ANNÉE 2018

THÈSE / UNIVERSITÉ DE RENNES 1
sous le sceau de l'Université Bretagne Loire

pour le grade de

DOCTEUR DE L'UNIVERSITÉ DE RENNES 1

Mention : Toxicologie

Ecole doctorale Biologie-Santé

présentée par

Jimmy Alarcan

Préparée à l'unité de recherche Toxicologie des Contaminants, Laboratoire de Fougères-ANSES en collaboration avec le Food Safety Department, German Federal Institute for Risk Assessment (BfR)

Effects of co-exposure to marine lipophilic biotoxins on the intestinal barrier, bioactivation and identification of molecular modes of action

Thèse soutenue à Rennes
le 15 Mai 2018

devant le jury composé de :

Luis BOTANA
Professeur, University of Santiago of Compostela / *rapporteur*

Albrecht SEIDEL
Professeur, Biochemical Institute for Environmental Carcinogens / *rapporteur*

Christine HERRENKNECHT Professeur, Université de Nantes / *président du jury*

Pascal LOYER
Docteur, Université de Rennes 1 / *examinateur*

Christopher MILES
Docteur, NRC Canada / *examinateur*

Valérie FESSARD
Docteur, ANSES-Fougères / *directeur de thèse*

Ludovic LE HEGARAT
Docteur, ANSES-Fougères / *co-encadrant de thèse*

Alfonso LAMPEN
Professeur, BfR Berlin / *directeur de thèse*

Acknowledgments

So many people to thank … I don´t know whom to begin with.

First of all, I would like to thank all the members of the jury, Luis Botana, Albrecht Seidel, Christine Herrenknecht, Pascal Loyer and Christopher Miles, for accepting to evaluate this work. My thanks go also to the members of my thesis committee Gregoire Michaud, Olivier Fardel and Fernando Rodrigues-Lima for their advices and opinions throughout this PhD.

I would like to introduce a new concept: the mother in sciences. This goes to you Valérie. Thanks for believing in me when I first steped in a research lab during my master internship. I will never forget these moments when during lunch you would scream/yell/say (rayer la mention inutile) “Jimmy we need to talk”. You get it right I did a PhD thesis. Thanks for always encouraging me in my not-always-relevant ideas. Thanks for all the corrections provided whether for the articles or the manuscript. Ludovic, you have been also my mentor since the very beginning. You received an organic chemist M2 student and turned him into a metabolism/toxicology PhD applicant. Thanks for all the knowledge you have transmitted, thanks for trusting me. And as well, thanks for all the corrections you provided.

Huge thanks go also to Estelle. You have been here since the very beginning too when I steped for my M2 internship. If co-PhD thesis would exist, I think you would clearly deserve it. Thanks for all the time you dedicated me with all the metabolism investigations. I am very happy you are doing a PhD thesis as well. You merit to be PhD graduated. A special thanks as well for Antoine aka PCR meister. Thanks for taking the time to show me every step of the art of the transcriptomic analysis. Thanks for accompanying me in Maisons Alfort. I am really glad our efforts were successful. Another special thanks to Kevin aka I´m Mister nice guy. Thanks for showing many protocols dealing with immunostaining (Arrayscan #1). “Bret Hart taking a huge Canadian backbreaker … oh no … wait … he got him … sharpshooter … the referee is asking … he tapped out … Bret Hart is the new world heavyweight champion”. This PhD thesis was based on *in vitro* experiments, especially with cell lines. That brings me to cell culture and it is now time to acknowledge Sylvie who taught me the art of cell culture. Without this skill, no PhD … so thanks again for teaching me this fundamental knowledge.

Once again a particular thank to my friend Ronel. Thanks a lot for your help in the review. And thanks as well for the great moments during the GdR conferences. The world of phycotoxins is clearly funnier with you. I would like to acknowledge another friend from the GdR, Romulo. Thanks for helping me with the SPX-1 metabolites and thanks for the nice moments during the GdR conferences.

A big thank goes to my friends from the lab: Kahina Kahina (Créteil connection … whenever you want to eat kebab, just call me … and finally I make you laugh), Pegah (fan #1 of Jean Moulin), Alexis (“tu vas niquer la batterie”), Romain (RIP my carpet), Vincent (and God made Rh123 and “putain”), Sarah (microbiologist … you are forgiven), Benjamin (fan #1 of CR7 and “ils prennent le bouillon !!!!!!!!!!”), Berengere (fan #1 of Tokyo Hotel … you are also forgiven), Océane (finally you are making sports … good luck with the marine biotoxins, tu reprends le flambeau), Pierre-Jean (“ah mais ca serait une autre étude ca” … man you are a genius for finding this), Manu (fan #1 of Pedro Miguel Pauleta (and also fan #1 of Francky Vincent, me being #2) … can´t wait PSG-Real Madrid in the final of champions´ league), Maleck (aka Bernard … you are truly one of kind), Rachelle (were we right about divorcing finally !? ...), Sophie (thumbs up to you for not having run away to a guy that was sending you papers

on psychoactive drugs, our discussions were deeply appreciated), Francesco (rital connection, les GdR étaient toujours un grand moment).

I would like then to acknowledge all my other colleagues from the lab who made these two years a really pleasant time. Particularly, I would like to thank Pascal Sanders for welcoming me in the lab and for its precious help through the registration for ECMNP.

This PhD thesis was also a unique opportunity for me to work/live in Berlin. I would like to thank everyone in the BfR who helped me. Alfonso, thanks for welcoming me in your department. Thank you for giving me the opportunity to stay 6 more months. Thanks for all your advices and the discussions (whether scientific or footballistic). Watching football games with you and Thorsten has always been a great pleasure. And maybe one day, your team will win.

A great thanks goes to Stefanie aka Steffi: thanks for caring about my good integration in the lab, thanks for helping me with the experiments and thanks for your corrections. I really enjoyed our meetings. One day I will try to visit Potsdam.

I would like to thank the secretaries Nicole and Sabine for their help with administrative tasks and all the nice moments and funny discussions. Your cheerfulnesses are really valuable.

I need to say thank you to all my labmates that helped me when I was lost or struggling to understand german indications. A special thanks to Conny (Arthur est un perroquet) who showed me almost all the experiments. Thanks to Claudia who helped me with the results of the transactivation assays. A big thank to Dorina who did the LC/MS-MS measurements for me. Another thank to Julia W (that RIP moment was really embarrassing for me, fortunately you laughed and saved me) that helped me with the HepaRG cells. A particular thank to my office colleagues: Holger and Jan. Jan, your “palm fett study” was really funny. A particular acknowledgment to Johanna, you are one of the sweetest people I have ever met.

Last but not least, I would like to say thank you to Jessica aka Jessy (sorry but you know I prefer Jessica). Thank you so much for always being there for me. I know I could always rely on you. Thank you for writing all the reports and projects for two. If you had to rely on my german, then it would have been pretty problematic. Thank you for all the nice moments in the lab and also in the congress. I think you deserve a special award for bearing all my stupid jokes.

I would like to say now a huge thanks to all my guys who made and makes this adventure here in Berlin extraordinary: (John) Cina (thumps up to you if you got the joke) (man we need to reunite “the marvelous idiots”), Miho-Chan (I would never thought you would laugh about “disguting”), Hannah (you are truly one of kind, my friend), Rami (fan #1 of Dave Mustaine, summer breeze will be remembered), Abd (who showed me the way of the dancefloors), Mika (I still keep the hope we will go dancing one day), Simin (you still owe me a restaurant I think), Michiel (I will visit you in Amsterdam), Rebecca (I will visit you in Lyon), Hector (so bad you moved from Berlin).

A very special thought goes to my *sensei* Christophe Dang. One entire life would not be enough to reach your level in việt quyền đạo (the Vietnamese way of killing with bare hands – no kidding it really means that more or less). I also want to express my gratitude to my other professors Raymond, Dominique, Boris, Kroa and all my mates.

Now, a really really really special thanks to my colegiala de amor: Alina Lourdes (aka las cosquillas, aka disculpe una preguntita por favor, aka eres un naco Jimmy, aka please Jimmy I say it with more style). Having you by my side helped me a lot. I will never forget our meeting when I did this seminar in your university.

Another special thought goes to my Nancy. We spent some crazy time together. I wish you the best. Take care of Marcellito and teach him French. One day we will meet again.

It is time now to acknowledge my professors and other people who played a role in my choice towards the path of sciences/toxicology. Particularly, I would like to thank Mrs Bemmoussat, my chemistry teacher in lycée, Mrs Zobiri my chemistry teacher in classes prépas, Prof Sylvie Condon, head of the master CMB, Pharmacist Hubert Corbé who introduced me to his colleague Pharmacist Philipe Vest to do my Bachelor internship in a toxicology lab and Philippe Vest for his mentorship during my very first lab experience.

I would like now to say a huge thank to my historic friends: Clément aka Clem aka oh marseillais, my brother in arms, Yannick ("allez on bosse là …"), Robert aka Bob (Finland is waiting for us), Enzo ("born to push you round … attends il chante là !!??"), Carole aka Cawole (we need to organize our trip), Jennifer (I never met a girl as busy as you), Yip-Ho (you need to show me Japan). We cannot meet as often as I wish but you are always with me.

Finally, it is time to acknowledge my family: a deep thought to all of them (ils se reconnaitront). Particularly, thanks to my brother Tony who gave me this "Master of puppets" CD when I was 17 … nothing was the same after that. Thanks for always caring of your little bro, even if sometimes you were a bit too jester (cf saint seiya armor in our cellar). Thanks also for your stylism advices. My mother Joëlle, thanks for everything, thanks for always being there for me. I forgive your crypto-communism. Finally, my father, Bernard: I have no words to express all my gratitude to you. Always there for me. You would turn the earth upside down if it was needed. Being raised with the military values is something that brought me a lot. I hope one day I will be able to reach your level.

Table of contents

Introduction 1

Chapter 1: From phytoplankton to shellfish poisoning 3

I. Phytoplankton and harmful algal blooms 3

II. Accumulation in filter bivalves 4

III. Human shellfish poisonings 4

IV. Legislation and monitoring of lipophilic phycotoxins 6

1. Codex Alimentarius 6

2. EFSA recommendations 7

3. Reference methods for monitoring 10

4. Alternative assays 10

V. Prospects 10

Chapter 2: Small intestine and liver, main targets of lipophilic phycotoxins 11

I. General considerations 11

1. Small intestine 11

a. Anatomical structure 11

b. Functions 12

c. Intestinal barrier 12

2. Liver 14

a. Anatomical structure 14

b. Functions 16

II. First-pass metabolism 16

1. General considerations 16

2. Barrier crossing 17

a. Paracellular passage 18

b. Transcellular passage 18

3. Xenobiotic-metabolizing enzymes 22

a. CYP 22

b. UGT 24

c. SULT 24

d. NAT 25

e. MT 26

f. GST 26

g. AMT 27

4. Metabolic bioactivation 27
5. Genetic polymorphism 28
6. Nuclear receptors 29
a. Classification and structure 29
b. Ligands 30
c. Activation 32
d. Protein-protein interaction and signaling crosstalk 35
e. Target genes 35
III. In vitro models 37
1. Intestine 37
2. Liver 37
Chapter 3: Lipophilic phycotoxins 39
I. Okadaic acid and analogues 39
1. Production by phytoplankton 39
2. Structure 39
3. *In vivo* toxicity 39
a. Lethal doses in rodents 39
b. Effects on the intestine 40
c. Effects on the liver 41
4. *In vitro* toxicity 42
a. Mechanism of action 42
b. Toxicological effects 42
5. ADME 43
a. Intestinal absorption 43
b. Metabolism 43
II. Pectenotoxins 44
1. Production by phytoplankton 44
2. Structure 44
3. *In vivo* toxicity 45
a. Lethal doses in rodents 45
b. Effects on the intestine 46
c. Effects on the liver 46
4. *In vitro* toxicity 47
a. Mechanism of action 47
b. Toxicological effects 47

5. ADME 47
a. Intestinal absorption 47
b. Metabolism 48
III. Spirolides 48
1. Production by phytoplankton 48
2. Structure 48
3. *In vivo* toxicity 49
a. Lethal doses in rodents 49
b. Effects on the intestine 50
c. Effects on the liver 51
4. *In vitro* toxicity 51
a. Mechanism of action 51
b. Toxicological effects 51
5. ADME 51
a. Intestinal absorption 51
b. Metabolism 51
IV. Yessotoxins 52
1. Production by phytoplankton 52
2. Structure 52
3. *In vivo* toxicity 53
a. Lethal doses in rodents 53
b. Effects on the intestine 55
c. Effects on the liver 55
4. *In vitro* toxicity 55
a. Mechanism of action 55
b. Toxicological effects 55
5. ADME 56
a. Intestinal absorption 56
b. Metabolism 56
V. Mixtures of phycotoxins 57
Publication #1: Mixtures of lipophilic phycotoxins: exposure data and toxicological assessment 57
Aims of the PhD project 82
Chapter 4: Material and Methods 83
I. *In vitro* cell lines 83
1. HepaRG/HepG2 83

2. HEK-T 83
3. Caco-2 84
II. Metabolism investigation 84
1. S9 incubations 84
2. Silensomes™ 85
3. LC/HRMS 85
III. High Content Screening 87
IV. Nuclear receptors activation 89
V. Mixture effects 89
1. Concept 89
2. Theoretical additivity method 90
3. Chou-Talalay method 91
Results 93
"Phycotoxins ADME" axis 93
Preliminary results: Investigation on the intestinal passage of the marine biotoxins PTX-2 and SPX-193
Publication #2: Metabolism of the Marine Phycotoxin PTX-2 and Its Effects on Hepatic Xenobiotic Metabolism: Activation of Nuclear Receptors and Modulation of the Phase I Cytochrome P450 104
Publication #3: Metabolism of the lipophilic phycotoxin 13-desmethylspirolide C in human and rat liver fractions 121
Preliminary results: Modulation of CYP3A4 and P-gp by okadaic acid and its associated mechanism: PXR inhibition and possible role of inflammation 140
Preliminary results: Effects of yessotoxin on mRNA expression in human hepatic HepaRG cells 154
"Mixture effects" axis 165
Publication #4: *In vitro* assessment of binary mixture effects of phycotoxins in human intestinal Caco-2 cells 165
Final summary 188
Discussion 189
Conclusion 194
Bibliography 195
Annexes 229
I. Training 229
II. Collaborations 229
III. Communications 229
1. Conference 229
2. Other 230

Figures

Figure 1: A bloom of the nontoxic dinoflagellate *Lingulodinium polyedrum* along the coast of La Jolla, San Diego County. Picture: Kai Schumann 3
Figure 2: Phycotoxins ways of exposure in humans (inspired from Berdalet et al., 2011) 4
Figure 3: Global distribution of shellfish poisoning events in humans (from whoi.edu/redtide) 6
Figure 4: Anatomy of the human digestive system (from humananatomywiki.com) 11
Figure 5: Intestinal barrier (from Gerbe et al., 2016) 13
Figure 6: Enterocytes (reproduced from Edwin R. Price et al., 2015) 13
Figure 7: Liver anatomy (from bannerhealth.com) 14
Figure 8: Hepatic lobule structure (Illustration from Anatomy & Physiology) 15
Figure 9: Cells population in the hepatic lobule (from Chu et al., 2013) 15
Figure 10: The different steps of the xenobiotics metabolism (reproduced from Pelkonen et al., 2014) 17
Figure 11: Paracellular and transcellular passage across enterocytes (reproduced from Sugano et al., 2010) 18
Figure 12: Passive transport mechanisms (reproduced from http://apbiology11.weebly.com/facilitated-diffision.html) 19
Figure 13: ABC efflux mechanism (from Kenneth J. Linton 2006) 20
Figure 14: Influx (green) and efflux (blue) transporters in enterocytes and hepatocytes (from Shugarts and Benet 2009) 21
Figure 15: Endocytosis mechanism (by Mariana Ruiz Villarreal 2007) 21
Figure 16: Crystalline structure of CYP3A4 (from Williams et al., 2004) 22
Figure 17: Repartition of CYP in the liver (reproduced from Paine et al., 2006) 24
Figure 18: Glucuronidation reaction (from Fujiwara et al., 2016) 24
Figure 19: Sulfation reaction (from Masahito et al., 2017) 25
Figure 20: N-acetylation and O-acetylation reactions (from Sim et al., 2013) 25
Figure 21: Methylation reaction (from Petra Jančová and Michal Šiller 2012) 26
Figure 22: Glutathione conjugation (from Townsend and Tew 2003) 27
Figure 23: Glycine conjugation on benzoic acid (from Petra Jančová and Michal Šiller 2012) 27
Figure 24: Nuclear receptor structure (inspired from Jenni Küblbeck 2012) 30
Figure 25: AhR structure (from Jenni Küblbeck 2012) 30
Figure 26: Direct activation of CAR, PXR and AhR (inspired from Mackowiak and Wang 2016) 34
Figure 27: Indirect activation of CAR, PXR and AhR (inspired from Mackowiak and Wang 2016) 34
Figure 28: Chemical structure of OA, DTX-1 and DTX-2 (from Larsen et al., 2007) 39
Figure 29: Chemical structure of PTX-2 and its analogues (from Halim and Brimble 2006) 45
Figure 30: Chemical structure of SPX-1 and other spirolides (from Rodríguez et al., 2013) 49
Figure 31: Chemical structure of YTX and its analogues (from Dominguez et al., 2010) 53
Figure 32: S9 and microsomes preparation (from Katrin Kittler 2012) 84
Figure 33: Example of CYP phenotyping assay (from Biopredic) 85
Figure 34: SPX-1 calibration curve 86
Figure 35: Metworks® software interface. Metabolites investigation is depicted with PTX-2 87
Figure 36: Principle of ArrayScan VTi Thermofischer 88
Figure 37: PXR transactivation assay principle (from Luckert et al., 2015) 89
Figure 38: Methodological tree for mixture effects 90

Figure 39: Characterization of mixture effects according to the theoretical additivity method (adapted from Smith et al., 2016) 91
Figure 40: Characterization of mixture effects according to the Chou-Talalay method (from Chou 2006)..... 92

Tables

Table 1: Classification of the main phycotoxins according to their chemical structure. Reported effects in humans are also presented (inspired from Gerssen et al., 2010) 5
Table 2: Maximum levels for marine biotoxins in live bivalve molluscs (from Regulation (EC) No 853/2004) 7
Table 3: Regulatory limits for the main lipophilic phycotoxins and ARfDs established by EFSA (EFSA Journal 2009) 8
Table 4: Probability of exceeding ARfD limits while being compliant with EU limits (EFSA Journal 2009) 8
Table 5: TEFs established by EFSA for the regulated lipophilic phycotoxins 9
Table 6: Ligands of AhR, CAR and PXR (from di Masi et al., 2009, Ramadoss et al., 2005, Mani et al., 2013) 31
Table 7: Target genes of AhR, CAR and PXR (from Beischlag et al., 2008, Jenni Küblbeck 2012, Wang et al., 2012, Chen et al., 2012) 36
Table 8: Main cell lines used for *in vitro* toxicokinetic studies on intestinal absorption 37
Table 9: Main *in vitro* hepatic cell lines used in toxicology (from Jenni Küblbeck 2012) 38
Table 10: Acute toxicity of OA in mice 40
Table 11: Acute toxicities of PTX-2 in mice 45
Table 12: Acute toxicities of SPX-1 in mice 50
Table 13: Acute toxicities of YTX in mice 54
Table 14: Co-factors for xenobiotic metabolism investigations using S9 fractions 85
Table 15: Limits of detection and quantification for the phycotoxins 86
Table 16: Markers used in High Content Screening investigations 88
Table 17: Summary of results 188

Abbreviations

ABC: ATP binding cassette

ADME: Administration, distribution, metabolism and excretion

AhR: Aryl hydrocarbon receptor

ARfD: Acute reference dose

ARNT: Aryl hydrocarbon receptor nuclear translocator

ASP: Amnesic shellfish poisoning

AZP: Azaspiracid shellfish poisoning

CAR: Constitutive androstane receptor

CYP: Cytochrome P450

DBD: DNA binding domain

DSP: Diarrheic shellfish poisoning

DTX: Dinophysistoxin

EFSA: European food safety authority

ENT: Equilibrative nucleoside transporter

EU: European union

FDA: Food and drug administration

GST: Glutathione S transferase

HAB: Harmful algal bloom

HCS: High content screening

HLM: Human liver microsome

HPLC/MS-MS: High pressure liquid chromatography/ mass spectrometry

HSP: Heat shock protein

hTERT: Human telomerase reverse transcriptase

IL: Interleukine

i.p: Intra peritoneal

LBD: Ligand binding domain

LBP: Ligand binding pocket

LC/HRMS: Liquid chromatography/High resolution mass spectrometry

LD_{50}: Lethal dose 50%

mAChR: muscarinic acetylcholine receptor

MBA: Mouse bioassay

MDR: Multi-drug resistance protein

MLD: Minimum lethal dose

MOA: Mode of action

MRP: Multi-drug resistance-assiocated protein

MS: Mass spectrometry

nAChR: Nicotinic acetylcholine receptor

NAT: N-acetyltransferase

NF-κB: Nuclear factor kappa B

NSP: Neurologic shellfish poisoning

OATP: Organic anion-transporting polypeptide

PDE: Phosphodiesterase

P-gp: P-glycoprotein

PP: Protein phosphatase

PSP: Paralytic shellfish poisoning

PTX-2: Pectenotoxin-2

PXR: Pregnane X receptor

RXR: Retinoid X receptor

SLC: Solute cation transporter

SPX-1: 13-desmethyl spirolide C

SULT: Sulfotransferase

TEF: Toxicological equivalency factor

UGT: UDP-glucuronosyltransferase

WHO: World health organization

XME: Xenobiotic metabolizing enzyme

XRE: Xenobiotic responsive element

XREM: Xenobiotic responsive element module

YTX: Yessotoxin

Introduction

Today, more than half of the world population is living in coastal zones. These particular areas between sea and land have been exploited since they display great natural resources, allowing a viable economy with industry implementation including tourism, aquaculture and seafood provision. Particularly, seafood industry has skyrocketed these past few decades. In 2013, the production of seafood in Europe was estimated over 10,000 million euros (from CBI market intelligence, 2015).

Seafood is increasingly becoming part of our diets and it is even seen as a substitute for meat products. Recognized as source of energy and protein with high biological value, it contributes to the intake of essential nutrients (iodine, selenium, calcium, vitamins, n-3 long-chain polyunsaturated fatty acids, etc.) with well-established health benefits. Data explicitly show that consumers in European countries increasingly demand seafood as part of a modern and healthy lifestyle and seafood is positively promoted as a healthy food in the media.

Nonetheless, a wide range of contaminants can be accumulated especially in high-level filtering shellfish (mussels, oysters etc.). Among them, natural products include phycotoxins that are produced by a restricted number of phytoplanktonic microalgal species. They accumulate in shellfish and can lead to human poisonings when contamined seafood is ingested. Several types of intoxications due to phycotoxins have been described so far. The symptoms, depending on the toxins incriminated, mainly imply neurological and gastro-intestinal disorders. Recurrent occurrence of emerging toxins in seafood has also been witnessed these last years. Indeed, some phycotoxins and toxic phytoplankton that were found only in tropical and subtropical areas are now detected in the temperate waters of the Atlantic Ocean and in the Mediterranean Sea. The climate change including global warming is one factor that may explain the spreading of sub-tropical species to temperate latitudes. Besides, their geographical expansion due to transport in ballast waters participates as well in this phenomenon. On the top of that, monitoring exposure and toxicity assessment of new emerging toxins keep up as challenging outcomes as the different groups of phycotoxins generally include several analogues. Finally, although mixtures of phycotoxins have been already described in seafood, facing both mixtures of well-known phycotoxins and potentially new mixtures with emerging phycotoxins will be a next step in human health protection from phycotoxins.

The establishment of regulatory levels for the main phycotoxins and the consequent monitoring programs for shellfish contamination to prevent acute human intoxications are based on hazard from animal studies and rare epidemiological data. In fact, data on toxic effects, if any, in humans are still missing for several toxins and the impact when mixtures of phycotoxins are ingested has been rarely addressed. To face this concern, including the involvement of emerging phycotoxins, health authorities need further exposure information and toxicological data to modify, when necessary, the regulatory levels.

Unfortunately, the studies on the toxicity of phycotoxins alone and in mixtures are confronted with several issues: i) the availability of pure compounds as only a limited number of toxins is commercialized by few suppliers; ii) the cost of *in vivo* studies due to the amount of toxins required

and iii) the lack of published data concerning phycotoxins mixtures found in seafood on both the co-occurring compounds and their concentrations.

Moreover, the behavior of phycotoxins after human ingestion has been rarely addressed. In fact, the extrapolation between the external exposure (level and toxin profile found in shellfish) and the internal exposure once the phycotoxins have been ingested by humans (level and toxin profile in organs and body fluids) is also a a challenging issue. Adressing the ADME of phycotoxins must help providing information to which toxins and metabolites and at which levels organs and body fluids are effectively exposed, and further on to correlate with the main harmful effects detected during *in vitro* studies.

This PhD work aims at contributing to the characterization of intestinal absorption, metabolism, toxicity and identification of the mechanisms of action of four main lipophilic phycotoxins alone or in mixture using *in vitro* approaches.

Chapter 1: From phytoplankton to shellfish poisoning

I. Phytoplankton and harmful algal blooms

Phytoplankton is the first nexus in marine food chain. It gathers different classes of microscopic algae which use photosynthesis to produce their vital resources. Among these classes, two are known to exhibit species that produce phycotoxins: diatoms and dinoflagellates (Anderson et al., 2012). The reason why certain species produce such toxins has not yet been elucidated although several hypotheses have been proposed such as defense mechanism against predators or potential energetic storage (Anderson et al., 2012).

Under specific circumstances, microalgae are able to proliferate rapidly, forming "harmful algal blooms" (HABs) (Berdalet et al., 2015). Sometimes HABs are spectacular changing the water color into red or green (Figure 1). High-nutrient conditions in water (especially nitrates and phosphorus) as well as high light conditions and temperature have been shown to favor the flourishing of HABs. Anthropic factors cannot be excluded as well since human activities such as urban constructions along the coasts (harbor, marina) or modern agriculture drastically change the environment of phytoplankton (Paerl 2014, Berdalet et al., 2015). When HABs involve phycotoxins producing species, the toxins accumulate in seafood products and eventually result in human intoxications (Pulido et al., 2016). Moreover, some toxins can drastically affect the local ecosystem. All these implications may strongly impact the coastal economic activities (fish and possibly shellfish mortality, shutting of fishing or seafood culture or harvest areas, and interruption of tourism-related activities) (Moore et al., 2013). Although some specific occurrences can be highlighted from one geographical region to one another, HABs is a worldwide phenomenon that affects all the continents.

Figure 1: A bloom of the nontoxic dinoflagellate *Lingulodinium polyedrum* along the coast of La Jolla, San Diego County. Picture: Kai Schumann

II. Accumulation in filter bivalves

Filter bivalves are a class of mollusks with about 12,000 species listed. They feed by filtering nutrients in surrounding water and essentially nourish from phytoplankton. When toxin-producing phytoplankton blooms occur, they accumulate toxins mainly in their digestive gland (hepato-pancreas). Food intoxications by contaminated shellfish are the principal way of human exposure to phycotoxins (Figure 2). The main filtering bivalves implied in shellfish poisonings are mussels, oysters, clams, scallops and cockles. In few cases phycotoxin-food intoxication is provoked by contaminated fish consumption (Rossini et al., 2010). Among these, ciguatera has the greatest impact of human cases reported worldwide (Friedman et al., 2017). Human exposure to phycotoxins can also occur through inhalation with aerosols as well as by skin contact for some specific phycotoxins (Rossini et al., 2010, Pulido 2016).

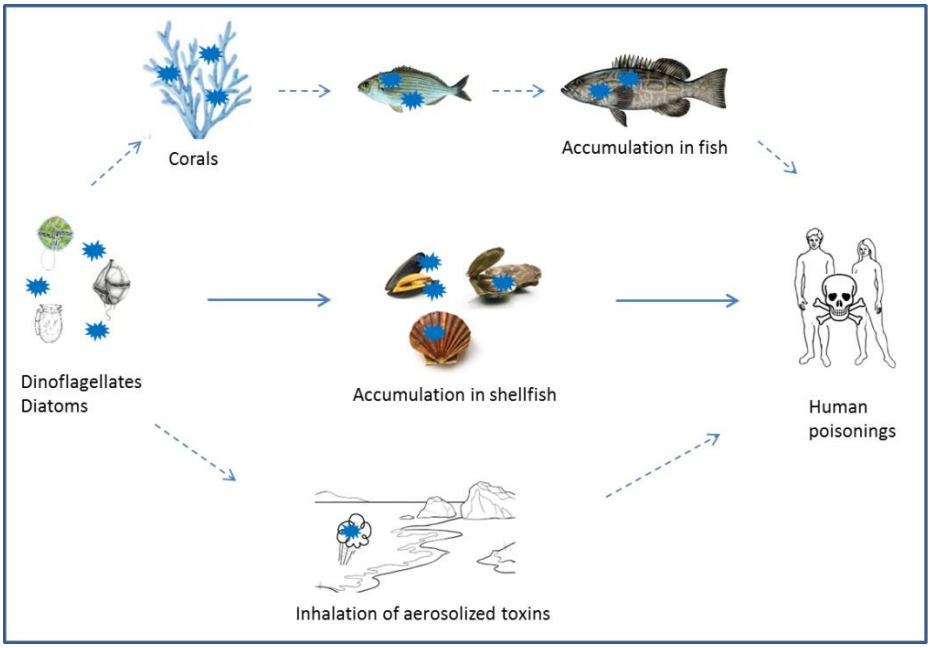

Figure 2: Phycotoxins ways of exposure in humans (inspired from Berdalet et al., 2011)

III. Human shellfish poisonings

Official data are not sufficient to get a precise number of human shellfish poisonings since underestimation is expected at least when no neurologic symptoms occur. Nevertheless, it is estimated that algal toxins are responsible for about 60,000 human intoxications each year (Van Dolah 2000). Phycotoxins display a large panel of symptoms in humans (Krahl 2009). A classification according to their chemical nature has been established (Table 1). Among the lipophilic toxins, more than 200 compounds have been described (Gerssen et al., 2011). Some groups of lipophilic phycotoxin (yessotoxins, cyclic imines) have not been linked to any human intoxication so far despite the fact that high levels were already reported in shellfish (Miles et al., 2010) and that they showed potent *in vivo* effects on rodents (Aune et al., 2008, Munday et al., 2012). Other phycotoxins have

also been reported in seafood but concern is rather for tropical areas (for instance ciguatoxin and palytoxin), although new records in temperate waters have been published (Otero et al., 2010, Silva et al., 2015, Biré et al., 2015). Besides, it cannot be excluded that non-monitored species such as sea urchins or crustaceans may be responsible for intoxications.

Table 1: Classification of the main phycotoxins according to their chemical structure. Reported effects in humans are also presented (inspired from Gerssen et al., 2010)

	Toxin	Syndrome	Symptoms	Genre
Hydrophilic	Domoic acid	ASP (amnesic shellfish poisoning)	short-term memory loss, headache, dizziness, nausea, vomiting	*Pseudo-nitzschia*
	Saxitoxins	PSP (paralytic shellfish poisoning)	tingling, numbness of the face, headache, dizziness. In case of high toxication, respiratory difficulties and other muscular paralytic effects	*Alexandrium / Gymnodinium / Pyrodinium*
Lipophilic	Brevetoxins	NSP (neurotoxic shellfish poisoning)	diarrhea, vomiting, cramps, rapid reduction of the respiratory rate and cardiac conduction disturbances	*Karenia / Chatonella*
	Okadaic acid and dinophysistoxins	DSP (diarrheic shellfish poisoning)	diarrhea, nausea, vomitting, abdominal pain	*Dinophysis / Prorocentrum*
	Pectenotoxins	Unknown	no effects reported in humans	*Dinophysis*
	Yessotoxins	Unknown	no effects reported in humans	*Protoceratium / Lingulodinium / Gonyaulax*
	Azaspiracids	AZP (azaspiracid shellfish poisoning)	diarrhea and abdominal cramps	*Azadinium*
	Cyclic imines	Unknown	no effects reported in humans	*Alexandrium / Vulcanodinium*
	Palytoxins	Not well-defined	myalgia, weakness, fever, nausea, vomitting	*Palythoa / Ostreopsis*
	Ciguatoxins	CFP (ciguatera fish poisoning)	diarrhea, nausea, vomitting, tingling, hypotension, bradycardia	Precursor from *Gambierdiscus toxicus*

If DSP, PSP and ASP are worldwide distributed, the other syndromes have been reported only in restricted areas (Figure 3). For instance, AZP has almost exclusively occurred along the European coasts whereas NSP has been only described along the coasts of North America and New-Zealand.

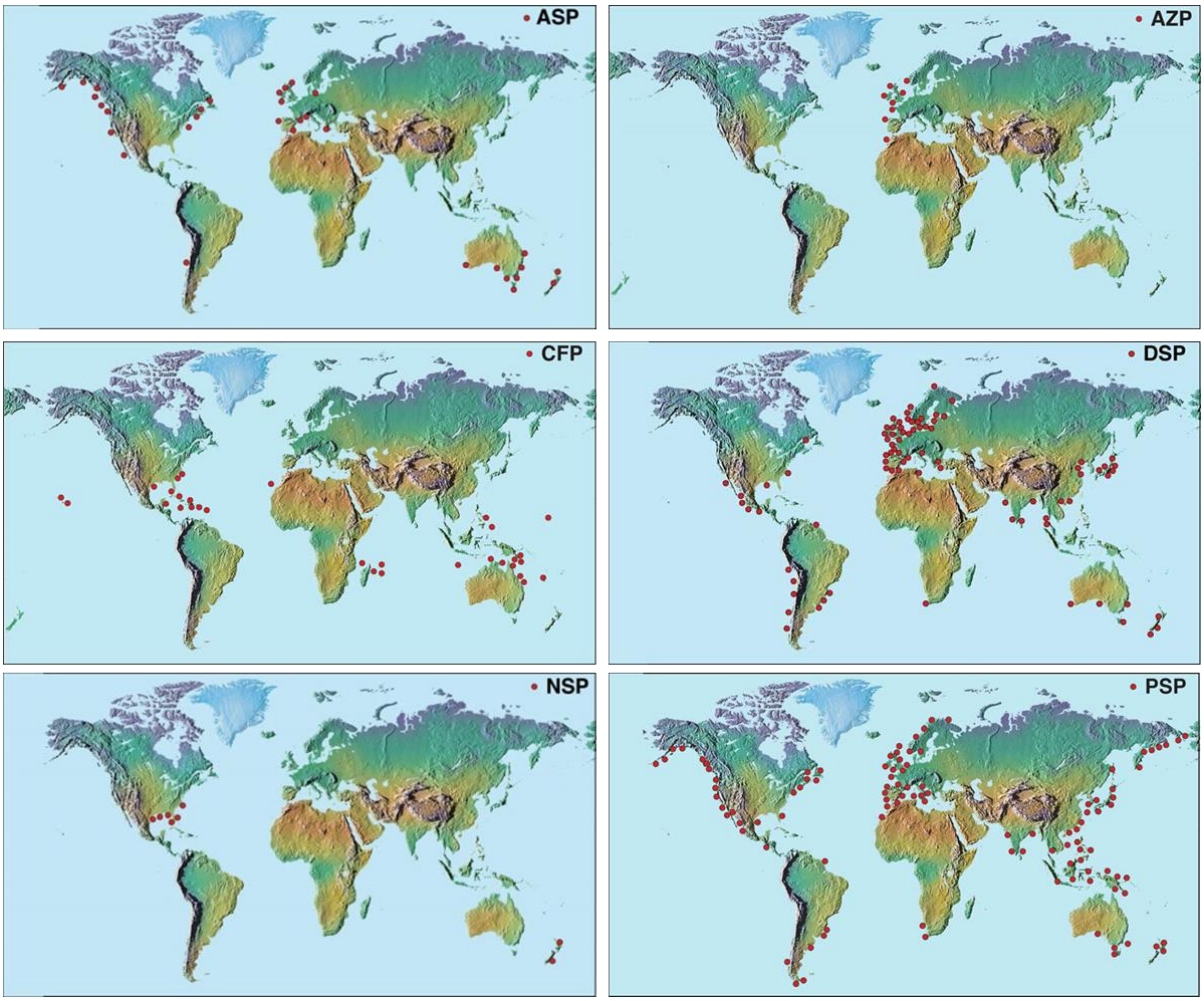

Figure 3: Global distribution of shellfish poisoning events in humans (from whoi.edu/redtide)

IV. Legislation and monitoring of lipophilic phycotoxins

1. Codex Alimentarius

The Codex Alimentarius Commission (CAC) is an intergovernmental group within the framework of the Joint Food Standards Programme established by the Food and Agriculture Organization of the United Nations (FAO) and the World Health Organization (WHO). Its purpose is to protect the health of consumers and to ensure fair practices in the food trade by providing food standards, guidelines, codes of practice and other recommendations. The Codex General Standard for Contamination and Toxins in Foods (CODEX STAN 193-1995) established regulatory limits for the main phycotoxin groups. These regulatory limits have been established in Europe in the document entitled "Regulation (EC) No 853/2004 of the European Parliament and of the Council of 29 April 2004 laying down specific hygiene rules for food of animal origin" with a specific paragraph for marine biotoxins in live bivalve molluscs (Table 2).

Table 2: Maximum levels for marine biotoxins in live bivalve molluscs (from Regulation (EC) No 853/2004)

2. They must not contain marine biotoxins in total quantities (measured in the whole body or any part edible separately) that exceed the following limits:

(a) for paralytic shellfish poison (PSP), 800 micrograms per kilogram;

(b) for amnesic shellfish poison (ASP), 20 milligrams of domoic acid per kilogram;

(c) for okadaic acid, dinophysistoxins and pectenotoxins together, 160 micrograms of okadaic acid equivalents per kilogram;

(d) for yessotoxins, 1 milligram of yessotoxin equivalent per kilogram;

and

(e) for azaspiracids, 160 micrograms of azaspiracid equivalents per kilogram.

For YTXs, the permitted level was adjusted to 3.75 milligrams of yessotoxin equivalent per kilogram in 2013 (COMMISSION REGULATION (EU) No 786/2013). Today no maximum limits have been set for spirolides and other cyclic imines since no cases of human intoxications involving these phycotoxins were reported.

2. EFSA recommendations

The European Food and Safety Authority (EFSA) is an official European agency that gives scientific opinions and recommendations in regards of risks associated with foodstuff. The CONTAM panel deals with the issues regarding food contaminants. Up to now, they have provided 13 reports on phycotoxins. In 2009, they published a key report dealing with the limits of regulated phycotoxins. Based on epidemiological data in humans (when available) or acute toxicity values in mice, they set up acute reference doses (ARfD) (Table 3). They calculated the maximum levels of phycotoxin to which humans can be exposed taking into account the higher levels of shellfish consumption from some European specific countries. It appears that all established ARfD (except for the YTX group) were below the EU regulatory limits (last column of the Table 3), suggesting that the established limit values are probably not sufficiently protective for the whole population including the big consumers.

Table 3: Regulatory limits for the main lipophilic phycotoxins and ARfDs established by EFSA (EFSA Journal 2009)

Toxin group	Current EU limits in shellfish meat (A)	Exposure from eating a 400 g portion at concentrations in samples on the EU market	ARfD	Corresponding dose for a 60 kg adult	Maximum concentration in shellfish meat to avoid exceeding the ARfD (B)	Ratio B/A
OA and analogues	160 µg OA eq/kg SM	64 µg OA eq/person	0.3 µg OA eq/kg b.w.	18 µg OA eq/person	45 µg OA eq/kg SM	0.28
AZA	160 µg AZA eq/kg SM	64 µg AZA1 eq/person	0.2 µg AZA1 eq/kg b.w.	12 µg AZA1 eq/person	30 µg AZA1 eq/kg SM	0.19
PTX	160 µg OA eq/kg SM	64 µg PTX2 eq/person	0.8 µg PTX2 eq/kg b.w.	48 µg PTX2 eq/person	120 µg PTX2 eq/kg SM	0.75
YTX	1 mg YTX eq/kg SM	400 µg YTX eq/person	25 µg YTX eq/kg b.w.	1500 µg YTX eq/person	3.75 mg YTX eq/kg SM	3.75

Additionally, a probabilistic analysis provided in the EFSA report concluded that the probability that contaminated shellfish had a toxin concentration exceeding the ARfD value was relevant mostly for OA and analogues (Table 4), with a probability of 20%.

Table 4: Probability of exceeding ARfD limits while being compliant with EU limits (EFSA Journal 2009)

Toxin group	Probability of exceeding the ARfD when consuming any single portion of shellfish on the EU market[(a)]	% of samples compliant with the EU limit but exceeding the concentration compatible with ARfD[(b)]
OA and analogues	20%	32%[(c)]
AZA	4%	8.5%
PTX	0.2%	0.3%
YTX	<0.2%	-

(a): probabilistic estimate based on the distribution of both occurrence and consumption

(b): the concentration was based on the 400 g portion size

(c): based on lower bound estimate

The case of spirolides and other cyclic imines was discussed in the EFSA report #1628. Currently, no ARfD limits have been established for cyclic imines including spirolides since no cases of human intoxications were reported. However, these toxins have been shown to exert potent toxicity in mice following oral or ip administration (Munday et al., 2012). The question of new emerging toxins was also discussed in two reports on brevetoxin and ciguatoxin groups. Besides, it was highlighted that, from the data of phycotoxins monitoring, co-contamination frequently occurs in shellfish (the EFSA

Journal, 2009). Co-exposure can be schematically divided into two categories: contamination by the same group (one toxin and its analogues) and contamination by different groups of toxins. Regarding phycotoxin mixtures issue, the EFSA opinion only focuses in the case of toxin analogues. Toxicity equivalence factors (TEF) have been proposed to convert the concentrations of the OA-, AZA-, YTX-, STX- and PTX analogues into respectively OA, AZA1, YTX, STX and PTX2 equivalents. TEFs approach relies on the additivity of the toxicity of the different analogues, assuming that they have the same mode of action.

TEFs for regulated phycotoxins were determined based on acute toxicity following i.p. administration to mice (Table 5).

Table 5: TEFs established by EFSA for the regulated lipophilic phycotoxins

Toxin group	Analogue	TEF
OA-group toxins	OA	1
	DTX1	1
	DTX2	0.6
AZA-group toxins	AZA1	1
	AZA2	1.8
	AZA3	1.4
YTX-group toxins	YTX	1
	1a-homoYTX	1
	45-hydroxyYTX	1
	45-hydroxy-1a-homoYTX	0.5
PTX-group toxins	PTX1	1
	PTX2	1
	PTX3	1
	PTX4	1
	PTX6	1
	PTX11	1

However, based on new oral data, different TEFs were proposed for the group of AZAs by the FAO (FAO /WHO Joint 2016): 0.7 and 0.5 for AZA2 and AZA3, respectively. Also, the TEF for DTX-2 was proposed to be revaluated to 0.5.

Due to the lack of studies regarding deleterious effects induced by combination of different groups of toxins, the EFSA recommends to provide further data in order to set proper regulatory limits that would take into account any combined effect when toxins co-occur.

3. Reference methods for monitoring

Phycotoxins screening in shellfish often steps in following alerts due to the levels of toxic phytoplankton found during water samplings analyses. The phytoplanktonic species give indications on which toxins are expected to be found in shellfish. The monitoring is therefore often a combination of phytoplankton monitoring and toxins screening in shellfish.

The Mouse bioassay (MBA) was largely employed in Europe for monitoring lipophilic phycotoxins in shellfish production areas and on the market. However, for such toxins, MBA has shown false positive responses due to interferences with lipids for example. Additionally, the use of animals for monitoring purposes raised ethical questions. Consequently, analytical methods have been developed and validated for lipophilic toxins detection and quantification. Liquid chromatography mass spectrometry is an appropriate tool for monitoring since it can detect levels of toxins below the current regulatory limits and can also be used for multi-toxin group detection/quantification (Gerssen et al., 2010, van den Top et al., 2011). Since 2011, this technique has been adopted as the EU reference method for OA, PTX, YTX and AZA-groups detection in shellfish (No. 15/2011). The main limit for this method is the requirement of certified standard solutions and the establishment of reliable TEFs. Moreover, some matrix effects have been reported and, for reasons not fully understood, some toxins are prone to signal enhancement or suppression (Zendong et al., 2015).

4. Alternative assays

Several alternative assays have been proposed as easy, fast and cheap ways to monitor toxins instead of MBA (see part III of Seafood and Freshwater Toxins: Pharmacology, Physiology, and Detection, Third Edition, 2014). They include ELISA assays, functional assays based on the mode of action and cell-based assays. Functional assays have been developed only for groups for which the mode of action was elucidated: OA and DTXs with protein phosphatase 2A (PP2A) inhibitor assays (Smienk et al., 2013) and SPXs with nicotinic inhibition assays (Vilarino et al., 2009). Recently, Diogène et al., 2017 proposed a double screening strategy based on both cell-based assays and LC/MS-MS analysis.

V. Prospects

The recommendations of the food safety agencies aim at addressing the mechanisms of toxicity to favor risk assessment. The data collected during reported events of human seafood intoxications showed that the gastrointestinal tract is the main target of lipophilic phycotoxins. *In vivo* experiments pinpointed alterations in the small intestine and in the liver following phycotoxins exposure. Since these two organs are involved in controlling the systemic level of phycotoxins after human ingestion, it is important to adress the ADME of phycotoxins and to study their harmful effects on these organs too.

Chapter 2: Small intestine and liver, main targets of lipophilic phycotoxins

I. General considerations

Intestine belongs to the gastro-intestinal (GI) tract whose primary functions are the intake of food, its digestion and the excretion of waste (Figure 4). In addition to the GI tract, several other organs such as liver participate in the digestion process. Altogether, the GI tract and the accessory organs of digestion (tongue, salivary glands, pancreas, liver, and gallbladder) form the digestive system (Schneeman 2002).

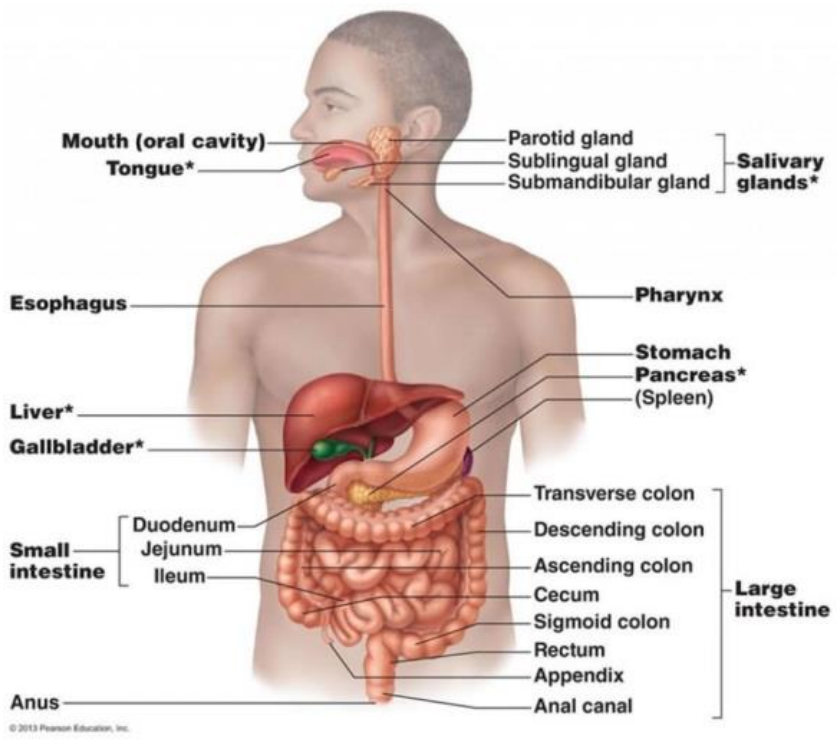

Figure 4: Anatomy of the human digestive system (from humananatomywiki.com)

1. Small intestine

a. Anatomical structure

The human small intestine is subdivided into 3 regions in humans:

- Duodenum, which starts after the stomach (pyloric sphincter), is the shortest region measuring around 25 cm. Featuring a C-shaped curve, it wraps around the head of the pancreas.

- Jejunum measures about 2.5 meters and follows the duodenum. Its mucosa lined with numerous wrinkles increases the total internal surface, allowing a better absorption of lipids, carbohydrates and proteins.
- Ileum is the final region of the small intestine, measuring about 3.5 meters. It is separated from the cecum (first portion of the large intestine) by the ileocecal valve.

The small intestine thus measures 6 to 7 meters in humans and exhibits about 200-300 m^2 of internal surface exchange. This large surface area plays a key role in the processes of digestion and absorption (Pappenheimer et al., 2003).

b. Functions

The small intestine ensures a key role in the digestion of food and absorption of nutrients (mainly proteins, carbohydrates and lipids) (Kong et al., 2008). The digestion of proteins into small peptides is carried out thanks to the release of pancreatic juice containing proteolytic enzymes such as trypsin or chymotrypsin (Moroz et al., 2016). Carbohydrates are partially converted into monosaccharides via pancreatic amylases (Schneeman 2002). Lipids digestion is assured by bile and pancreatic lipases which degrade them into free fatty acids and glycerol.

Absorption of nutrients is driven through diffusion and active transport. The epithelial tissue of small intestine features capillaries called villi that enable the increase of the exchange surface area (Pappenheimer et al., 2003).

Last, the small intestine plays a role in the immune system thanks to lymphoid follicles (called Peyer´s patches) associated to the epithelia of jejunum and ileum (Reboldi and Cyster 2016).

c. Intestinal barrier

The intestinal epithelium constitutes a complex barrier which ensures a double function: allowing the absorption of key elements such as nutrients as well as protecting the organism from xenobiotics and pathogens (Groschwitz and Hogan 2009). Different types of cells are found in this epithelium: enterocytes, Paneth cells, goblet cells, M cells, tuft cells, intestinal stem cells (Gerbe et al., 2016) (Figure 5). All these cells are specifically arranged, forming a villus that considerably enhances the exchange surface area between lumen and lamina propria.

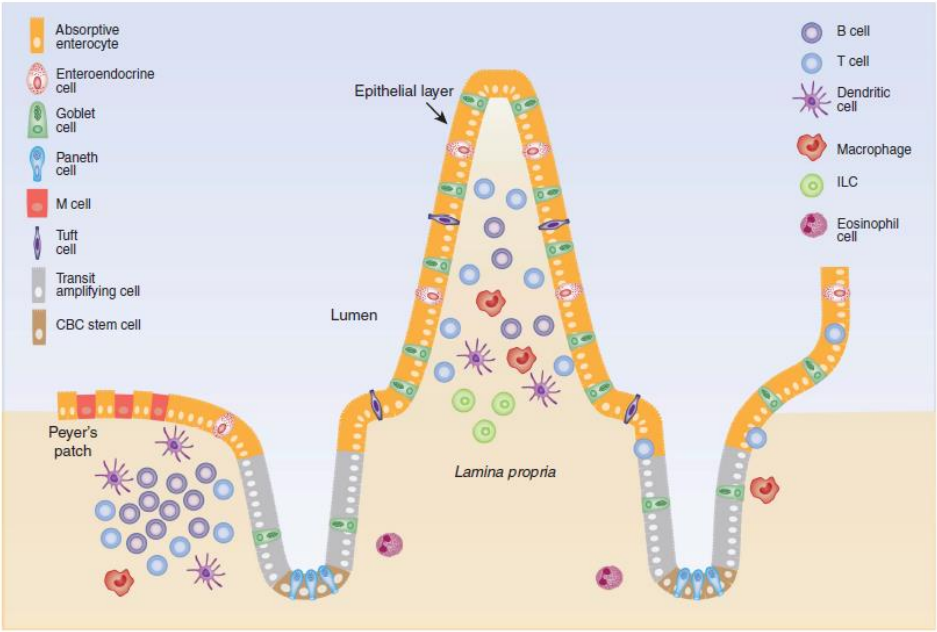

Figure 5: Intestinal barrier (from Gerbe et al., 2016)

Enterocytes are polarized cells with an apical side facing the lumen and a basolateral side facing the lamina propria. On the apical side, enterocytes display microvilli arranged in brush border. These microvilli greatly expand the exchange surface area and are the place of absorption of many compounds (Krause 2005) (Figure 6). Indeed, in addition to various transporters, enzymes located in the membrane of microvilli will terminate proteins and carbohydrates digestion enabling their uptake.

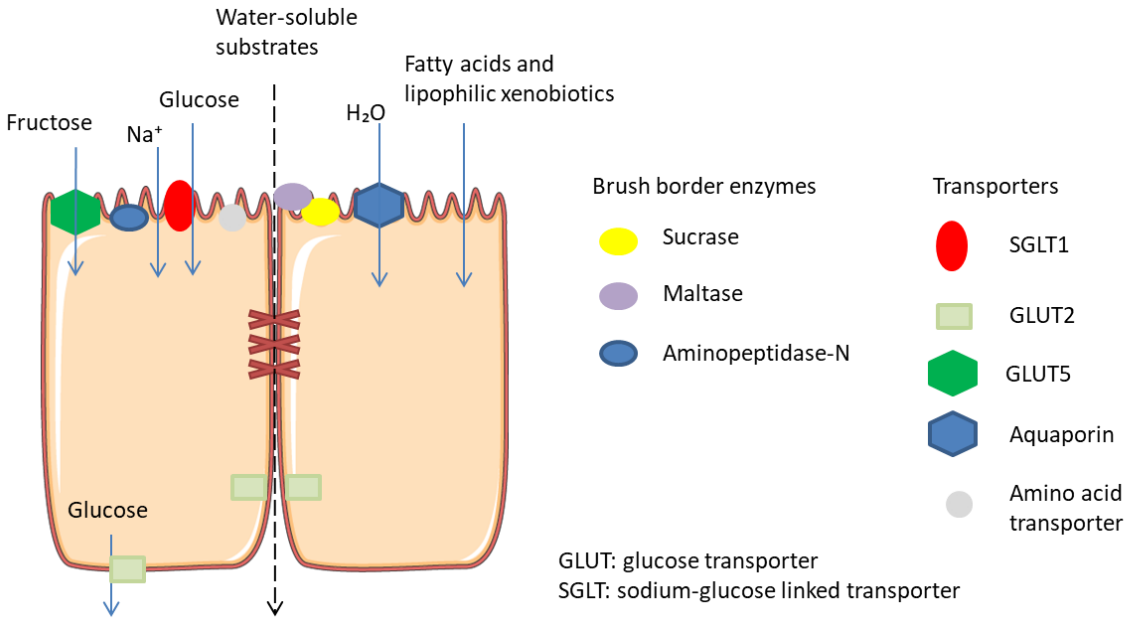

Figure 6: Enterocytes (reproduced from Edwin R. Price et al., 2015)

2. Liver

a. Anatomical structure

The human liver is located on top of the stomach in the upper right-hand portion of the abdominal cavity and beneath the diaphragm (Figure 7). It is divided into two lobes in humans.

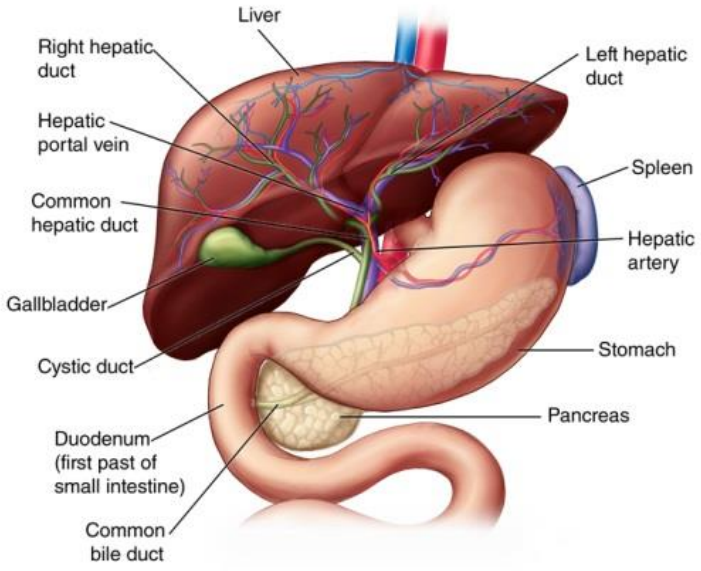

Figure 7: Liver anatomy (from bannerhealth.com)

The liver is a highly vascularized organ supplied in blood by the hepatic portal vein and the hepatic artery (Abdel-Misih and Bloomston 2010). The hepatic portal vein carries blood rich in bile and nutrients to the small intestine. The hepatic artery supplies the liver with O_2-charged blood from the heart. The blood coming from the hepatic portal vein and the hepatic artery will enter the hepatic lobules through small capillaries called sinusoids (Abdel-Misih and Bloomston 2010). Lobules with hexagonal structure are the functional units of the liver consisting of plates of hepatocytes organized around a central vein that further joins the hepatic vein (Figure 8). At each corner of the lobule the portal triads are found: they gather a hepatic artery branch, a hepatic portal vein branch and a bile duct. It is through these portal triads that the blood enters sinusoids and comes into contact with the hepatocytes and then is drained to the central vein. The bile ducts carry the bile which is produced by the hepatocytes (Boyer 2013). The bile is then addressed to the gall bladder before being discharged in the duodenum. About 95% of the bile delivered to the duodenum is reabsorbed by the ileum before transportation again to the hepatic lobules via the portal vein (Boyer 2013).

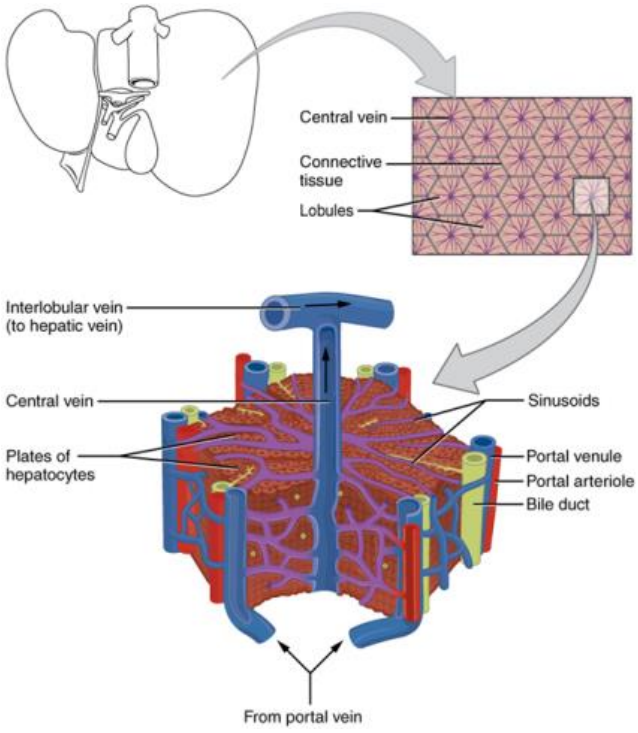

Figure 8: Hepatic lobule structure (Illustration from Anatomy & Physiology)

Different cell types compose the hepatic lobules (Figure 9). In addition to the hepatocytes, endothelial cells and Kupffer cells are present along the sinusoids. The Kupffer cells are macrophages (Dixon et al., 2013). Sinusoidal endothelial cells form a barrier against pathogenic agents and also serve as a selective sieve for substances passing from the blood to the hepatocytes (De Leeuw et al., 1990, Knolle et al., 2016). Moreover, they participate in the metabolic and clearance functions of the liver (De Leeuw et al., 1990).

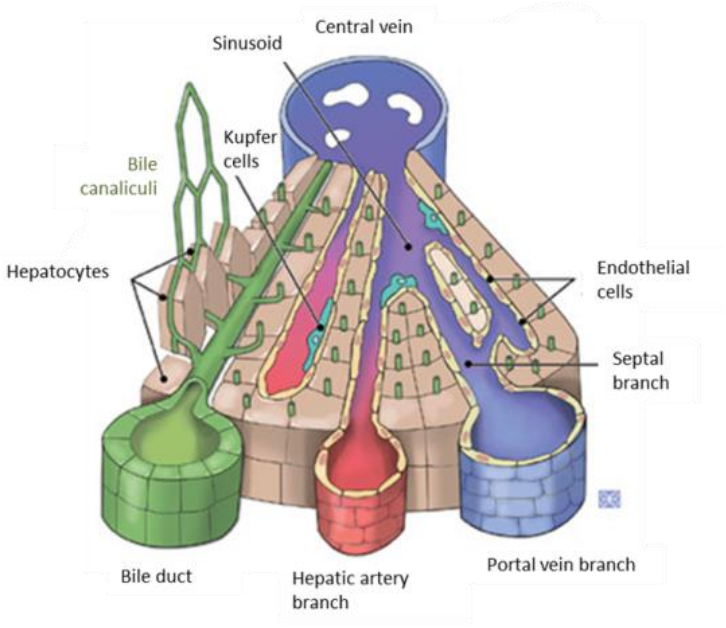

Figure 9: Cells population in the hepatic lobule (from Chu et al., 2013)

b. Functions

The liver ensures a wide spectrum of key functions for the organism:

- during digestion, the liver hepatocytes produces the bile that will be delivered to the small intestine. The bile is transported via bile canaliculi and is then either drained directly into the duodenum thanks to the bile duct or is stored in the gall bladder via the cystic duct (Boyer 2013).

- it participates in the metabolism of carbohydrates and lipids. From glucose it synthesizes glycogen which is stored and can be released later on when needed (glycogenolysis) (Raddatz and Ramadori 2007). It can also itself produce glucose from amino acid, lactate or glycerol (gluconeogenesis). It is responsible for the synthesis of cholesterol and triglycerides (lipogenesis), as well as many lipoproteins (Postic et al., 2004).

- it produces key proteins such as albumin, blood clotting factors or growth factors (Levitt and Levitt 2016). It is also responsible for the breakdown of insulin and other hormones. It breaks bilirubin and converts ammonia into urea (Wang et al., 2006).

- it stores a multitude of key substances such as vitamins (A, D, B12 or K), metals (iron, copper), folic acid, glucose, etc (Kmieć 2001).

- it plays a major role in the metabolism of xenobiotics where compounds are biotransformed and then excreted (Brockmoller and Roots 1994). This part is further detailed below.

II. First-pass metabolism

1. General considerations

First-pass metabolism refers to an ensemble of processes whereby the concentration of a xenobiotic is reduced, and consequently lowering the xenobiotic concentration in the systemic blood circulation. The liver is considered to be the major site of first-pass metabolism, but the importance of the intestine is being increasingly reviewed since enterocytes express also some of the key xenobiotic-metabolizing enzymes (XME) involved in first-pass metabolism (Jones et al., 2016).

Globally, after ingestion, a xenobiotic can undergo primary metabolic modifications when crossing the intestinal barrier through enterocytes. Then it reaches liver through the hepatic vein where it undergoes hepatic metabolism before being excreted into urine by kidneys.

As previously highlighted, both enterocytes and hepatocytes are responsible for the biotransformation and excretion of xenobiotics (pharmaceutical drug, contaminant, toxin, etc). The hydrophobic compounds will more easily permeate inside the cells. The metabolism consists in increasing their hydrophilicity, favoring their excretion outside the cells with less possibility to permeate through again. For this purpose, XME modify the chemical structure of the compounds. The metabolic process is divided in three main steps called phases including enzymatic (phases I and

II) and efflux (phase III) mechanisms (Pelkonen et al., 2014) (Figure 10). An additional phase 0 could be added to describe the influx when xenobiotics, rather hydrophilic, are uptaken by specific transporters. Phase I metabolism depicts mainly oxidation or hydrolysis reactions which permit the formation of hydrophilic functions such as hydroxyl (-OH), amine (-NH_2) or acid (-COOH) groups on the molecules. The produced metabolites are generally more hydrophilic than the parent compound and can be effluxed by transporters (for instance P-glycoprotein), or further biotransformated by Phase II enzymes. Phase II metabolism consists of the conjugation of small hydrophilic molecules whether on phase I metabolites or on parent compound. This conjugation favors the hydrophilicity of the molecule and then its excretion via bile and further urine. Following biotransformation from previous phases, metabolites are then excreted out of the cells by transporters. In some cases, xenobiotics can be directly excreted by transporters without undergoing biotransformation. There are two major superfamilies of transporters, the ATP-binding cassette (ABC) and the solute carriers (SLC).

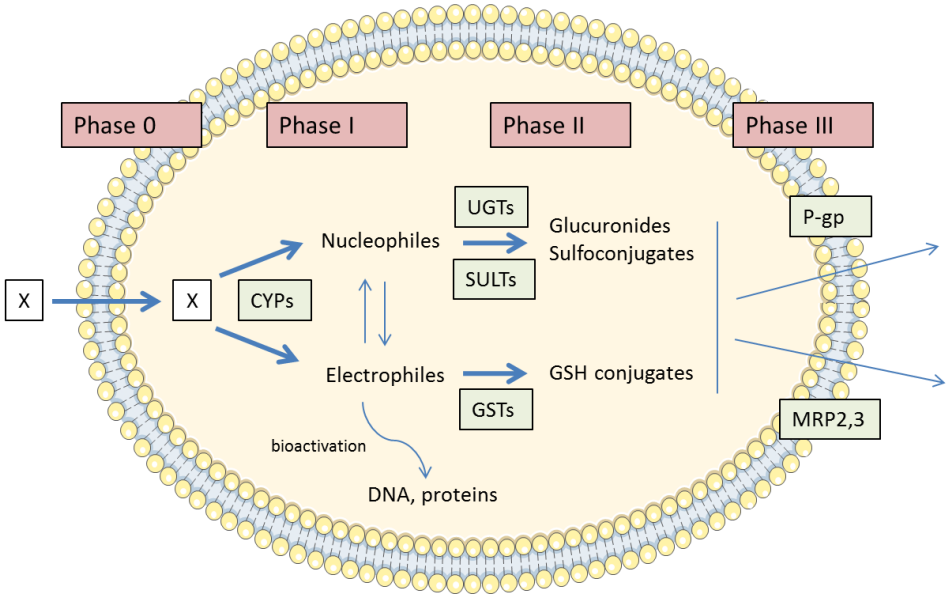

Figure 10: The different steps of the xenobiotics metabolism (reproduced from Pelkonen et al., 2014)

2. Barrier crossing

The absorption of molecules through the intestinal epithelium is mediated whether by paracellular or transcellular passage (El-Kattan and Varma 2012) (Figure 11).

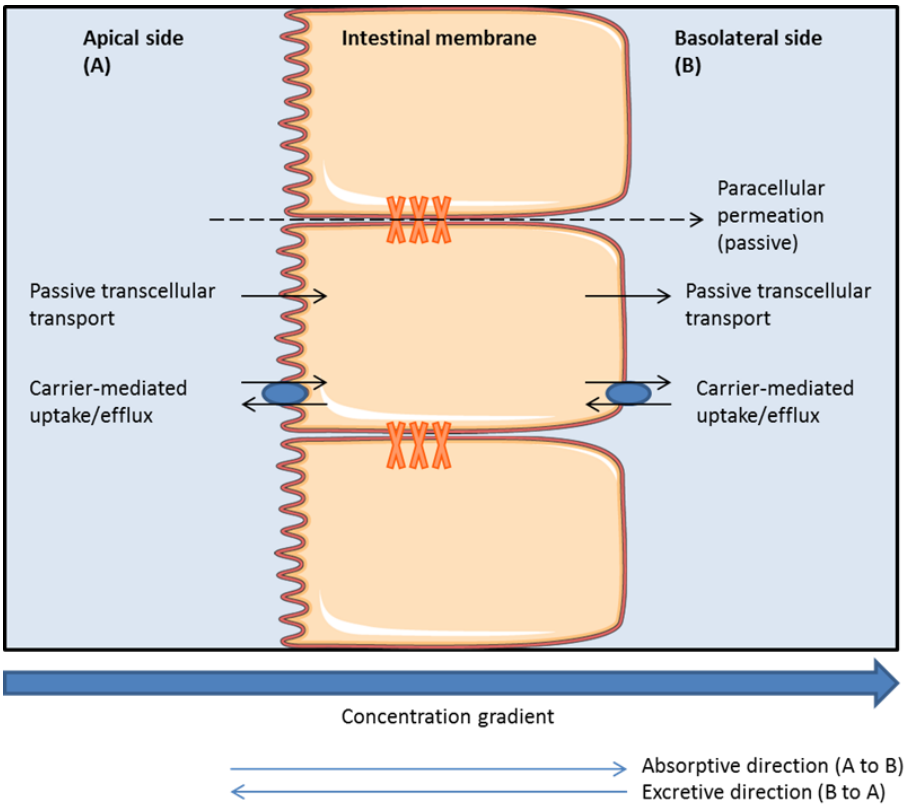

Figure 11: Paracellular and transcellular passage across enterocytes (reproduced from Sugano et al., 2010)

a. Paracellular passage

The paracellular pathway describes the passage of substances across the barrier by passive diffusion between the epithelial cells linked together through tight junction proteins. This free-energy mechanism is concentration gradient-dependent, and concerns mostly small molecules (molecular weight MW < 250 g/mol) that are hydrophilic and positively charged (El-Kattan and Varma 2012).

b. Transcellular passage

The transcellular pathway describes the passage of substances through enterocytes. Diffusion and transport are the two mechanisms involved in the transcellular passage:

- In addition to simple diffusion, facilitated diffusion is also involved in free-energy drug passage (Figure 12). It relies on membrane proteins to help larger, charged, hydrophilic and polar molecules that cannot diffuse on their own through the hydrophobic bilayer. Two types of integral membrane proteins have been described: the first are carrier proteins, which bind a molecule to facilitate the transport through the cell membrane (Friedman 2008), the second are channel proteins, which create a passageway to transport molecules and ions through the cell membrane. This channel protein creates a pore through the hydrophobic region that allows polar molecules just to pass right through (Friedman 2008).

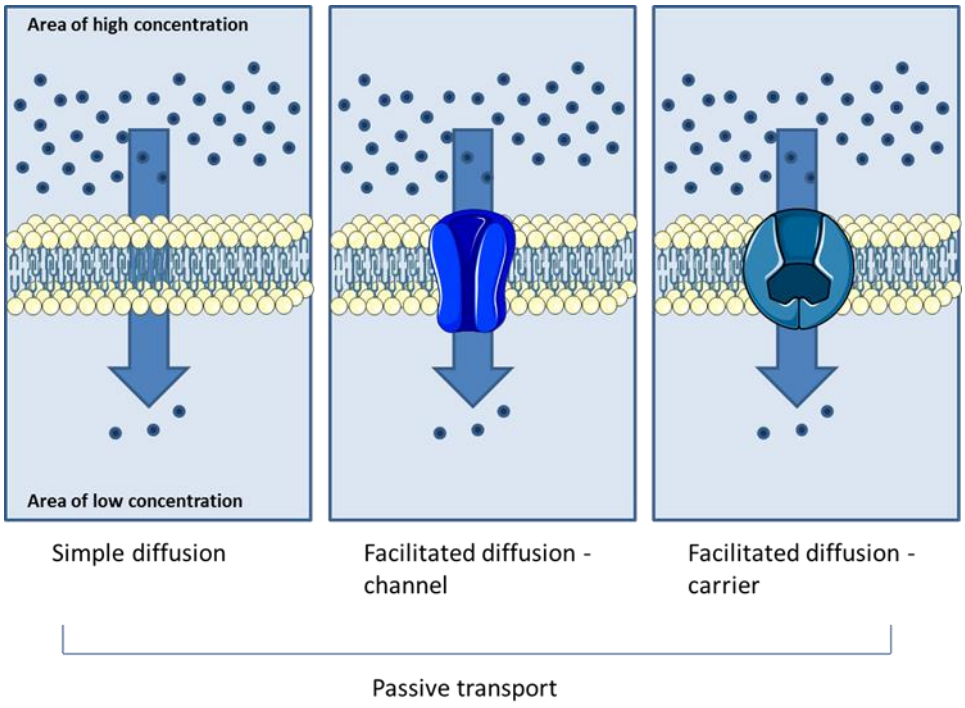

Figure 12: Passive transport mechanisms (reproduced from http://apbiology11.weebly.com/facilitated-diffision.html)

- Membrane transporters are mainly divided into two major families: the ATP binding cassette (ABC) family and the solute carrier (SLC/SLCO) family.
    - ATP binding cassette (ABC) carriers are primary active carriers that use the energy from ATP hydrolysis to transport their substrates through the cell membrane. These efflux pumps all possess consensus regions which allow the recognition of the molecules, as well as a hydrolysis site releasing an inorganic phosphate accompanied by an ADP molecule (Kenneth J. Linton 2006) (Figure 13). These carriers are found in the intestine but also in the liver and the brain (Shugarts and Benet 2009, Yano et al., 2018). They are located whether on the apical or the basolateral side of the cells (some, as MRP4, are located on both sides), favoring the efflux of xenobiotics outside them (Larsen et al., 2007). The ABC transporter family is divided into subfamilies coded from A to G. Forty-eight different proteins have been identified which are involved in the transport of a wide variety of xenobiotics (Wilkens 2015). Sugars, lipids, proteins, hydrophobic molecules or even metal ions are also well-known substrates. The most important ABC transporters involved in drug passage are P-gp (ABCB1), multidrug resistance-associated proteins MRPs (ABCC subfamily), bile salt export pump BSEP (ABCB11) and breast cancer resistance protein BCRP (ABCG2) (Shugarts and Benet 2009, Liang et al., 2015).

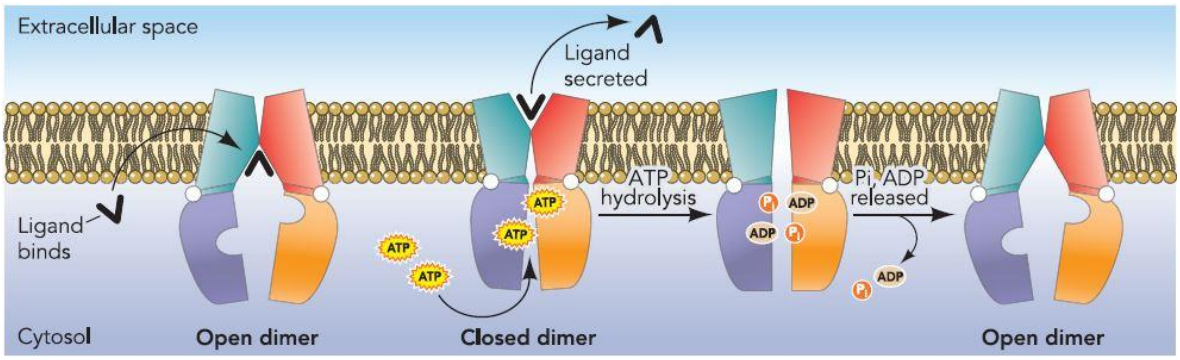

Figure 13: ABC efflux mechanism (from Kenneth J. Linton 2006)

- On the contrary, the SLC/SLCO transporters generally use energy from a chemiosmotic gradient created by translocation of ions across the membrane. Solute carriers (SLC/SLCO) are a group of membrane transporters with approximately 400 members in 52 families (Xie et al., 2018). Some of these SLC/SLCOs are involved in the transport of xenobiotics (Kovacsics et al., 2016). These transporters are found on the apical membrane of the cells and are involved in the influx of certain xenobiotics. SLC/SLCOs are found in many tissues, including liver, intestine and brain (Roth et al., 2012). The most important SLC families are the organic anion transporters (OAT), the organic cation transporters (OCT), the concentrative nucleoside transporters (CNT), the peptide transporters (PEPT), and the equilibrative nucleoside transporters (ENT) (Shugarts and Benet 2009, Hediger et al., 2004). The SLCO family also gathers the organic anion transporting polypeptides (OATP).

Both uptake and efflux transporters play a key role in the bioavailability of most xenobiotics. The figure 14 shows the main transporters involved in uptake and efflux of drugs at the intestinal and hepatic levels. While P-gp, BCRP, MRP2 and MRP4 are mainly implicated in the excretion of drugs, OATP1A2, OATP2B1, PEPT1, OCT3, MCT1 or CNT1 are responsible for drugs uptake (Shugarts and Benet 2009). Additionally, transporters play a key role in drug-drug interactions (Yu et al., 2017).

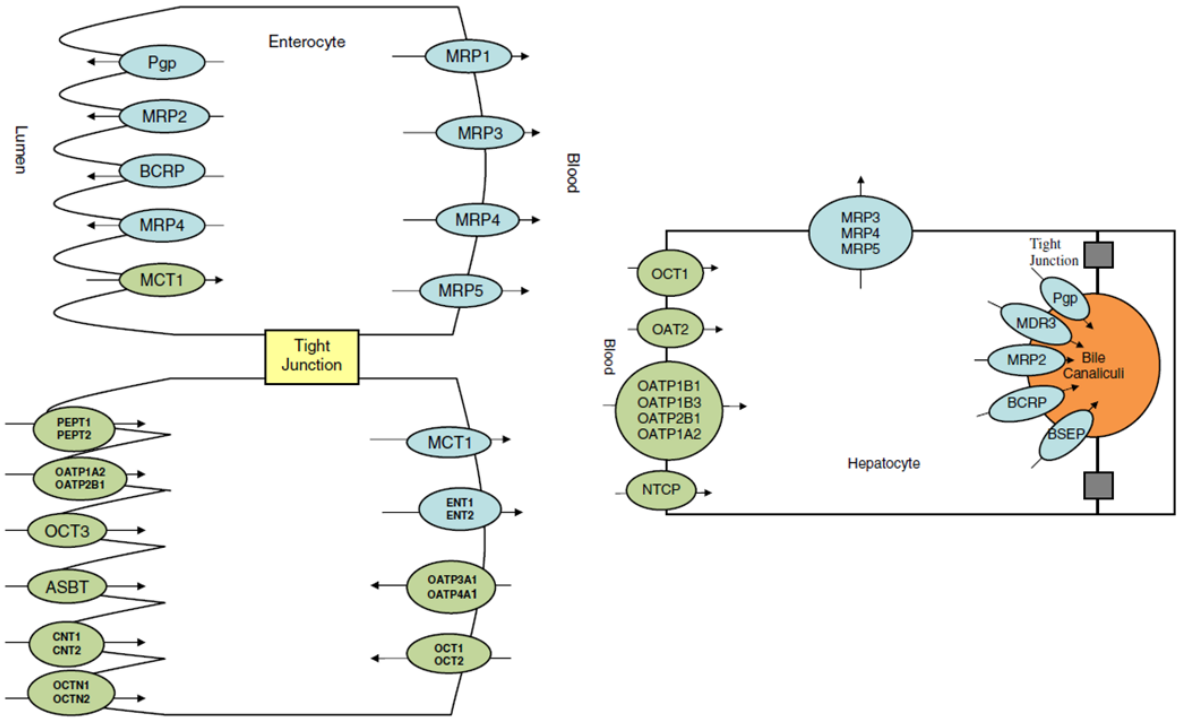

Figure 14: Influx (green) and efflux (blue) transporters in enterocytes and hepatocytes (from Shugarts and Benet 2009)

Finally, endocytosis describes a particular process of transport where compounds are internalized into the cells (Figure 15). The membrane surrounds the compound to be internalized and then migrates inside the cell forming a vesicle which traps the compound. This process targets macromolecules and particles. Ingestion of material such as bacteria occurs through phagocytosis whereas smaller material is internalized through pinocytosis. Additionally, some specific molecules (for instance cholesterol) can enter the cell through specific receptor-mediated endocytosis (Cooper 2000).

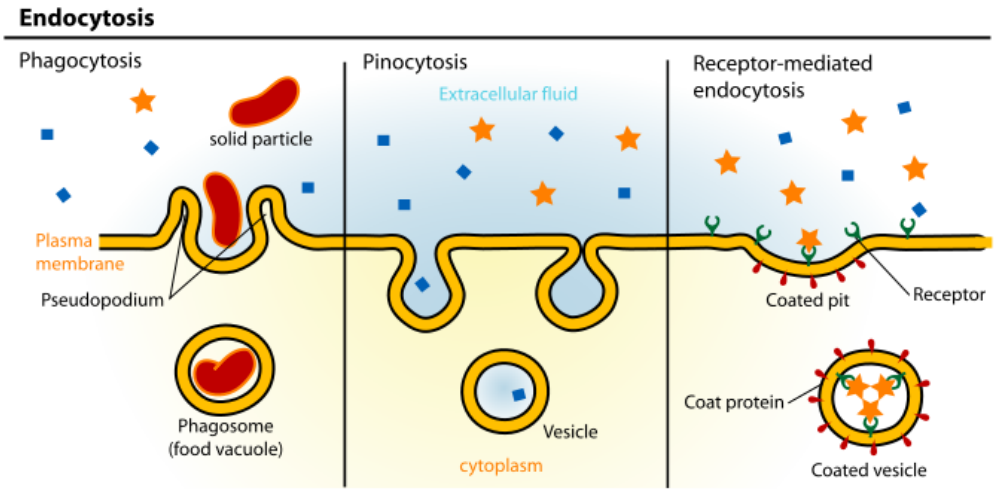

Figure 15: Endocytosis mechanism (by Mariana Ruiz Villarreal 2007)

3. Xenobiotic-metabolizing enzymes

XME designates both phase I and II enzymes that participate in the biotransformation of xenobiotics. Phase I enzymes comprise hydrolases which gather different varieties of enzymes (lipases, glucosidases, epoxide hydrolases, etc.) and oxido-reductases which gather monooxygenases (cytochromes P450 and flavin-containing monooxygenases), cyclooxygenases and alcohol-dehydrogenases (Foti and Dalvie, 2016).

There are six main phase II enzyme families: UDP-glucuronosyltransferases, sulfotransferases, N-acetyltransferases, N- and O-methyltransferases, glutathione S-transferases and amino acid transferases (Omiecinski et al., 2011).

a. CYP

Cytochromes P450 represent a superfamily of enzymes involved in the metabolism of xenobiotics and certain endogenous molecules. They are mostly expressed in the liver but are also present in lower amounts in the intestine, lungs, kidneys, heart, brain and skin (Pelkonen et al., 2008). In the liver, cytochromes are predominantly located in the endoplasmic reticulum membrane of hepatocytes. From a structural point of view, the P450s are hemoproteins consisting of a protein part called apoprotein and a prosthetic group called heme with a porphyrin nucleus linked to an iron atom (Figure 16).

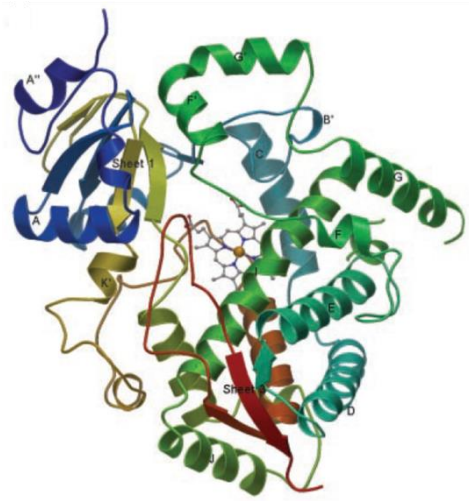

Figure 16: Crystalline structure of CYP3A4 (from Williams et al., 2004)

Coded by 57 genes in humans, this enzymatic family presents a multitude of isoforms classified according to the following nomenclature: cytochrome / family / subfamily / isoform (Guengerich et al., 2005). For example, CYP1A2 designates the second isoform of the cytochrome belonging to family 1 and subfamily A. Only the isoforms belonging to the three main families CYP1, 2 and 3 will be presented.

CYP1:

This family includes CYP1A1, CYP1A2 and CYP1B1, and is known to be involved in the detoxification of many prescribed drugs. CYP1A2 plays a major role in the metabolism of xenobiotics featuring planar polyaromatic amides or amines (ethoxyresorufin, caffeine or phenacetin) (Zhou et al., 2010).

CYP2:

It is the family with the most isoforms and metabolizing a wide range of drugs (Pelkonen et al., 2008). Among these enzymes are CYP2A6, CYP2B6, CYP2C which themselves contain several isoforms (CYP2C8, CYP2C9 or CYP2C19), CYP2D6 and CYP2E1.

- CYP2A6: weakly expressed, its substrates are mostly small planar molecules (Lewis 2004). It is predominant in the metabolism of nicotine.
- CYP2B6: It catalyzes in particular the transformation of neutral molecules, not planar or having a weakly basic property. Among its substrates, mention may be made of bupropion, cyclophosphamide, ketamine and also propofol (Turpeinen et al., 2006).
- CYP2C9: predominant form of CYP2C, it metabolizes a large number of commonly used drugs such as fluoxetine, fluvastatin or diclofenac (Rostami-Hodjegan and Tucker, 2007).
- CYP2C19: the least expressed isoform of CYP2C, it is however involved in the biotransformation of many compounds including diazepam, citalopram, mephenytoin or omeprazole (Pelkonen et al., 2008).
- CYP2D6: it is the isoform with the greatest genetic polymorphism (Eichelbaum et al., 2006). Its action is major in the metabolism of propanolol, fluoxetine, bufuralol and certain antipsychotics like risperidone.
- CYP2E1: well-expressed at the liver level, its action is mainly known in the bioactivation of certain organic apolar solvents as well as the metabolism of ethanol (Raucy et al., 1993, Lieber 2004). Its typical substrate is hydrophobic and of low molecular weight (Lewis 2004).

CYP3:

Accounting for approximately 40% of the "material" P450 in the liver (Figure 17), this family is the most important in the biotransformation of drugs (Paine et al., 2006). It includes the CYP3A4, CYP3A5 and CYP3A7 (Pelkonen et al., 2008).

- CYP3A4: the most expressed metabolic enzyme in the liver, its role is essential since it intervenes in the metabolism of about 50% of the drugs (Pelkonen et al., 2008). Among these, antibiotics (erythromycin), benzodiazepines (midazolam, triazolam) and statins (simvastatin).
- CYP3A5: polymorphic enzyme poorly expressed in liver but consistently expressed in extra-hepatic tissues (Daly 2006). It shares many substrates with CYP3A4.
- CYP3A7: this isoform is especially present during embryonic and fetal development where it is involved in the hydroxylation of endogenous substances like retinoic acid and steroid hormones (Daly 2006). In the adult liver, it is a minor form.

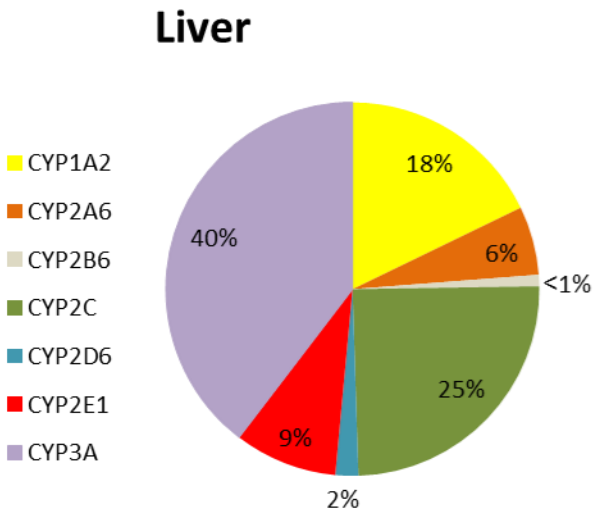

Figure 17: Repartition of CYP in the liver (reproduced from Paine et al., 2006)

b. UGT

UDP-glucuronosyltransferases (UGTs) gather 19 enzymes in humans that are divided into two families (UGT1A and UGT2) (Fujiwara et al., 2016, Yang et al., 2017). These enzymes catalyze the addition of glucose onto nitrogen or oxygen atom of their substrate (Figure 18). Nonetheless, N-glucuronidation reactions are solely catalyzed by UGT1A family. UGTs are located in the endoplasmic reticulum membrane of the cells. They are expressed in several tissues but some isoforms are tissue-specific (for instance UGT2As are predominantly expressed in the olfactory epithelium) (Fujiwara et al., 2016, Yang et al., 2017). It is estimated that about 35% of the prescribed drugs metabolized by Phase II enzymes undergo metabolism by UGTs (Fujiwara et al., 2016, Yang et al., 2017).

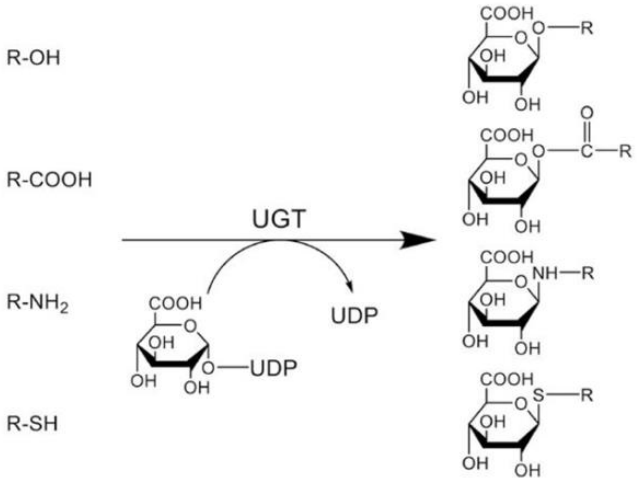

Figure 18: Glucuronidation reaction (from Fujiwara et al., 2016)

c. SULT

Sulfotransferases (SULTs) gather 15 enzymes divided into four families (SULT1, 2, 4 and 6). These enzymes catalyze the transfer of the sulfonate group from the active sulfate, 3'-phosphoadenosine

5'-phosphosulfate (PAPS) to compounds containing an hydroxyl or an amino group (Figure 19). SULTs are present in the cytosol in soluble form, or bound to the membranes of the Golgi apparatus. Golgi membrane-bound SULTs are responsible for the sulfation of proteins, proteoglycans, and glycolipids whereas SULTs present in the cytosol are involved in the sulfation of xenobiotics (Masahito et al. 2017).

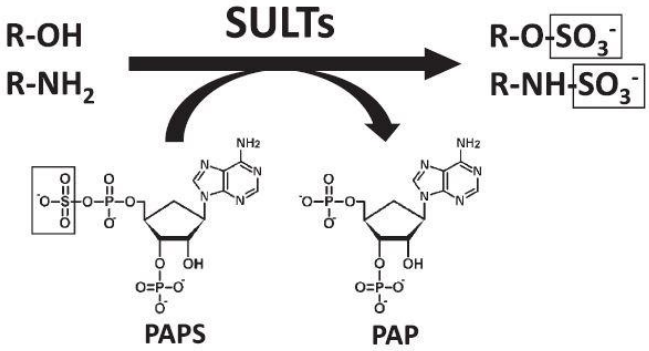

Figure 19: Sulfation reaction (from Masahito et al., 2017)

d. NAT

N-acetyltransferases (NATs) gather only two isoenzymes, NAT1 and NAT2 (Sim et al., 2013). These enzymes catalyze the transfer of the acetyl group from acetyl-coenzyme A to compounds containing whether an arylamine, hydrazine or hydroxylamin group (Figure 20). NATs are present in the cytosol. NAT2 is mainly expressed in the liver and the gut whereas NAT1 is found in many tissues (Sim et al., 2013). Besides, NATs are highly polymorphic enzymes. They have raised concern since they were found out to be linked with many cancers (Agúndez 2008).

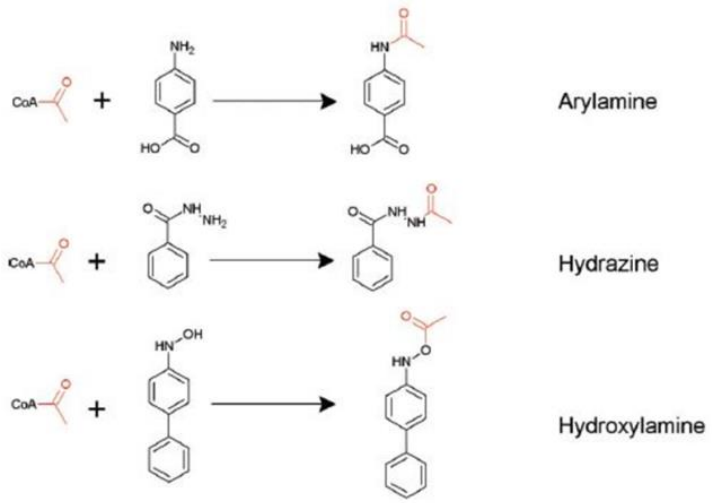

Figure 20: N-acetylation and O-acetylation reactions (from Sim et al., 2013)

e. MT

Methyltransferases gather a large number of enzymes (over 150 described) divided into five structurally distinct families. These families use S-adenosyl-Lmethionine (SAM or Ado-Met) as methyl donor (Figure 21). A large spectrum of compounds is substrate for methyltransferases. Nonetheless, this metabolic pathway is generally minor in the biotransformation of xenobiotics. Methylation plays a key role in neurotransmitters metabolism. Methyltransferases are whether present in the cytosol or bound to membranes. They are expressed in many different tissues (Petra Jančová and Michal Šiller 2012).

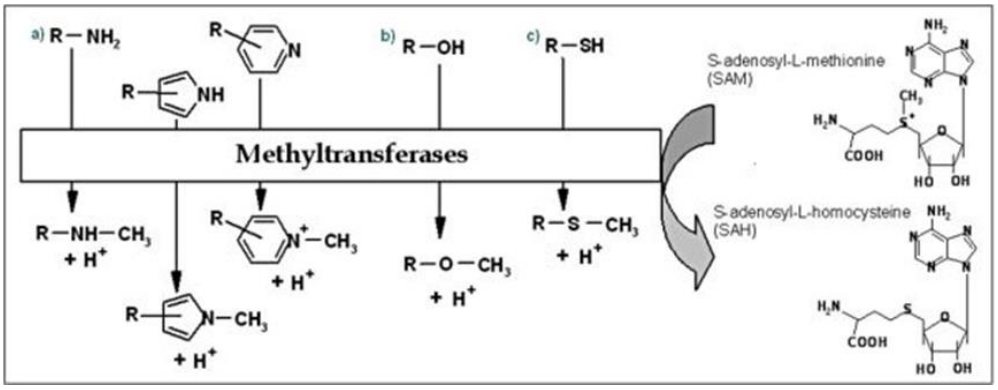

Figure 21: Methylation reaction (from Petra Jančová and Michal Šiller 2012)

f. GST

Glutathione S-transferases (GSTs) gather a wide number of enzymes divided into three distinct superfamilies: cytosolic or mitochondrial GSTs which are further divided into eight different classes (alpha, kappa, mu, omega, pi, sigma, theta and zeta) and microsomal GSTs which include six members (Mohana and Achary 2017). They play a great role in protecting macromolecules from attack by reactive electrophiles. These enzymes catalyze the addition of glutathione (GSH) to compounds (Figure 22). GSTs exhibit a large tissue distribution (Mohana and Achary 2017, Townsend and Tew 2003). Besides, GSTs constitute a key defense mechanism against oxidative stress (Mohana and Achary 2017, Townsend and Tew 2003).

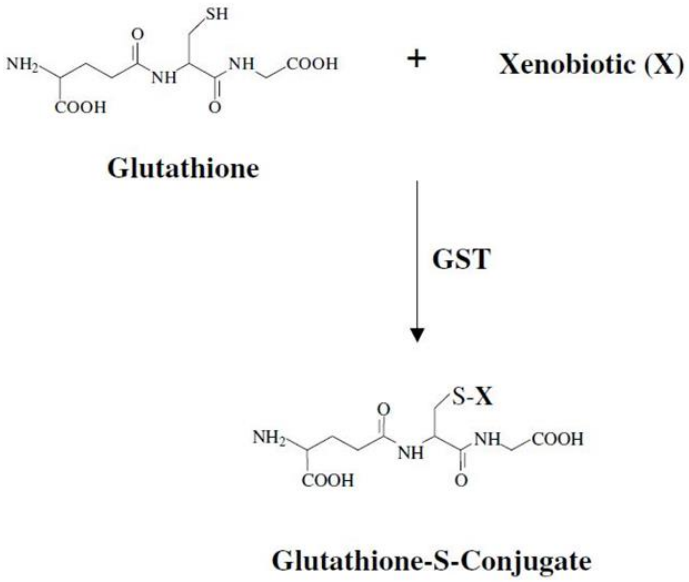

Figure 22: Glutathione conjugation (from Townsend and Tew 2003)

g. AMT

Amino acid transferases pathway is not well-characterized due to the small numbers of known substrates. Enzymes are located in mitochondria. Amino acid conjugation is a two-steps mechanism and involves first formation of a xenobiotic acyl-CoA thioester that is then conjugated principally with glycine (Figure 23). Xenobiotics containing a carboxylic acid group are more likely to undergo amino acid conjugation. Amino acid transferases are principally found in the liver and the kidney (Petra Jančová and Michal Šiller 2012).

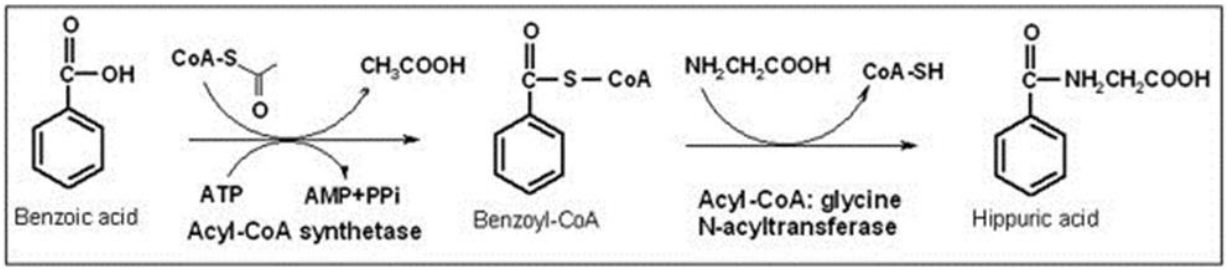

Figure 23: Glycine conjugation on benzoic acid (from Petra Jančová and Michal Šiller 2012)

4. Metabolic bioactivation

Although the role of XME is to detoxify xenobiotics, it can happen that their action generates highly toxic metabolites. This process is known as metabolic bioactivation. For instance, oxidation reactions generate electrophilic reactive metabolites whereas reduction reactions lead to the formation of free radicals.

Electrophilic metabolites are deficient in electron and therefore display an affinity for nucleophilic molecules such as proteins and nucleic acids. CYP has been shown to generate such intermediates by

converting aromatic compounds into epoxides (Guengerich 2003). Aside epoxides, quinone imines are other class of electrophilic metabolites. Electrophilic metabolites can bind irreversibly by covalent bond to the DNA. This occurs on the amino group of the purine or pyrimidine bases. This alteration can lead to mutation and eventually to cancer. Examples of metabolism-induced DNA alterations include aflatoxin B1, metabolized to a compound that form 8-oxo-guanine adducts leading to liver tumors (Wild and Turner 2002) or benzo[a]-pyrene, responsible for lung tumors after bioactivation by CYP1A (Kasala et al., 2015). Apart from nucleic acids, electrophilic metabolites can also bind covalently to the proteins via the amine groups and/or the thiol groups of the amino acid residues (cysteine, lysine, arginine, methionine and histidine). This results in the inactivation of the protein and can lead eventually to toxicity. A well-known example is the metabolic bioactivation of paracetamol. Indeed, in case of paracetamol overdose, N-acetyl-p-benzo-quinone imine (NAPQI) is formed and display high toxicity to liver cells (Albano et al., 1985, Gonzalez 2007).

Free radicals are intermediates that feature a single electron responsible for their high reactivity. They can bind irreversibly to macromolecules (proteins, unsaturated lipids). They are also responsible for the lipid peroxidation phenomenon where a free radical snatches a hydrogen atom out of a polyunsaturated fatty acid forming a radical lipid that further reacts with oxygen to form peroxide radical which, in turn, reacts with another polyunsaturated fatty acid to form a hydroperoxide and a new lipid radical. This scheme propagates along the membrane and induces eventually its disruption. One example of free radical-induced lipid peroxidation is the conversion of carbon tetrachloride (CCl_4) into trichloromethyl radical ($CCl_3^{\bullet}$) (Weber et al., 2003).

Even though the liver is the main place for xenobiotic metabolism, metabolic bioactivation is not only restricted to this organ as some reactive metabolites can be produced in another organ where they will induce damage. For instance, glucuronides conjugates of N-hydroxylamine, initially formed in the liver, migrate to urine where they are hydrolysed to carcinogenic N-hydroxylamines. For example, N-naphthylamine and 4-aminobiphenyl were shown to induce bladder cancer (Zenser et al., 1998).

5. Genetic polymorphism

Xenobiotics can display different effects between two people. One of the main reasons for the inter-individual variation is the genetic polymorphism of XME. The polymorphism results from mutations on genes coding for enzymes detoxification which causes decrease, increase or absence of expression or activity of a protein by various molecular mechanisms (Meyer et Zanger 1997). Genetic polymorphism has been described for many XME as well as transporters: CYP (CYP2C9, 2C19, 2D6, 3A5, etc.), NAT (NAT2), GST (GSTM1, GSTT1, etc.) and P-gp (Martiny and Miteva 2013; Yiannakopoulou, 2013; Hoffmeyer et al., 2000). This finding has led to distinguish subgroups in the population, according to their ability to metabolize certain molecules. For instance, in the case of CYP2D6 whose polymorphism affects the pharmacokinetics of approximately 50% of its drug substrates (Ingelman-Sundberg 2005), four main groups have been described: poor metabolizer, intermediate metabolizer, extensive metabolizer, or ultra-rapid metabolizer. Considering a pharmaceutical drug, the consequences of polymorphism may be manifested by either adverse effects due to the accumulation of the drug in poor metabolizers, or by a decreased or lack of response to treatment in extensive or ultra-rapid metabolizers. Codeine is a prodrug converted into

the active metabolite morphine by the CYP2D6. The absence of the CYP2D6 in 7% of Caucasians leads therefore to inefficiency in analgesic effects. In addition, the population of slow metabolizers is likely to suffer from adverse effects of codeine, mainly nausea (Caraco et al., 1996). Regarding P-gp, about fifty SNPs (Single Nucleotide Polymorphisms) were identified on the MDR1 gene (Hoffmeyer et al., 2000). This polymorphism may affect absorption and tissue concentrations of many substrates of P-gp.

6. Nuclear receptors

a. Classification and structure

The expression level of metabolic enzymes is regulated by several transcription factors. These transcription factors act as xenosensors, meaning that they will trigger the induction of metabolism-associated genes in response to the presence of xenobiotics (Timsit and Negishi 2007). Three main receptors are responsible for the induction of XME: the Pregnane X receptor (PXR), the Constitutive Androstane receptor (CAR) and the Aryl Hydrocarbon receptor (AhR) (Omiecinski et al., 2011, Ramadoss et al., 2005).

PXR and CAR belong to the superfamily of nuclear receptors, especially the type I group (Pavek 2016). This group gathers receptors which form heterodimers with the retinoid X receptor (RXR) inside the nucleus prior to binding to DNA sequence. The group I features also receptors for thyroid hormone (RT), retinoic acid (RAR) and vitamin D (RVD). In 1999, a unified nomenclature system for the nuclear receptor superfamily was established by a committee of experts. PXR and CAR are respectively identified by the code NR1I2 and NR1I3.

Structurally, nuclear receptors feature a well-conserved structure with five different regions, each depicting a specific function (Omiecinski et al., 2011, Küblbeck 2012) (Figure 24):

- The N-terminal domain (A/B) contains the ligand-independent activation zone (activation function 1, AF1). It is also able to bind specific co-factors and features multiple phosphorylation sites that can regulate the transcriptional activity of the receptor.
- The DNA-binding domain (DBD) or C domain is able to target specific gene sequences (response elements). It also plays a role in receptor dimerization.
- The D domain gives protein flexibility and enables for instance the rotation of the ligand binding domain (LBD). It contains also phosphorylation sites that can affect the transcriptional activity of the receptor as well as nuclear localization signals.
- The ligand-binding domain (LBD) or E domain is essential for the interaction of the ligand and contains also a site for the dimerization of the receptor. A special pocket, ligand binding pocket (LBP), is located in the middle of the domain. This pocket is preferably binding hydrophobic compounds. The AF2 sequence constitutes a recognition and interaction site with the various cofactors.
- The C-terminal domain (F) is not present in all receptors and its function is still to be discovered.

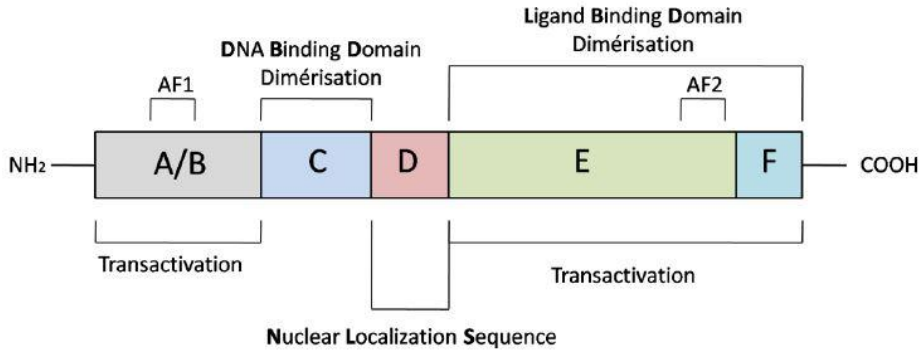

Figure 24: Nuclear receptor structure (inspired from Jenni Küblbeck 2012)

PXR and CAR feature structural specificities which confer them unique properties. They both do not exhibit any N-terminal (A/B) and C-terminal (F) domains. PXR displays a large and flexible LBP which permits the binding of ligands of various sizes and shapes (Timsit and Negishi 2007, Küblbeck 2012). CAR displays an additional α helix in its LBD pocket which allows CAR activation even in the absence of ligand (Xu et al., 2004).

AhR does not belong to the superfamily of nuclear receptors but to the family of basic-helix-loop-helix/Per-Arnt-Sim (bHLH/PAS) transcription factors (Omiecinski et al., 2011). AhR structure share similarities with NR structure (Omiecinski et al., 2011, Küblbeck 2012) (Figure 25). The N-terminal bHLH motif is responsible for DNA binding (basic region, b) and protein-protein interactions (HLH). It also contains the nuclear localization and nuclear export signals (NLS and NES) which mediate the translocation from the cytoplasm to the nucleus. The two PAS domains (A and B) interact with other PAS domain containing proteins, for instance the aryl hydrocarbon receptor nuclear translocator (ARNT) and it also features the ligand binding site. Finally, the C-terminal part contains the large transactivation domain (TAD), consisting of several subregions involved in co-activator recruitment and transactivation/repression.

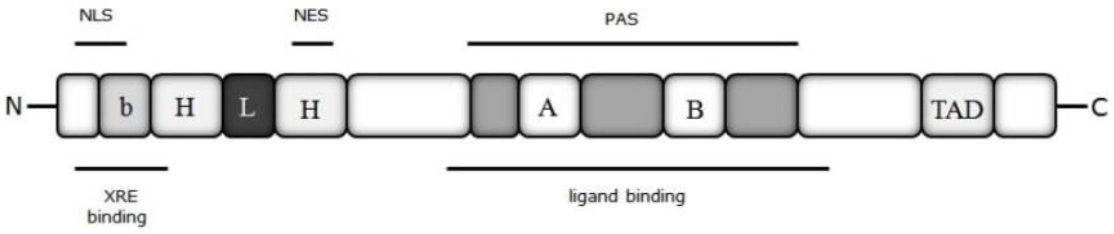

Figure 25: AhR structure (from Jenni Küblbeck 2012)

b. Ligands

AhR, CAR and PXR display a wide variety of ligands including drugs, pesticides, herbal compounds, toxins, hormones, etc. The table 6 sums briefly known ligands for AhR, CAR and PXR.

Table 6: Ligands of AhR, CAR and PXR (from di Masi et al., 2009, Ramadoss et al., 2005, Mani et al., 2013)

Receptor	Ligand	
	Agonist	**Antagonist**
AhR	2,3,7,8-Tetrachlorodibenzo-p-dioxin, Benzo-[a]-pyrene, 3-Methylcholanthrene, Thiabendazole, Omeprazole	6,2',4'-trimethoxyflavone
	Agonist	**Inverse agonist**
CAR	16,17-Androstane-3-ol, CITCO, Di(2-ethylhexyl) phthalate, 17β-Estradiol, Estrone, (5β)-Pregnane-3,20-dione, TCPOBOP	5α-Androstan-3α-ol, 5α-Androst-16-en-3α-ol, Clotrimazole, Meclizine, Progesterone, Testosterone
	Agonist	**Antagonist**
PXR	Artemisinin, Betamethasone, Carbamazepine, 5β-Cholestan-3α,7α,12α-triol, CITCO, Clotrimazole, Colupulone, Corticosterone, Dexamethasone, Dexamethasone-t-butylacetate, 6,16α-Dimethylpregnenolone, 17β-Estradiol, Ferutinine, 17-Hydroxy-pregnenolone, 17-Hydroxy-progesterone, 3α-Hydroxy-5β-pregnane-3,20-dione-methansulphonate, Hyperforin, Indomethacin, Lansoprazole, Lovastatin, Mono(2-ethylhexyl) phthalate, Nifedipine, Omeprazole, Paclitaxel, Pantoprazole, PCN, Pregnenolone, Progesterone, (5β)-Pregnane-3,20-dione, Phenobarbital, Phenytoin, Primaquine, Rabeprazole, Rifampicin, RU486, (-)S20, (+)S20, Schisandrin, SR12813, T0901317, TCPOBOP, Troglitazone, Warfarin, Verapamil, Zearalenone	A792611, Allyl isothiocyanate, Camptothecin, Coumestrol, Ecteinascidin-743, Enilconazole, Fluconazole, Fucoxanthin, Ketoconazole, Metformin, Ochratoxin A, Sesamin, Sulforaphane

Additionally, some molecules have been shown to inhibit CAR or PXR without interacting with the LBP but instead interacting supposedly with the outer surface of receptors. Examples of CAR and PXR inhibitors include sesamin, ketoconazole or leflunomide (Chai et al., 2016).

c. Activation

The activation of CAR, PXR, and AhR has been described through two mechanisms (Mackowiak and Wang 2016):

- a direct activation mechanism where a ligand binds to the receptor and induce a conformational change to its active form (Figure 26).

- an indirect activation mechanism where a cellular signaling is altered and change the phosphorylation status of the receptor without any direct ligand interaction (Figure 27).

If CAR and AhR´s indirect activation mechanism is fully admitted, there is some controversial regarding the indirect activation of PXR.

CAR:

Under normal physiological conditions, CAR is located in the cytoplasm in an inactive state due to a multi-protein retention complex constituted of heat-shock protein (HSP) 90 and CAR cytoplasmic retention protein (CCRP). HSP70 has also been shown to stabilize this complex in the inactive state (Yoshinari et al., 2003, Timsit et al., 2014).

CAR activation mechanism starts by its cellular translocation from the cytoplasm to the nucleus, followed by the heterodimerization with RXR and other transcriptional proteins to stimulate the expression of target genes (Kawamoto et al., 1999, Li et al., 2009).

In the case of a direct activation mechanism, a ligand binds to the receptor and induces a conformational change to its active form which releases the multi-protein retention complex. CAR translocates to the nucleus where it dimerizes with RXR, followed by the binding to the promoter regions of the target genes, XREM (Xenobiotic Responsive Element Module) (Küblbeck 2012).

Indirect activation mechanism of CAR has been particularly highlighted with phenobarbital (PB). Mutoh et al., 2013 showed that PB inhibits the epidermal growth factor receptor (EGFR) to induce indirectly CAR activation in the liver. Upon activation, EGFR signaling pathway leads normally to the inhibition of CAR activation via the ERK1/2-mediated inhibition of CAR dephosphorylation. Following PB binding and inhibition of the EGFR signaling pathway, RACK1 is dephosphorylated, which promotes the dephosphorylation of CAR by PP2A, leading to its nuclear translocation and further activation (Mutoh et al., 2013).

It is noteworthy that CAR was shown to be localized in the nucleus and constitutively active in immortalized cell lines (Kawamoto et al., 1999, Kanno et al., 2005). For instance, it was shown in transfected HepG2 cells that CAR spontaneously accumulates in the nucleus and exhibits constitutive activation of its target genes (Choi et al., 1997; Kawamoto et al., 1999). However, some studies support the hypothesis that nuclear activation is required in CAR-mediated gene regulation. Indeed, pretreatment of primary hepatocytes with PP2A inhibitor OA inhibits PB-induced CAR nuclear translocation but does not repress CAR-mediated activation of reporter genes in HepG2 cells where CAR is localized in the nuclei (Kawamoto et al., 1999; Swales et al., 2005).

PXR:

The cellular localization of PXR is still under discussion. Like CAR, PXR is consistently localized in the nucleus in immortalized cell lines (Saradhi et al., 2005). Nevertheless, such auto-accumulation in the nucleus is not sufficient for PXR to induce transcription of its target genes.

Following ligand binding and conformational change to its active form which releases the multi-protein retention complex, PXR translocates to the nucleus where it dimerizes with RXR and other transcriptional proteins to stimulate the expression of target genes.

Unbound PXR in the nucleus is silenced by corepressors SMRT and NcoR. After binding with an agonist, corepressors are dissociated and coactivators such as SRC-1 and GRIP1 are recruited (di Masi et al., 2009). Then, PXR dimerizes with RXR and binds to the promoter regions of XREM (Orans et al., 2005).

Indirect activation mechanism of PXR is still unclear but several studies reported that compounds-mediated disturbances of some signaling pathways affected the phosphorylation, the nuclear translocation and the activation of PXR. For instance, it was shown that the dephosphorylation by PP1 was essential to xenobiotic-induced nuclear translocation of PXR while phosphorylation by Ca^{2+}/calmodulin dependent protein kinase II led to repression of PXR nuclear translocation (Lichti-Kaiser et al., 2009; Sugatani et al., 2014). Other studies showed that PKC signaling represses PXR activity, potentially by strengthening PXR interaction with corepressor NcoR1, while PKA signaling enhances the recruitment of SRC-1 to PXR, potentiating target gene transcription (Ding and Staudinger, 2005). Finally, Lin et al., 2008 found that inhibitors of Cdk2 induced PXR-mediated gene expression in HepG2 luciferase assays, while activation of the Cdk2 pathway led to repression of PXR-mediated CYP3A4 activation.

AhR:

AhR is sequestered in the cytoplasm by a protein complex containing HSP90, hepatitis B virus protein X-associated protein 2 (XAP2) and p23. Following ligand binding, AhR translocates to the nucleus while still bound to HSP90 (Tsuji et al., 2014; Ikuta et al., 2000; Kazlauskas et al., 2001). Once inside the nucleus, AhR breaks away from HSP90 and heterodimerizes with the aryl hydrocarbon nuclear translocator (ARNT) protein, enabling the AhR:ARNT complex to bind to the xenobiotic response element (XRE) in the regulatory region of target genes which lead to the transcription of the genes (Reisz-Porszasz et al., 1994).

Indirect AhR activation mechanism rose when the known activator omeprazole was found not to directly bind to AhR and instead mediate its effects through indirect mechanisms (Lesca et al., 1995; Daujat et al., 1992). Investigations on the exact omeprazole-mediated mechanism of AhR showed that both genistein, a tyrosine kinase inhibitor, and daidzein, a casein kinase II inhibitor, were able to inhibit the indirect activation of AhR by omeprazole (Backlund et al., 1997). It was found later that c-src kinase plays a role in omeprazole-mediated AhR activation (Backlund et al., 2005). Indeed, indirect activation of AhR by omeprazole was enhanced when c-src signaling was inhibited. Nonetheless, the finding that tyrosine kinase inhibitor Sunitinib was indirectly activating AhR independently of ligand-binding, suggests that the protein tyrosine kinase signaling cascade is probably playing an ambivalent role in the activation of AhR (Maayah et al., 2013).

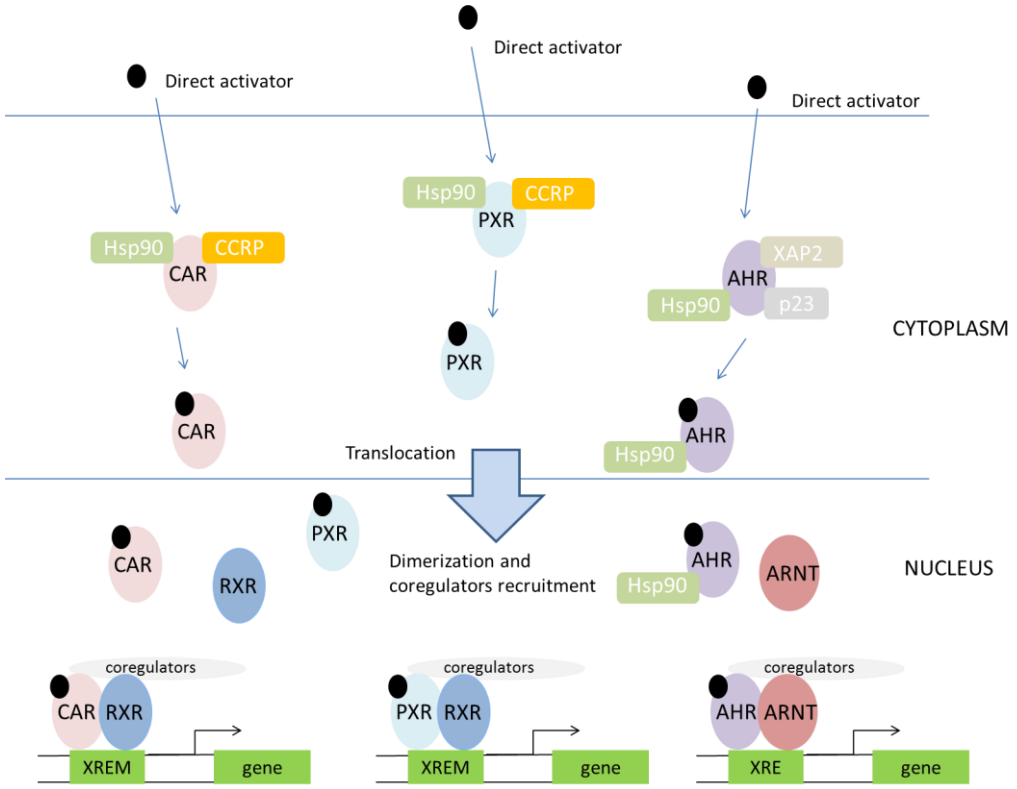

Figure 26: Direct activation of CAR, PXR and AhR (inspired from Mackowiak and Wang 2016)

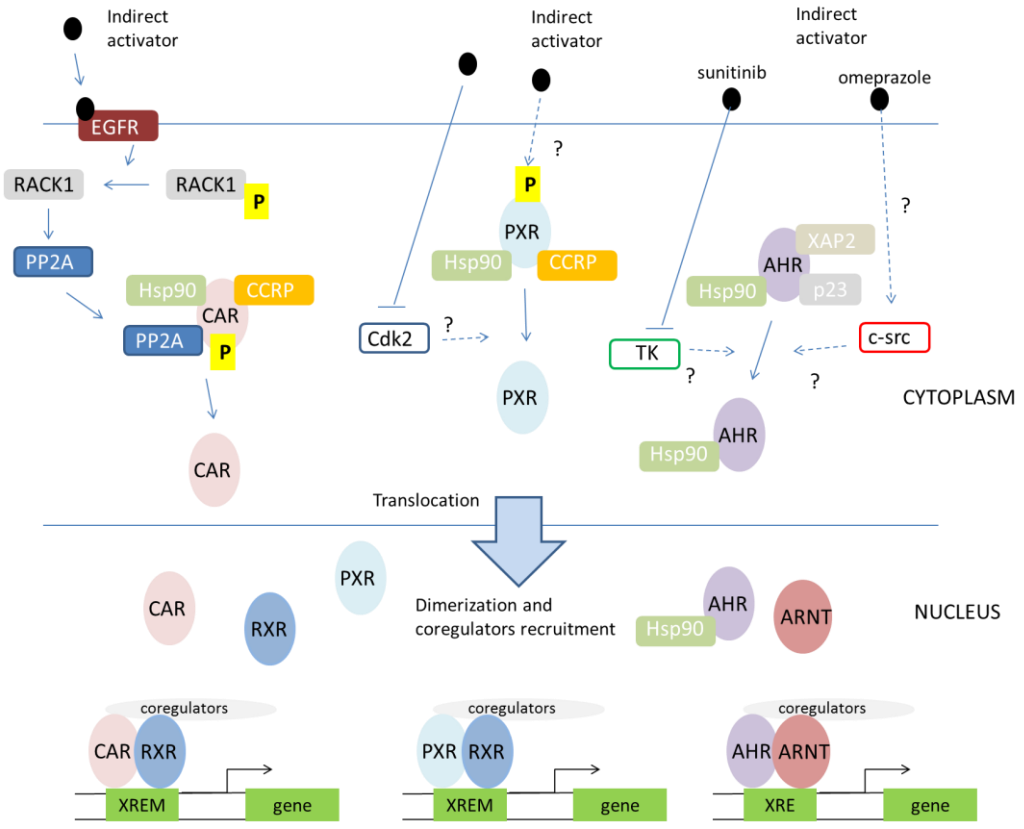

Figure 27: Indirect activation of CAR, PXR and AhR (inspired from Mackowiak and Wang 2016)

d. Protein-protein interaction and signaling crosstalk

Apart from activation mechanisms, nuclear receptors are also under the regulation of protein and signaling crosstalk. Reviewing all of the protein-protein interactions and signaling crosstalks that affect nuclear receptors is beyond the scope of this section. Instead a focus on few key proteins and signaling crosstalks will be made.

It is a long-standing observation that pathological conditions affect drug metabolism by reducing PXR and CAR activities. For instance, CYP3A4 expression is suppressed by inflammation due to interference of NF-κB with PXR's transactivation function. Indeed, the p65 subunit of NF-κB was found to disrupt DNA binding of the PXR/RXRα complex on the CYP3A4 gene promoter region (Gu et al., 2006). Additionally, the interleukin 6 (IL-6) was shown to specifically inhibit RIF- and PB-mediated induction of the CYP2B6, CYP2C8/9, and CYP3A4 genes. This was due to the IL-6-dependent repression of PXR and CAR mRNA levels (Pascussi et al., 2000). Besides, hepatic steatosis leads to reduced PXR and CAR activity through SREBP-1-mediated inhibition of interaction between coactivator and CAR or PXR (Roth et al., 2008).

Forkhead box protein O1 (FoxO1) is a transcription factor that plays important roles in regulating gluconeogenesis by insulin signaling. Kodama et al., 2004 showed that FoxO1 binds directly to CAR and PXR to promote CYP3A4 expression (Kodama et al., 2004).

Posttranslational modifications have also been reported to play a role in nuclear receptors activity. For instance, acetylation status of PXR was shown to play a role in PXR transcriptional activity. Indeed, PXR was shown to be acetylated in its unstimulated state, and deacetylated in response to RIF (Pasquel et al., 2016). PXR was shown to be directly acetylated by p300. The authors also demonstrated that PXR deacetylation was mediated partly by sirtuin 1 (SIRT1), resulting in activation of PXR's lipogenic functions in a ligand-independent manner.

Finally, *in vitro* studies showed that the mRNAs for many ADME related genes were targeted directly by one or more miRNAs (Rieger et al., 2013; Yu et al., 2012). For instance, miR-27b directly regulates CYP1B1 and CYP3A4 expression, PXR expression is regulated by miR-148a, the MDR1 transporter by miR-45. Nonetheless, these miRNA-dependent regulations must be confirmed *in vivo*.

e. Target genes

The target genes of PXR, CAR and AhR include not only Phase I enzymes such as CYP but also Phase II transferases as well as many transporters involved in both uptake and efflux of drugs (Table 7). If they are able to regulate a common set of genes, certain genes are preferentially under the regulation of one specific xenosensor: for example CYP3A4 is preferably regulated by PXR, CYP1A1 and 1A2 by AhR whereas CYP2B6 is the prototypical gene targeted by CAR.

Table 7: Target genes of AhR, CAR and PXR (from Beischlag et al., 2008, Jenni Küblbeck 2012, Wang et al., 2012, Chen et al., 2012)

Class	Gene	Receptor
Phase I drug metabolism enzymes	CYP1A1/2	**AhR**/CAR
	CYP1B1	AhR
	CYP2A4	CAR
	CYP2A6	PXR
	CYP2B1/2/6	**CAR**/PXR
	CYP2B10	**PXR**/CAR
	CYP2C8/9/19	**PXR**/CAR
	CYP2C29/37	CAR
	CYP2S1	AhR
	CYP3A2	PXR
	CYP3A4/5/7	**PXR**/CAR
	CYP3A11	**PXR**/CAR
	CYP3A23	PXR
	CYP4F12	PXR
	CYP7A1	PXR
	ALDH1	**PXR**/CAR
	AKR1C1/2	PXR
	AKR1B7	**PXR**/CAR
Phase II drug metabolism enzymes	UGT1A1	**CAR**/PXR/AhR
	UGT1A3/4	PXR
	UGT1A6/9	**PXR**/CAR
	UGT2B1	CAR
	UGT2B5	PXR
	GSTA1/2	**PXR**/CAR
	GSTM1	**PXR**/CAR
	SULT1A1	**PXR**/CAR
	SULT1A2	CAR
	SULT1B1	PXR
	SULT1E1	**PXR**/CAR
	SULT2A1	PXR
	NAT1	CAR
Drug transporters	MDR1	**PXR**/CAR/AhR
	MRP1	CAR
	MRP2/3	**PXR**/CAR
	MRP4	CAR
	SLCO1A4	PXR
	BCRP	AhR
	OATP1A2	PXR
	OATP1B3	CAR

III. In vitro models

1. Intestine

The study of substances absorption across the intestinal barrier can be performed with several intestinal cell lines. The Table 8 sums some of the most used cell lines. The Caco-2 cells have been extensively used because they can differentiate into enterocyte-like cells displaying tight junctions, microvilli on the apical side and functional enzymes (Hidalgo et al., 1989, Sambuy et al., 2005). After seeding the cells on Transwell microplates, the passage from the apical to the basolateral compartment can be measured. Other cell lines such as HT29-MTX or MDCKII have been also used complementary to predict the absorption of drugs or to investigate the role of a specific transporter (Behrens et al., 2001, Pontiers et al., 2001, Ehlers et al., 2014). If the Caco-2 cells represent a suitable model, they still don´t fully mimic the complexity of the human intestinal barrier. To gain even better predictability, several models of co-culture of intestinal cells were proposed such as a co-culture of Caco-2 and HT29-MTX cells (Béduneau et al., 2014).

Table 8: Main cell lines used for *in vitro* toxicokinetic studies on intestinal absorption

Cell line	Cell type	Main features	Metabolic status	Reference
Caco-2/TC7*	enterocytes	After differentiation, polarized cells with brush border (microvilli) on apical side. Tight junctions	Low CYP, high Transporters (ie P-gp)	Sambuy et al., 2005
HT29-MTX	goblet cells	Secretion of mucine	No P-gp expression	Pontiers et al., 2001
MDCKII	canine epithelial cells	Widely used for permeability assays after transfection of P-gp for instance	No CYP, no UGTs	Ehlers et al., 2004

*several clones exist with different relevancies in regard to drug passage investigation. The clone TC7 is the most suitable for such purpose

When intestinal toxicity is investigated, the Caco-2 and HT29-MTX are rather used because of their relevance as human enterocytes-like or mucus cells and also due to an easy maintenance.

2. Liver

The choice of suitable *in vitro* model depends largely on the aim of the study. For instance, investigation of drug metabolism is mostly performed using human liver microsomes or CYP recombinants whereas CYP induction studies rely on the use of cell lines. Besides, for toxicity purposes, various hepatic cell models are currently available and used (Table 9). It is noteworthy, that for many years, *in vitro* hepatotoxicity has been assessed using cell lines with low metabolic competence such as HepG2 cells (Gomez-Lechon et al., 2017). Nearly 10 years ago, the establishement of the HepaRG cell line has offered a relevant alternative to human hepatocytes

(Guillouzo et al., 2007, Andersson et al., 2012). If primary cells are still considered as the gold standard, they feature limited supply, rapid decline of liver-specific functions and also donor variability (Dvorak 2016).

Table 9: Main *in vitro* hepatic cell lines used in toxicology (from Jenni Küblbeck 2012)

Cell model	Main features	Metabolic status
Human hepatocytes	Considered as the gold standard	Depends on the donor, all enzymes presumably present
HepaRG	Differentiated cells showing hepatic morphology. The closest cell line in terms of human metabolic content. Has been used for studies on metabolism, uptake as well as toxicity.	High phase I and phase II enzyme expression, efficiently inducible
HepG2	Adherent and epithelial-like. Secretes plasma proteins (e.g. albumin). High variability in gene expression depending on cell culture conditions	Low CYP, poorly inducible
Hep3B	Adherent and epithelial-like. Secrete plasma proteins (e.g. albumin). Mainly used to study apoptosis and toxicity	Poor CYP (except for CYP1A1). Higher phase II enzyme activity than in HepG2.
BC2	Differentiates at confluency and remains differentiated for several weeks. Mainly used in (repeated) toxicity studies	Proper CYP and phase II enzymes, efficiently inducible
HuH7	Secretes plasma proteins (e.g. AFP, albumin). Used in various studies related to hepatitis virus C infection, hepatotoxicity and gene regulation	Low CYP, poorly inducible

Chapter 3: Lipophilic phycotoxins

I. Okadaic acid and analogues

1. Production by phytoplankton

Intoxications due to seafood contaminated with OA and analogues have been first reported in the Netherlands and in Japan in the 1970´s, followed by a French outbreak in 1983-1984 (James et al., 2010, Reguera et al., 2014). In Europe, OA is usually the main toxin involved in DSP whereas DTX-1 prevails in Japan. In humans, symptoms such as diarrhea, nausea, vomiting and abdominal pain are displayed. Yasumoto et al., 1985 were the first to discover one of the causative organisms *Dinophysis fortii*. Since, numerous *Dinophysis* species have been identified to produce OA toxin group (Reguera et al., 2014). Additionally, some *Prorocentrum* have been identified as productive species (Granade et al., 1992). *Prorocentrum* species are benthic whereas *Dinophysis* species are pelagic.

OA and its analogues are mainly found in mussels, oysters, clams, cockles and sometimes in crustaceans (The EFSA Journal (2008) 589, Torgersen et al., 2005).

2. Structure

The chemical structure of OA and its analogue DTX-1 was fully elucidated by Tachibana et al., 1981 and Murata et al., 1982. DTX-2 structure was only determined in 1992 by Hu et al. OA and DTX-2 are isomers. Additionally, OA and its analogues can undergo shellfish metabolism leading to a variety of acylated derivatives that have been collectively named DTX-3 (Yasumoto et al., 1985).

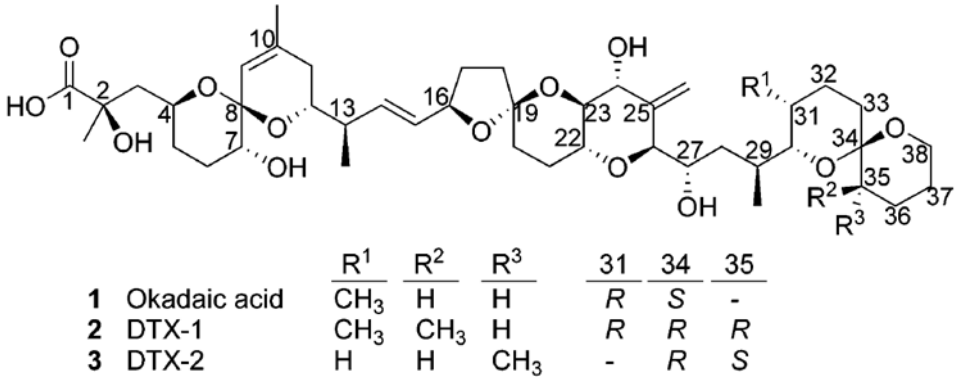

		R^1	R^2	R^3	31	34	35
1	Okadaic acid	CH_3	H	H	*R*	*S*	-
2	DTX-1	CH_3	CH_3	H	*R*	*R*	*R*
3	DTX-2	H	H	CH_3	-	*R*	*S*

Figure 28: Chemical structure of OA, DTX-1 and DTX-2 (from Larsen et al., 2007)

3. *In vivo* toxicity

a. Lethal doses in rodents

Multiple studies have been conducted to determine acute toxicity of OA in rodents. OA displays a high toxicity following i.p. injection with a LD_{50} around 200 µg/kg while a LD_{50} between 400 and 1000 µg/kg were reported by oral administration (Ito et al., 2002, Tubaro et al., 2003). More recently, Aune et al., 2012 estimated a precise LD_{50} of 880 µg/kg by oral administration (Table 10). Although they feature very similar chemical structure, DTXs have been shown to induce toxic effects following i.p administration with a different potency, DTX-1 being the most toxic compound with a median lethal dose estimated at 160 µg/kg (Murata et al., 1982) and DTX-2 the least toxic with a median

lethal dose estimated at 352 µg/kg (Aune et al., 2007). Ogino et al., (1997) reported an oral lethal dose of DTX-1 at approximately 300 µg/kg. Data for DTX-1 should be taken with caution as the studies are limited and old.

Table 10: Acute toxicity of OA in mice

Toxin	Strain/gender	Mode of administration	Parameter	Acute toxicity	Reference
OA	?	Intra-periteonal	LD_{50}	192 µg/kg	Tachibana et al., 1981
OA	ddY/male	Intra-periteonal	MLD	3.6 µg/kg	Yanagi et al., 1989
OA	HLA: (SW)BR/female	Intra-periteonal	LD_{50}	210 µg/kg	Dickey et al., 1990
OA	CD-1/female	Intra-periteonal	LD_{50}	225 µg/kg (95%, 176-275)	Tubaro et al., 2003
OA	CD-1/female	Intra-periteonal	LD_{50}	204 µg/kg	Aune et al., 2007
OA	ICR/male	Gavage	LD_{50}	400 µg/kg	Ito et al., 2002
OA	CD-1/female	Gavage	LD_{50}	1000-2000 µg/kg	Tubaro et al., 2003
OA	Swiss/female	Gavage	LD	600 µg/kg	Le Hégarat et al., 2006
OA	NMRI/female	Gavage	LD_{50}	880 µg/kg	Aune et al., 2012

b. Effects on the intestine

Mice treated with i.p. injections of OA (200–400 µg/kg) showed hyperemia of the duodenum and the jejunum as well as an accumulation of pale fluid after 24 h (Tubaro et al., 2003). Histological examination revealed epithelium erosions, lamina propria congestion as well as shortening and flattening of villi in the duodenum and/or the jejunum.

Oral administration features similar characteristics as i.p. injections. After oral administration of 150 µg/kg to mice, erosion and hypersecretion of the epithelium was observed as well as eroded villi with disconnected cells and components of edema floating in the lumen (Ito et al., 2002).

Tubaro et al., 2003 reported congestion of the small intestine after 24 h oral treatment of 1 or 2 mg/kg of OA. Moreover, the small intestine was distended and contained a pale or bloody fluid in its

lumen. An accumulation of pale fluid was observed also in the large intestine with 2 mg/kg of OA. Histological examination showed a degeneration of the duodenal villi, consisting in areas of moderate erosion of the epithelium, congestion of lamina propria and shortening of villi. In a short term study (7 days oral daily administration), the same team showed that the small and large intestine of mice were hyperaemic and contained a pale and bloody fluid in response to oral administration of 1 mg/kg/day of OA (Tubaro et al., 2004).

Aune et al., 2012 investigated the effects of orally administrated doses of OA (from 660 up to 1140 µg/kg) in mice. After 24 h, they reported a dilatation of the small intestine and the contents were more watery than normal. In the duodenum, the villi were slightly shortened and blunt with signs of exfoliation of epithelium. Infiltration of neutrophils was seen in the lamina propria and the jejunum featured severe atrophy of the villi.

c. Effects on the liver

Tubaro et al., 2003 reported the presence of dark areas in the liver of mice treated by i.p. injection of OA (200–400 µg/kg), with death occurring between 2 and 12 h. Moreover, histological examination revealed isolated cell necrosis and/or vacuolisation of hepatocytes. Slight acute inflammation was also reported.

Similarly to what they found by i.p. injection, Tubaro et al., 2003 reported dark areas on the liver of mice orally treated with 1 or 2 mg/kg of OA for 24 h. Histological examination showed degenerative modifications of hepatocytes such as slight-moderate cytoplasmic vacuolation. In a short term study (7 days oral daily administration), Tubaro et al., 2004 reported dark areas on the liver of mice treated 1 mg/kg/day of OA. A marked atrophy of the hepatocytes was also observed.

After 24 h of an oral administration of 700 µg OA /kg to mice, Vieira et al., 2013 reported important liver injuries. Aggregates of necrotic hepatocytes were observed accompanied with dilation and a congestion of sinusoids. Neighboring hepatocytes showed cellular swelling, lipid vacuoles of different sizes and either pleomorphic or pyknotic nuclei. Additionally, scant polymorphonuclear inflammatory infiltrates were seen.

Aune et al., 2012 reported only a change in the colour of the liver (varying from pale to dark and blood filled), but without microscopic modifications after 24 h of oral administration of 660 up to 1140 µg OA/kg in mice.

Le Hégarat et al., 2006 reported histopathological injuries in the liver of mice treated by gavage from 115 µg/kg OA. Apoptotic cells were also reported in the liver for both 115 and 230 µg/kg doses at 24 and 36 h.

With a lower oral dose of 150 µg/kg to mice, the liver did not show any alterations (Ito et al., 2002).

4. *In vitro* toxicity

a. Mechanism of action

It was first demonstrated that OA inhibited myosin phosphatases (Takai et al., 1987) before showing that OA was specifically targeting protein serine/threonine phosphastases PP1 and PP2A (Bialojan and Takai 1988). This mode of action was later confirmed by different studies (Haystead et al., 1989; Holmes et al., 1990). Today, OA is considered as one of the most potent protein phosphatase inhibitor with IC_{50} between 0.1 and 1 nM for PP2A and IC_{50} between 10 and 100 nM for PP1 (Cruz et al., 2013) and is widespread used in research to confirm the involvement of PP2A in the regulation of a pathway.

b. Toxicological effects

Due to the importance of protein phosphorylation status in cell signaling, OA-phosphatases inhibition can disturb many cellular pathways. OA main toxic effects feature apoptosis, cytoskeleton disruption, cell cycle alteration, inflammation/immunotoxicity and genotoxicity.

Apoptosis induction is certainly the most documented hallmark of OA toxicity. OA was shown to induce apoptosis in intestinal cells (Lago et al., 2005, Ferron et al., 2014), neuronal cells (Leira et al., 2001, Cabado et al., 2004), hepatic cells (Ferron et al., 2016), leukemia cells (Riordan et al., 1998), etc. The caspase pathway was often the mechanism involved in OA-induced apoptosis (Lago et al., 2005, Rossini et al., 2001).

OA was shown to alter cytoskeleton in different cell lines. OA induced disturbance of keratin and tubulin filaments in intestinal and hepatic cells (Berven et al., 2001). Additionally, OA induced changes in the organization of F-actin in intestinal cells (Fiorentini et al., 1996) or fibroblasts (Diogène et al., 1995). Human blood cells and neuronal cells are also subjected to cytoskeletal disorganization (Leira et al., 2001, Valdiglesias et al., 2011). Opsahl et al., 2013 showed that OA regulated the phosphorylation status and location of proteins associated with the actin cytoskeleton, microtubules and cell adhesion structures in SH-SY5Y cells.

OA was shown to induce cell cycle alterations, particularly mitotic arrest, in different cell types: leukemia cells (Lerga et al., 1999), intestinal cells (Ferron et al., 2014), lymphocytes (Gotoh et al., 1995), fibroblasts (Yamashita et al., 1990), ovary cells (Le Hégarat et al., 2006) and neuronal cells (Valdiglesias et al., 2011). These effects are likely due to the imbalance in phosphorylation/dephosphorylation of cell cycle control proteins. In addition, Lerga et al., 1999 showed that the mitotic arrest found in OA-treated cells was due to PP2A inhibition as PP1/PP2A activity is required for metaphase–anaphase transition (Wardlaw 2010, Sivakumar and Gorbsky 2017).

OA was shown to induce inflammation in human monocytes. Indeed low doses of OA increased IL-1 production (Hokama et al., 1989). OA was also shown to increase the production of pro-inflammatory cytokines such as IL-8 in HL-60 cells (human myelocytes) (Sonoda et al., 1997). Additionally, Ferron et al., 2014 showed that OA induced translocation of NF-κB from cytoplasm to nucleus in intestinal cells. NF-kB is a transcription factor which regulates the transcription of a variety of genes involved in the inflammatory response (Schottelius and Baldwin, 1999). Martín-López et al.,

2012 showed that low doses of OA induced down-regulation of T cell receptor expression levels in T lymphocytic EL-4 cells. OA-mediated inflammatory cell activation has been observed also *in vivo* in spleen and thymus with recruitment of granulocytes, a higher number of active macrophages and an increase of immunoreactivity to cytokines (Franchinia et al., 2005).

Genotoxic effects of OA are well-documented. Fessard et al., 1996 showed that exposure to low nanomolar doses of OA induced DNA adducts in hamster fibroblasts and human keratinocytes. OA was also shown to induce the formation of micronuclei in the Caco-2 intestinal cell line, in mice gut cells and in CHO-K1 cells (Carvalho et al., 2006, Le Hégarat et al., 2006). Furthermore, Valdiglesias et al., 2011 and Ferron et al 2014 showed the induction of double strand breaks, evidenced by the phosphorylation of histone H2AX in human neuroblastoma SHSY5Y and hepatic HepG2 and intestinal Caco2 cell lines, although this marker was rather due to apoptosis than to a genotoxic effect (Ferron et al. 2014).

Finally, several medium-term two-stage carcinogenesis studies both *in vitro* and *in vivo* showed that OA is a tumor promoter (Fujiki et al., 1988; Suganuma et al., 1988; Messner et al., 2001). This tumor promoting activity was suggested to be mediated through by the transcription factor AP-1 (Peng et al., 1997; Thompson et al., 2002) and the TNFalpha (Suganuma et al., 1999 and Suganuma et al., 2002).

5. ADME

a. Intestinal absorption

In vivo studies suggest that OA can be absorbed across the intestinal barrier as it distributes into several systemic tissues after oral administration (Matias et al., 1999; Le Hégarat et al., 2006). *In vitro*, OA has been shown to cross poorly Caco-2 monolayers. Indeed, after 24h incubation, only 2% of the initial 200 nM dose was detected in the basolateral chamber (Ehlers et al., 2011). Moreover, when assessing OA transport from the basolateral to the apical side, it was found that OA was excreted to a certain extent (up to 18% for 200 nM OA). Fernandez et al., 2014 confirmed that OA (up to 100 nM) were almost unable to cross the Caco-2 cell monolayer after 24h exposure. A similar behavior was noticed for DTX1 and DTX2.

Concerning the role of transporters, first evidence of P-gp involvement was given by Chambers et al., 1993 who showed that overexpressing P-gp human KB-V1 cells were less sensitive to OA cytotoxicity than the parental KB-3 cells. More recently, transport studies were conducted with MDCK transfected cell monolayers over-expressing human P-gp (Ehlers et al., 2014). Compared to wild type MDCK cells, the efflux of OA was enhanced over time. In the same paper, the involvement of P-gp was also confirmed using P-gp inhibitor cyclosporine A on Caco-2 cells monolayers. In regard to cell uptake, the role of OATP1B3 (and possibly OATP1B1) was demonstrated by Ikema et al., 2015 using stably transfected HEK 293 cells. Indeed, OA was found to be more toxic and PP2A activity more inhibited in OATP1B3 transfected cells in comparison to wild type HEK 293 cells.

b. Metabolism

Using CYP recombinants, four hydroxylated metabolites were detected after 30 min incubation with 50 µM OA (Guo et al., 2010). These metabolites were specifically generated by the CYP3A4 and

CYP3A5. The same four metabolites were also detected using human liver microsomes after 30 min incubation with 5 µM OA. These hydroxylation reactions were totally inhibited with 10 µM ketoconazole (CYP3A inhibitor).

Using rat S9 fractions, Kittler et al., 2010 confirmed the four metabolites previously reported and detected 5 others metabolites which are isomers of mono-hydroxylated metabolites after 3 h incubation with 310 nM OA. No glutathione and glucuronides conjugates were observed.

The role of CYP3A4 was also confirmed by Kittler et al., 2014 in HepaRG cells. Using the CYP3A4 inhibitor ketoconazole, they showed an increased cytotoxicity as well as the absence of hydroxylated metabolites. Additionally, Ferron et al., 2016 also showed increased toxicity of OA in HepaRG cells when CYP3A4 was inhibited. Moreover, they showed that OA induced PXR luciferase activity in transfected HepG2 cells but no induction of the main CYP (1A2, 2C9, 2C19 and 3A4) was observed in HepaRG cells following 72 h of incubation with 4 nM OA.

Metabolic bioactivation of OA was reported in several studies. Le Hégarat et al., 2006 reported an increased induction of micronucleus (MN) by OA in CHO-K1 cells treated with rat S9. Using HepG2 transformants, Hashizume et al., 2009 showed that genotoxic effects of OA (induction of MN) was significantly induced in transformants expressing CYP1A2 compared with the other CYP isoforms or the HepG2 control cells. The role of CYP1A2 in OA metabolic bioactivation was confirmed when MN induction was suppressed by treatment with a CYP1A2 specific inhibitor and with siRNA CYP1A2.

In a comparative human-rat metabolism study, Kolrep et al., 2016 showed that human recombinant CYP3A enzymes led to the formation of hydroxylated metabolites, associated with decreased cytotoxicity in HepG2 cells. Detoxification by rat Cyp3a1 was lower compared to human CYP3A and bioactivation of OA by Cyp3a2 was even observed. However, human and rat CYP1A2 seemed to bioactivate OA into cytotoxic intermediates.

II. Pectenotoxins

1. Production by phytoplankton

Pectenotoxin-1 and -2 were simultaneously discovered in contaminated scallops *Pactinopecten yessoensis* in Japan (Yasumoto et al., 1985). Later, different analogues (resulting mostly of shellfish metabolism) have been described. PTX-2 is produced by several species of *Dinophysis*: *D. fortii*, *D. acuta* , *D. norvegica*, *D. acuminata*, *D. caudata* and *D. rotundata* (Draisci et al., 1996, Suzuki et al., 2003, MacKenzie et al., 2005, Fernández et al., 2006). PTX-2 is mainly found in mussels, oysters, clams and scallops (the EFSA Journal, 2009).

2. Structure

The chemical structure of PTX-2 and its analogues features polyether lactones, also called macrolide. PTX-1 and PTX-4 are in fact hydroxylated PTX-2. The form seco-acid of PTX-2 results from the metabolism of shellfish where hydrolases open the cycle.

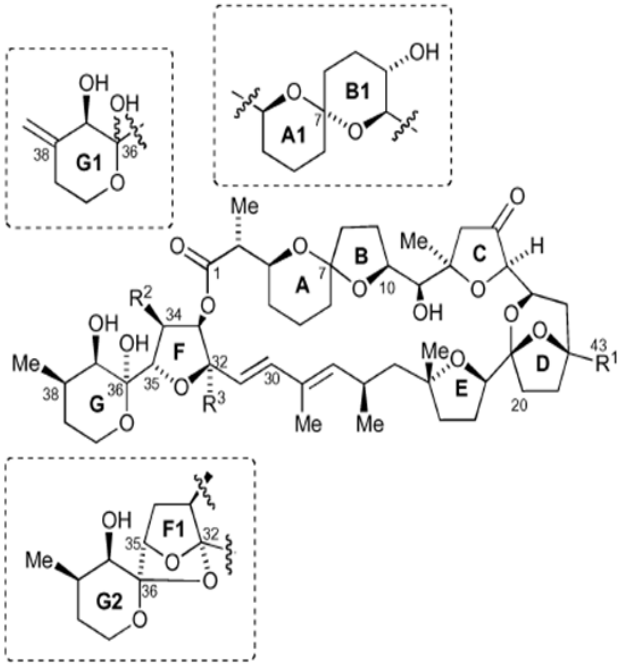

		R^1	R^2	R^3	C-7	C-36
1	PTX1	CH_2OH	H	H	*R*	α-OH
2	PTX2	CH_3	H	H	*R*	α-OH
3	PTX3	CHO	H	H	*R*	α-OH
4	PTX4	CH_2OH	H	H	*S*	α-OH
5	PTX6	COOH	H	H	*R*	α-OH
6	PTX7	COOH	H	H	*S*	α-OH
7	PTX11	CH_3	OH	H	*R*	α-OH
	Structure	***A1/B1/G***				
8	PTX8	CH_2OH	H	H	*S*	α-OH
9	PTX9	COOH	H	H	*S*	α-OH
	Structure	***A/B/G1***				
10	36*S*-PTX12	CH_3	H	H	*R*	α-OH
11	36*R*-PTX12	CH_3	H	H	*R*	β-OH
12	PTX13	CH_3	H	OH	*R*	α-OH
	Structure	***A/B/G2/F1***				
13	PTX14	CH_3	-	-	*R*	–
	Unidentified					
	PTX5	unidentified				
	PTX10	unidentified				

Figure 29: Chemical structure of PTX-2 and its analogues (from Halim and Brimble 2006)

3. *In vivo* toxicity

a. Lethal doses in rodents

First studies on acute toxicity showed a minimum lethal dose (MLD) of 260 µg/kg after i.p injection in mice (Yasumoto et al., 1985). Two ip LD_{50} were described: 411 µg/kg (Yoon and Kim, 1997) and 219 µg/kg (Miles et al., 2004), and the difference could be due to the mice strain or to the purification level of the compound. The oral toxicity of PTX-2 was scarcely investigated and discrepancies exist between studies. Ogino et al., 1997 estimated an oral LD_{50} around 200 µg/kg whereas Miles et al., 2004 reported no mortality with doses up to 5000 µg/kg. Table 11 sums the actual knowledge.

Table 11: Acute toxicities of PTX-2 in mice

Toxin	Strain/gender	Mode of administration	Parameter	Acute toxicity	Reference
PTX-2	?	Intra-periteonal	MLD	260 µg/kg	Yasumoto et al., 1985
PTX-2	?	Intra-periteonal	MLD	230 µg/kg	Yasumoto et al., 1988
PTX-2	ICR/male	Intra-periteonal	LD_{50}	411 µg/kg	Yoon et Kim 1997
PTX-2	Swiss mice/female	Intra-periteonal	LD_{50}	219 µg/kg	Miles et al., 2004

PTX-2	ddY/male	Oral	LD_{50}	200 µg/kg	Ogino et al., 1997
PTX-2	Swiss mice/female	Gavage	LD_{50}	> 5 mg/kg	Miles et al., 2004

Regarding analogues, no death was recorded in mice treated with a maximum dose of 1.6mg/kg PTX-2 seco acid (Burgess 2003). Besides, PTX-2 seco acid or 7-epi-PTX-2 seco acid did not exert toxic changes in mice injected intraperitoneally at a dose of 5000 µg/kg (Miles et al., 2006).

b. Effects on the intestine

Neither Yasumoto et al., 1985 nor Yoon et Kim 1997 nor Miles et al., 2004 reported particular toxic effects on the intestine after i.p injections of PTX-2 to mice.

Nonetheless, several teams reported effects following oral administration to rodents. Ishige et al. (1988) observed swollen intestine filled with fluid after oral administration of 250 µg/kg but only one single mouse was tested. Vacuole formation was observed in the epithelial cells of the small intestine. These effects were confirmed by Ito (2006) after administration of a single dose of 400 µg/kg while no effects were observed at 300 µg/kg.

In another oral study, PTX-2 caused intestinal fluid secretion in mice as well as in rats at 500 and 1500 µg/kg, respectively (Ito et al., 2008). The intestines of mice depicted a swelling appearance. Slight changes in lamina propria (presence of vacuoles) were also observed and gaps with accompanying debris were depicted at the surface of the villi top. Besides, PTX-6 was found to induce erosion of the villi of jejunum–ileum following gavage to rats with 2 mg/kg (Ito et al., 2008).

Histological examination of duodenum and jejunum revealed no abnormalities after PTX-2 seco acid or 7-epi-PTX-2 seco acid treatment in mice (5000 µg/kg i.p. injection) (Miles et al., 2006).

c. Effects on the liver

Discrepancies exist in regard to the toxic effects of PTX-2 on the liver. No particular hepatic toxicity was reported after i.p. (up to 325 µg/kg) administration of PTX-2 in rodents (Miles et al., 2004). Similarly, a repeated i.p. administration of low doses of PTX-2 (20 or 100 µg/kg) in mice over one or two weeks did not cause any changes in the liver (Yoon and Kim., 1997). However, Munday 2008 reported hepatic congestion after 250 µg PTX2/kg i.p. in mice.

After gavage, hyaline droplets and vacuolar degeneration were observed in liver of mice treated at 1000 µg/kg and above (Ishige et al., 1988). However, Miles et al., 2004 reported no particular hepatic toxicity after oral (5000 µg/kg) administration of PTX-2 in rodents. Besides, PTX-6 was found to induce bleeding and membrane vacuolization in mice 6 h after 500 µg/kg i.p. treatment (Ito et al., 2008).

No abnormalities were reported in liver after i.p administration of 5000 µg/kg PTX-2 seco acid or 7-epi-PTX-2 seco acid to mice (Miles et al., 2006).

4. *In vitro* toxicity

a. Mechanism of action

PTX-2 was shown to interact with the actin cytoskeleton. Based on crystallography studies, PTX-2 was shown to form a complex with F-actin located in the growing (+) barbed end of the filament (Allingham et al., 2007). This interaction prevents the fixation of G-actin and thus stops the elongation of the filament. This mechanism is known as "capping effect". Additionally, PTX-2 was also shown to sequester monomeric G-actin (Hori et al., 1999). Butler et al., 2012 showed that PTX-2 inhibition of actin polymerization was unspecific and affected similarly skeletal muscle actin, smooth muscle actin, cardiac muscle actin, and non-muscle actin (IC_{50} values between 19 and 94 nM). Interestingly, PTX2 seco acid exhibited no inhibitory effects, suggesting a key role of the lactone ring for bioactivity.

b. Toxicological effects

In vitro studies upon toxicity of PTX-2 showed particularly effects towards cell cycle, inflammation, apoptosis and telomerase activity.

PTX-2 was found to induce cell cycle arrest at G2/M phase in different cancer cells (Moon et al., 2008; Shin et al., 2011). Reduced levels of Cdc2 and cyclin B1, increased levels of phospho-histone 3 and increased phosphorylation of Cdc25C were found to be initial events leading to induction of G2/M phase arrest.

Regarding inflammatory effects, Kim et al., 2008 found that PTX-2 inhibited constitutive NF-κB activation and also down-regulated gene expression and protein levels of Cox-2, IAP-1, IAP-2 and XIAP in different leukemia cell lines. This suppression of NF-κB activity was shown to sensitize apoptosis.

PTX-2 was reported to induce apoptosis through different pathways. Shin et al., 2008 observed that PTX-2 induced proteolytic activation of caspases 3, 8 and 9 in hepatic Hep3B cells. They also found out that apoptosis-induced by PTX-2 was associated with the down-regulation of anti-apoptotic Bcl-2 members and IAP family proteins as well as the up-regulation of pro-apoptotic Bax protein. Moon et al., 2008 reported a PTX-2-induced apoptosis through the ERK and JNK pathways in human leukemia cells.

PTX-2 was shown to suppress telomerase activity in human leukemia cells (Kim et al., 2008). This suppression is mediated via reductions in c-Myc and Sp1 activities, which leads to the transcriptional downregulation of human telomerase reverse transcriptase (hTERT). In parallel, PTX-2 was also shown to interfere with the Akt pathway, which is in charge of the phosphorylation of hTERT, one key event in the telomerase activation pathway.

5. ADME

a. Intestinal absorption

In vivo studies by Burgess 2003 showed that only 19% of PTX-2 was detected following 24 h administration of a single oral dose to mice (5.7 µg PTX-2/animal). PTX-2 was found in the

gastrointestinal content and faeces, with only traces in the gastro-intestinal tissue. No detectable amounts were found in other internal organs and urine. Similarly, Espenes et al., 2009 reported that 24 h after gavage with 1 or 5 mg/kg b.w to mice, PTX-2 was detected by far in the stomach followed by the intestines whereas internal organs and whole blood showed only traces. Nonetheless, the fact that *in vivo* effects on the liver were reported after an oral administration (Ishige et al., 1988) suggests that PTX-2 is able to cross the intestinal barrier. No data has been published using *in vitro* systems to study the intestinal passage of PTX-2.

b. Metabolism

Regarding PTX-2 metabolism, few studies have been conducted. Using rat S9, Kittler et al., 2010 described 5 metabolites after 3 h incubation with 100 nM PTX-2: one hydroxylated metabolite, three isomers of double hydroxylated metabolite and finally one triple hydroxylated metabolite. No glutathione and glucuronide conjugates were observed. Ferron et al., 2016 showed that inhibition of CYP3A4 activity resulted in higher PTX-2 toxic responses in HepaRG cells, suggesting that CYP3A4 may play a role in PTX-2 metabolism. Finally, Sandvik et al., 2017 showed that PTX-2 was rapidly converted into two major and several oxidized metabolites using suspensions of rat hepatocytes.

III. Spirolides

1. Production by phytoplankton

Spirolides (B and D) were first discovered in contaminated shellfish in Canada in 1995 (Hu et al., 1995). In 2001, the same team discovered new members in contaminated shellfish, including spirolides A, C and SPX-1. Spirolides are exclusively produced by the species *Alexandrium ostenfeldii* and *A. peruvianum* (Cembella et al., 2000, Touzet et al., 2008). Spirolides are mainly found in mussels, oysters and clams (the EFSA Journal, 2008).

2. Structure

The group of spirolides belongs to the family of spiroimine which gathers multiple other different groups: gymnodimines, prorocentrolides, pteriatoxins, pinnatoxins. All these groups share a common cyclic imine structure. A particular feature of the spirolides is the presence of a spiro-linked tricyclic ether group (Figure 30).

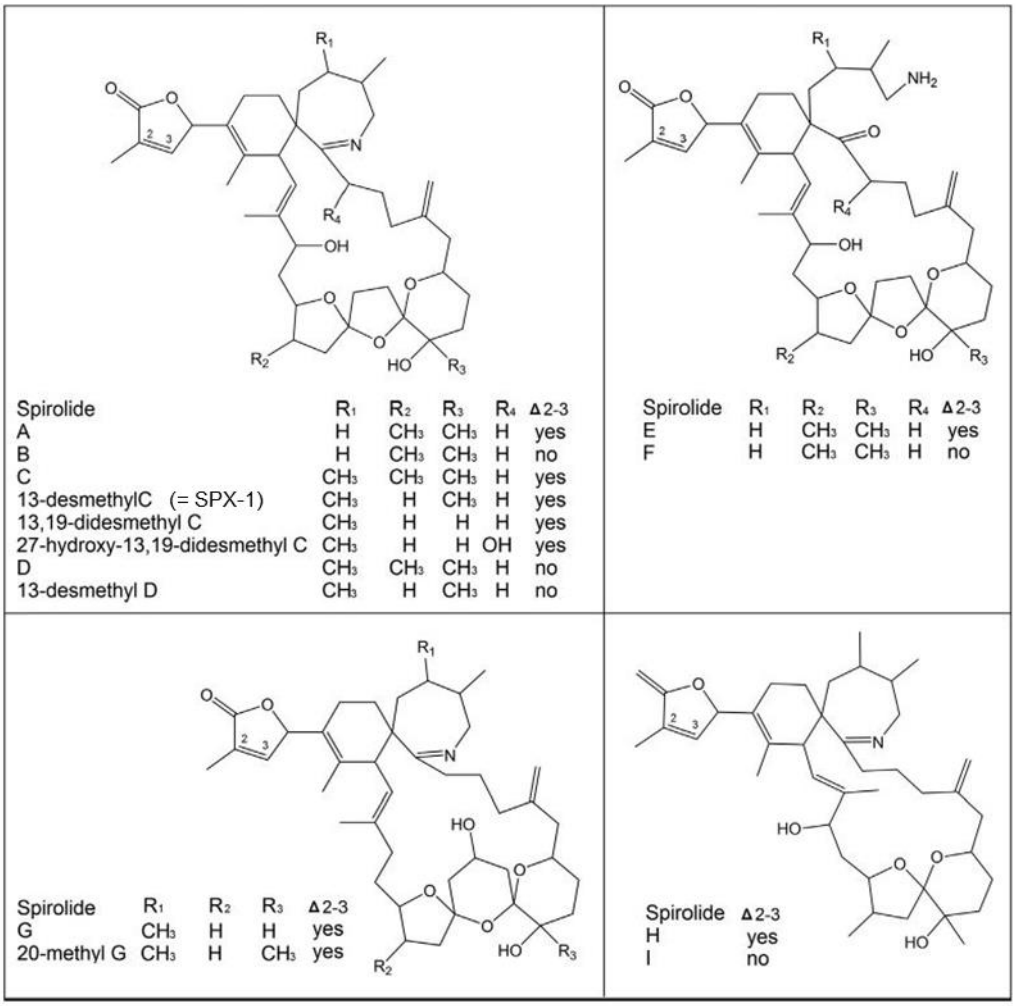

Figure 30: Chemical structure of SPX-1 and other spirolides (from Rodríguez et al., 2013)

3. *In vivo* toxicity

a. Lethal doses in rodents

Studies on the acute toxicity of SPX-1 showed low LD_{50} of 6.9 and 27.9 µg/kg after i.p injection in mice (Munday et al., 2012; Otero et al., 2012). SPX-1 by gavage was less toxic with value around 130 µg/kg (Munday et al., 2012). It is noteworthy that after injection or gavage, death occurred between 3 and 20 min after administration of the toxin. Administration by feeding was even less toxic (LD_{50} = 500 µg/kg) (Munday et al., 2012). Spirolide C showed similar LD_{50} values whereas LD_{50} values for spirolides A and B were higher (Munday et al., 2012). Spirolides E and F showed no toxicity at 1000 µg/kg (Hu et al., 1996). Table 12 sums the current knowledge for SPX-1.

Table 12: Acute toxicities of SPX-1 in mice

Toxin	Strain/gender	Mode of administration	Parameter	Acute toxicity	Reference
SPX*	CD-1/female	Intra-periteonal	LD_{50}	40 µg/kg	Richard et al., 2001
SPX-1	CD-1/female	Intra-periteonal	LD_{100}	75 µg/kg	Gill et al., 2003
SPX-1	Swiss mice	Intra-periteonal	LD_{50}	27.9 µg/kg	Otero et al., 2012
SPX-1	Swiss albino mice/female	Intra-periteonal (fed/fasted)	LD_{50}	6.9 µg/kg (95%, 5.0-8.0)	Munday et al., 2012
SPX*	CD-1/female	Oral (intragastric)	LD_{50}	1 mg/kg	Richard et al., 2001
SPX-1	Swiss albino mice/female	Gavage (fed)	LD_{50}	160 µg/kg (95%, 123-198)	Munday et al., 2012
SPX-1	Swiss albino mice/female	Gavage (fasted)	LD_{50}	133 µg/kg (95%, 87-166)	Munday et al., 2012
SPX-1	Swiss albino mice/female	Feeding	LD_{50}	1000 µg/kg (95%, 861-1290)	Munday et al., 2012
SPX-1	Swiss albino mice/female	Feeding (fasted)/ dry mousefood	LD_{50}	630 µg/kg (95%, 547-829)	Munday et al., 2012
SPX-1	Swiss albino mice/female	Feeding (fasted)/ moist mousefood	LD_{50}	590 µg/kg (95%, 500-625)	Munday et al., 2012
SPX-1	Swiss albino mice/female	Feeding (fasted)/ cream cheese	LD_{50}	500 µg/kg (95%, 381-707)	Munday et al., 2012

*crude extract of cultured *A. ostenfeldii*

b. Effects on the intestine

No macroscopic abnormalities towards the intestine were reported after oral or i.p administration of SPX-1, even at LD_{50} (Munday et al., 2012). Similarly, Gill et al., 2003 reported no histological changes at doses of 75, 260 and 2000 µg/kg administrated i.p to mice.

c. Effects on the liver

As for intestine, no macroscopic or microscopic abnormalities were reported in liver after oral or i.p administration of doses from 5 up to 2000 µg/kg SPX-1 (Munday et al., 2012, Gill et al., 2003).

4. *In vitro* toxicity

a. Mechanism of action

SPX-1 has been shown to interact with muscarinic acetylcholine receptors (mAChR). Wandscheer et al., 2010 reported that SPX-1 inhibited the acetylcholine-induced calcium signal and reduced the binding of muscarinic ligands to neuroblastoma cells. In parallel, a potent antagonism of SPX-1 was revealed for both muscle-type and neuronal nicotinic acetylcholine receptors (nAChR) (Bourne et al., 2010). Later, Hauser et al., 2012 showed that interaction of SPX-1 with muscarinic receptors was minimal whereas SPX-1 displayed great affinity for nicotinic receptors, especially the α7 receptor. This was confirmed by Araoz et al., 2015. The authors concluded that the rapid death observed in mice was explained by SPX-1 specific high affinity interaction with muscle-type nAChRs existing at the neuromuscular junction of skeletal muscle and with the major neuronal nAChRs present in the peripheral and central nervous system.

b. Toxicological effects

In vitro toxicity of SPX-1 has been scarcely investigated. Espiña et al., 2011 reported no cytotoxicity in Caco-2 cells after 10 h treatment with 1 µM dose. Moreover, Munday et al., 2012 showed that SPX-1 induced no evidence of cytotoxicity after 24 h treatment in a panel of cell lines (hepatic, neuroblastoma, adipocyte, ovarian cancer, skeletal muscle and macrophage). Besides, Ferron et al., 2016 reported no toxic effects of SPX-1 up to 262 nM after 24 h treatment in hepatic HepaRG cells.

5. ADME

a. Intestinal absorption

SPX-1 is able to cross the intestinal barrier as shown by Otero et al., 2012 who detected SPX-1 in blood and urine of mice treated orally with a single dose of 27.9 µg/kg b.w. This was confirmed in vitro by Espiña et al., 2011 who showed that SPX-1 was able to readily cross intestinal Caco-2 monolayers. After 10 h exposure, almost half of the loaded 1 µM SPX-1 was detected in the basolateral compartment. No alterations in the monolayer integrity were observed as shown by TEER values. Based on Papp calculations, the authors predicted a human intestinal permeability ≥ 80% for SPX-1.

b. Metabolism

Using human liver microsomes (HLM), Hui et al., 2012 detected a total of nine metabolites through a 32 h kinetic study using a single initial dose of 10.2 µM. The biotransformations observed included

hydroxylation, dihydroxylation, oxidation of a quaternary methyl group to hydroxymethyl or carboxylic acid groups, dehydrogenation and hydroxylation, as well as demethylation and dihydroxylation reactions. No glucuronides were detected. The stability plot of SPX-1 showed first-order kinetics and the intrinsic clearance was calculated to be 41 µL/min/mg.

Ferron et al., 2016 studied the impact of the modulation of CYP3A4 activity on SPX-1 toxic responses in HepaRG cells. Rifampicin-induced CYP3A4 activity led to decreased cell counts following treatment with SPX-1, suggesting that the CYP3A4 may play a role in SPX-1 metabolism.

IV. Yessotoxins

1. Production by phytoplankton

Yessotoxins were first discovered in Japan by Murata et al., in 1987 in contaminated scallops. Several species have been found to produce yessotoxins: *Prorocentrum reticulatum* was the first identified (Satake et al., 1999), followed by *Lingulodinium polyedrum* and *Gonyaulax spinifera* (Paz et al., 2004, Rhodes et al., 2006). Yessotoxins are mainly found in mussels and oysters (the EFSA Journal, 2008).

2. Structure

Yessotoxin structure was fully established using NMR by Murata et al., 1987. It features a unique ladder-like skeleton of polycyclic polyethers terminated by two sulfate groups at one of its extremity. The other extremity differs depending on the analogue (Figure 31).

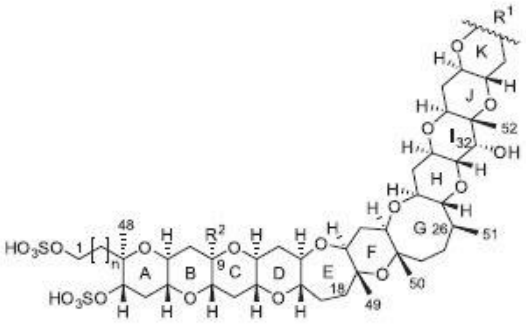

Name	R^1	R^2	n
Yessotoxin (YTX)	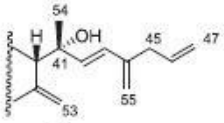	H	1
45-Hydroxy-YTX (45-OH-YTX)	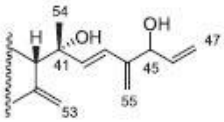	H	1
45,46,47-Trinor-YTX	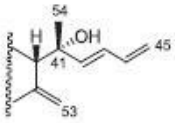	H	1
45,46,47-Trinorhomo-YTX	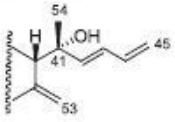	H	2
Homo-YTX (1a-Homo-YTX)	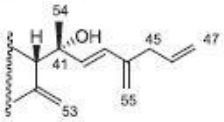	H	2
45-OH-HomoYTX	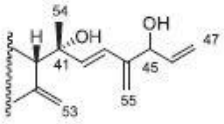	H	2

Figure 31: Chemical structure of YTX and its analogues (from Dominguez et al., 2010)

3. *In vivo* toxicity

a. Lethal doses in rodents

The LD_{50} values via i.p injection range from 100 µg/kg to 500 µg/kg (Table 13). Depending on the dose, death occurred in mice within the first hour to few hours after injection. However, YTX did not show acute toxicity after oral administration up to 54 mg/kg in mice (Ogino et al., 1997, Tubaro et al., 2010). These results suggest a low passage of YTX through the intestinal barrier although some toxicitiy to heart tissue was reported after repeated acute or subacute exposure (Tubaro et al., 2008, Ferreiro et al., 2017). Homo-YTX and 45-hydroxy-YTX were shown to be approximately as toxic as YTX, based on the LD_{50} results reported after i.p injection (Tubaro et al., 2003, Satake et al., 1997).

Hovewer, no mortality was observed for homo-YTX and 45-hydroxy-YTX orally administered at 5 mg/kg in mice (Tubaro et al., 2004).

Table 13: Acute toxicities of YTX in mice

Strain/gender	Mode of administration	Parameter	Acute toxicity	Reference
ICR/male	Intra-periteonal	LD_{50}	286 µg/kg (95%, 96-131)	Terao et al., 1990
ddY/male	Intra-periteonal	LD_{50}	80-100 µg/kg	Ogino et al., 1997
NMRI/female	Intra-periteonal	LD_{50}	500-750 µg/kg	Aune et al., 2002
CD/female	Intra-periteonal	LD_{50}	512 µg/kg (95%, 312-618)	Tubaro et al., 2003
?	Intra-periteonal	LD_{50}	<100 µg/kg	Ciminiello et al., 2003
Swiss albino/female	Intra-periteonal	LD_{50}	112 µg/kg (95%, 96-131)	Botana et al., 2008
C57 black/female	Intra-periteonal	LD_{50}	136 µg/kg (95%, 112-166)	Botana et al., 2008
ICR/male	Intra-periteonal	LD_{50}	462 µg/kg (95%, 353-603)	Aune et al., 2008
ICR/female	Intra-periteonal	LD_{50}	380 µg/kg (95%, 357-407)	Aune et al., 2008
CFW-1/male	Intra-periteonal	LD_{50}	328 µg/kg (95%, 294-375)	Aune et al., 2008
CFW-1/female	Intra-periteonal	LD_{50}	269 µg/kg (95%, 221-330)	Aune et al., 2008
NMRI/male	Intra-periteonal	LD_{50}	412 µg/kg (95%, 337-505)	Aune et al., 2008
NMRI/female	Intra-periteonal	LD_{50}	314 µg/kg (95%, 285-346)	Aune et al., 2008

b. Effects on the intestine

Discordant results have been published regarding toxic effects of YTX on the intestine. Tubaro et al., 2003 observed no effects after i.p injection up to 750 µg/kg. Aune et al., 2002 also reported the absence of pathological changes after i.p administration of doses from 100 up to 1000 µg/kg. On the contrary, Franchini et al., 2004 reported inflammation in the small intestine of mice treated by i.p administration of 420 µg/kg of YTX. Macrophages and lymphocytes were indeed detected in the epithelium of the duodenum.

After oral administration of YTX up to 10 mg/kg to mice, no effects were reported (Aune et al., 2002). Tubaro et al., 2003 also observed no morphological changes after 24 h treatment of 1 and 2 mg/kg of YTX. The same team reported no changes after a 7 days study (YTX being repeatedly administrated by gavage at 2 mg/kg/day) (Tubaro et al., 2004).

c. Effects on the liver

No particular effects towards the liver were reported after oral or i.p administration of YTX up to 2000 or 750 µg/kg, respectively (Aune et al., 2002; Tubaro et al., 2003, 2004).

4. *In vitro* toxicity

a. Mechanism of action

No clear mechanism of action has been reported for YTX. In fact, YTX has been shown to target different pathways depending on the cellular model employed. However, interaction with phosphodiesterases (PDEs) was clearly demonstrated: kinetic equilibrium dissociation constant (K_D) between YTX and PDE1, PDE3 and PDE4 were established by Pazos et al., 2004, 2005, 2006. The binding was confirmed by measuring the fluorescence polarization of a specific PDE-dye (Alfonso et al., 2005). YTX was also found to bind to exonuclease PDE I.

b. Toxicological effects

In vitro studies upon toxicity of YTX revealed effects towards calcium flux, cell death, cytoskeleton and mitochondria.

YTX was found to increase cytosolic calcium in many cell lines: HL7702 human liver cells (Pang et al., 2012), Bel7402 human hepatoma cell line (Pang et al., 2014), primary cultures of rat cerebellar neurons (Perez-Gomez et al., 2006) or human lymphocytes (De la Rosa et al., 2001, Malagoli et al., 2006). Another study showed no modification in cytosolic calcium levels of rat cardiomyocytes (Dell'Ovo et al., 2008).

The apoptotic effect of YTX has been reported in different cell lines: BE(2)-M17 neuroblastoma cell line (Leira et al., 2002), HL7702 human liver cells (Pang et al., 2012), Bel7402 human hepatoma cell line (Pang et al., 2011), rodent myoblast cell lines (Korsnes et al., 2006), HeLa cells (Malaguti et al.,

2002). The YTX mediated-apoptosis was found to be both intrinsic and extrinsic (Fernández-Araujo et al., 2014, 2015). Besides, YTX was also shown to induce cellular death by paraptosis mechanism in BC3H1 myoblast cell lines (Korsnes et al., 2011, 2013). Autophagy pathway was described by Rubiolo et al., 2014 in glioma cells as a consequence of endoplasmic reticulum-stress, cell cycle arrest in G1 and inhibition of protein synthesis. Since YTX is able to induce cell death by different mechanisms (apoptosis, paraptosis and autophagy), it has been suggested as potential anti-cancer agent (Korsnes et al., 2012).

A progressive depolymerization of actin microfilaments was described after YTX treatment in different cell lines such as insect IPLB-LdFB cells, mouse fibroblasts NIH3T3 cells and cultured rat cerebellar neurons (Malagoli et al., 2006, Franchini et al., 2010, Perez-Gomez et al., 2006). Moreover, disassemble of F-actin and translocation of tensin was observed in L6 and BC3H1 myoblast cell lines (Korsnes et al., 2007). Besides, the disruption of F-actin cytoskeleton was also observed in mouse T-lymphocytic EL-4 cells (Martín-López et al., 2012).

The effects of YTX on mitochondrial activity have been well characterized. Decreased mitochondrial membrane potential was described in neuroblastoma cells after YTX exposure (Leira et al., 2002). This was confirmed later by Bianchi et al., 2004 who not only reported changes in mitochondrial membrane potential but also in the opening of the permeability transition pore after YTX exposure in hepatic cells. Besides, changes in permeability of the outer mitochondrial membrane and production of pro-apoptotic factors together with swelling of mitochondria were also described after incubation with YTX in myoblast cell lines (Korsnes et al., 2006).

5. ADME

a. Intestinal absorption

Data on YTX distribution are scarce but several *in vivo* studies reported a passage through the intestinal barrier as YTX was detected in the kidneys, the spleen and the heart (Aasen et al., 2011, Tubaro et al., 2008). Nonetheless, only high doses of oral YTX (1 mg/kg b.w) exhibit passage.

No *in vitro* data has been published on the intestinal passage of YTX.

b. Metabolism

Regarding YTX metabolism, few studies have been conducted. Using rat S9, Kittler et al., 2010 described one hydroxylated metabolite after 3 h incubation with a single dose of 92 nM YTX. No glutathione or glucuronides were observed. Ferron et al., 2016 studied the impact of the modulation of CYP3A4 activity on YTX toxic responses in HepaRG cells. YTX was not toxic whatever the treatment condition, making it impossible to draw any conclusions on the role of CYP3A4.

Publication #1: Mixtures of lipophilic phycotoxins: exposure data and toxicological assessment

Review published in Mar. Drugs 2018, 16, 46; doi:10.3390/md16020046.

Review

Mixtures of Lipophilic Phycotoxins: Exposure Data and Toxicological Assessment

Jimmy Alarcan [1], Ronel Biré [2], Ludovic Le Hégarat [1] and Valérie Fessard [1,*]

[1] Toxicology of Contaminants Unit, French Agency for Food, Environmental and Occupational Health and Safety, ANSES, 35300 Fougères, France; jimmy.alarcan@anses.fr (J.A.); ludovic.lehegarat@anses.fr (L.L.H.)
[2] Marine Biotoxins Unit, French Agency for Food, Environmental and Occupational Health and Safety, ANSES, 94706 Maisons-Alfort, France; ronel.bire@anses.fr
* Correspondence: valerie.fessard@anses.fr; Tel.: +33-02-99-17-27-47

Received: 06 December 2017; Accepted: 29 January 2018; Published: 31 January 2018

Abstract: Lipophilic phycotoxins are secondary metabolites produced by phytoplanktonic species. They accumulate in filter-feeding shellfish and can cause human intoxication. Regulatory limits have been set for individual toxins, and the toxicological features are well characterized for some of them. However, phycotoxin contamination is often a co-exposure phenomenon, and toxicological data regarding mixtures effects are very scarce. Moreover, the type and occurrence of phycotoxins can greatly vary from one region to another. This review aims at summarizing the knowledge on (i) multi-toxin occurrence by a comprehensive literature review and (ii) the toxicological assessment of mixture effects. A total of 79 publications was selected for co-exposure evaluation, and 44 of them were suitable for toxin ratio calculations. The main toxin mixtures featured okadaic acid in combination with pectenotoxin-2 or yessotoxin. Only a few toxicity studies dealing with co-exposure were published. In vivo studies did not report particular mixture effects, whereas in vitro studies showed synergistic or antagonistic effects. Based on the combinations that are the most reported, further investigations on mixture effects must be carried out.

Keywords: phycotoxins; mixtures; exposure; toxicological assessment

1. Introduction

1.1. Problematic of Phycotoxins Contamination

Marine biotoxins are secondary metabolites produced by approximately 100 phytoplanktonic species [1]. From a chemical point of view, hydrophilic, lipophilic and amphiphilic toxins are distinguished. Among the group of lipophilic toxins, several main families have been depicted: okadaic acid (OA) and dinophysistoxins (DTXs), pectenotoxins (PTXs), yessotoxins (YTXs), azaspiracids (AZAs) and, finally, cyclic imines (spirolides (SPXs), pinnatoxins (PnTXs), pteriatoxins and gymnodimines (GYMs)). To prevent human intoxications, the European Union (EU) has set regulatory limits in shellfish [2] (Table 1).

Table 1. Current EU limits, exposure levels resulting from consumption of shellfish on the EU market and acute reference doses (ARfDs) set by the European Food Safety Authority (EFSA) (taken from EFSA Report #1306, [2]).

Toxin Group	Current EU Limits in Shellfish Meat	Exposure by Eating a 400-g Portion at the EU Limit	ARfD
OA and analogues	160 μg OA eq./kg SM	64 μg OA eq./person	0.3 μg OA eq./kg b.w.
AZA	160 μg AZA eq./kg SM	64 μg AZA1 eq./person	0.2 μg AZA1 eq./kg b.w.
PTX	160 μg OA eq./kg SM	64 μg PTX2 eq./person	0.8 μg PTX2 eq./kg b.w.
YTX	1 mg YTX eq./kg SM	400 μg YTX eq./person	25 μg YTX eq./kg b.w.
STX	800 μg PSP/kg SM	320 μg STX eq./person	0.5 μg STX eq./kg b.w.
DA	20 mg DA/kg SM	8 mg DA/person	30 μg DA/kg b.w.

SM: shellfish meat; eq.: equivalents; b.w.: body weight; ARfD: acute reference dose; PSP: paralytic shellfish poison; EU: European Union; OA: okadaic acid; PTX: pectenotoxin; YTX: yessotoxin; STX: saxitoxin; DA: domoic acid; AZA, azaspiracid.

However, several gaps exist in the current management of phycotoxins risk. For instance, no regulatory limits have been set up for cyclic imines, though these toxins are frequently detected and found to be very potent in vivo [3]. Regarding mixtures, the European Food Safety Authority (EFSA) opinion was only stated in the case of analogues based on toxicological equivalent factors (TEF) established from acute toxicity in rodents [2]. Although some publications reported the combined effects of a few binary mixtures of phycotoxins, a proper setting of regulation limits that would take into account risk when toxins co-occur is missing. Besides, it is noteworthy to investigate to which mixtures of phycotoxins the consumers can be exposed and to which respective levels. It is well known that some species can produce different analogues belonging to the same family, but also toxins of different families (Table 2). Moreover, as the conditions favoring the proliferation of deleterious phytoplankton, such as harmful algal bloom (HAB), can be similar for one species to another, several toxins are likely to co-occur.

Table 2. Global overview of the key phytoplanktonic species producing the main lipophilic phycotoxins. SPX, spirolide.

Phycotoxins	Species	Ref.
OA/DTXs	*Dinophysis mitra*, *Dinophysis tripos*, *Prorocentrum lima*, *Prorocentrum concavum*	[4,5]
OA/DTXs and PTXs	*Dinophysis fortii*, *Dinophysis acuta*, *Dinophysis acuminata*, *Dinophysis norvegica*, *Dinophysis rotundata*	[4,6–9]
YTXs	*Protoceratium reticulatum*, *Lingulodinium polyedrum*, *Gonyaulax spinifera*	[10,11]
AZAs	*Azadinium spinosum*	[12]
SPXs	*Alexandrium ostenfeldii*, *Alexandrium peruvianum*	[13,14]

1.2. Methodology for Mixture Hazard Assessment

Investigation of mixture effects is certainly one of the greatest challenges for hazard characterization nowadays. Hazard evaluation based on a single compound has restricted application since chemical contamination is often multiple and the interaction of compounds could result in a non-additive toxicity (whether higher or lower than expected). The combined effects of mixtures have been well established and classified [15]. This categorization relies on compounds sharing or not the same mode of action (MOA). Three different scenarios have been thus defined: (i) when compounds share the same MOA (analogues), the "dose addition" approach is employed: it considers that all these compounds behave as if they were a simple dilution of each other and the concentrations of each analogue are pondered using TEFs when available; (ii) when compounds have different MOAs, but no interaction is observed, the "response addition" approach is employed, and the global toxicity is calculated as the sum of each individual toxicity; (iii) when compounds interact, neither dose addition nor response addition are suitable approaches. Interaction is considered when the effect of a mixture differs from additivity based on the dose-response relationships of each individual compound. Then,

effects are classified as lower (antagonism, inhibition, masking) or greater (synergism, potentiation) than additive. Figure 1 summarizes the different cases.

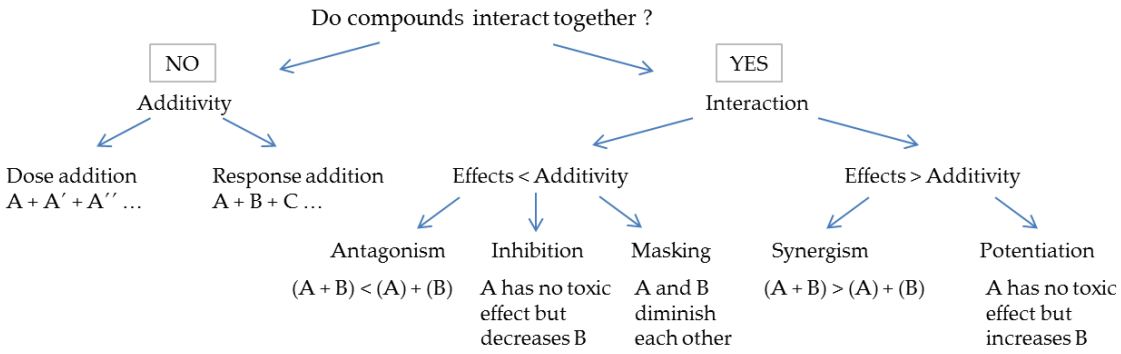

Figure 1. Methodology tree for mixture effect classification established according to the EFSA report [15].

Such strategies have been successfully employed to characterize the mixture effects of pesticides, dioxins or heavy metals [16–18].

1.3. Toxicological Features of Phycotoxins

Okadaic acid and dinophysistoxins were first reported as responsible for diarrhetic shellfish poisoning (DSP), causing various symptoms in humans, such as diarrhea, nausea, abdominal pain or vomiting [19]. OA is a potent inhibitor of protein phosphatase 2A (PP2A) and to a lesser extent of PP1 [20]. The group of pectenotoxins, especially PTX-2, its main representative, used to be associated with DSP, but they were further removed from the diarrhetic toxins due to the lack of evidence for their implication in gastro-intestinal symptoms [21]. Nevertheless, according to the regulation, OA, DTXs and PTX-2 are summed together for the established limit of 160 µg of OA equivalent per kg of shellfish. The major deleterious effect of PTX-2 involves actin depolarization leading to cytoskeleton disruption [22]. The group of yessotoxins has not been reported to affect humans, but in vivo studies showed potent toxicity in rodents with intra-peritoneal administration and specific cardiotoxic effects with oral administration [23,24]. Many studies also claimed in vitro toxicity [25,26]. The mechanism of action is unknown, but YTX has been shown to interfere with the autophagy pathway [27]. Although the group of azaspiracids displays symptoms similar to DSP [28], in vivo studies in mice showed more severe effects than OA toxins [29]. AZAs were found to act as potassium channel blockers [30]. No food intoxication related to the group of cyclic imines has been reported so far. Still, cyclic imines have been shown to exert neurological effects in mice [31], and most spirolides including SPX-1 were shown to selectively inhibit nicotinic acetylcholine receptors [32].

2. Exposure Data

2.1. Case Study of Multi-Phycotoxins Contamination in Shellfish

For this review, we analyzed the literature dealing with multi-phycotoxins contamination using the Scopus and PubMed databases. One thousand one hundred seventy one references were retrieved from the Scopus database using the keywords dinophysistoxin, pectenotoxin, spirolide and yessotoxin. In PubMed, a total of 686 references was retrieved using the same keywords. Only studies including shellfish contamination with the different toxin-groups were considered for analysis excluding contamination data with different analogues of the same group (Table 3). Among these papers, only some were suitable for a case study analysis so as to estimate toxin ratios when co-exposure occurred. The papers for which toxin ratios were not reported or could not be determined

were considered as unsuitable. The grey literature was not included in the search strategy, neither were the data collected from the national monitoring programs.

A total of 79 publications dealing with the co-occurrence of toxins in shellfish was retrieved. The mixtures reported depend on the toxins that were investigated. Table 3 sums the information on the toxin mixtures that were investigated in these studies. Among these 79 publications, only 44 were suitable for analysis. Geographical repartition is depicted in Figure 2. According to Table 3, many studies did not investigate the presence of spirolides in shellfish. For instance, no data from the U.S., Japan or Korea were available. In Europe also, among the 36 references, 23 did not investigate the presence of spirolides. Similarly, the presence of azaspiracids or yessotoxins was not investigated in any of the studies.

Table 3. List of publications where multi-phycotoxins contamination in shellfish were reported. Red color indicates that the data were unsuitable for analysis.

Authors	Ref.	Area	Toxins Investigated	Toxins Mixtures Reported
Taleb et al., 2006	[33]	Morocco	OA, DTX-1, DTX-2, AZA-1, AZA-2, AZA-3	mixtures of OA, DTX-2, AZA-2 and AZA-1
Elgarch et al., 2008	[34]	Morocco	OA, DTX-1, DTX-2, AZAs	mixtures of OA, DTX-2 and traces of AZA-2. OA found in highest concentrations
Ben Haddouch et al., 2015	[35]	Morocco	OA, DTXs, PTXs, AZAs, GYMs, SPXs, YTXs	mixtures of OA, DTXs, YTX, PTXs, AZA-2 and sometimes GYM
Pitcher et al., 2011	[36]	South Africa	OA, DTX-1, DTX-2, PTXs, AZA-1, GYM, SPXs, YTX, DA	mixtures of OA, DTX-1 and traces of PTXs
Turner et al., 2015	[37]	Argentina	OA, DTX-1, DTX-2, PTX-1, PTX-2, PTX-11, AZA-1, AZA-2, AZA-3, GYM, SPX-1, 20 Me SPX-G, YTX, 45-OH-YTX, homoYTX, 45-OH-homoYTX	YTX/OAs
McCarron et al., 2014	[38]	Canada	DA, OA, DTXs, AZAs, PTXs, YTXs, GYMs, SPXs, PnTXs.	mixtures of high levels of DTX-1, PTXs, YTXs and trace levels of cyclic imines
Alvarez et al., 2010	[39]	Chile	OA, DTX-1, PTX-1, PTX-2, PTX-2 sa, AZA-1, SPX-1, YTX	mixtures of AZA-1 and SPX-1; levels were below LOQ
Garcia et al., 2012	[40]	Chile	OA, DTX-1, DTX-2, PTX-2, YTX, AZA-1	DTX-1/PTX-2/YTX
Zamorano et al., 2013	[41]	Chile	OA, DTX-1, DTX-2, PTX-2, AZA-1, AZA-2, AZA-3, YTX, STX, neo-STX, GTXs	OAs/PTX-2/AZA-1/YTX/STXs
Alves de Souza et al., 2014	[42]	Chile	OA, DTX-1, DTX-2, DTX-3, PTX-2, YTX, 45-OH-YTX	mixture of 45-OH-YTX and traces of PTX-2
García et al., 2015	[43]	Chile	OA, DTX-1, DTX-2, PTX-2, AZA-1, AZA-2, AZA-3, YTX, STX, neo-STX, GTXs	mixtures of STXs and OA/DTX-1; hydrophilic toxins were subjected to shellfish metabolism
Garcia et al., 2016	[44]	Chile	OA, DTX-1, DTX-2, DTX-3, PTX-2, PTX-2 sa, AZA-1, AZA-2, AZA-3, YTX, homoYTX, COOH-YTX	OAs/PTX-2/YTX and OAs/YTX
García-Mendoza et al., 2014	[45]	Mexico	OA, DTX-1, DTX-2, PTX-1, PTX-2, PTX-11, AZA-1, AZA-2, AZA-3, GYM, SPX-1, YTX, 45-OH-YTX, homoYTX, 45-OH-homoYTX	mixtures mainly of OA, PTX-2, YTX and low levels of SPX-1 and AZA-1
Trainer et al., 2013	[46]	U.S.	OA, DTX-1, DTX-2, PTX-2, AZA-1, AZA-2, AZA-3, YTX	OA/YTX/PTX-2 and OA/PTX-2 and OA/YTX and OA/PTX-2/AZA-2 and OA/YTX/PTX-2/AZA-2
Hattenrath-Lehmann et al., 2013	[47]	U.S.	OA, DTX-1, DTX-2, PTX-2, PTX-11	OAs/PTXs
Eberhart et al., 2013	[48]	U.S.	OA, DTX-1, DTX-2, YTX	mixtures of DTX-1 and YTX
Wu et al., 2005	[49]	China	OA, DTX-1, STX, neo-STX, GTXs	mixtures of OA and GTX-2/3
Liu et al., 2011	[50]	China	OA, DTX-1, DTX-2, PTX-1, PTX-2, AZA-1, AZA-2, AZA-3, GYM, SPX-1, SPX-A, YTX, 45-OH-YTX,	GYM/OA and PTX-2s/OA

			homoYTX, 45-OH-homoYTX	
Li et al., 2012	[51]	China	OA, DTX-1, DTX-2, PTX-2, PTX-2 sa, AZA-1, AZA-2, AZA-3, GYM, SPX-1, YTX, 45-OH-YTX	OAs/PTX-2s
Guo et al., 2012	[52]	China	OA, DTX-1, PTX-2, YTX	OAs/PTX-2
Zhang et al., 2012	[53]	China	OA, DTX-1, PTXs	mixture of OA, DTX-1, 7-epi-PTX-2sa and PTX-2sa
Li et al., 2014	[54]	China	OA, DTX-1, DTX-3, PTXs, AZA-1, AZA-2, AZA-3, GYM, SPX-1, YTX	PTX-2s/GYM and PTX-2s/GYM/OAs and PTX-2s/OAs
Fang et al., 2014	[55]	China	PTX-2, AZA-2, GYM, SPX-1	SPX-1/PTX-2
Wu et al., 2014	[56]	China	OA, DTX-1, DTX-2, PTX-2, AZA-1, AZA-2, AZA-3, GYM, SPX-1, YTX, PbTXs	mixtures of OA, SPX-1, PTX-2, AZAs, PbTx-3 and traces of YTX
Wang et al., 2015	[57]	China	OA, DTX-1, DTX-2, PTX-2, AZA-1, AZA-2, AZA-3, GYM, SPX-1, YTX	mixtures of OA, DTX-1, PTX-2 and GYM
Wu et al., 2015	[58]	China	OA, PTX-2, AZA-1, GYM, SPX-1	OA/PTX-2/GYM/SPX-1 and OA/AZA-1/PTX-2/GYM/SPX-1 and OA/PTX-2/GYM
Li et al., 2016	[59]	China	OA, DTX-1, PTXs, AZA-1, AZA-2, AZA-3, GYM, SPX-1, YTXs	STXs/SPXs/YTXs and PTX-2/SPXs and STX/SPXs and OA/didesMe-SPX-C
Jiang et al., 2017	[60]	China	OA, DTX-1, DTX-2, PTX-1, PTX-2, PTX-2 sa, AZA-1, AZA-2, AZA-3, GYM, SPX-1, YTXs, DA	PTX-2s/OA/GYM and DTX-1/GYM
Suzuki et al., 2000	[61]	Japan	OA, DTX-1, PTX-6	PTX-6/OAs
Ito et al., 2001	[62]	Japan	OA, DTX-1, PTX-6, YTX	mixtures constituted of OA, DTX-1, YTX and PTX-6
Suzuki et al., 2005	[63]	Japan	OA, DTX-1, DTX-2, PTXs, YTXs	PTX-2s/OAs/YTXs and OAs/YTXs
Hashimoto et al., 2006	[64]	Japan	OA, DTX-1, DTX-3, PTX-1, PTX-2, PTX-6, YTX, 45-OH-YTX	PTX-2s/YTXs/OAs
Suzuki et al., 2011	[65]	Japan	OA, DTX-1, DTX-2, PTXs, YTXs	PTX-2s/OAs/YTXs and OAs/YTXs
Matsushima et al., 2015	[66]	Japan	OA, DTX-1, DTX-3, PTX-1, PTX-2, PTX-3, PTX-6	mixtures mainly of PTX-6 and DTX-3
Kim et al., 2010	[67]	Korea	OA, DTX-1, PTX-2, YTX	mixtures of OA, DTX-1 and traces of PTX-2, YTX
Lee et al., 2011	[68]	Korea	OA, DTX-1, PTX-2, YTX	mixtures mainly constituted of OA and DTX-1; DSP toxin content 10-times higher in mussels than in oysters
Vershinin et al., 2006	[69]	Russia	OA, DTX-1, PTXs, YTXs, AZAs, SPX-1	OAs/PTXs/YTXs
Morton et al., 2009	[70]	Russia	OA, DTX-1, PTXs	mixtures of OA, DTX-1, PTX-2 and PTX-2 sa
Orellana et al., 2017	[71]	Belgium	OA, DTX-1, DTX-2, PTX-2, AZA-1, AZA-2, AZA-3, SPX-1, YTX	mixtures of OA, DTX-2, SPXs and their ester metabolites

Pavela-Vrancic et al., 2001	[72]	Croatia	OA, DTX-2, PTX-2 sa, 7-epi-PTX-2 sa	mixtures of OA and 7-epi-PTX-2sa
Pavela-Vrancic et al., 2002	[73]	Croatia	OA, DTX-1, DTX-2, PTX-2, PTX-2 sa, 7-epi-PTX-2 sa	OA/7-epi-PTX-2SA
Pavela-Vrancic et al., 2006	[74]	Croatia	OA, DTX-1, DTX-2, PTX-2 sa, 7-epi-PTX-2 sa	OA/7-epi-PTX-2SA
Ninčević Gladan et al., 2008	[75]	Croatia	OA, DTX-1, DTX-2, PTX-2, PTX-2 sa, PTX-6, AZAs, GYM, SPX, YTX, COOHYTX, 45-OH-YTX, homoYTX, 45-OH-homoYTX	YTXs/OA and OA/YTXs
Ninčević Gladan et al., 2010	[76]	Croatia	OA, DTX-1, DTX-2, PTXs, YTXs, GYM, SPX-1	YTXs/OA and OA/YTXs/PTX-2s and OA/PTX-2s
Čustović et al., 2014	[77]	Croatia	OA, DXT-3, YTX, PSP	YTX/OAs
Amzil et al., 2007	[78]	France	OA, DTX-1, DTX-2, DTX-3, PTXs, AZAs, YTXs, SPXs, GYMs	OA/PTX-2/SPXs and OA/SPXs and PTX-2/OA
Amzil et al., 2008	[79]	France	OA, DTXs, PTXs, PTX-6, AZAs, GYMs, SPXs, YTXs	mixtures of OA, AZA-1 and AZA-2
Picot et al., 2012	[80]	France	OA, SPX-1	OA/SPX-1
Fernandez Puente et al., 2004	[81]	Ireland	OA, DTX-1, DTX-2, PTX-2, PTX-2 sa	OAs/PTX-2s
Fux et al., 2009	[82]	Ireland	OA, DTX-1, DTX-2, PTX-2, YTX, SPX, AZA-1, AZA-2, AZA-3	AZAs/OAs and OAs/AZAs and OAs/AZAs/YTX
Campbell et al., 2014	[83]	Ireland	OA, DTX-1, DTX-2, DA, STX, palytoxin	PSP/OAs/DA
Ciminiello et al., 1997	[84]	Italy	OA, YTX	YTX/OA
Draisci et al., 1999	[85]	Italy	OA, YTX, homoYTX	OA/YTX
Draisci et al., 1999	[86]	Italy	OA, DTX-1, DTX-2, PTXs, YTX	mixture of YTX, PTXs and OA
Ciminiello et al., 2010	[87]	Italy	OA, DTX-1, DTX-2, PTXs, AZA-1, AZA-2, AZA-3, YTXs, SPXs, DA	SPXs/PTX-2sa
Nincevic Gladan et al., 2011	[88]	Italy	OA, DTX-1, DTX-2, PTX-1, PTX-2, PTX-2 sa, 7-epi-PTX-2 sa, PTX-6, GYM, SPX-1, YTX, 45-OH-YTX, homoYTX, 45-OH-homoYTX	OA/homoYTX and OA/homoYTX/PTX-2sa and OA/PTX-2sa
Buratti et al., 2011	[89]	Italy	OA, YTX, 45-OH-YTX, homoYTX, COOH-YTX	mixtures mainly of YTX and homoYTX. HomoYTX found in highest concentrations
Bacchiocchi et al., 2015	[90]	Italy	OA, DTX-1, DTX-2, PTX-1, PTX-2, AZA-1, AZA-2, AZA-3, YTX, 45-OH-YTX, homoYTX, 45-OH-homoYTX	mixtures mainly of OA and YTX plus traces of AZA-2
Gerssen et al., 2010	[91]	The Netherlands	OA, PTX-2, AZA-1, YTX, SPX-1	YTX/OA/AZA-1/PTX-2/SPX-1
Van den Top et al., 2011	[92]	The Netherlands	OA, DTX-1, DTX-2, PTX-2, AZA-1, AZA-2, AZA-3, YTX, 45-OH-YTX	OAs/AZAs/YTXs/PTX-2 and YTXs/OAs and YTXs/OAs/AZAs
Gerssen et al., 2011	[93]	The Netherlands	OA, DTXs, PTXs, AZAs, YTXs	OAs/AZAs/PTX-2s and OAs/AZAs/YTXs/PTX-2s and PTX-2s/OAs/YTXs

Lee et al., 1988	[94]	Norway	OA, DTX-1, PTX-2, YTX	mixtures of DTX-1 and YTX
Ramstad et al., 2001	[95]	Norway	OA, DTX-1, YTX	mixtures constituted of OA/DTX-1 and YTX
Torgersen et al., 2008	[96]	Norway	OA, DTXs, PTXs	mixtures of PTXs, OA and DTXs
Vale et al., 2004	[97]	Portugal	OA, DTX-1, DTX-2, PTX-2, PTX-2 sa, 7-epi-PTX-2 sa	mixtures of OA/DTX-2 and PTX-2/PTX-2sa
Vale et al., 2006	[98]	Portugal	OA, DTX-1, DTX-2, PTX-2, PTX-2 sa, 7-epi-PTX-2 sa	mixtures of OA/DTX-2 and PTX-2/PTX-2sa
Gago-Martinez et al., 1996	[99]	Spain	OA, DTX-1, DTX-2, DTX-3, STXs, GTXs, neo-STXs	mixtures mainly of OA, DTX-2, GTXs and traces of STX
Villar Gonzalez et al., 2006	[100]	Spain	OA, DTX-1, DTX-2, DTX-3, SPX-1	mixtures of OA, DTX-2 and traces of SPX-1
Villar Gonzalez et al., 2007	[101]	Spain	OA, DTX-1, DTX-2, PTX-1, PTX-2, PTX-2 sa, AZA-1, YTX, SPX-1	OA/PTX-2sa and OA/PTX-2sa/SPX-1
de la Iglesia et al., 2009	[102]	Spain	PTX-6, YTX, 45-OH-YTX	mixtures of PTX-6 and YTXs
Rodriguez et al., 2015	[103]	Spain	OA, DTX-1, DTX-2, PTX-1, PTX-2, AZA-1, AZA-2, AZA-3, YTX, 45-OH-YTX, homoYTX, 45-OH-homoYTX	YTX/OA and OAs/YTX and YTXs/OA/PTX-2
García-Altares et al., 2016	[104]	Spain	OA, DTX-1, DTX-2, PTX-1, PTX-2, AZA-1, AZA-2, AZA-3, GYM, SPX-1, YTX, 45-OH-YTX, homoYTX, 45-OH-homoYTX	mixtures of OA and PTX-2
Stobo et al., 2005	[105]	UK	OA, DTX-1, DTX-2, PTX-1, PTX-2, AZA-1, AZA-2, AZA-3, YTX, 45-OH-YTX, homoYTX, 45-OH-homoYTX	YTX/OA and OA/AZA-1 and OA/YTX/PTX-2 and OA/PTX-2 and OA/YTX
Stobo et al., 2008	[106]	UK	OA, DTX-1, DTX-2, DTX-3, PTX-1, PTX-2, AZA-1, AZA-2, AZA-3, YTX, 45-OH-YTX, homoYTX, 45-OH-homoYTX	mixtures of OA, DTXs, PTXs and DA
Madigan et al., 2006	[107]	Australia	OA, PTX-2, GYM, YTX, DA	PTX-2s/OA
Takahashi et al., 2007	[108]	Australia	OA, DTXs, PTX-2, PTX-2 sa, GYM, DA	GYM/DA/PTX-2 and PTX-2s/OA/DA/GYM and PTX-2/OA
Ajani et al., 2017	[109]	Australia	OA, PTX-2, GYM, YTX, DA	PTX-2s/OA
MacKenzie et al., 2002	[110]	New Zealand	OA, DTX-1, PTXs, AZA-1, GYM, YTX, 45-OH-YTX, homoYTX, DA	YTXs/OA/PTX-2s/GYM/DA
McNabb et al., 2005	[111]	New Zealand	OA, DTX-1, DTX-2, PTXs, AZA-1, AZA-2, AZA-3, YTXs, GYM, SPXs, DA	PTX-2s/OA/YTXs/GYM and DA/OAs/PTX-2 and OAs/GYM/PTX-2/AZA-1/YTX

AZAs: azaspiracids; DTXs: dinophysistoxins; GTXs: gonyautoxins; GYMs: gymnodimines; PnTXs: pinnatoxins; PTXs: pectenotoxins; SPXs: spirolides; STXs: saxitoxins; YTXs: yessotoxins.

When establishing a toxin ratio A/B, A always corresponds to the toxin found in the highest concentration. For instance, in their paper, Pavela-Vrancic et al., 2002 [65], reported 0.133 and 0.090 µg/g hepato-pancreas (HP) of OA and 7-epi-PTX-2SA, respectively. Therefore, the ratio OA/7-epi-PTX-2SA equals 1.5 (= 0.133/0.090). When multiple analogues of the same toxin-group were reported, they were arithmetically summed without taking into account TEF values when available and named as equivalent to the corresponding toxin leader (OA, PTX-2, AZA-1, YTX and SPX-1). This choice was made to circumvent the fact that TEFs are not available for all of the toxins. Furthermore, one cannot be sure that the TEFs would still be valid for mixtures of toxins belonging to different groups. For instance, data for OA, DTX-1 and DTX-2 were summed and called OA equivalent (OA eq.). The complete and detailed analysis of each publication is supplied in the Supplementary Data Table S1.

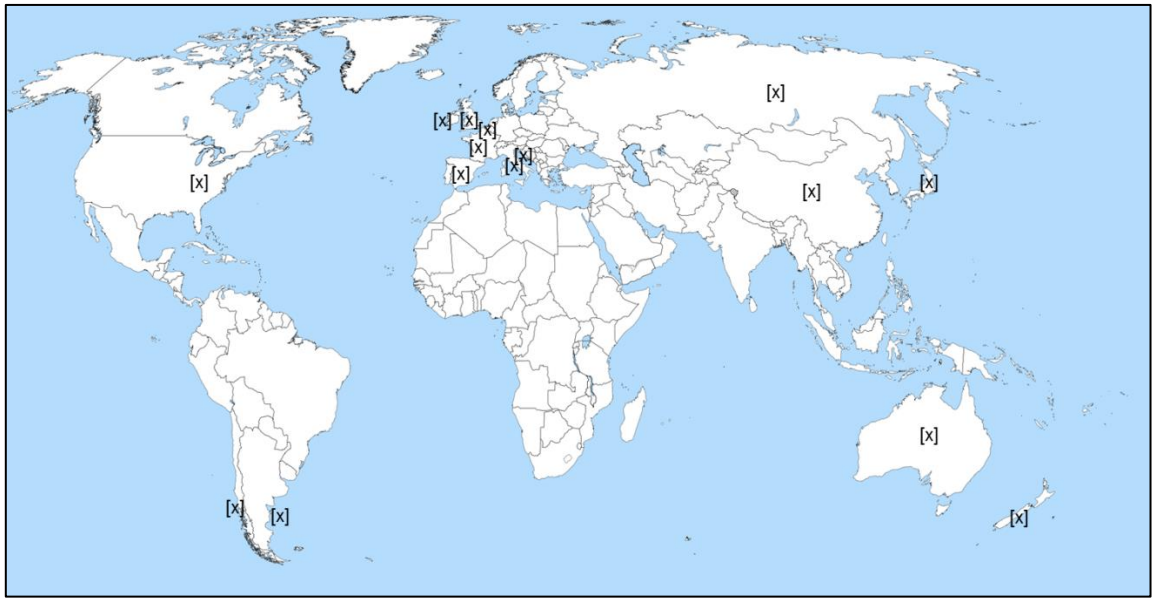

Figure 2. Case study of toxin-mixture contaminations. Countries where contaminations were reported are shown as [x]. A total of 44 publications considered as suitable was analyzed.

From these analyses, it appears that OA was the most often recorded lipophilic toxin in mixtures, as well as the predominant toxin (amount) whatever the mixture. Binary and trinary mixtures were also reported and sometimes even more complex cocktails (up to five toxins). In order to give a global view of mixtures, data from all publications were compiled and gathered according to shellfish species and geographic localization (Figures 3–6). Data in Figures 3–6 depict only the ratios for binary combinations. For instance, a trinary mixture OA/YTX/SPX-1 (OA being the predominant toxin) is represented by two dots considering the predominant toxin: one dot for OA/YTX and the other for OA/SPX-1. For each binary combination, the toxin ratios and their median values were calculated and presented by dots and horizontal lines, respectively. Different patterns were used to depict data and are solely meant to ease the reading of the figures, without specific correspondences.

Figure 3 shows the data regarding the contamination of mussels. In Asia, six combinations were reported: OA/YTX with a median ratio of eight and all the other combinations (OA/PTX-2, YTX/OA, PTX-2/OA, PTX-2/GYM and GYM/PTX-2) with a median ratio between one and five. In America, ten combinations were reported: OA/YTX, OA/STX, YTX/OA, PTX-2/OA with similar median ratios of 3–4, OA/PTX-2 with a median ratio of 15, OA/AZA-1 and STX/OA with median ratios between 5 and 8, STX/AZA-1 with a ratio around 28, YTX/PTX-2 with a ratio of 60, and STX/YTX with a ratio around 90. In Europe, 18 combinations were reported: OA/SPX-1 and PTX-2/OA with similar median ratios of 16, OA/PTX-2 and YTX/PTX-2 with similar median ratios of 8–9, STX/OA with a median ratio of 33, OA/DA with a median ratio of 58, STX/DA with a median ratio of 200, SPX-1/PTX-2 with a ratio of 350

and all other combinations (OA/YTX, OA/STX, YTX/OA, PTX-2/SPX-1, OA/AZA-1, YTX/SPX-1, YTX/AZA-1, PTX-2/YTX, AZA-1/OA and AZA-1/YTX) with median ratios between 1 and 7. In Oceania, seven combinations were reported: YTX/PTX-2 and PTX-2/YTX with median ratios between 1 and 4, YTX/OA and PTX-2/OA with similar median ratios of 13–14, YTX/GYM with a median ratio of 21, YTX/DA with a median ratio of 60 and PTX-2/GYM with a median ratio around 750.

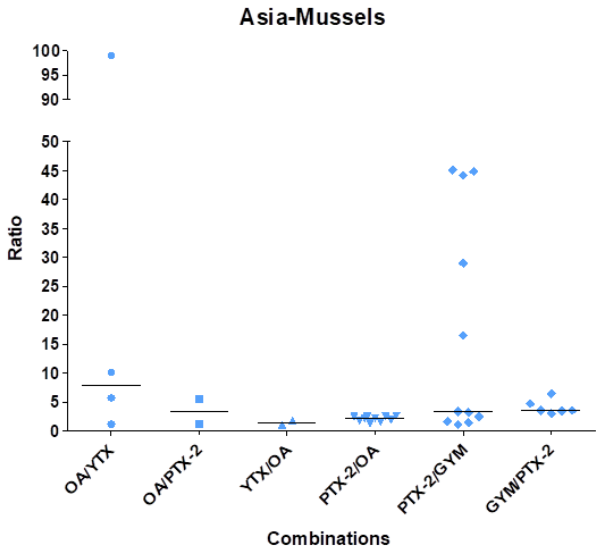

(**a**)

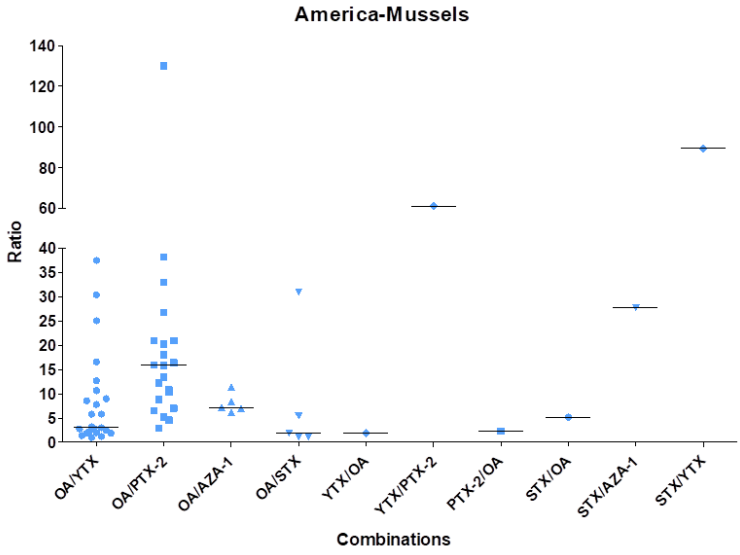

(**b**)

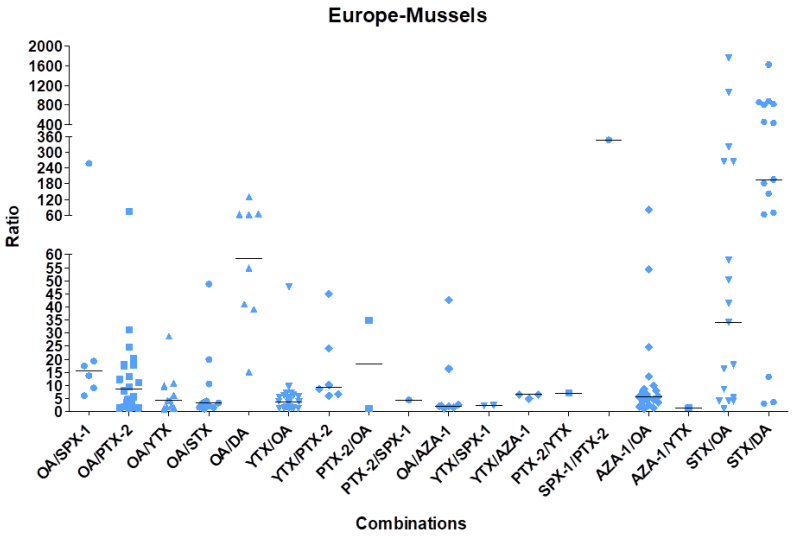

(**c**)

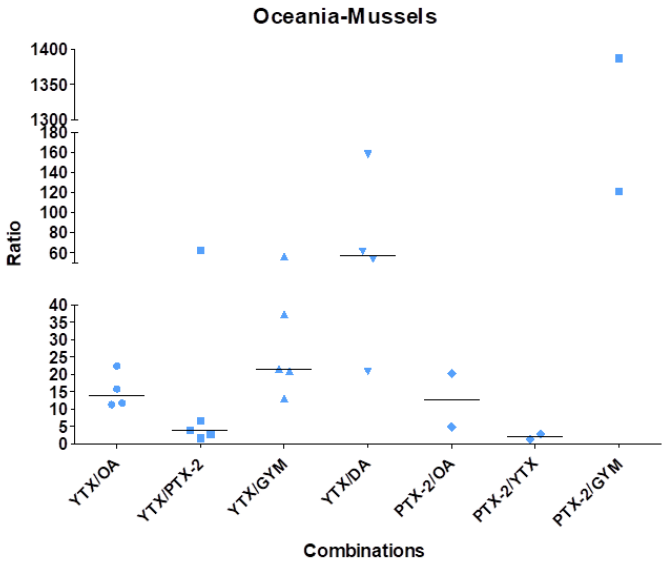

(**d**)

Figure 3. Mixture ratios found in mussels based on the analysis of 44 publications. (**a**) Data for Asia, (**b**) for America, (**c**) for Europe and (**d**) for Oceania.

Figure 4 shows the data regarding the contamination of oysters. In Asia, six combinations were reported: OA/GYM, GYM/PTX-2 and SPX-1/PTX-2 with ratios between 1 and 4, PTX-2/OA with a median ratio of 16, PTX-2/GYM with a ratio of 125 and GYM/OA with a ratio around 200. In America, three combinations were reported: OA/YTX and PTX-2/OA with similar median ratios of 3–4 and OA/PTX-2 with a median ratio of eight. In Europe, 10 combinations were reported: OA/PTX-2 with a ratio around 16, STX/DA with a ratio of 21, STX/OA with a ratio of 60 and all the other combinations (OA/SPX-1, SPX-1/PTX-2, PTX-2/OA, YTX/OA, YTX/PTX-2, YTX/SPX-1 and YTX/AZA-1) with a median ratio between 2 and 6. In Oceania, only the mixture PTX-2/OA with a ratio of six was reported.

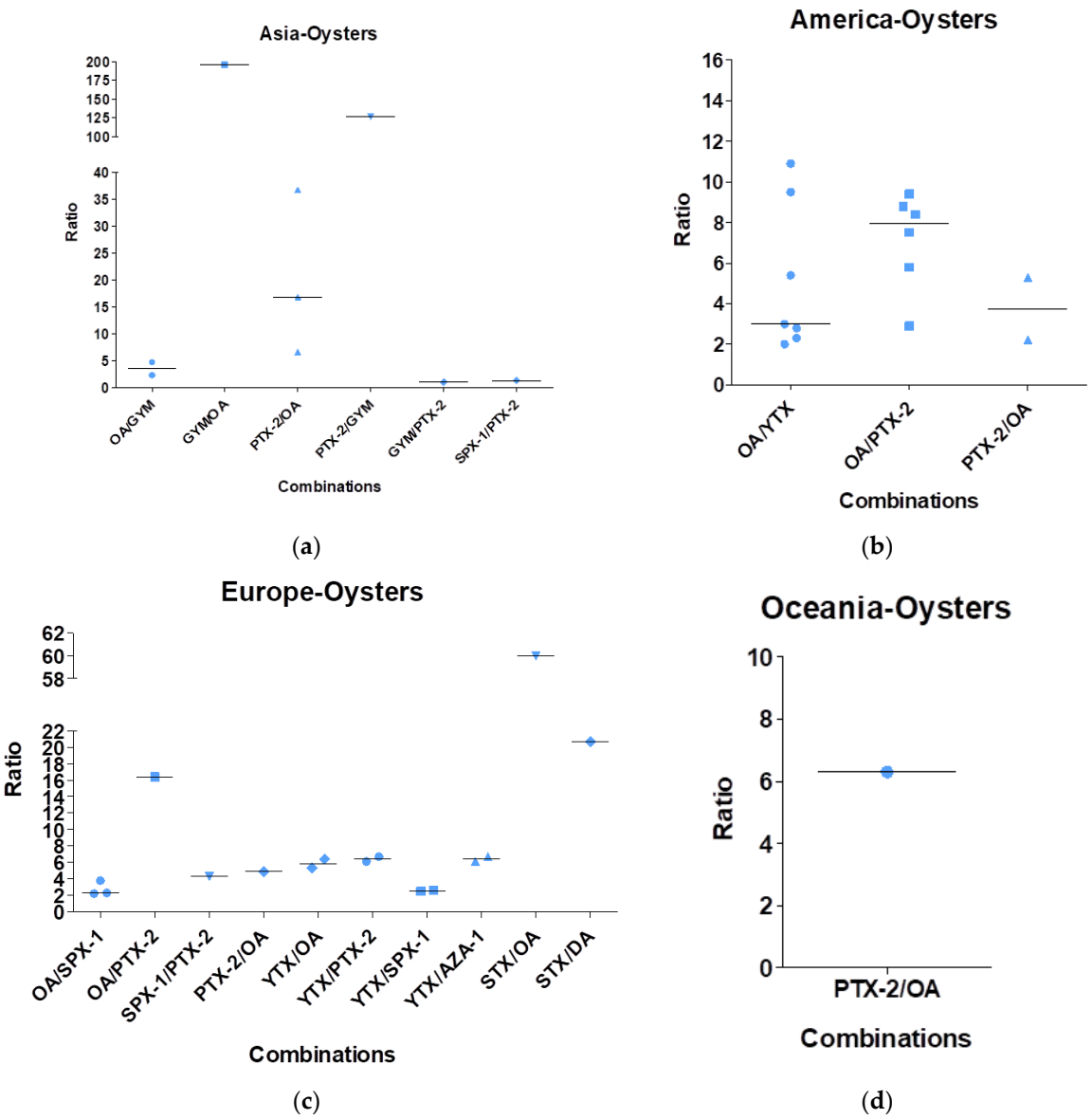

Figure 4. Mixture ratios found in oysters based on the analysis of the 44 publications. (**a**) Data for Asia, (**b**) for America, (**c**) for Europe and (**d**) for Oceania.

Figure 5 shows the data regarding the contamination of scallops. In Asia, five combinations were reported: PTX-2/YTX and YTX/PTX-2 with similar median ratios of 3, YTX/OA and OA/PTX-2 with similar median ratios of 5 and PTX-2/OA with a median ratio of 6. In America, only the mixture YTX/OA with a ratio around two was reported. In Europe, nine combinations were reported: OA/PTX-2 with a ratio of 29 and all the other combinations (OA/AZA-1, YTX/OA, OA/STX, OA/DA, STX/OA, STX/DA, DA/OA and DA/STX) with a median ratio between 2 and 6. In Oceania, only the mixture PTX-2/OA with a ratio around 30 was reported.

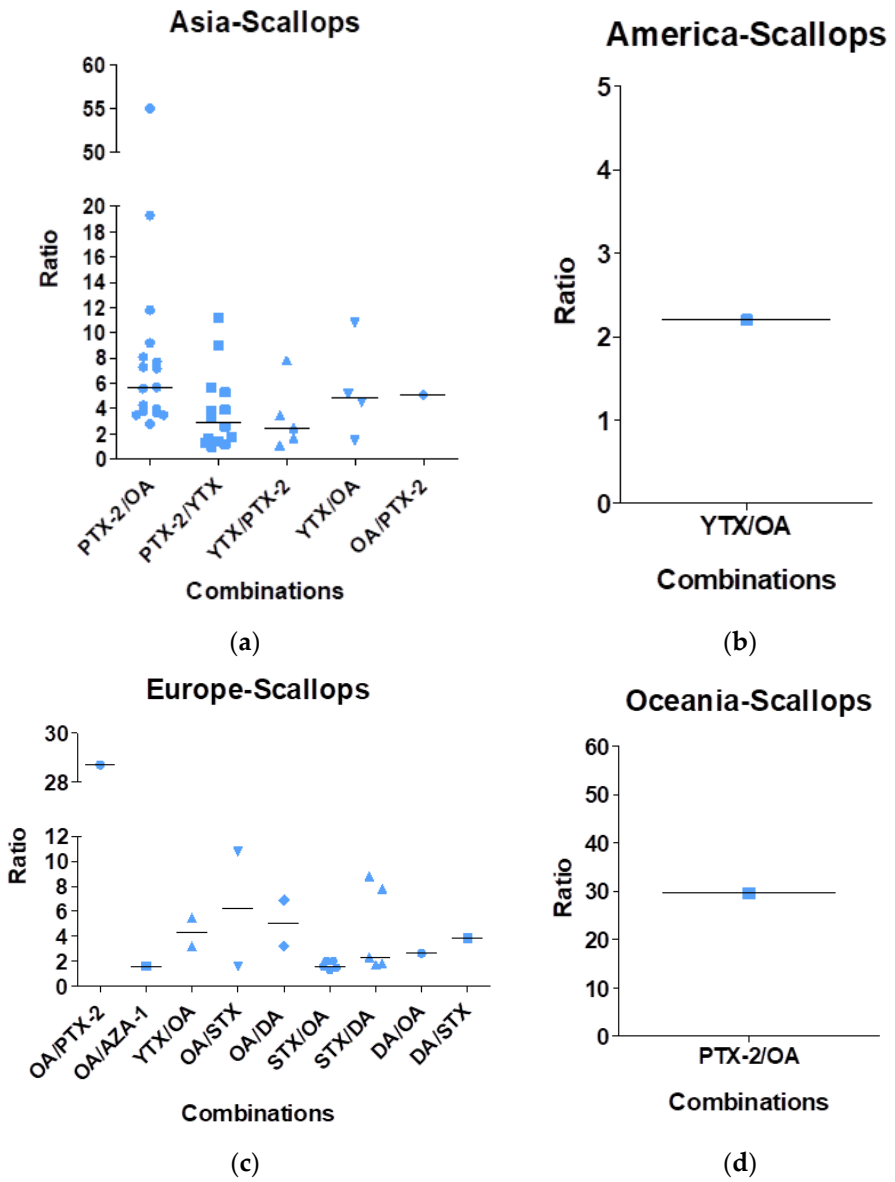

Figure 5. Mixture ratios found in scallops based on the analysis of the 44 publications. (**a**) Data for Asia, (**b**) for America, (**c**) for Europe and (**d**) for Oceania.

Figure 6 shows the data regarding the contamination of clams. In Asia, three combinations were reported: PTX-2/SPX-1 with a ratio of 3, STX/SPX-1 with a ratio of 34 and PTX-2/OA with a ratio of 225. In America, three combinations were reported: OA/YTX and PTX-2/OA with similar median ratios of three and OA/PTX-2 with a median ratio of 11. In Europe, two combinations were reported: OA/PTX-2 with a median ratio of 13 and OA/SPX-1 with a median ratio of 20. No mixtures were reported in Oceania in this particular matrix.

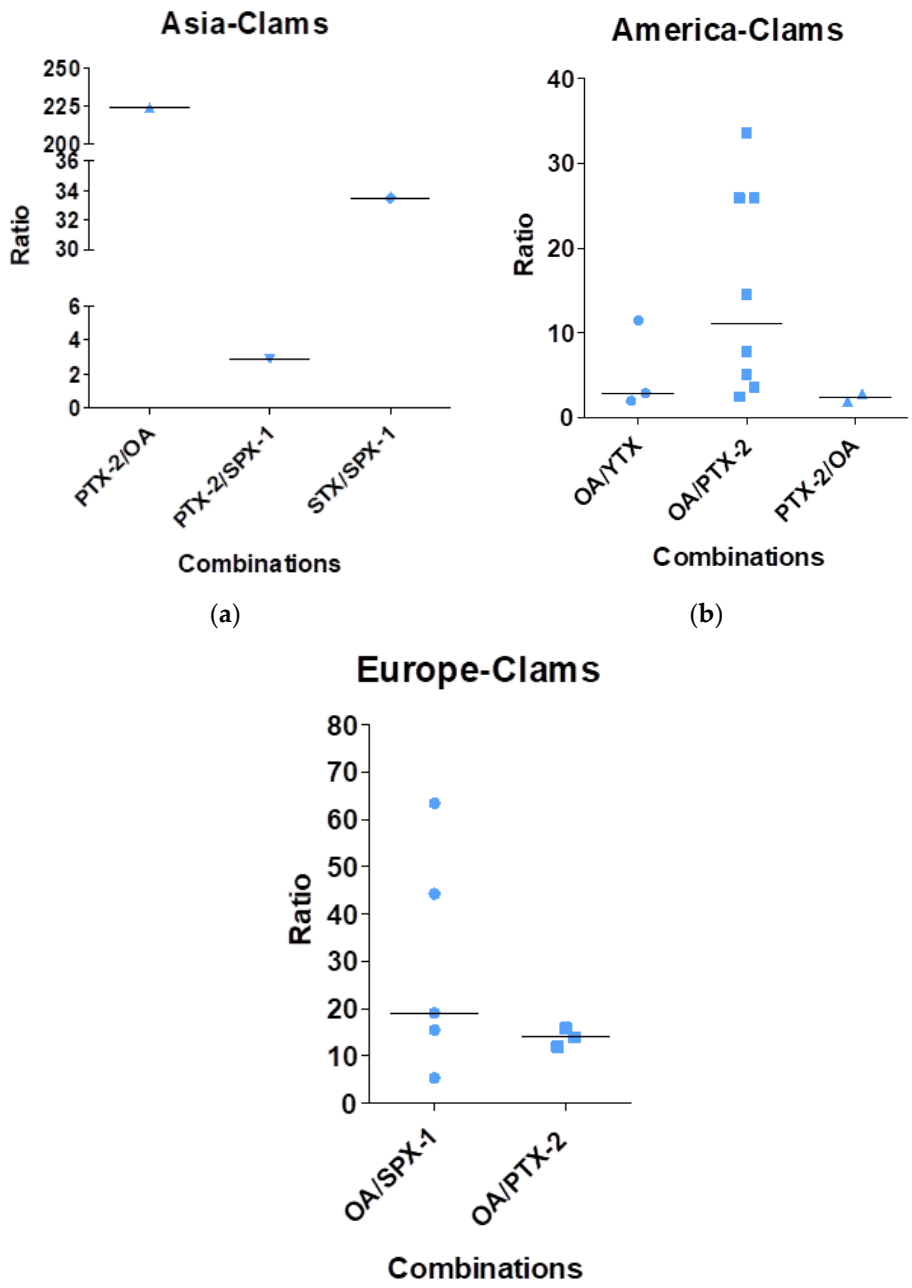

Figure 6. Mixture ratios found in clams based on the analysis of the 44 publications. (**a**) Data for Asia, (**b**) for America and (**c**) for Europe.

From our cases study, it appears that shellfish contamination by mixtures depends on the location. For instance, mixtures involving SPX-1 were often reported in Europe and in several shellfish types (mussel, oyster, clam, scallop and cockle), whereas it was scarcely described in Asia. In fact, in Japan and Korea, neither SPXs, nor AZAs were investigated. In Oceania, OA was found to be minor in mixtures, whereas it was predominant in mixtures reported in Europe and America. As for the ratios, Figure 7 shows box plots for the main reported combinations. Except in Asia, the median value ratio for the combination OA/PTX-2 is superior to 10 and higher in Europe compared to America. The median value ratio for the combination OA/YTX is around 3.5, except in Asia, where it yields six. For the combination OA/SPX-1, it reaches 11.5, but this combination is only reported in Europe. The combinations PTX-2/OA and YTX/OA share a similar value of the median ratios for a defined zone, but these ratios are continent-dependent (around 2 for America, 4-5 in Europe and

14 in Oceania). In Asia, median values ratios for PTX-2/OA and YTX/OA combinations are around 3–4. Besides, data also show that the distribution of the ratio values can be very wide for some combinations, with an upper extreme value more than 10-times higher than the median value for other combinations.

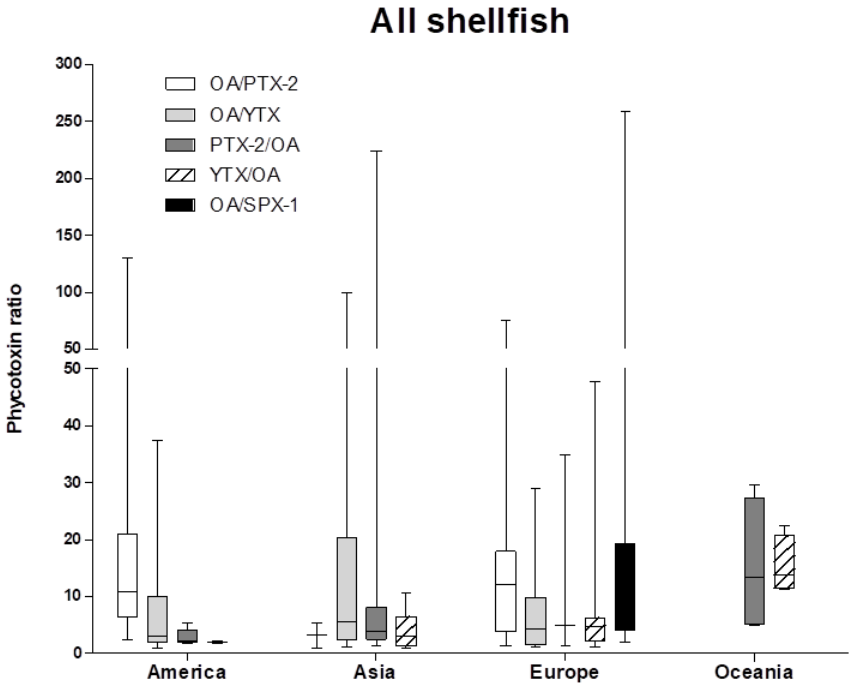

Figure 7. Box and whisker plots of phycotoxins ratios calculated for the main reported mixtures according to the location. The minimum, the lower quartile, the median, the upper quartile and the maximum are shown in the box and whisker plots.

Regarding the other publications that describe multi-toxins contamination, but which were not selected for the case study, the information is reported in Table 3. In Africa, most of the data concern Morocco. The main mixtures featured OA, DTXs and AZAs. In America, the mixtures featured often OA or DTX-1 with PTX-2, YTX and traces of spirolides and AZAs. In Asia, OA was found predominantly in association with PTX-2. In Europe, the main mixtures featured OA, DTXs and PTX-2 or YTX.

2.2. Multi-Phycotoxins Contamination in Other Matrices

Throughout our literature analysis, we found some papers describing multi-phycotoxin contamination in matrices other than shellfish (Table 4). Most of the time, the matrix was gastropods. Compared to shellfish, new combinations were described such as OA/PnTXs, OA/ciguatoxin (CTX) or OA/DA/Brevetoxin 3 (PbTx-3).

Table 4. Contamination with phycotoxin mixtures in other matrices.

Authors	Area	Toxin Mixtures	Matrix	Ref.
Zamorano et al., 2013	Chile	OAs/PTX-2/AZA-1/YTX/STXs	Gastropods	[41]
García et al., 2015	Chile	STXs/OA/DTX-1	Gastropods	[43]
García et al., 2016	Chile	OAs/PTX-2/YTX and OAs/YTX	Gastropods	[44]
Ganal et al., 1993	Hawaii	OA/CTX	Fish	[112]
Fire et al., 2011	U.S.	OA/DA/PbTx-3	Bottlenose dolphin	[113]
Wang et al., 2015	U.S.	OA/DTXs/PTX-2	Bottlenose dolphin	[114]
Kim et al., 2012	Korea	OA/YTX	Gastropods	[115]
Lee et al., 2012	Korea	OA/YTX	Gastropods	[116]
MacKenzie et al., 2011	New Zealand	OA/PnTxs	Gastropods	[117]

2.3. Conclusions and Perspectives Regarding Multi-Phycotoxins Contamination in Shellfish

Multi-phycotoxins contamination of seafood has been detected worldwide. The variability of analogues and bivalve filtering species, as well as discrepancies between geographical areas make it very challenging to establish a proper picture of multi-toxin contamination. From our literature analysis, it appears that the most frequent mixtures imply OA in combination with PTX-2 or YTX. If OA/PTX-2 mixtures depicted a median value ratio superior to 10 in America and Europe, a lower median ratio (inferior to five) was observed for PTX-2/OA mixtures. On the contrary, OA/YTX and YTX/OA mixtures share a similar ratio-value (around 3–4). Finally, even if OA/SPX-1 was only reported in Europe with a median value ratio of 11.5, the occurrence of this mixture could be underestimated since SPX-1 was not often included in the monitoring of non-European countries. In our review, the focus was on lipophilic toxins, but mixtures of both lipophilic and hydrophilic toxins have been also observed in a few cases. As depicted in Table 3, many studies did not investigate the presence of toxins such as spirolides, azaspiracids and even sometimes yessotoxins. Consequently, some of the mixtures that were described may not be fully accurate. For the purposes of this work, the toxins belonging to the same group were expressed as the equivalent of the main analogue. Besides, all the mixtures featuring more than two compounds were converted into binary mixtures. Most of the data were obtained from shellfish sampling in a short period that does not reflect any seasonal variability. In order to improve toxin mixtures' identification, it could be worth creating a network to analyze phycotoxin contamination with a shared database between institutes in charge of toxin monitoring. The better our knowledge on data exposure, the better we will be able to assess mixture effects. Indeed providing sufficient exposure data will enable selecting the most relevant mixtures (concentrations and ratios) before performing in vitro and in vivo assays, especially as in vivo investigations are toxin and money-consuming.

3. Toxicological Assessment

3.1. In Vivo Studies

So far, only a few studies have been conducted regarding possible mixture effects. Two of them consisted of one single dose treatment, whereas a third one mimicked a short-term repeated exposure. For all studies, the oral route was the way of administration. Table 5 summarizes the experimental conditions and the results.

In the study of Aasen et al. [118], female NMRI mice were given by gavage 1 or 5 mg/kg YTX, either alone or together with 200 mg/kg AZA-1. The results indicated no particular mixture effects in regards to clinical effects and pathological changes of internal organs. However, an increase in YTX levels was observed in stomach tissue suggesting higher YTX absorption in stomach when YTX was combined with AZA-1. After determination of the lethal doses of OA or AZA-1 by gavage to female NMRI mice, Aune et al. [119] examined the combined toxicity of OA and AZA-1 when given at both LD_{10} and LD_{50}/LD_{10} doses. No combined effects on lethality when AZA-1 and OA were given together were reported. Similarly, the pathological effects along the gastro-intestinal tract were not increased. The absorption of OA and AZA-1 from the GI tract was very low for each toxin separately, and it was reduced when toxins were given together. The in vivo toxicity by repeated oral exposure to a combination of YTX and OA (1 mg YTX/kg and 0.185 mg OA/kg, daily for seven days) was investigated in female CD-1 mice [120]. The results indicated no mortality, signs of toxicity, diarrhea and hematological changes, neither with the toxins alone, nor when co-administration. Thus, the co-exposure of YTX and OA did not show any combined toxic effects in mice. Franchini et al., 2005 [121], also featured mixtures of toxins (OA/YTXs), but since the effects of YTXs alone were not investigated, it is not possible to conclude about any mixture effect.

Table 5. Summary of in vivo studies.

Ref.	Animal	Treatment	Toxin (mg/kg b.w.)	Results Toxins alone		Results Mixtures	
				Distribution in Internal Organs [a,b]	Macro- and Micro-scopical Examination	Distribution in Internal Organs	Macro- and Micro-scopical Examination
Aasen et al., 2011 [118]	Female NMRI mice	single intake by gavage	YTX: 1 or 5 AZA-1: 200 YTX/AZA-1: 1/200 or 1/500	- Highest levels of AZA-1 found in stomach, duodenum and jejunum - Highest levels of YTX found in duodenum, jejunum, ileum and colon	YTX: no effects AZA-1: retention of material in the stomach and dilatation of the upper 1/3 of the small intestine with increased fluidity; contraction and bluntness of villi from duodenum, extension of cryptal compartments and extensive infiltration of neutrophils in lamina propria	- Enhanced levels of YTX and AZA-1 in stomach - Enhanced levels of YTX in duodenum, jejunum and colon - Reduced level of YTX in liver	No mixture effect
Aune et al., 2012 [119]	Female NMRI mice	single intake by gavage	OA: 0.6; 0.82; 0.9; 0.98 or 1.14 AZA-1: 0.42; 0.54; 0.6; 0.66 or 0.78 OA/AZA-1 *: LD_{10}/LD_{10} or LD_{50}/LD_{10}	- Highest levels of OA in GI tract - Highest levels of AZA-1 in stomach	OA: dilatation of stomach; shortened villi in the duodenum and jejunum and infiltration of neutrophils in lamina propria AZA-1: severe increase amount of content in stomach and dilatation of small intestine; shortened villi in the duodenum and infiltration of neutrophils in lamina propria	lower level for both toxins	No mixture effect
Sosa et al., 2013 [120]	Female CD-1 mice	repeated intake for 7 days by gavage	YTX: 1 OA: 0.185 YTX/OA: 1/0.185	Not investigated	YTX: ultrastructural changes in cardiomyocytes/OA: inflammation of the forestomach submucosa and ultrastructural changes in cardiomyocytes	Not investigated	No mixture effect

[a] Brain, heart, lungs, thymus, liver, spleen, kidneys, stomach, small intestine (duodenum, middle and lower jejunum) and colon. * Lethal doses (LD) were estimated from individual toxin experiments. [b] Brain, heart, lungs, thymus, liver, spleen, kidneys, stomach, small intestine (duodenum, middle and lower jejunum) and colon.

3.2. In Vitro Studies

Data concerning in vitro effects of toxins mixtures are scarce. Nevertheless, it has been pinpointed that a combination of toxins can result in greater or lower toxicity compared to toxins alone. For example, Sala et al., 2009 [122], showed a synergistic effect on the protein expression of heat shock protein β-1 isoforms and superoxide dismutase in human breast adenocarcinoma cells after 24 h of co-treatment with OA and gambierol (50/50 nM). Nonetheless, the characterization of those interactions using a mathematical model is missing in order to fully conclude about a mixture effect.

Ferron et al., 2016 [123], used the combination index-isobologram equation developed by Chou and Talalay [124] in order to deeply characterize the interactions between binary mixtures of phycotoxins incubated with human intestinal cells (Table 6).

Table 6. Summary of the study by Ferron et al., 2016 [123].

Cell Model	Treatment	Endpoint	Toxin Mixture (nM)		Mixture Effect
			Mixture	Molar Ratio *	
Caco-2	24-h incubation	Neutral red uptake	AZA-1/YTX	1:0.8	additive
				1:1.3	synergistic
				1:2.4	
				1:3.6	
			AZA-1/OA	1:51	antagonistic
				1:27.2	
				1:15.3	
				1:8.2	
			YTX/OA	1:26.5	antagonistic
				1:14.1	additive
				1:7.9	
				1:4.2	
Human intestinal epithelial crypt-like HIEC	24-h incubation	Neutral red uptake	AZA-1/YTX	1:0.8	synergistic
				1:1.3	
				1:2.4	
				1:3.6	additive
			AZA-1/OA	1:51	antagonistic
				1:27.2	additive
				1:15.3	
				1:8.2	antagonistic
			YTX/OA	1:26.5	synergistic
				1:14.1	antagonistic
				1:7.9	additive
				1:4.2	

* Molar ratios were based on IC_{50} values established for each toxin alone (OA: 78.52 nM, AZA-1: 4.03 nM and YTX: 4.08 nM).

All kinds of mixture effects, i.e., synergism, additivity and antagonism, were depicted in this study. Although Rodriguez et al. [103] showed a greater toxicity in human neuroblastoma cells when OA was co-incubated with YTX or DTX-2, only an additive effect could be concluded from their results, as they did not take into account the additivity of the effects.

3.3. Conclusions and Perspectives Regarding Multi-Phycotoxins' Toxicological Assessment

Except some modification in the absorption of toxins, no particular in vivo combined effects have been depicted so far. On the contrary, in vitro studies reported synergism, antagonism and additivity. Interestingly, the mixtures that failed to induce any in vivo combined effects were potent on cell lines. At least one of the most common mixtures OA/YTX showed a panel of responses from antagonism to synergism depending on the molar ratios. In vitro models are certainly the most suitable tools for screening combined effects as a large range of toxins concentrations and ratios can be investigated.

Surprisingly, no in vivo studies featuring mixtures of OA/SPX-1 and OA/PTX-2 were conducted, although these two combinations were commonly found in contaminated seafood.

4. Conclusions

The purpose of this review was to summarize the knowledge about published data dealing with seafood contamination by mixtures of lipophilic phycotoxins. Since mixtures can modulate the toxicity, the combined effects are worth investigating to identify the mixtures with higher potencies that may affect human health. For this purpose, relevant combinations (toxin composition and ratios between the toxins) must be established before performing toxicological surveys. As stated before, giving a complete overview of the occurrence of phycotoxins mixtures is challenging. Nevertheless, this review points out which combinations were most reported in the literature and which ratios were displayed. Additional data on mixtures of lipophilic phycotoxins, both on exposure and on toxicity, are required to state if the current regulations are sufficient and relevant to protect consumers' health.

Supplementary Materials: The following are available online at www.mdpi.com/link: Table S1: Calculation of ratio mixtures for each publication from the case study.

Acknowledgments: This work did not receive any financial support.

Author Contributions: Jimmy Alarcan, Ronel Biré, Valérie Fessard and Ludovic Le Hégarat conceived of and designed the review. Jimmy Alarcan analyzed the data. Jimmy Alarcan, Ronel Biré, Valérie Fessard and Ludovic Le Hégarat wrote the paper.

Conflicts of Interest: The authors declare no conflict of interest.

References

1. Visciano, P.; Schirone, M.; Berti, M.; Milandri, A.; Tofalo, R.; Suzzi, G. Marine biotoxins: Occurrence, toxicity, regulatory limits and reference methods. *Front. Microbiol.* **2016**, *7*, 1051, doi:10.3389/fmicb.2016.01051.
2. Alexander, J.; Benford, D.; Boobis, A.; Ceccatelli, S.; Cravedi, J.-P.; Di Domenico, A.; Doerge, D.; Dogliotti, E.; Edler, L.; Farmer, P.; et al. Scientific Opinion of the Panel on Contaminants in the Food Chain on a request from the European Commission on Marine Biotoxins in Shellfish—Summary on regulated marine biotoxins. *EFSA J.* **2009**, *1306*, 1–23.
3. Alexander, J.; Benford, D.; Boobis, A.; Ceccatelli, S.; Cravedi, J.-P.; Di Domenico, A.; Doerge, D.; Dogliotti, E.; Edler, L.; Farmer, P.; et al. Scientific Opinion on marine biotoxins in shellfish—Cyclic imines (spirolides, gymnodimines, pinnatoxins and pteriatoxins). *EFSA J.* **2010**, *8*, 1628, doi:10.2903/j.efsa.2010.1628.
4. Lee, J.-S.; Igarashi, T.; Fraga, S.; Dahl, E.; Hovgaard, P.; Yasumoto, T. Determination of diarrhetic shellfish toxins in various dinoflagellate species. *J. Appl. Phycol.* **1989**, *1*, 147–152.
5. An, T.; Winshell, J.; Scorzetti, G.; Fell, J.W.; Rein, K.S. Identification of okadaic acid production in the marine dinoflagellate Prorocentrum rhathymum from Florida Bay. *Toxicon* **2010**, *55*, 653–657.
6. Draisci, R.; Lucentini, L.; Giannetti, L.; Boria, P.; Poletti, R. First report of pectenotoxin-2 (PTX-2) in algae (Dinophysis fortii) related to seafood poisoning in Europe. *Toxicon* **1996**, *34*, 923–935.
7. Suzuki, T.; Beuzenberg, V.; Mackenzie, L.; Quilliam, M.A. Liquid chromatographymass spectrometry of spiroketal stereoisomers of pectenotoxins and the analysis of novel pectenotoxin isomers in the toxic dinoflagellate Dinophysis acuta from New Zealand. *J. Chromatogr. A* **2003**, *992*, 141–150.
8. MacKenzie, L.; Beuzenberg, V.; Holland, P.; McNabb, P.; Suzuki, T.; Selwood, A. Pectenotoxin and okadaic acid-based toxin profiles in Dinophysis acuta and Dinophysis acuminata from New Zealand. *Harmful Algae* **2005**, *4*, 75–85.
9. Luisa Fernández, M.; Reguera, B.; González-Gil, S.; Míguez, A. Pectenotoxin-2 in single-cell isolates of Dinophysis caudata and Dinophysis acuta from the Galician Rías (NW Spain). *Toxicon* **2006**, *48*, 477–490.
10. Satake, M.; Ichimura, T.; Sekiguchi, K.; Yoshimatsu, S.; Oshima, Y. Confirmation of yessotoxin and 45,46,47-trinoryessotoxin production by Protoceratium reticulatum collected in Japan. *Nat. Toxins* **1999**, *7*, 147–150.
11. Pistocchi, R.; Guerrini, F.; Pezzolesi, L.; Riccardi, M.; Vanucci, S.; Ciminiello, P.; Dell'Aversano, C.; Forino, M.; Fattorusso, E.; Tartaglione, L.; et al. Toxin levels and profiles in microalgae from the north-Western Adriatic Sea—15 years of studies on cultured species. *Mar. Drugs* **2012**, *10*, 140–162.

12. Tillmann, U.; Elbrächter, M.; Krock, B.; John, U.; Cembella, A. *Azadinium spinosum* gen. et sp. nov. (Dinophyceae) identified as a primary producer of azaspiracid toxins. *Eur. J. Phycol.* **2009**, *44*, 63–79.
13. Cembella, A.D.; Lewis, N.I.; Quilliam, M.A. The marine dinoflagellate Alexandriumostenfeldii (Dinophyceae) as the causative organism of spirolide shellfish toxins. *Phycologia* **2000**, *39*, 67–74.
14. Touzet, N.; Franco, J.M.; Raine, R. Morphogenetic diversity and biotoxin composition of Alexandrium (dinophyceae) in Irish coastal waters. *Harmful Algae* **2008**, *7*, 782–797.
15. Alexander, J.; Benford, D.; Leblanc, J.-C.; Hougaard-Bennekou, S.; Dorne, J.-L.; Binaglia, M.; Castoldi, A.; Chiusolo, A.; Cortinas-Abrahantes, J.; Heraud, F.; et al. European Food Safety Authority, 2013. International Frameworks Dealing with Human Risk Assessment of Combined Exposure to Multiple Chemicals. *EFSA J.* **2013**, *11*, 3313, doi:10.2903/j.efsa.2013.3313.
16. Takakura, N.; Sanders, P.; Fessard, V.; Le Hégarat, L. In vitro combined cytotoxic effects of pesticide cocktails simultaneously found in the French diet. *Food Chem. Toxicol.* **2013**, *52*, 153–162.
17. Walker, N.J.; Crockett, P.W.; Nyska, A.; Brix, A.E.; Jokinen, M.P.; Sells, D.M.; Hailey, J.R.; Easterling, M.; Haseman, J.K.; Yin, M.; et al. Dose-additive carcinogenicity of a defined mixture of "dioxin-like compounds. *Environ. Health Perspect.* **2004**, *113*, 43–48.
18. Zhou, Y.X.; Xu, J.; Zhang, X.; Xu, S.; Du, Q. Combined toxic effects of heavy metals and antibiotics on a pseudomonas fluorescens strain zy2 isolated from swine wastewater. *Int. J. Mol. Sci.* **2015**, *16*, 2839–2850.
19. Valdiglesias, V.; Prego-Faraldo, M.V.; Pásaro, E.; Méndez, J.; Laffon, B. Okadaic acid: More than a diarrheic toxin. *Mar. Drugs* **2013**, *11*, 4328–4349.
20. Takai, A.; Murata, M.; Torigoe, K.; Isobe, M.; Mieskes, G.; Yasumoto, T. Inhibitory effect of okadaic acid derivatives on protein phosphatases. A study on structure-affinity relationship. *Biochem. J.* **1992**, *284 Pt 2*, 539–544.
21. Ito, E.; Suzuki, T.; Oshima, Y.; Yasumoto, T. Studies of diarrhetic activity on pectenotoxin-6 in the mouse and rat. *Toxicon* **2008**, *51*, 707–716.
22. Allingham, J.S.; Miles, C.O.; Rayment, I. A Structural Basis for Regulation of Actin Polymerization by Pectenotoxins. *J. Mol. Biol.* **2007**, *371*, 959–970.
23. Aune, T.; Aasen, J.A.B.; Miles, C.O.; Larsen, S. Effect of mouse strain and gender on LD_{50} of yessotoxin. *Toxicon* **2008**, *52*, 535–540.
24. Tubaro, A.; Giangaspero, A.; Ardizzone, M.; Soranzo, M.R.; Vita, F.; Yasumoto, T.; Maucher, J.M.; Ramsdell, J.S.; Sosa, S. Ultrastructural damage to heart tissue from repeated oral exposure to yessotoxin resolves in 3 months. *Toxicon* **2008**, *51*, 1225–1235.
25. Korsnes, M.S. Yessotoxin as a Tool to Study Induction of Multiple Cell Death Pathways. *Toxins* **2012**, *4*, 568–579.
26. Tubaro, A.; Dell'Ovo, V.; Sosa, S.; Florio, C. Yessotoxins: A toxicological overview. *Toxicon* **2010**, *56*, 163–172.
27. Fernández-Araujo, A.; Alfonso, A.; Vieytes, M.R.; Botana, L.M. Key role of phosphodiesterase 4A (PDE4A) in autophagy triggered by yessotoxin. *Toxicology* **2015**, *329*, 60–72.
28. McMahon, T.; Silke, J. West coast of Ireland; winter toxicity of unknown aetiology in mussels. In *Harmfull Algae News*; The Intergovernmental Oceanographic Commission of UNESCO: Paris, France, 1996.
29. Kilcoyne, J.; Jauffrais, T.; Twiner, M.J.; Doucette, G.J.; Aasen-Bunes, J.A.; Sosa, S.; Krock, B.; Séhet, V.; Nulty, C.; Salas, R.; et al. Azaspiracids—Toxicological Evaluation, Test Methods and Identification of the Source Organism (ASTOX II). Available online: http://oar.marine.ie/handle/10793/970 (accessed on 19 February 2017).
30. Twiner, M.J.; Doucette, G.J.; Rasky, A.; Huang, X.-P.; Roth, B.L.; Sanguinetti, M.C. Marine Algal Toxin Azaspiracid Is an Open-State Blocker of hERG Potassium Channels. *Chem. Res. Toxicol.* **2012**, *25*, 1975–1984.
31. Munday, R.; Quilliam, M.A.; LeBlanc, P.; Lewis, N.; Gallant, P.; Sperker, S.A.; Ewart, H.S.; MacKinnon, S.L. Investigations into the Toxicology of Spirolides, a Group of Marine Phycotoxins. *Toxins* **2011**, *4*, 1–14.
32. Molgó, J.; Marchot, P.; Aráoz, R.; Benoit, E.; Iorga, B.I.; Zakarian, A.; Taylor, P.; Bourne, Y.; Servent, D. Cyclic imine toxins from dinoflagellates: A growing family of potent antagonists of the nicotinic acetylcholine receptors. *J. Neurochem.* **2017**, *142* (Suppl. S2), 41–51.
33. Taleb, H.; Vale, P.; Amanhir, R.; Benhadouch, A.; Sagou, R.; Chafik, A. First detection of azaspiracids in mussels in North West Africa. *J. Shellfish Res.* **2006**, *25*, 1067–1070.
34. Elgarch, A.; Vale, P.; Rifai, S.; Fassouane, A. Detection of Diarrheic Shellfish Poisoning and Azaspiracids Toxins in Moroccan Mussels: Comparison of LC-MS Method with the Commercial Immunoassay Kit. *Mar. Drugs* **2008**, *6*, 587–594.

35. Ben Haddouch, A.; Amanhi, R.; Amzil, Z.; Taleb, H.; Rovillon, G.-A.; Adly, F.; Loutfi, M. Lipophilic Toxin Profile in Mytilus galloprovincialis from the North Atlantic Coast of Morocco: LC-MS/MS and Mouse Bioassay Analyses. *Int. J. Sci. Res.* **2017**, *6*, 186. Available online: http://archimer.ifremer.fr/doc/00372/48342/ (accessed on 2 August 2017).
36. Pitcher, G.C.; Krock, B.; Cembella, A.D. Accumulation of diarrhetic shellfish poisoning toxins in the oyster Crassostrea gigas and the mussel Choromytilus meridionalis in the southern Benguela ecosystem. *Afr. J. Mar. Sci.* **2011**, *33*, 273–281.
37. Turner, A.D.; Goya, A.B. Occurrence and profiles of lipophilic toxins in shellfish harvested from Argentina. *Toxicon* **2015**, *102*, 32–42.
38. McCarron, P.; Wright, E.; Quilliam, M.A. Liquid Chromatography/Mass Spectrometry of Domoic Acid and Lipophilic Shellfish Toxins with Selected Reaction Monitoring and Optional Confirmation by Library Searching of Product Ion Spectra. *J. AOAC Int.* **2014**, *97*, 316–324.
39. Álvarez, G.; Uribe, E.; Ávalos, P.; Mariño, C.; Blanco, J. First identification of azaspiracid and spirolides in Mesodesma donacium and Mulinia edulis from Northern Chile. *Toxicon* **2010**, *55*, 638–641.
40. Garcia, C.; Rodriguez-Unda, N.; Contreras, C.; Barriga, A.; Lagos, N. Lipophilic toxin profiles detected in farmed and benthic mussels populations from the most relevant production zones in Southern Chile. *Food Addit. Contam. Part A* **2012**, *29*, 1011–1020.
41. Zamorano, R.; Marín, M.; Cabrera, F.; Figueroa, D.; Contreras, C.; Barriga, A.; Lagos, N.; García, C. Determination of the variability of both hydrophilic and lipophilic toxins in endemic wild bivalves and carnivorous gastropods from the Southern part of Chile. *Food Addit. Contam. Part A* **2013**, *30*, 1660–1677.
42. Alves-de-Souza, C.; Varela, D.; Contreras, C.; de La Iglesia, P.; Fernández, P.; Hipp, B.; Hernández, C.; Riobó, P.; Reguera, B.; Franco, J.M.; et al. Seasonal variability of *Dinophysis* spp. and Protoceratium reticulatum associated to lipophilic shellfish toxins in a strongly stratified Chilean fjord. *Deep-Sea Res. Part II Top. Stud. Oceanogr.* **2014**, *101*, 152–162.
43. García, C.; Pérez, F.; Contreras, C.; Figueroa, D.; Barriga, A.; López-Rivera, A.; Araneda, O.F.; Contreras, H.R. Saxitoxins and okadaic acid group: Accumulation and distribution in invertebrate marine vectors from Southern Chile. *Food Addit. Contam. Part A* **2015**, *32*, 984–1002.
44. García, C.; Oyaneder-Terrazas, J.; Contreras, C.; del Campo, M.; Torres, R.; Contreras, H.R. Determination of the toxic variability of lipophilic biotoxins in marine bivalve and gastropod tissues treated with an industrial canning process. *Food Addit. Contam. Part A* **2016**, *33*, 1711–1727.
45. García-Mendoza, E.; Sánchez-Bravo, Y.A.; Turner, A.; Blanco, J.; O'Neil, A.; Mancera-Flores, J.; Pérez-Brunius, P.; Rivas, D.; Almazán-Becerril, A.; Peña-Manjarrez, J.L. Lipophilic toxins in cultivated mussels (Mytilus galloprovincialis) from Baja California, Mexico. *Toxicon* **2014**, *90*, 111–123.
46. Trainer, V.; Moore, L.; Bill, B.; Adams, N.; Harrington, N.; Borchert, J.; da Silva, D.A.; Eberhart, B.T. Diarrhetic Shellfish Toxins and Other Lipophilic Toxins of Human Health Concern in Washington State. *Mar. Drugs* **2013**, *11*, 1815–1835.
47. Hattenrath-Lehmann, T.K.; Marcoval, M.A.; Berry, D.L.; Fire, S.; Wang, Z.; Morton, S.L.; Gobler, C.J. The emergence of Dinophysis acuminata blooms and DSP toxins in shellfish in New York waters. *Harmful Algae* **2013**, *26*, 33–44.
48. Eberhart, B.-T.; Moore, L.; Harrington, N.; Adams, N.; Borchert, J.; Trainer, V. Screening Tests for the Rapid Detection of Diarrhetic Shellfish Toxins in Washington State. *Mar. Drugs* **2013**, *11*, 3718–3734.
49. Wu, J.-Y.; Zheng, L.; Wang, J.-H. Contamination of shellfish from Shanghai seafood markets with paralytic shellfish poisoning and diarrhetic shellfish poisoning toxins determined by mouse bioassay and HPLC. *Food Addit. Contam.* **2005**, *22*, 647–651.
50. Liu, R.; Liang, Y.; Wu, X.; Xu, D.; Liu, Y.; Liu, L. First report on the detection of pectenotoxin groups in Chinese shellfish by LC–MS/MS. *Toxicon* **2011**, *57*, 1000–1007.
51. Li, A.; Ma, J.; Cao, J.; McCarron, P. Toxins in mussels (Mytilus galloprovincialis) associated with diarrhetic shellfish poisoning episodes in China. *Toxicon* **2012**, *60*, 420–425.
52. Guo, M.; Tan, Z.; Wu, H.; Li, Z.; Zhai, Y. Simultaneous determination of okadaic acid, dinophysistoxin, pectenotoxin and yessotoxin in shellfish by liquid chromatography-tandem mass spectrometry. *Chin. J. Chromatogr.* **2012**, *30*, 256–261.
53. Zhang, X.; Cai, X. Isolation and identification of shellfish toxins from contaminated blue mussel (Mytilus edulis) from the East China Sea. *J. Hyg. Res.* **2012**, *41*, 819–823.

54. Li, A.; Sun, G.; Qiu, J.; Fan, L. Lipophilic shellfish toxins in Dinophysis caudata picked cells and in shellfish from the East China Sea. *Environ. Sci. Pollut. Res.* **2015**, *22*, 3116–3126.
55. Fang, L.; Yao, X.; Wang, L.; Li, J. Solid-Phase Extraction-Based Ultra-Sensitive Detection of Four Lipophilic Marine Biotoxins in Bivalves by High-Performance Liquid Chromatography-Tandem Mass Spectrometry. *J. Chromatogr. Sci.* **2015**, *53*, 373–379.
56. Wu, H.; Guo, M.; Tan, Z.; Cheng, H.; Li, Z.; Zhai, Y. Liquid chromatography quadrupole linear ion trap mass spectrometry for multiclass screening and identification of lipophilic marine biotoxins in bivalve mollusks. *J. Chromatogr. A* **2014**, *1358*, 172–180.
57. Wang, X.-Z.; Cheng, Y.; Li, N.; Wen, H.-M.; Liu, R.; Shan, C.-X.; Chai, C.; Wu, H. Occurrence and Seasonal Variations of Lipophilic Marine Toxins in Commercial Clam Species along the Coast of Jiangsu, China. *Toxins* **2015**, *8*, 8, doi:10.3390/toxins8010008.
58. Wu, H.; Yao, J.; Guo, M.; Tan, Z.; Zhou, D.; Zhai, Y. Distribution of Marine Lipophilic Toxins in Shellfish Products Collected from the Chinese Market. *Mar. Drugs* **2015**, *13*, 4281–4295.
59. Li, A.; Chen, H.; Qiu, J.; Lin, H.; Gu, H. Determination of multiple toxins in whelk and clam samples collected from the Chukchi and Bering seas. *Toxicon* **2016**, *109*, 84–93.
60. Jiang, T.; Liu, L.; Li, Y.; Zhang, J.; Tan, Z.; Wu, H.; Jiang, T.; Lu, S. Occurrence of marine algal toxins in oyster and phytoplankton samples in Daya Bay, South China Sea. *Chemosphere* **2017**, *183*, 80–88.
61. Suzuki, T.; Yasumoto, T. Liquid chromatography-electrospray ionization mass spectrometry of the diarrhetic shellfish-poisoning toxins okadaic acid, dinophysistoxin-1 and pectenotoxin-6 in bivalves. *J. Chromatogr. A* **2000**, *874*, 199–206.
62. Ito, S.; Tsukada, K. Matrix effect and correction by standard addition in quantitative liquid chromatographic–mass spectrometric analysis of diarrhetic shellfish poisoning toxins. *J. Chromatogr. A* **2002**, *943*, 39–46.
63. Suzuki, T.; Jin, T.; Shirota, Y.; Mitsuya, T.; Okumura, Y.; Kamiyama, T. Quantification of lipophilic toxins associated with diarrhetic shellfish poisoning in Japanese bivalves by liquid chromatography–mass spectrometry and comparison with mouse bioassay. *Fish Sci.* **2005**, *71*, 1370–1378.
64. Hashimoto, S.; Suzuki, T.; Shirota, Y.; Honma, M.; Itabashi, Y.; Chyounan, T.; Kamiyama, T. Lipophilic toxin profiles associated with diarrhetic shellfish poisoning in scallops, Patinopecten yessoensis, collected in Hokkaido and comparison of the quantitative results between LC/MS and mouse bioassay. *J. Food Hyg. Soc. Jpn.* **2006**, *47*, 33–40.
65. Suzuki, T.; Quilliam, M.A. LC-MS/MS analysis of diarrhetic shellfish poisoning (DSP) toxins, okadaic acid and dinophysistoxin analogues, and other lipophilic toxins. *Anal. Sci.* **2011**, *27*, 571–571.
66. Matsushima, R.; Uchida, H.; Nagai, S.; Watanabe, R.; Kamio, M.; Nagai, H.; Kaneniwa, M.; Suzuki, T. Assimilation, Accumulation, and Metabolism of Dinophysistoxins (DTXs) and Pectenotoxins (PTXs) in the Several Tissues of Japanese Scallop Patinopecten yessoensis. *Toxins* **2015**, *7*, 5141–5154.
67. Kim, J.H.; Lee, K.J.; Suzuki, T.; Kang, Y.S.; Ho Kim, P.; Song, K.C.; Lee, T.S. Seasonal Variability of Lipophilic Shellfish Toxins in Bivalves and Waters, and Abundance of *Dinophysis* spp. in Jinhae Bay, Korea. *J. Shellfish Res.* **2010**, *29*, 1061–1067.
68. Lee, K.J.; Mok, J.S.; Song, K.C.; Yu, H.; Jung, J.H.; Kim, J.H. Geographical and Annual Variation in Lipophilic Shellfish Toxins from Oysters and Mussels along the South Coast of Korea. *J Food Prot.* **2011**, *74*, 2127–2133.
69. Vershinin, A.; Moruchkov, A.; Morton, S.L.; Leighfield, T.A.; Quilliam, M.A.; Ramsdell, J.S. Phytoplankton composition of the Kandalaksha Gulf, Russian White Sea: Dinophysis and lipophilic toxins in the blue mussel (Mytilus edulis). *Harmful Algae* **2006**, *5*, 558–564.
70. Morton, S.L.; Vershinin, A.; Smith, L.L.; Leighfield, T.A.; Pankov, S.; Quilliam, M.A. Seasonality of *Dinophysis* spp. and Prorocentrum lima in Black Sea phytoplankton and associated shellfish toxicity. *Harmful Algae* **2009**, *8*, 629–636.
71. Orellana, G.; Van Meulebroek, L.; De Rijcke, M.; Janssen, C.R.; Vanhaecke, L. High resolution mass spectrometry-based screening reveals lipophilic toxins in multiple trophic levels from the North Sea. *Harmful Algae* **2017**, *64*, 30–41.
72. Pavela-Vrančič, M.; Meštrović, V.; Marasović, I.; Gillman, M.; Furey, A.; James, K.K. The occurrence of 7-epi-pectenotoxin-2 seco acid in the coastal waters of the central Adriatic (Kaštela Bay). *Toxicon* **2001**, *39*, 771–779.
73. Pavela-Vrančič, M.; Meštrović, V.; Marasović, I.; Gillman, M.; Furey, A.; James, K.J. DSP toxin profile in the coastal waters of the central Adriatic Sea. *Toxicon* **2002**, *40*, 1601–7.

74. Pavela-Vrančić, M.; Ujević, I.; Ninčević Gladan, Ž.; Furey, A. Accumulation of Phycotoxins in the mussel Mytilus galloprovincialis from the Central Adriatic Sea. *Croat. Chem. Acta* **2006**, *79*, 291–297.
75. Ninčević-Gladan, Ž.; Skejić, S.; Bužančić, M.; Marasović, I.; Arapov, J.; Ujević, I.; Bojanić, N.; Grbec, B.; Kušpilić, G.; Vidjak, O. Seasonal Variability in *Dinophysis* spp. Abundances and Diarrhetic Shellfish Poisoning Outbreaks Along the Eastern Adriatic Coast. *Bot. Mar.* **2008**, 51, 449–463. Available online: https://www.degruyter.com/view/j/bot.2008.51.issue-6/bot.2008.067/bot.2008.067.xml (accesssed on 14 September 2017).
76. Gladan, Ž.N.; Ujević, I.; Milandri, A.; Marasović, I.; Ceredi, A.; Pigozzi, S.; Arapov, J.; Skejić, S.; Orhanović, S.; Isajlović, I. Is Yessotoxin the Main Phycotoxin in Croatian Waters? *Mar. Drugs* **2010**, *8*, 460–470.
77. Čustović, S.; Orhanović, S.; Skejić, S.; Pavela-Vrančič, M. The predominant occurrence of YTX in the Eastern-mid Adriatic sea (Vranjic basin, Croatia). *Fresenius Environ. Bull.* **2014**, *23*, 3453–3458.
78. Amzil, Z.; Sibat, M.; Royer, F.; Masson, N.; Abadie, E. Report on the first detection of pectenotoxin-2, spirolide-A and their derivatives in French shellfish. *Mar. Drugs* **2007**, *5*, 168–179.
79. Amzil, Z.; Sibat, M.; Royer, F.; Savar, V. First report on azaspiracid and yessotoxin groups detection in French shellfish. *Toxicon* **2008**, *52*, 39–48.
80. Picot, C.; Roudot, A.-C. A Practical Example of Risk Assessment—Risk Assessment to Phycotoxins in a Recreational Shellfish Harvester's Subpopulation. In *Novel Approaches and Their Applications in Risk Assessment*; InTech: Lexington, KY, USA, 2012. Available online: https://www.intechopen.com/download/pdf/35499 (accesssed on 2 August 2017).
81. Puente, P.F.; Sáez, M.J.F.; Hamilton, B.; Lehane, M.; Ramstad, H.; Furey, A.; James, K.J. Rapid determination of polyether marine toxins using liquid chromatography-multiple tandem mass spectrometry. *J. Chromatogr. A* **2004**, *1056*, 77–82.
82. Fux, E.; Bire, R.; Hess, P. Comparative accumulation and composition of lipophilic marine biotoxins in passive samplers and in mussels (*M. edulis*) on the West Coast of Ireland. *Harmful Algae* **2009**, *8*, 523–537.
83. Campbell, K.; McNamee, S.E.; Huet, A.C.; Delahaut, P.; Vilarino, N.; Botana, L.M.; Poli, M.; Elliott, C.T. Evolving to the optoelectronic mouse for phycotoxin analysis in shellfish. *Anal. Bioanal. Chem.* **2014**, *406*, 6867–6881.
84. Ciminiello, P.; Fattorusso, E.; Forino, M.; Magno, S.; Poletti, R.; Satake, M.; Viviani, R.; Yasumoto, T. Yessotoxin in mussels of the northern Adriatic Sea. *Toxicon* **1997**, *35*, 177–183.
85. Draisci, R.; Ferretti, E.; Palleschi, L.; Marchiafava, C.; Poletti, R.; Milandri, A.; Ceredi, A.; Pompei, M. High levels of yessotoxin in mussels and presence of yessotoxin and homoyessotoxin in dinoflagellates of the Adriatic Sea. *Toxicon* **1999**, *37*, 1187–93.
86. Draisci, R.; Palleschi, L.; Giannetti, L.; Lucentini, L.; James, K.J.; Bishop, A.G.; Satake, M.; Yasumoto, T. New approach to the direct detection of known and new diarrhoeic shellfish toxins in mussels and phytoplankton by liquid chromatography-mass spectrometry. *J. Chromatogr. A* **1999**, *847*, 213–221.
87. Ciminiello, P.; Dell'Aversano, C.; Fattorusso, E.; Forino, M.; Tartaglione, L.; Boschetti, L.; Rubini, S.; Cangini, M.; Pigozzi, S.; Poletti, R. Complex toxin profile of Mytilus galloprovincialis from the Adriatic sea revealed by LC-MS. *Toxicon* **2010**, *55*, 280–288.
88. Nincevic Gladan, Z.; Ujevic, I.; Milandri, A.; Marasovic, I.; Ceredi, A.; Pigozzi, S.; Arapov, J.; Skejic, S. Lipophilic Toxin Profile in Mytilus galloprovincialis during Episodes of Diarrhetic Shellfish Poisoning (DSP) in the N.E. Adriatic Sea in 2006. *Molecules* **2011**, *16*, 888–899.
89. Buratti, S.; Franzellitti, S.; Poletti, R.; Ceredi, A.; Montanari, G.; Capuzzo, A.; Fabbri, E. Bioaccumulation of algal toxins and changes in physiological parameters in Mediterranean mussels from the North Adriatic Sea (Italy): Effects of Algal Toxins on Marine Mussels. *Environ. Toxicol.* **2013**, *28*, 451–470.
90. Bacchiocchi, S.; Siracusa, M.; Ruzzi, A.; Gorbi, S.; Ercolessi, M.; Cosentino, M.A.; Ammazzalorso, P.; Orletti, R. Two-year study of lipophilic marine toxin profile in mussels of the North-central Adriatic Sea: First report of azaspiracids in Mediterranean seafood. *Toxicon* **2015**, *108*, 115–125.
91. Gerssen, A.; van Olst, E.H.W.; Mulder, P.P.J.; de Boer, J. In-house validation of a liquid chromatography tandem mass spectrometry method for the analysis of lipophilic marine toxins in shellfish using matrix-matched calibration. *Anal. Bioanal. Chem.* **2010**, *397*, 3079–3088.
92. Van den Top, H.J.; Gerssen, A.; McCarron, P.; van Egmond, H.P. Quantitative determination of marine lipophilic toxins in mussels, oysters and cockles using liquid chromatography-mass spectrometry: Inter-laboratory validation study. *Food Addit. Contam. Part A* **2011**, *28*, 1745–1757.

93. Gerssen, A.; Mulder, P.P.J.; de Boer, J. Screening of lipophilic marine toxins in shellfish and algae: Development of a library using liquid chromatography coupled to orbitrap mass spectrometry. *Anal. Chim. Acta* **2011**, *685*, 176–185.
94. Lee, J.S.; Tangen, K.; Yasumoto, T.; Dahl, E.; Hovgaard, P.; Yasumoto, T. Diarrhetic shellfish toxins in norwegian mussels. *Nippon Suisan Gakkaishi* **1988**, *54*, 1953–1957.
95. Ramstad, H.; Hovgaard, P.; Yasumoto, T.; Larsen, S.; Aune, T. Monthly variations in diarrhetic toxins and yessotoxin in shellfish from coast to the inner part of the Sognefjord, Norway. *Toxicon* **2001**, *39*, 1035–1043.
96. Torgersen, T.; Sandvik, M.; Lundve, B.; Lindegarth, S. Profiles and levels of fatty acid esters of okadaic acid group toxins and pectenotoxins during toxin depuration. Part II: Blue mussels (Mytilus edulis) and flat oyster (Ostrea edulis). *Toxicon* **2008**, *52*, 418–427.
97. Vale, P. Differential dynamics of dinophysistoxins and pectenotoxins between blue mussel and common cockle: A phenomenon originating from the complex toxin profile of Dinophysis acuta. *Toxicon* **2004**, *44*, 123–134.
98. Vale, P. Differential dynamics of dinophysistoxins and pectenotoxins, part II: Offshore bivalve species. *Toxicon* **2006**, *47*, 163–173.
99. Gago-Martinez, A.; Rodriguez-Vazquez, J.A.; Thibault, P.; Quilliam, M.A. Simultaneous occurrence of diarrhetic and paralytic shellfish poisoning toxins in Spanish mussels in 1993. *Nat. Toxins* **1996**, *4*, 72–79.
100. González, A.V.; Rodríguez-Velasco, M.L.; Ben-Gigirey, B.; Botana, L.M. First evidence of spirolides in Spanish shellfish. *Toxicon* **2006**, *48*, 1068–1074.
101. Villar-González, A.; Rodríguez-Velasco, M.L.; Ben-Gigirey, B.; Botana, L.M. Lipophilic toxin profile in Galicia (Spain): 2005 toxic episode. *Toxicon* **2007**, *49*, 1129–1134.
102. De la Iglesia, P.; Gago-Martínez, A. Determination of yessotoxins and pectenotoxins in shellfish by capillary electrophoresis-electrospray ionization-mass spectrometry. *Food Addit. Contam. Part A* **2009**, *26*, 221–228.
103. Rodríguez, L.; González, V.; Martínez, A.; Paz, B.; Lago, J.; Cordeiro, V.; Blanco, L.; Vieites, J.M.; Cabado, A.G. Occurrence of Lipophilic Marine Toxins in Shellfish from Galicia (NW of Spain) and Synergies among Them. *Mar. Drugs* **2015**, *13*, 1666–1687.
104. García-Altares, M.; Casanova, A.; Fernández-Tejedor, M.; Diogène, J.; de la Iglesia, P. Bloom of Dinophysis spp. dominated by D. sacculus and its related diarrhetic shellfish poisoning (DSP) outbreak in Alfacs Bay (Catalonia, NW Mediterranean Sea): Identification of DSP toxins in phytoplankton, shellfish and passive samplers. *Reg. Stud. Mar. Sci.* **2016**, *6*, 19–28.
105. Stobo, L.A.; Lacaze, J.-P.C.; Scott, A.C.; Gallacher, S.; Smith, E.A.; Quilliam, M.A. Liquid chromatography with mass spectrometry—Detection of lipophilic shellfish toxins. *J. AOAC Int.* **2005**, *88*, 1371–1382.
106. Stobo, L.A.; Lacaze, J.-P.C.L.; Scott, A.C.; Petrie, J.; Turrell, E.A. Surveillance of algal toxins in shellfish from Scottish waters. *Toxicon* **2008**, *51*, 635–648.
107. Madigan, T.L.; Lee, K.G.; Padula, D.J.; McNabb, P.; Pointon, A.M. Diarrhetic shellfish poisoning (DSP) toxins in South Australian shellfish. *Harmful Algae* **2006**, *5*, 119–123.
108. Takahashi, E.; Yu, Q.; Eaglesham, G.; Connell, D.W.; McBroom, J.; Costanzo, S.; Shaw, G.R. Occurrence and seasonal variations of algal toxins in water, phytoplankton and shellfish from North Stradbroke Island, Queensland, Australia. *Mar. Environ. Res.* **2007**, *64*, 429–442.
109. Ajani, P.; Harwood, D.; Murray, S. Recent Trends in Marine Phycotoxins from Australian Coastal Waters. *Mar. Drugs* **2017**, *15*, 33, doi:10.3390/md15020033.
110. MacKenzie, L.; Holland, P.; McNabb, P.; Beuzenberg, V.; Selwood, A.; Suzuki, T. Complex toxin profiles in phytoplankton and Greenshell mussels (Perna canaliculus), revealed by LC-MS/MS analysis. *Toxicon* **2002**, *40*, 1321–1330.
111. McNabb, P.; Selwood, A.I.; Holland, P.T. Multiresidue method for determination of algal toxins in shellfish: Single-laboratory validation and interlaboratory study. *J. AOAC Int.* **2005**, *88*, 761–772.
112. Ganal, C.A.; Asahina, A.Y.; Hokama, Y.; Miyahara, J.T. Characterization of marine toxin(s) in Myripristis sp. by immunological, mouse toxicity, and guinea pig assays. *J. Clin. Lab. Anal.* **1993**, *7*, 41–45.
113. Fire, S.E.; Wang, Z.; Byrd, M.; Whitehead, H.R.; Paternoster, J.; Morton, S.L. Co-occurrence of multiple classes of harmful algal toxins in bottlenose dolphins (Tursiops truncatus) stranding during an unusual mortality event in Texas, USA. *Harmful Algae* **2011**, *10*, 330–336.
114. Wang, Z.; Broadwater, M.H.; Ramsdell, J.S. Analysis of diarrhetic shellfish poisoning toxins and pectenotoxin-2 in the bottlenose dolphin (Tursiops truncatus) by liquid chromatography-tandem mass spectrometry. *J. Chromatogr. A* **2015**, *1416*, 22–30.

115. Kim, J.H.; Lee, K.J.; Suzuki, T.; Mok, J.S.; Park, K.; Kwon, J.Y.; Son, K.T.; Song, K.C. First report of contamination of the abalone Haliotis discus hannai by okadaic acid and yessotoxin. *J. Shellfish Res.* **2012**, *31*, 1199–1203.
116. Lee, K.J.; Mok, J.S.; Song, K.C.; Yu, H.; Lee, D.S.; Jung, J.H.; Kim, J.H. First Detection and Seasonal Variation of Lipophilic Toxins Okadaic Acid, Dinophysistoxin-1, and Yessotoxin in Korean Gastropods. *J. Food Prot.* **2012**, *75*, 2000–2006.
117. MacKenzie, L.A.; Selwood, A.I.; McNabb, P.; Rhodes, L. Benthic dinoflagellate toxins in two warm-temperate estuaries: Rangaunu and Parengarenga Harbours, Northland, New Zealand. *Harmful Algae* **2011**, *10*, 559–566.
118. Aasen, J.A.B.; Espenes, A.; Miles, C.O.; Samdal, I.A.; Hess, P.; Aune, T. Combined oral toxicity of azaspiracid-1 and yessotoxin in female NMRI mice. *Toxicon* **2011**, *57*, 909–917.
119. Aune, T.; Espenes, A.; Aasen, J.A.B.; Quilliam, M.A.; Hess, P.; Larsen, S. Study of possible combined toxic effects of azaspiracid-1 and okadaic acid in mice via the oral route. *Toxicon* **2012**, *60*, 895–906.
120. Sosa, S.; Ardizzone, M.; Beltramo, D.; Vita, F.; Dell'Ovo, V.; Barreras, A.; Yasumoto, T.; Tubaro, A. Repeated oral co-exposure to yessotoxin and okadaic acid: A short term toxicity study in mice. *Toxicon* **2013**, *76*, 94–102.
121. Franchini, A.; Marchesini, E.; Poletti, R.; Ottaviania, E. Swiss mice CD1 fed on mussels contaminated by okadaic acid and yessotoxins: Effects on thymus and spleen. *Eur. J. Histochem.* **2005**, *49*, 179–188.
122. Sala, G.L.; Ronzitti, G.; Sasaki, M.; Fuwa, H.; Yasumoto, T.; Bigiani, A.; Rossini, G.P. Proteomic Analysis Reveals Multiple Patterns of Response in Cells Exposed to a Toxin Mixture. *Chem. Res. Toxicol.* **2009**, *22*, 1077–1085.
123. Ferron, P.-J.; Dumazeau, K.; Beaulieu, J.-F.; Le Hégarat, L. Fessard, V. Combined Effects of Lipophilic Phycotoxins (Okadaic Acid, Azapsiracid-1 and Yessotoxin) on Human Intestinal Cells Models. *Toxins* **2016**, *8*, 50, doi:10.3390/toxins8020050.
124. Chou, T.-C. Theoretical Basis, Experimental Design, and Computerized Simulation of Synergism and Antagonism in Drug Combination Studies. *Pharmacol. Rev.* **2006**, *58*, 621–681.

Aims of the PhD project

This project aims at bringing new information on two main research axes: absorption, distribution, metabolism and excretion (ADME) of single lipophilic toxins as well as mixture effects.

As described before, only limited information is known regarding the intestinal absorption and the metabolism of PTX-2, SPX-1 or YTX. If previous data has been published, a complete characterization is missing: to which extent is these toxins absorbed, which transporters are involved, to which extent is these toxins metabolized, the involved enzymes in the biotransformation processes, the metabolites produced, their structural elucidation as well as their activity are all questions to be answered. Establishing pharmacokinetic data using *in vivo* experiments is beyond the scope of this Ph.D project. Instead, a combination of *in vitro* tools will be employed to answer the raised questions. Besides, lipophilic toxins are often co-occurring in shellfish matrices. Many different mixtures have been reported. Thus, it is of importance to assess the toxicity of these mixtures since it could result in increased toxicity. Preliminary investigation will pinpoint, based on combinations mostly reported, which harmful effects can be highlighted due to mixtures exposure in *in vitro* assays.

Therefore, the main goals of this project were to:

- Assess the intestinal passage of lipophilic phycotoxins through Caco-2 monolayers
- Assess the metabolism of lipophilic phycotoxins using liver fractions and HRMS method
- Decipher the metabolic pathways involved in lipophilic phycotoxins biotransformation
- Investigate the molecular modes of action by q-PCR approach and transactivation assay
- Assess possible mixture effects using a panel of *in vitro* toxicity endpoints on intestinal cells

Chapter 4: Material and Methods

I. *In vitro* cell lines

1. HepaRG/HepG2

HepaRG is a cell line derived from a human hepatocarcinoma isolated at the end of the 1990s. This cell line differentiates into morphologically and functionally human hepatocytes-like cells (Guillouzo et al., 2007). Indeed, after low density seeding, the cells proliferate to confluence and differentiate into two cell types: hepatocytes that form cell aggregates surrounded by biliary-like cells. At the end of the differentiation period, the hepatocyte population reaches approximately 50% and exhibits the following metabolic characteristics: expression of most phase I and II enzymes, expression of major membrane transporters, CYP inducibility via nuclear receptors, bioactivation of toxic metabolites (Kanebratt et al., 2008). The expression of the majority of CYP makes the HepaRG model a remarkable model for *in vitro* studies (Andersson et al., 2012). In addition, the CYP mRNAs are expressed at levels comparable to those of human hepatocytes in primary culture (Antherieu et al., 2012). The same is oserved for the phase II enzymes and efflux transporters: GST and UGT as well as MDR and MRP carriers. The activities are also regulated by the presence of the AhR, CAR and PXR receptors, whose mRNAs are expressed at levels comparable to those found in human hepatocytes in primary culture. Thus, HepaRG cells represent a formidable alternative to human hepatocytes in primary culture, which are still considered as "gold standard" despite certain disadvantages (low availability, moderate proliferation, limited lifetime and loss of metabolic activity over time and reproducibility due to variability in donors' phenotypes).

HepG2 is also a cell line derived from a human hepatocarcinoma. It is the "historical" hepatic cell line which has been used since the early 1980s. Easy to handle, numerous studies on drug metabolism and toxicology have been published with this model despite poor levels of metabolic enzymes expression such as CYP and low inducibility (Gomez-Lechon et al., 2017). Some clones have shown to exhibit higher CYP levels as well as a better inducibility. The HepG2 can also be used in the investigation of metabolic bioactivation when incubated with external system such as S9 liver fraction. In this purpose, Yoshitomi et al., 2001 have established transformants expressing differents CYP subtypes in HepG2 which were used for examining the genotoxicity of metabolites (Hashizume et al., 2011).

2. HEK-T

HEK-T is a cell line derived from human embryonic kidney isolated at the end of the 1970s. This cell line has been extensively used in stably transfected forms to study cellular processes in different areas such as neurobiology or toxicology (Thomas et al., 2005). HEK-T cells are successful due to easy and fast maintenance, easy-to-do transfection using a wide variety of methods and high efficiency of transfection and protein production (Thomas et al., 2005). Plasmid constructs to study the activation of nuclear receptors such as PXR were developed successfully (Luckert et al., 2013).

3. Caco-2

Caco-2 is a cell line derived from a human colocarcinoma and was isolated in the early 1970s (Fogh and Trempe, 1975). This cell line differentiates into morphologically and functionally human enterocytes-like cells (Hidalgo et al., 1989). Indeed, the cells proliferate to confluence and naturally differentiate into intestinal enterocytes. The expression levels of CYP in Caco-2 cells are highly variable and may depend on the state of differentiation, the different cell clones and the culture conditions specific to each laboratory (Sambuy et al., 2005). On the other hand, GST and sulfotransferase enzymes are widely expressed. As they express the majority of intestinal carriers and produce tight junctions mimicking an epithelial monolayer, Caco-2 cells are attractive as a remarkable model for studying the intestinal absorption of xenobiotics (passive diffusion and active transport) (Artursson et al., 2001; Matsson et al., 2005).

II. Metabolism investigation

1. S9 incubations

The use of an external metabolic activation system has been widely spread for investigation of drug metabolism. It represents a very useful tool for preliminary studies since it is cheap, easy to use and fast. Moreover, a large variety of different S9 species are available commercially, allowing a pre-screening investigation for animal specific responses. S9 are obtained from centrifuged liver homogenates (Figure 32) whether from animals treated with metabolic enzymes inducers or not. They gather both cytosol and microsomes, permitting both phase I and II investigations.

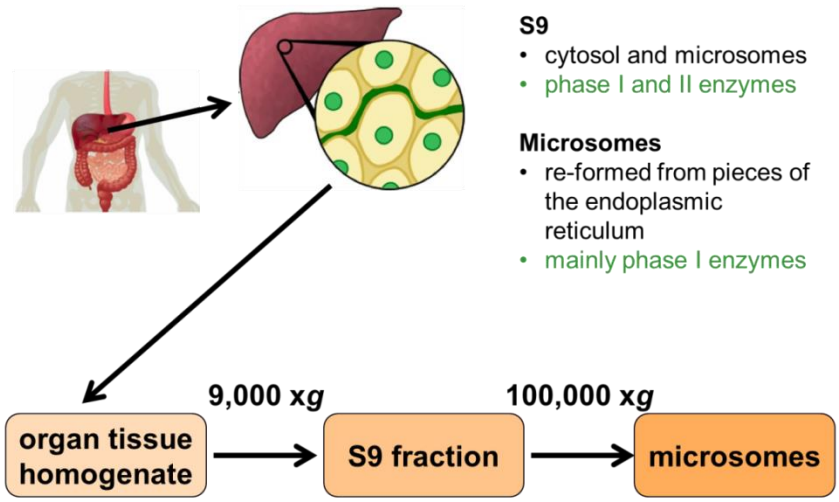

Figure 32: S9 and microsomes preparation (from Katrin Kittler 2012)

S9 fractions allow the screening of multiple biotransformation reactions depending on which specific co-factors are added to the incubation medium. Table 14 sums the different reactions that have been investigated in this work:

Table 14: Co-factors for xenobiotic metabolism investigations using S9 fractions

Hxdroxylation	Sulfation	Glucuronidation	GSH conjugation	Methylation
Na/H_3PO_4 buffer	Na/H_3PO_4 buffer	Na/H_3PO_4 buffer	Na/H_3PO_4 buffer	Na/H_3PO_4 buffer
NADP+	PAPS	Alamethicin	GSH reduced	SAM
Glucose-6-phosphate	$MgCl_2$	UDPGA/ d-saccharolactone	$KCl/MgCl_2$	$MgCl_2$
$KCl/MgCl_2$		$MgCl_2$		

2. Silensomes™

Silensomes™ are a new *in vitro* tool developed by Biopredic International. Silensomes™ are human pooled liver microsomes in which a single CYP has been chemically and irreversibly inactivated using mechanism based inhibitors. It proved to have better predictability than recombinant CYP towards several drug CYP-mediated metabolism studies. Nine Silensomes™ have been developed to date: CYP1A2, 2A6, 2B6, 2C8, 2C9, 2C19, 2D6, 2E1 and 3A4. By comparing the depletion curves of silensomes and their controls, it is possible to determine the contribution of a CYP (fm) to the metabolism of a tested compound (Figure 33).

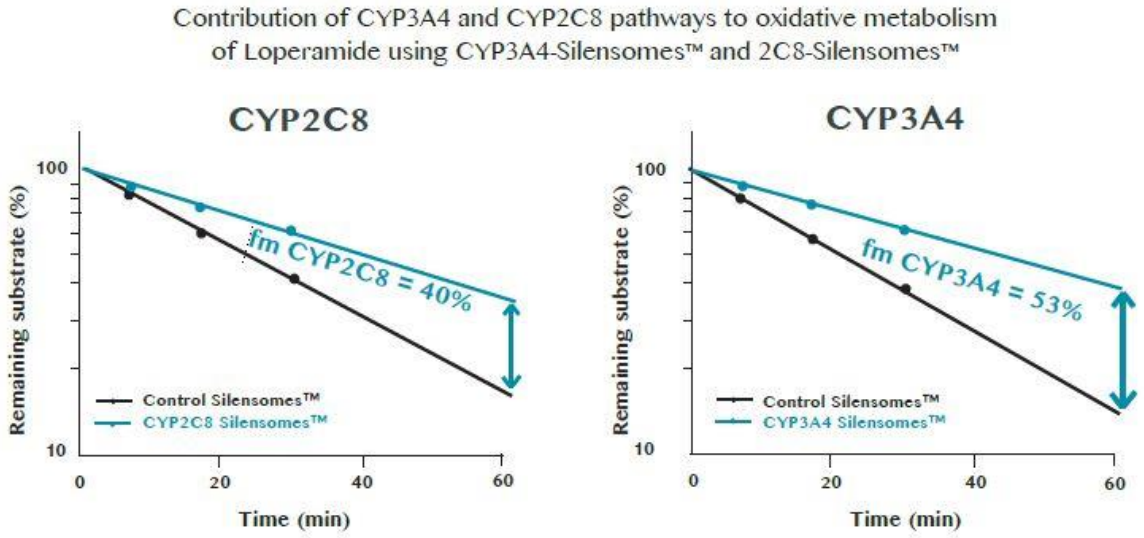

Figure 33: Example of CYP phenotyping assay (from Biopredic)

3. LC/HRMS

S9 or silensomes incubations allow the formation of metabolites but their detection and identification require analytical tools. In this Ph.D project, we used a combined approach to perform

the quantification of the tested compounds as well as the investigation of metabolites formation using liquid chromatography coupled to mass spectrometry. We developed a dosing method using high-resolution mass spectrometry: this technique allows the screening of a large window of m/z (typically 100 to 2000 m/z), which is appropriate for metabolites investigation (characterized by gain or loss of m/z compared to the m/z of the parent compound). The establishment of a calibration curve (Figure 34) allows the quantification of the remaining tested compound after S9 or silensomes incubations. The table 15 sums the different parameters of the HRMS method. The loss of the tested compound is a first indication for metabolism process involvement.

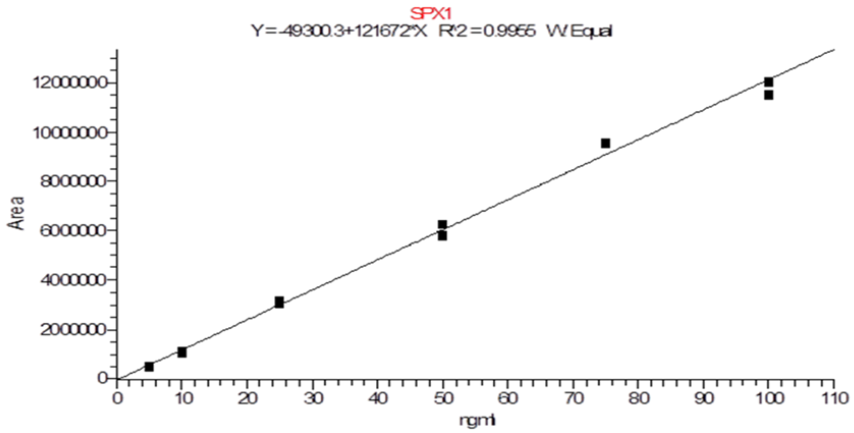

Figure 34: SPX-1 calibration curve

Table 15: Limits of detection and quantification for the phycotoxins

Phycotoxin	ESI	m/z	RT (min)	LOD (ng/ml)	LOQ (ng/ml)
OA	-	803.46	5.25	0.31	1.4
YTX	-	1141.47	5.31	0.37	1.7
PTX-2	+	876.51	8.48	0.25	1.1
SPX-1	+	692.45	5.74	0.76	3.4

Metabolites investigation was performed with the metabolite research software MetWorks® 1.3. This bank of metabolic reactions is based on mass shifts. After indicating the m/z of the tested compound, theoretical masses corresponding to biotransformation reactions are automatically calculated. If a metabolite is detected inside the 100 → 2000 m/z window, then the peak corresponding to the theoretical reaction is outlined. An example is depicted in Figure 35: first row corresponds to the PTX-2 and second and third rows show peaks of hydroxylated PTX-2. MetWorks® contains about 80 reactions grouped in different modules: phase I reactions, phase II reactions, phase I+II reactions, etc.

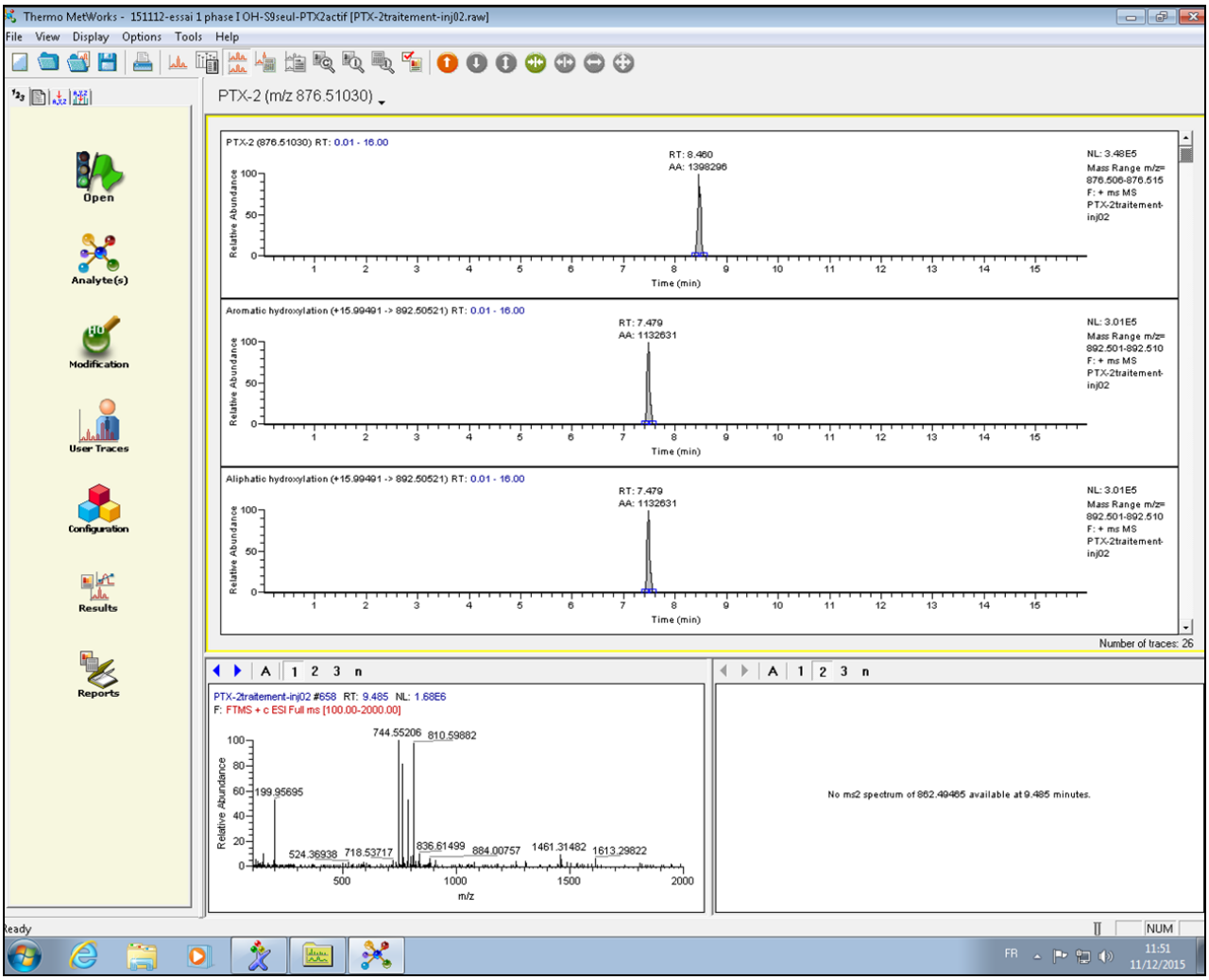

Figure 35: Metworks® software interface. Metabolites investigation is depicted with PTX-2

III. High Content Screening

High Content Analysis designates an approach widely used in drug discovery. It consists of simultaneous screening of multiple cellular markers. The immunostaining of proteins is certainly the most common analysis. By selecting distinct wavelengths for the fluorescent antibodies, it is possible to measure generally up to 4-5 markers concomittantly.

After treatment with the test substance, the cells are fixed then labeled with the antibodies. The cell nuclei are first detected through DNA-staining (ie DAPI), and then the cytoplasm is delimited (Figure 36). Once each cell is fully distinguished, fluorescence is measured at different wavelengths in the selected compartments. The results are displayed both through cell images and mean values of fluorescence for each channel.

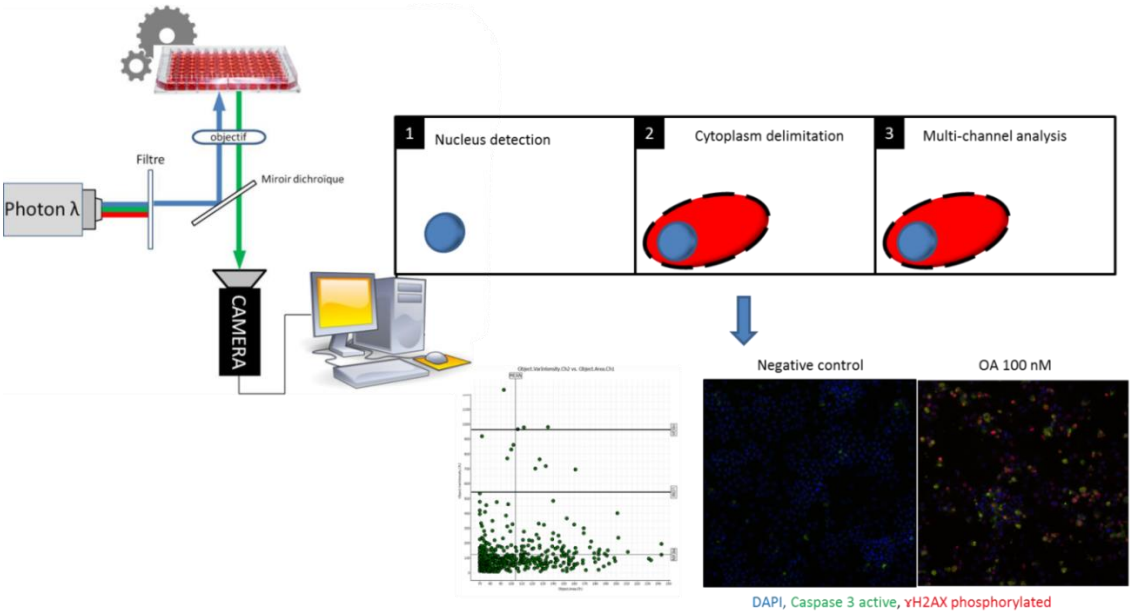

Figure 36: Principle of ArrayScan VTi Thermofischer

Markers used in toxicology cover a wide range of cellular events: apoptosis, genotoxicity, inflammation, oxidative stress, receptor translocation, cell cycle, mitochondrial toxicity, etc. The table 16 sums the different markers that have been investigated in this work:

Table 16: Markers used in High Content Screening investigations

Biological Pathway	Protein	Antibody
Apoptosis	Caspase 3	rabbit anti active caspase-3 (ab13847): 1/1000
Genotoxicity	H2AX	mouse anti γH2AX ser139 (ab2893): 1/1000
	CYP3A4	rabbit anti-CYP3A4 (ab3572): 1/1000
Metabolism	CYP1A2	mouse anti-CYP1A2 S19 (ab22717): 1/1000
	AhR	mouse anti-AhR RTP1 (TF #MA1-514): 1/1000
Oxidative stress	Nrf-2	rabbit anti-Nrf2 (ab31163): 1/1000

IV. Nuclear receptors activation

Investigation of the activation of nuclear receptors such as PXR or CAR by toxins was made using transactivation assays. The principle of such assay is schematized in Figure 37: two plasmids are transfected in a host cell. One plasmid expresses a chimeric transcription factor composed of the DNA-binding domain (DBD) fused to the ligand-binding domain (LBD). The second plasmid expresses the reporter gene firefly luciferase under the transcriptional control of a thymidine kinase promoter (TK) and an upstream activation sequence (UAS). Following the binding of a ligand to the LBD, the transcription factor is then activated and binds to UAS, thereby activating the expression of firefly luciferase which can be measured by chemiluminescence.

Experimentally, HEK-T or HepG2 cells are transfected with the plasmids. After four to six hours, cells are incubated with the compound to test for 24 h. Then the cells are lysed and after centrifugation a small volume of supernatant is analyzed for luciferase activity by chemiluminescence.

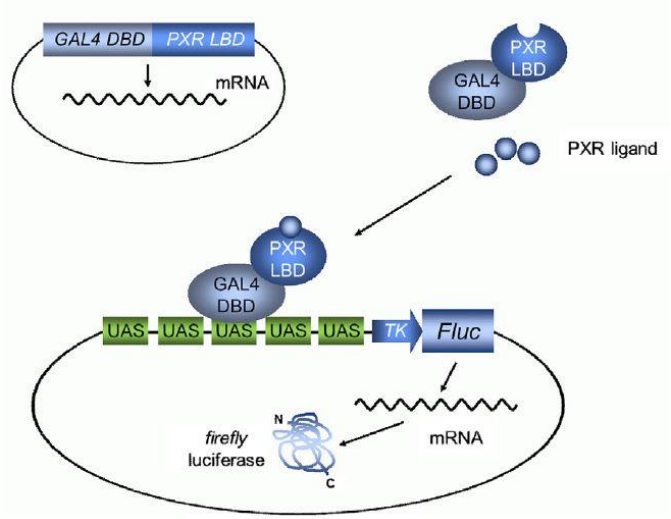

Figure 37: PXR transactivation assay principle (from Luckert et al., 2015)

V. Mixture effects

1. Concept

Mixture effect has become the new great challenge for hazard characterization. Although risk assessment is based on single compounds, chemical contamination is often multiple (exposome concept for instance) and it was shown that compounds could interact resulting in a different toxicity than additivity (whether higher or lower). Mixture effects have been well characterized and several types of responses were depicted depending on the fact that compounds share or not the same mode of action (MOA). Three different scenarios are thus considered: i) when compounds share the same MOA, the “Dose Addition” approach is employed: it considers that all these compounds behave as if they were a simple dilution of each other ii) when compounds have different MOAs but their individual effects have no repercussions on the toxicity of others, the “Response Addition” approach is employed and the final global toxicity is calculated as the sum of each individual toxicity iii) when

compounds are found to interact and thus neither dose addition nor response addition is a suitable approach. Interaction is considered when the effect of a mixture is different from additivity based on the dose-response relationships of the individual compounds. Then, effects are classified as lower than additive (antagonism, inhibition, masking) or greater (synergism, potentiation). Figure 38 sums the different possible cases.

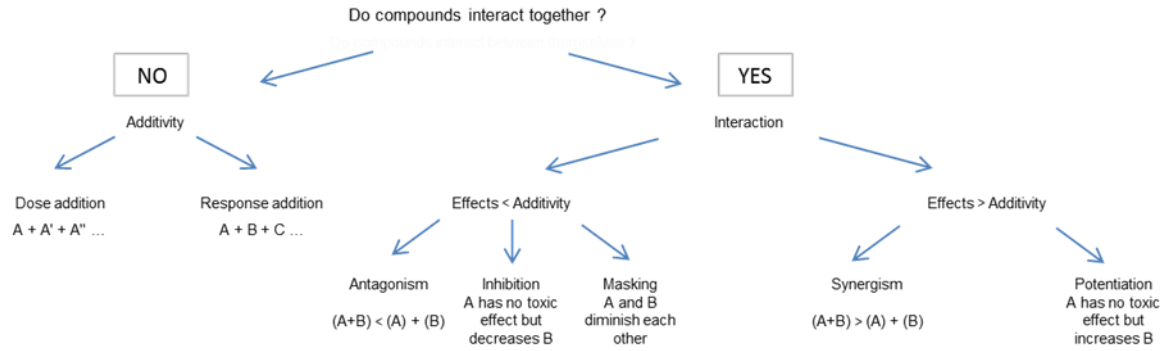

Figure 38: Methodological tree for mixture effects

2. Theoretical additivity method

This method compares the theoretical predicted values calculated from results with single compounds with the measured values obtained with mixtures. In our study with binary phycotoxin combination, the predicted mixture effect value was calculated as follows:

Mix(A+B) predicted value = (mean value A + mean value B) – mean value solvent control

For data expressed as fold change compared to solvent control, mean value of solvent control = 1. Mix(A+B) predicted value < , = and > Mix(A+B) measured value indicate respectively synergism, additive effect and antagonism.

For cell viability analysis, mean value of solvent control = 100. Mix(A+B) predicted value < , = and > Mix(A+B) measured value indicate respectively antagonism, additive effect and synergism.

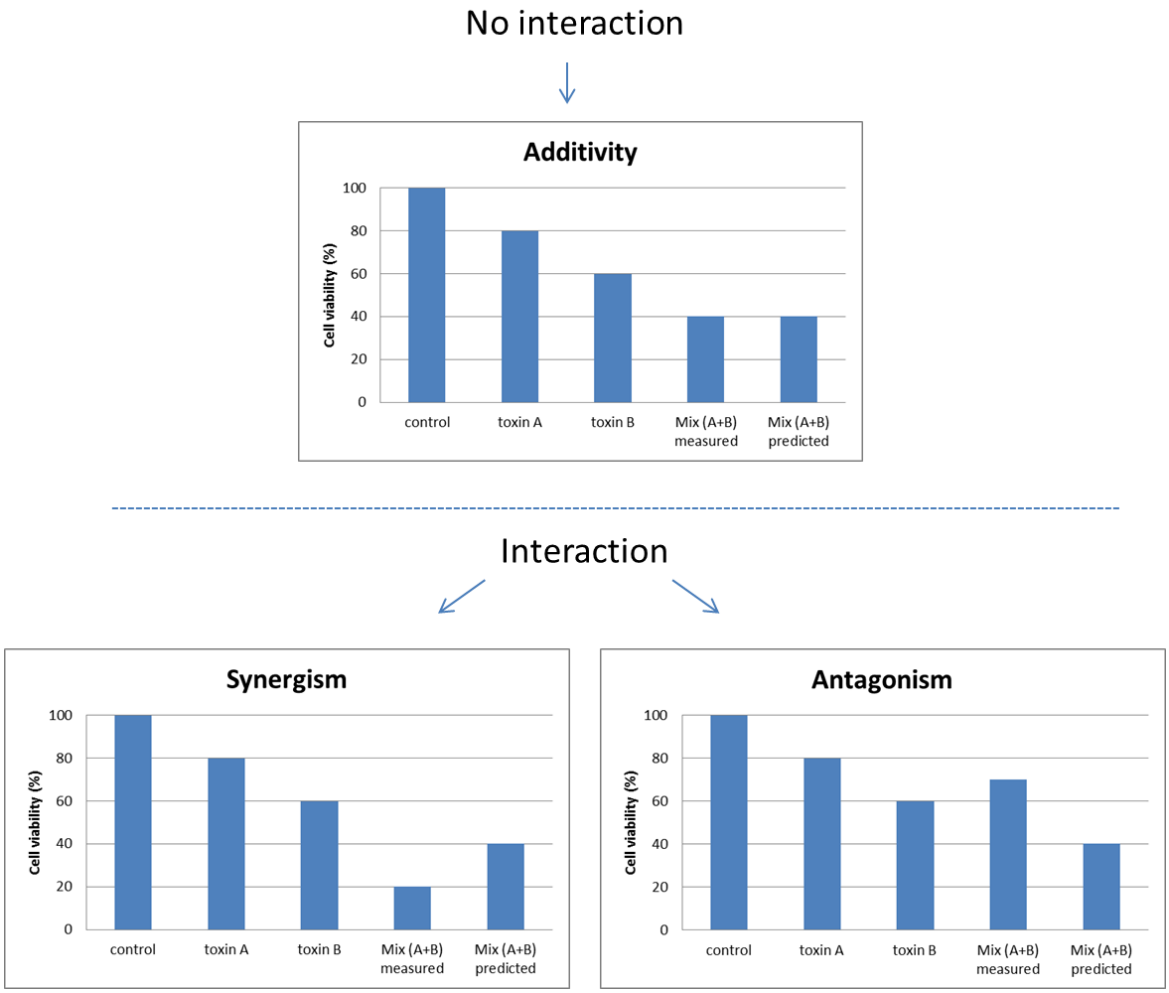

Figure 39: Characterization of mixture effects according to the theoretical additivity method (adapted from Smith et al., 2016)

3. Chou-Talalay method

The Chou-Talalay method (Chou and Talalay 1984) is commonly used to analyze interactions between drugs. For each endpoint, dose-response relationships for toxin alone or in binary combination are modeled using the median-effect equation of the mass action law (Chou 2006):

$fa/fu = (D/D_m)^m$

where D is the dose of the toxin, D_m is the median-effect dose, fa is the fraction affected by D, fu is the fraction unaffected (fu = 1 − fa) and m is the coefficient signifying the shape of the dose–effect relationship (m = 1, m > 1, and m < 1 indicate hyperbolic, sigmoidal and flat sigmoidal dose–effect curves, respectively).

Interactions between toxins are analyzed using the combination index method (Chou 2006):

$(CI)_x = (D)_1/(D_x)_1 + (D)_2/(D_x)_2$

where $(CI)_x$ is the combination index at x% effect, $(D)_1$ and $(D)_2$ are the doses of toxins that exert x% effect in binary combination, $(D_x)_1$ and $(D_x)_2$ are the doses of each toxin alone that exerts x% effect. CI < 1, =1 and >1 indicate respectively synergism, additive effect and antagonism.

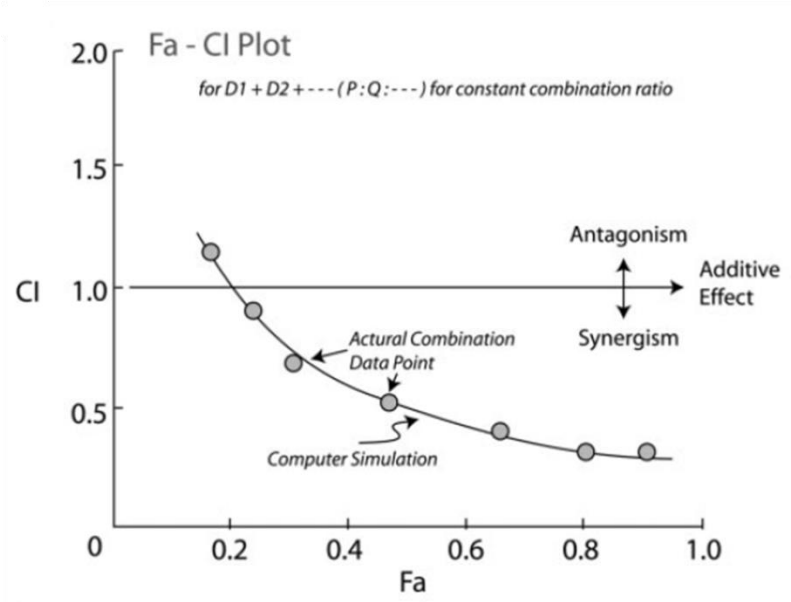

Figure 40: Characterization of mixture effects according to the Chou-Talalay method (from Chou 2006)

Results

"Phycotoxins ADME" axis

Preliminary results: Investigation on the intestinal passage of the marine biotoxins PTX-2 and SPX-1

In this section, we present the preliminary results obtained from our investigation on the passage of PTX-2 and SPX-1. OA passage was not assessed since published data already exist (Ehlers et al., 2011, 2014). YTX passage could not be investigated due to technical issues (binding to the membrane of the Transwell). Although the results are presented using the structure of a research article, additional data including both repetitions of some assays and addition of other selected assays are necessary before submitting this work. Complementary studies will be suggested in the discussion section.

1. Introduction

Phycotoxins are some of the main food contaminants stemming from the seas. Produced by a restricted variety of phytoplanktonic species (Lee et al., 1989, Draisci et al., 1996, Cembella et al., 2000), they accumulate in bivalve filtering species and can cause harm to humans. Phycotoxins have been classified into different families according to their structure and effects. Among the group of pectenotoxins, pectenotoxin 2 (PTX-2) is the most documented compound. If no direct correlation between PTX-2 shellfish contamination and human poisoning syndrome could be ascertained (Miles et al., 2004, Ito et al., 2008), some gastro-intestinal symptoms have been observed in rodents. For instance, increase of intestinal fluid after oral administration to mice has been depicted (Ito et al., 2008, Ishige et al., 1988) and some hepatic injuries after intraperitoneal injection were also observed (Terao et al., 1986). The mode of action of PTX-2 was shown *in vitro* to be actin depolarization leading to cytoskeleton disruption (Espina et al., 2008).
Spirolide 1 - or 13-desmethyl spirolide C - (SPX-1) belongs to the group of cyclic imines. Although no effects in humans have been reported so far, SPX-1 was shown to be particularly potent in rodents, inducing rapid death to mice by intra-peritoneal injection (ip) or gavage (Munday et al., 2011). SPX-1 acts through inhibition of muscle and neuronal nicotinic acetylcholine receptors with high affinity interaction (Aráoz et al., 2015). SPX-1 was shown to easily cross a monolayer of intestinal Caco-2 cells (Espina et al., 2011), suggesting a wide distribution to systemic organs that was also highlighted *in vivo* since SPX-1 was found in blood, urine and faeces after a single oral administration to mice (Otero et al., 2012).
Although both PTX-2 and SPX-1 can apparently cross the intestinal barrier, some quantitative data on the bioavailability for the two toxins are still missing and the pathways involved must be clarified. Bioavailability is linked to the systemic toxicity of a compound. Paracellular and transcellular processes regulate the absorption of compounds across the intestinal epithelium. Hydrophilic molecules are more likely to permeate through the paracellular way although membrane-bound transporters can also be involved for some hydrophilic drugs to enter into the cells (El-Kattan and Varma 2012).
In this study we assessed the passage of PTX-2 and SPX-1 using monolayers of Caco-2 cells.

2. Materials and Methods

2.1. Chemicals

PTX-2 and SPX-1 standards were purchased from the National Research Council Institute for Marine Biosciences (Halifax, NS Canada). Neutral red powder (N4638) and fluorescein isothiocyanate–dextran (average mol wt 10,000) were purchased from Sigma-Aldrich (St. Louis, MO, USA). All other chemicals including acetonitrile (ACN), methanol (MeOH) and dimethyl sulfoxide (DMSO) were of analytical grade and purchased from Fisher Scientific (Leicestershire, England). Formic acid was purchased from Merck (Darmstadt, Germany). Deionised water was prepared using a Milli-Q system (Millipore, Bedford, MA, USA).

2.2. Cell culture

Caco-2 cells were obtained from the European Collection of Cell Cultures (Porton Down, UK). Cells (passages 30–35) were seeded at 60,000 cells/cm^2 in 12-transwell inserts (1.12 cm^2 growth area, 0.4 µm pore size, polycarbonate membranes; Corning Incorporated Costar, Cambridge, MA, USA) plates in culture medium (Dulbecco's modified Eagle's medium, supplemented with 10% fetal bovine serum, 100 IU/ml penicillin and 100 µg/ml streptomycin). Cells were cultured for 3 weeks with renewal of medium every 2 to 3 days. For cytotoxicity assays, cells were seeded at 10,000 cells/cm^2 in 96-well microplates.

2.3. Cytotoxicity assays

Following 24 h treatment with the toxins, cells were rinsed in PBS. Neutral red solution was added to each well and incubated 2 h at 37°C. Cells were then rinsed in PBS, and 100 µL of solubilization solution (1% acetic acid in 50% ethanol) were added to each well. Absorbance was read at 540 nm using a Fluostar Omega microplate reader (BMG Labtek), and viability was calculated as the percentage of mean absorbance to the solvent control condition.

2.4. Transwell assays

Transport experiments were conducted by changing the culture medium with new medium without FBS containing PTX-2 (1.14 % MeOH) or SPX-1 (0.7 % MeOH) at concentrations of 50 or 500 nM loaded whether in the apical or in the basolateral compartment for PTX-2 and only in the basolateral compartment for SPX-1 since apical passage was previously studied (Espina et al., 2011). At different times, medium from both chambers of the transwell was collected and stored at −20°C until HPLC–MS/MS analysis. As an endpoint for monolayer integrity, the passage of the paracellular leakage marker sodium fluorescein was determined. After the addition of 50 µM fluorescein isothiocyanate–dextran to the apical side, crossing of fluorescein in the basolateral medium was measured at different time points with a Fluoroskan Ascent (Thermo Scientific, Waltham, MA, USA) (excitation wavelength 485 nm, emission wavelength 520 nm).

2.5. Calculation of the permeability coefficient P app

The permeability coefficient P app was calculated using the following formula:

$$P_{app}\ (cm/s) = (c \times V) / (t \times A \times c0)$$

where c, V, t, A and c0 represent the concentration in acceptor compartment (ng/ml), the volume of acceptor compartment (cm^3), the time (s), the surface area (cm^2) and the initial concentration in donor compartment (ng/ml), respectively.

2.6. LC/MS-MS analysis

The analyses were conducted on the Thermo Fisher Scientific Ultimate 3000 (Thermo Fisher, Bremen, Germany) system coupled to a TSQ Quantiva mass spectrometer. Chromatographic separation was

carried out on a Thermo Hypersil Gold C18 column (Thermo Fisher, Bremen, Germany) (150 × 2.1 mm, 1.9 µm) using two mobile phase preparations, consisting of mobile phase (A), 100% water, and mobile phase (B), 5% water and 95% acetonitrile. Both mobile phases contained 2 mM of ammonium formate and 50 mM of formic acid. The gradient conditions were as follows: from 0 to 1 min, 90% of mobile phase A, then from 1 to 6 min, linear ramp from 90% to 10% of mobile phase A and hold for 6 min, then ramp back over 0.5 min to initial conditions and hold for 5 min to re-equilibrate the system. The flow rate was set at 0.2 mL× min^{-1}, the injection volume was 10 µL, and the column oven was maintained at 40 °C. PTX-2 and SPX-1 were quantified using a calibration curve with toxin standards at 0, 5, 10, 25, 50, 75, and 100 ng/mL in MeOH-water (66.6:33.3, v/v). The mass spectrometer was operated with an electrospray ionization probe in positive mode using the following source parameters: sheath gas flow rate: 40 arb; auxiliary gas flow rate: 10 arb; sweep gas flow rate: 1 arb; ion spray voltage: 4.0 kV; capillary temperature: 335 °C. The analytes were detected by Selected Reaction Monitoring (SRM). For analyte identification and quantification, toxin specific transitions to product ions were chosen: PTX-2, 876.7>823.5 (CE: 22 V) and 876.7>805.5 (CE: 24 V) for identification and 876.7>787.5 (CE: 27 V) for quantification; SPX-1, 692.6>674.5 (CE: 29 V) and 692.6>444.4 (CE: 36 V) for identification and 692.6>164.1 (CE: 45 V) for quantification. The mass spectrometer was operated in unit resolution (0.7 amu). The toxin recoveries were calculated as follows: Ri = (ci × 100)/c0, where ci is the measured concentration of the sample i, and c0 is the initial concentration. Based on S/N, LOD and LOQ were estimated at 7.5 and 25 pg/ml, respectively.

3. Results

3.1. Effects of PTX-2 and SPX-1 on cell viability

After 24 h treatment, neither PTX-2 up to 500 nM nor SPX-1 up to 510 nM had effect on cell viability (Figure 1). Based on these results, we selected two concentrations for passage investigation: one low (50 nM) and one high (500 nM).

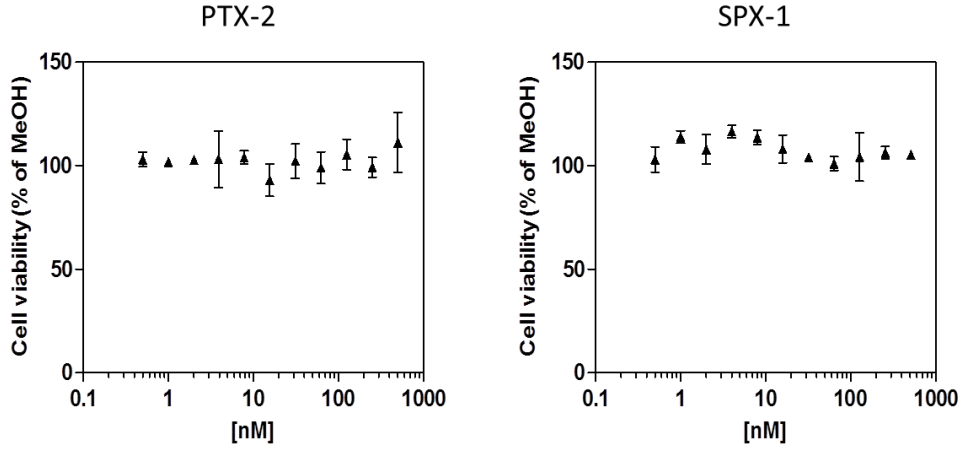

Figure 1. Cell viability in differentiated Caco-2 cells. After 24 h of treatment with different concentrations of PTX-2 or SPX-1, cytotoxicity was measured using NRU assay. The results were obtained from three independent experiments performed in triplicate (mean ± SD).

3.2. Effects of PTX-2 and SPX-1 on the integrity of Caco-2 monolayers

The disruption of monolayers integrity was assessed with the permeability of fluorescein (Fluorescein isothiocyanate–dextran). The monolayer integrity is considered altered when a P app ≥ 10^{-6} cm/s is obtained. No effect of the solvent control (up to 1.14% MeOH) was observed when incubated in the apical or in the basolateral compartment. A low concentration (50 nM) of apical PTX-2 induced a

weak leakage of FITC-dextran only after 24 h of incubation (Figure 2a) but without altering the monolayer integrity (P app < 10^{-6} cm/s). On the contrary, a high concentration (500 nM) of apical PTX-2 largely affected the FITC-dextran passage after only 2 h of treatment. FITC-dextran passage reached a maximum after 6 h. When a low concentration (50 nM) of PTX-2 was loaded in the basolateral compartment, a potent leakage of FITC-dextran occurred only after 24 h of incubation (Figure 2b). With a high concentration (500 nM) of basolateral PTX-2, FITC-dextran crossed largely after 6 and 24 h of treatment. These results show that a high concentration of PTX-2 disrupts the Caco-2 cell monolayer. Regarding SPX-1, no effect on the permeability of the FITC-dextran was detected (P app < 5.10^{-7} cm/s) with a 10 h treatment up to 500 nM in the basolateral compartment.

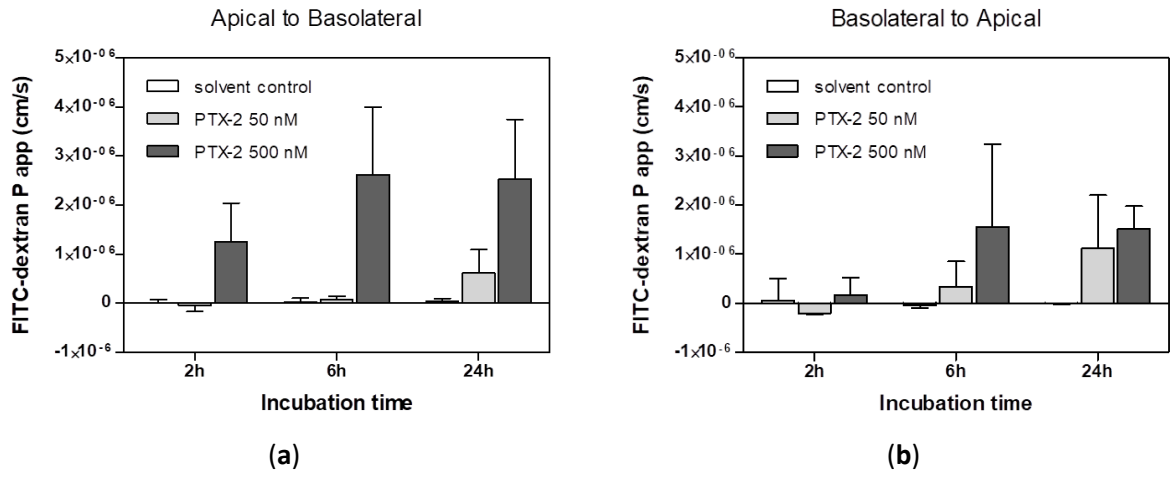

Figure 2. PTX-2 effects on the paracellular permeability of the monolayers of Caco-2 cells. Fluorescein was incubated in the apical compartment and measured in the basolateral compartment. (a) and (b) depict fluorescein passage after PTX-2 treatment in the apical or in the basolateral compartment. Results were obtained from three independent experiments. Data represents means ± SD.

3.3. Passage of PTX-2 and SPX-1 throught monolayers of Caco-2 cells

3.3.1. Transport of PTX-2

In order to assess if PTX-2 can cross the intestinal barrier, the amount of toxin in the two compartments was measured only for the time points where no alteration of the integrity of the Caco-2 monolayers was reported. From apical to basolateral, 50 nM PTX-2 was barely detected in each compartment respectively (Figure 3).

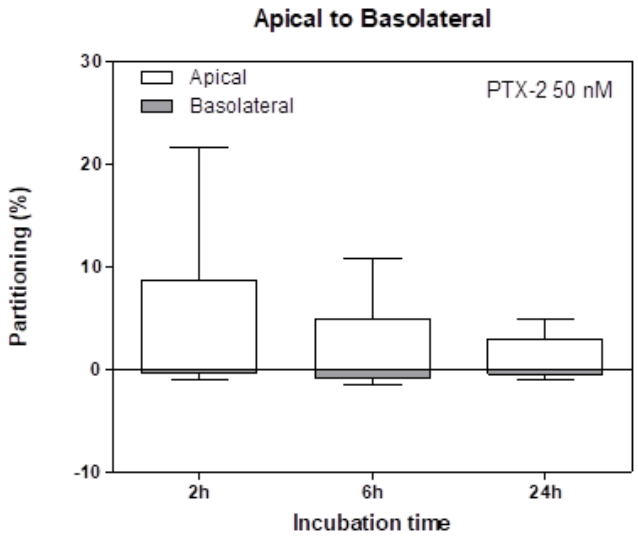

Figure 3. PTX-2 partitioning after incubation with monolayers of Caco-2 cells. 50 nM of PTX-2 was loaded in the apical compartment and incubated for different times. Recoveries were determined by measuring the PTX-2 amount in both apical and basolateral compartments. Results were obtained from three independent experiments. Data represents means ± SD.

Calculations of passage and coefficient of permeability indicated almost no crossing whatever the time of treatment (Table 1).

Table 1. PTX-2 transport accross Caco-2 cell monolayers. 50 nM of PTX-2 was loaded in the apical compartment and incubated for different times. PTX-2 was then dosed in each compartment. Results were obtained from three independent experiments. Data represents means ± SD.

Incubation time	Passage (%)	P app (cm/s)
2h	0.4 ± 0.6	$6.8\times10^{-7} \pm 1.2 \times10^{-6}$
6h	1.0 ± 0.6	$6.0\times10^{-7} \pm 3.8 \times10^{-7}$
24h	0.5 ± 0.5	$8.0\times10^{-8} \pm 7.1 \times10^{-8}$

For the passage from basolateral to apical, PTX-2 was detected in the apical compartment (Figure 4).

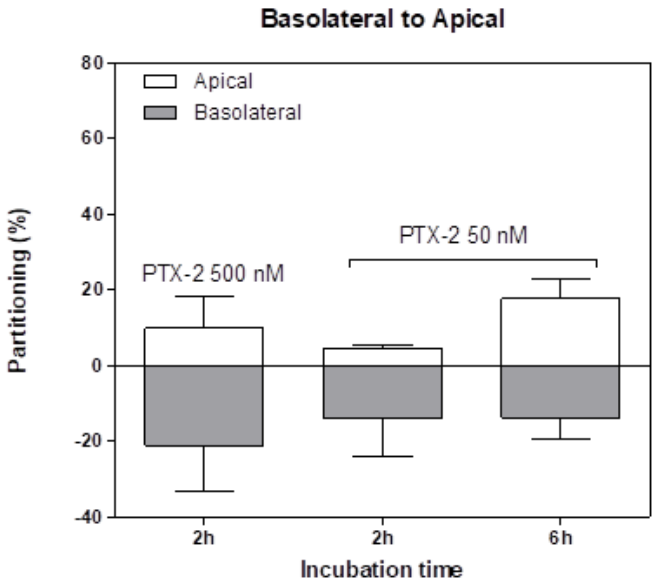

Figure 4. PTX-2 partitioning after incubation with monolayers of Caco-2 cells. 50 and 500 nM of PTX-2 were loaded in the basolateral compartment and incubated for different times. Recoveries were determined by measuring the PTX-2 amount in each compartment. Results were obtained from two independent experiments. Data represents means ± SD.

The passage was dose- and time-dependent with a maximal crossing around 18% for 50 nM of PTX-2 and 6 h incubation (Table 2). This higher passage was confirmed by higher P app values (Table 2). The calculation of efflux ratios (P app B/A ÷ P app A/B) showed an extensive role of elimination process at 6 h for 50 nM of PTX-2 (Figure 5).

Table 2. PTX-2 efflux through Caco-2 cell monolayers. 50 and 500 nM of PTX-2 were loaded in the basolateral compartment and incubated for different times. PTX-2 was then dosed in each compartment. Results were obtained from two independent experiments. Data represents means ± SD.

Incubation time	Passage (%)	P app (cm/s)
PTX-2 (500 nM) 2h	4.6 ± 1.1	$2.8\times10^{-6} \pm 6.5 \times10^{-7}$
PTX-2 (50 nM) 2h	9.7 ± 8.5	$6.0\times10^{-6} \pm 5.3 \times10^{-6}$
PTX-2 (50 nM) 6h	17.8 ± 4.9	$3.7\times10^{-6} \pm 1.0 \times10^{-6}$

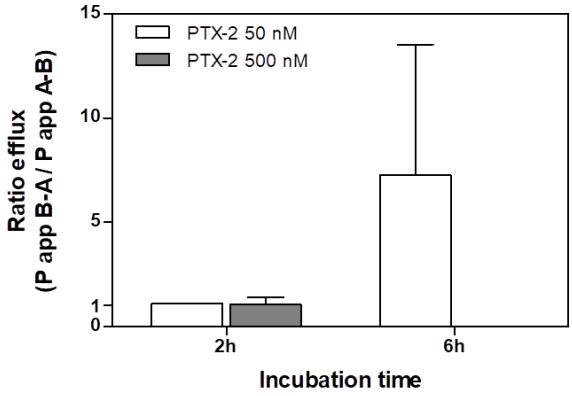

Figure 5. Efflux ratios for PTX-2 transport assay through Caco-2 cell monolayers. 50 and 500 nM of PTX-2 were loaded whether in the apical or in the basolateral compartment and incubated for different times. Results were obtained from two independent experiments. Data represents means ± SD.

3.3.2. Basolateral-apical passage of SPX-1

In order to assess if SPX-1 elimination can occur, the passage from the basolateral to the apical compartment was investigated with two concentrations (50 and 500 nM) at different times using monolayers of Caco-2 cells. SPX-1 was highly detected in the apical compartment (Figure 6). The passage was dose but not time dependent (Figure 7a). With the high dose of SPX-1, more than half of the loaded amount was detected in the apical compartment after 3 h. The longer incubation times did not show any increase of SPX-1 crossing. With the low dose of SPX-1, approximately one third of the loaded amount was detected in the apical compartment after 3 h. The longer incubation times depicted only a slight increase of SPX-1 crossing. For all cases P app values were in the 10^{-5} cm/s range (Figure 7b).

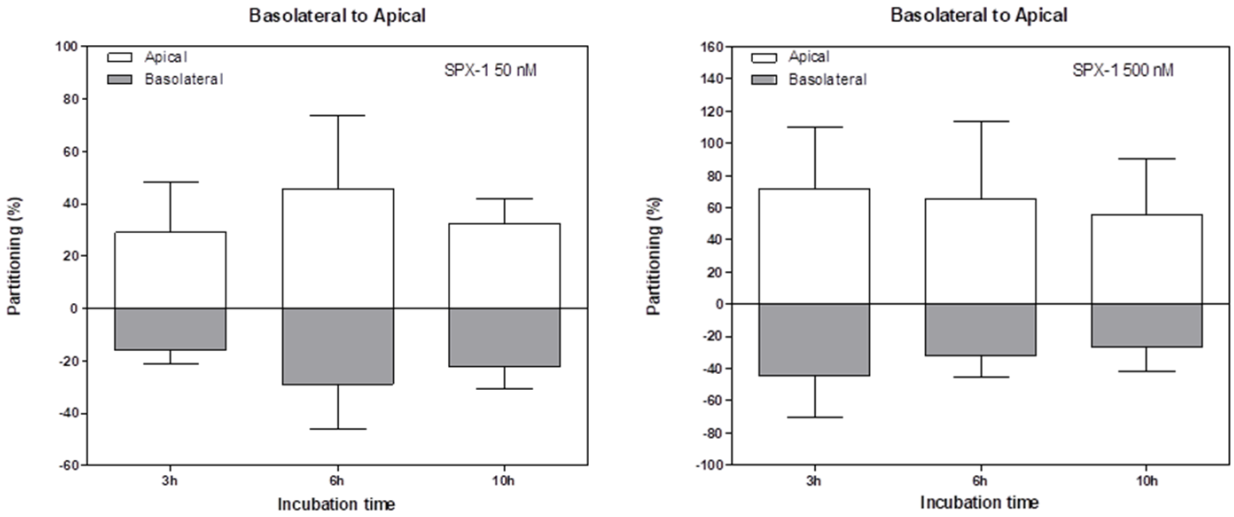

Figure 6. SPX-1 partitioning after incubation with monolayers of Caco-2 cells. 50 and 500 nM of SPX-1 were loaded in the basolateral compartment and incubated for different times. Recoveries were determined by measuring the SPX-1 amount in each compartment. Results were obtained from three independent experiments. Data represents means ± SD.

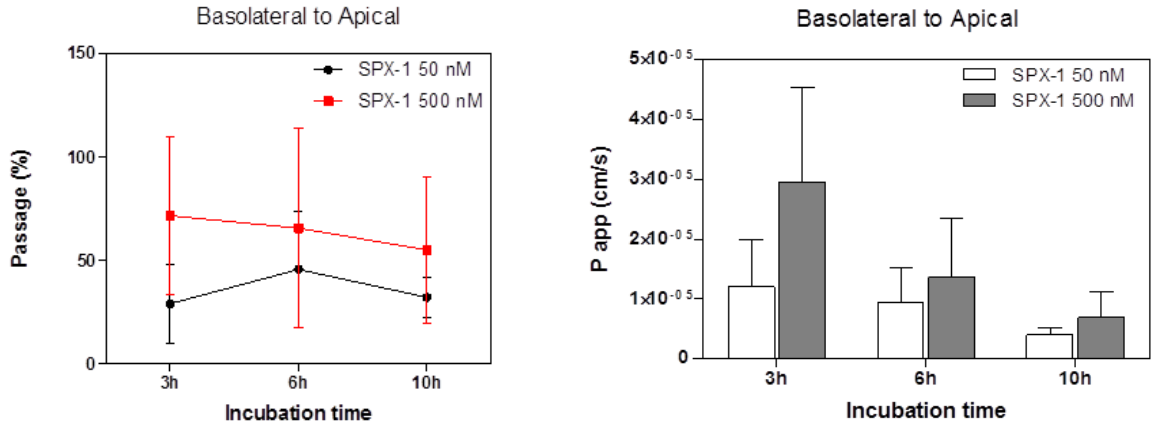

(a) (b)

Figure 7. SPX-1 passage through Caco-2 cell monolayers. 50 and 500 nM of SPX-1 were loaded in the basolateral compartment and incubated for different times. SPX-1 was then dosed in each compartment. (a) depicts the percentage of crossing and (b) depicts the coefficients of apparent permeability. Results were obtained from three independent experiments. Data represents means ± SD.

4. Discussion

In this study, we investigated the transport of PTX-2 and SPX-1 through monolayers of Caco-2 cells. Our results on fluorescein permeability showed that 500 nM of PTX-2 induces leakage of the fluorescein after only 2 h. This indicates that PTX-2 disrupts the tight junctions. This particular network between two adjacent cells is composed mainly of claudins and occludins (Anderson and Itallie 2009). In fact, other proteins such as ZO-1 that play a scaffold role between these transmembrane proteins and the actin filaments inside the cell are also found (Itoh et al., 1997). PTX-2 is known to induce the depolymerization of actin filaments that could provoke the disruption of the tight junctions, explaining the passage of fluorescein.

Our data showing low recoveries correlate with *in vivo* studies by Burgess 2003 that showed that only 19% of PTX-2 was detected in the whole body following 24 h after administration of a single oral dose of 5.7 µg per mice. PTX-2 was found in the gastrointestinal content and faeces, with only traces in the gastro-intestinal tissue. No detectable amounts were found in other internal organs and urine (Burgess 2003). As the amount found in the apical chamber was below 10% of the loaded amount and that only a weak amount was detected in the basolateral, we expect that a great extent of PTX-2 entered the cells. Possible explanation implies that PTX-2 was kept inside the cells or rather was extensively biotransformed. For instance, using S9 liver fractions, we previously showed that PTX-2 undergoes hepatic phase I metabolism leading to the formation of hydroxylated metabolites (Alarcan et al., 2017). Although the whole metabolic capacity of enterocytes is far lower than hepatocytes, they display some phase I enzymes such as CYP450 which may metabolize PTX-2. In fact, the Caco-2 cells poorly express CYP450 but exhibit high levels of UGTs (Zhang et al., 2011), which could be implicated in PTX-2 metabolism too. Flavin-containing monooxygenases (FMO) that are also expressed in the small intestine catalyze hydroxylation reactions (Cashman and Zhang 2006), but no information is available regarding their expression in Caco-2 cells. A screening of metabolites in both compartments using high-resolution mass spectrometry would help to clarify if any metabolism had occurred. Besides, the dosage of the intra-cellular content should also be performed for possible trapped PTX-2. Nonetheless, it cannot be excluded that these low recoveries result also, to some

extent, from technical issues such as toxin adsorption on the membrane of the Transwell or matrix effect during PTX-2 ionisation.
Our results on the efflux ratios showed a higher basolateral to apical transport compared to the apical to basolateral passage after 6 h. This could suggest the involvement of active transport mechanisms to excrete PTX-2 from the cell. Transporters such as P-gp are known to be implicated in the efflux of a wide variety of compounds and are highly expressed in Caco-2 cells (Elsby et al., 2008). The role of P-gp in the efflux of okadaic acid, another marine biotoxin, was already demonstrated (Ehlers et al., 2014). P-gp may not be the only ABC transporters involved in the efflux of PTX-2 since it was shown that PTX-2 induced an up-regulation of mRNA levels of ABCG2 coding for BRCP in human hepatic cells (Alarcan et al., 2017).

Espiña et al. solely investigated the apical to basolateral passage of SPX-1 and demonstrated a high permeability predicting a human absorption superior to 80%. In this work, as a mean of comparison, we investigated the basolateral to apical passage of SPX-1. However, we did not use a concentration as high as the one by Espiña et al. (0.5 µM versus 1 µM). No permeability to fluorescein was observed after basolateral incubation with SPX-1 up to 10 h indicating no particular disruption of the tight junctions. Recoveries calculated for the high dose of SPX-1 ranged from 82 to 116%, indicating that no biotransformation processes occurred. However, with the low dose, the recoveries were lower, ranging from 45 to 75%. In their paper, Espiña et al. reported no particular loss of compound with their high dose treatment. Our passage data show that SPX-1 is highly excreted to the apical side. This passage is dose-dependent as the higher dose of SPX-1 led to a higher passage to the apical side. However, no time dependency was reported, SPX-1 transport reaching an equilibrium status after 3 h. Contrary to PTX-2, this suggests rather a paracellular or a passive transcellular transport (diffusion or facilitated diffusion) from the basolateral to the apical side of the monolayers. Further assays are needed to decipher by which mechanism SPX-1 is excreted to the apical side.
No human intoxication involving SPX-1 has been reported so far. If Espiña et al. predicted a human absorption superior to 80%, we showed that SPX-1 can be also highly excreted to the apical side. Although the major amount of SPX-1 is likely to reach the bloodstream, it was shown that this toxin undergoes extensive hepatic metabolism (Hui et al., 2012). Therefore, even if a large amount of SPX-1 is absorbed through the intestinal epithelium, the high rate of first-pass metabolism is certainly a crucial element explaining the absence of reported effects in humans.

5. Concluding remarks

From our preliminary investigations, it seems that PTX-2 could undergo a strong biotransformation in enterocytes. However, this assumption needs to be ascertained. Besides, we suggest that only a limited amount of SPX-1 would presumably reach systemic organs due to SPX-1 efflux in intestine coupled to a high rate of metabolism in liver.

6. Experiments planned

Due to some variability between experiments (as evidenced by high standard deviation) as well as a problem in TEER measurement, new experiments should be made to confirm these results. Since 500 nM of PTX-2 disrupted rapidly monolayer integrity, lower doses should be used. Before undergoing experiments with cells, possible adsorption of PTX-2 on the Transwells needs to be checked. After this preliminary verification, the hypothesis of intestinal metabolism can be assessed. For this purpose, the analytical measurements of PTX-2 should be carried on using HRMS in order to investigate possible metabolites. The intra-cellular content should also be checked for possible trapped PTX-2. Finally, it would be of interest to assess the role of few main transporters by competitive inhibition assays. For such purpose, the use of so-called specific fluorescent substrates could be a convenient way to investigate the role of P-gp (rhodamine 123), MRP2 (CDFDA) or BCRP (Bodipy-prazosin).

References

Alarcan J, Dubreil E, Huguet A, Hurtaud-Pessel D, Hessel-Pras S, Lampen A, Fessard V, Le Hegarat L. Metabolism of the Marine Phycotoxin PTX-2 and Its Effects on Hepatic Xenobiotic Metabolism: Activation of Nuclear Receptors and Modulation of the Phase I Cytochrome P450. Toxins (Basel). 2017 Jul 5;9(7).

Anderson JM, Van Itallie CM (2009) Physiology and function of the tight junction. Cold Spring Harb Perspect Biol 1: a002584.

Aráoz R, Ouanounou G, Iorga BI, Goudet A, Alili D, Amar M, et al. The Neurotoxic Effect of 13,19-Didesmethyl and 13-Desmethyl Spirolide C Phycotoxins Is Mainly Mediated by Nicotinic Rather Than Muscarinic Acetylcholine Receptors. Toxicol Sci. 2015 Sep;147(1):156–67.

Burgess VA, 2003. Toxicology investigation with the Pectenotoxin-2 seco acids. National Research Centre for Environmental Toxicology and the School of Public Health. Brisbane, Queensland, Australia, Griffith University, PhD thesis, February 2003.

Cashman J.R., Zhang J. Human flavin-containing monooxygenases. Annu. Rev. Pharmacol. Toxicol. 2006;46:65–100.

Cembella, A.D., Lewis, N.I., Quilliam, M.A., (2000). The marine dinoflagellate Alexandriumostenfeldii (Dinophyceae) as the causative organism of spirolide shellfish toxins. Phycologia 39, 67–74.

Draisci, R., Lucentini, L., Giannetti, L., Boria, P., and Poletti, R. (1996). First report of pectenotoxin-2 (PTX-2) in algae (Dinophysis fortii) related to seafood poisoning in Europe. Toxicon Off. J. Int. Soc. Toxinology 34, 923–935.

Ehlers, A., These, A., Hessel, S., Preiss-Weigert, A., Lampen, A., 2014. Active elimination of the marine biotoxin okadaic acid by P-glycoprotein through an in vitro gastrointestinal barrier. Toxicol. Lett. 225, 311–317.

Ayman El-Kattan and Manthena Varma (2012). Oral Absorption, Intestinal Metabolism and Human Oral Bioavailability, Topics on Drug Metabolism, Dr. James Paxton (Ed.), InTech, DOI: 10.5772/31087. Available from: https://www.intechopen.com/books/topics-on-drug-metabolism/oral-absorption-intestinal-metabolism-and-human-oral-bioavailability-.

Elsby R, Surry DD, Smith VN, Gray AJ (2008). Validation and application of Caco-2 assays for the in vitro evaluation of development candidate drugs as substrates or inhibitors of P-glycoprotein to support regulatory submissions. Xenobiotica 38: 1140–1164.

Espiña B, Louzao MC, Ares IR, Cagide E, Vieytes MR, Vega FV, et al. Cytoskeletal toxicity of pectenotoxins in hepatic cells. Br J Pharmacol. 2008;155(6):934–944.

Espiña B, Otero P, Louzao MC, Alfonso A, Botana LM. 13-Desmethyl spirolide-c and 13,19-didesmethyl spirolide-c trans-epithelial permeabilities: Human intestinal permeability modelling. Toxicology. 2011 Sep;287(1–3):69–75.

Hui JPM, Stuart Grossert J, Cutler MJ, Melanson JE. (2012). Strategic identification of in vitro metabolites of 13-desmethyl spirolide C using liquid chromatography/high-resolution mass spectrometry: Identification of in vitro metabolites of 13-desmethyl spirolide C. Rapid Commun Mass Spectrom. 26(3), 345–54.

Ishige, M.; Satoh, N.; Yasumoto, T. Pathological studies on mice administered with the causative agent of diarrhetic shellfish poisoning (okadaic acid and pectenotoxin-2). Hokkaidoritsu Eisei Kenkyushoho 1988, 38, 15–18.

Ito E, Suzuki T, Oshima Y, Yasumoto T. Studies of diarrhetic activity on pectenotoxin-6 in the mouse and rat. Toxicon. 2008 Mar;51(4):707–16.

Itoh M, Nagafuchi A, Moroi S, Tsukita S. Involvement of ZO-1 in cadherin-based cell adhesion through its direct binding to alpha catenin and actin filaments. J Cell Biol. 1997;138(1):181–92.

Lee, J.-S., Igarashi, T., Fraga, S., Dahl, E., Hovgaard, P., and Yasumoto, T. (1989). Determination of diarrhetic shellfish toxins in various dinoflagellate species. J. Appl. Phycol. 1, 147–152.

Miles CO, Wilkins AL, Munday R, Dines MH, Hawkes AD, Briggs LR, et al. Isolation of pectenotoxin-2 from Dinophysis acuta and its conversion to pectenotoxin-2 seco acid, and preliminary assessment of their acute toxicities. Toxicon. 2004 Jan;43(1):1–9.

Munday R, Quilliam MA, LeBlanc P, Lewis N, Gallant P, Sperker SA, et al. Investigations into the Toxicology of Spirolides, a Group of Marine Phycotoxins. Toxins. 2011 Dec 30;4(12):1–14.

Otero P, Alfonso A, Rodríguez P, Rubiolo JA, Cifuentes JM, Bermúdez R, et al. (2012). Pharmacokinetic and toxicological data of spirolides after oral and intraperitoneal administration. Food Chem Toxicol. 50(2), 232–7.

Terao, K.; Ito, E.; Yanagi, T.; Yasumoto, T. Histopathological studies on experimental marine toxin poisoning. I. Ultrastructural changes in the small intestine and liver of suckling mice induced by dinophysistoxin-1 and pectenotoxin-1. Toxicon 1986, 24, 1141–1151.

Zhang H, Tolonen A, Rousu T, Hirvonen J, Finel M (2011) Effects of cell differentiation and assay conditions on the UDP-glucuronosyltransferase activity in caco-2 cells. Drug Metabolism and Disposition 39: 456–464.

In vivo studies on PTX-2 effects showed some hepatic damage after oral administration, meaning that PTX-2 is able to reach the bloodstream. Therefore, we assessed the hepatic metabolism of PTX-2 using rat and human S9 fractions. We also investigated its molecular mode of actions on the liver using HepaRG cells.

Publication #2: Metabolism of the Marine Phycotoxin PTX-2 and Its Effects on Hepatic Xenobiotic Metabolism: Activation of Nuclear Receptors and Modulation of the Phase I Cytochrome P450

Article published in Toxins 2017, 9, 212; doi:10.3390/toxins9070212

Metabolism of the Marine Phycotoxin PTX-2 and Its Effects on Hepatic Xenobiotic Metabolism: Activation of Nuclear Receptors and Modulation of the Phase I Cytochrome P450

Jimmy Alarcan [1], Estelle Dubreil [2], Antoine Huguet [1], Dominique Hurtaud-Pessel [2], Stefanie Hessel-Pras [3], Alfonso Lampen [3], Valérie Fessard [1] and Ludovic Le Hegarat [1,*]

[1] Toxicology of Contaminants Unit, French Agency for Food, Environmental and Occupational Health & Safety, ANSES, 35306 Fougères, France; jimmy.alarcan@anses.fr (J.A.); antoine.huguet@anses.fr (A.H.); valerie.fessard@anses.fr (V.F.)

[2] Analysis of Residues and Contaminants Unit, French Agency for Food, Environmental and Occupational Health & Safety, ANSES, 35306 Fougères, France; estelle.dubreil@anses.fr (E.D); dominique.pessel@anses.fr (D.H.-P.)

[3] Federal Institute for Risk Assessment, Department of Food Safety, Max-Dohrn-Straße 8-10, 10589 Berlin, Germany; Stefanie.Hessel-Pras@bfr.bund.de (S.H-P.); Alfonso.Lampen@bfr.bund.de (A.L.)

* Correspondence: ludovic.lehegarat@anses.fr; Tel.: +33-02-9917-2747

Academic Editor: Luis M. Botana
Received: 15 June 2017; Accepted: 1 July 2017; Published: 5 July 2017

Abstract: PTX-2 is a marine biotoxin frequently found in shellfish that can lead to food intoxication in humans. Information regarding PTX-2 metabolism is scarce, and little is known of its effect on xenobiotic-metabolizing enzymes (XME) or its molecular pathways. The aim of this study was consequently to examine PTX-2 Phase I metabolism using rat and human liver S9 fractions, and also to assess the capability of PTX-2: (i) to modulate the gene expression of a panel of Phase I (CYP) and II (UGT, SULT, NAT, and GST) enzymes, as well as the Phase III or 0 (ABC and SLCO) transporters in the human hepatic HepaRG cell line using qPCR; (ii) to induce specific CYP in HepaRG cells measured by immunolabeling detection and the measurement of the cells' activities; and (iii) to activate nuclear receptors and induce CYP promoter activities in HEK-T and HepG2 transfected cell lines using transactivation and reporter gene assay, respectively. Our results indicate that PTX-2 hydroxylation occurred with both rat and human S9 fractions. Whereas PTX-2 mostly upregulated the gene expression of CYP1A1 and 1A2, no induction of these two CYP activities was observed. Lastly, PTX-2 did not act as an agonist of CAR or PXR. Due to its effects on some key XME, more attention should be paid to possible drug–drug interactions with phycotoxins, especially as shellfish can accumulate several phycotoxins as well as other kinds of contaminants.

Keywords: PTX-2; metabolism; CYP; nuclear receptors

1. Introduction

Pectenotoxins (PTXs) are a group of marine biotoxins whose structure is based on polyether lactones produced by a restricted variety of phytoplanktonic species [1–3]. Among this group, pectenotoxin 2 (PTX-2, see Figure 1) is the best documented compound. Although no correlation between PTX-2 contamination and diarrhea has been ascertained [4,5], PTX-2 has been recurrently associated with diarrhetic shellfish poisoning with gastrointestinal symptoms observed in humans. Moreover, the small intestine and the liver have been depicted as the two main target organs of this toxin in rodents, with an increase of intestinal fluid after oral administration to mice [6], and some hepatic damage after intraperitoneal injection [7]. The major deleterious effects of PTX-2 at the cellular level are mediated via actin depolymerization leading to cytoskeleton disruption [8]. The apoptosis or suppression of NF-κB activity has also been described [9,10]. We previously showed that PTX-2 was cytotoxic in the human metabolic competent hepatoma cell line HepaRG, inducing apoptosis and DNA damage [11]. We also showed that PTX-2 failed to induce PXR translocation in HepG2 cells [11]. Regarding liver metabolism, although a decrease of hepatic protein content was observed, no effect on several enzymatic detoxification activities (total CYP, cytochrome b5, NADPH-cytochrome c reductase, and aminopyrine *N*-demethylase) was detected in mice [12]. In addition, the formation of several hydroxylated metabolites using rat liver S9 supernatants has been described [13]. We also showed that CYP3A4's inhibition by ketoconazole highly increases the cytotoxicity of PTX-2 in HepaRG cells, suggesting the implication of Phase I metabolism in PTX-2 detoxification [11].

Taken together, these data suggested that PTX-2 could be metabolized by rat S9 fractions and that Phase I metabolism, such as by CYP3A4, participates in reducing the toxicity of PTX-2. However, the role of the human liver's metabolism and the question as to whether PTX-2 can regulate its own metabolism remains unclear. In fact, the expression of Phase 0, I, II, and III metabolism proteins is orchestrated by several nuclear receptors and transcription factors (AhR, NRF-2, PXR, and CAR) that recognize xenobiotics as ligands [14–17]. These regulatory processes enable cells to activate detoxification, and protect them from xenobiotics [17].

In this study, we compared the metabolism of PTX-2 by human and rat liver S9 fractions, and we investigated the capability of PTX-2: (i) to modulate the gene expression of a panel of Phase I (CYP) and II (UGT, SULT, NAT and GST) enzymes, as well as the Phase 0 and III (ABC and SLCO) transporters in the human hepatic HepaRG cell line using qPCR; (ii) to induce specific CYP in HepaRG cells measured by immunolabeling detection and the measurement of the cells' activities; and (iii) to activate nuclear receptors and induce CYP promoter activities in HEK-T and HepG2 transfected cell lines using transactivation and reporter gene assays, respectively.

2. Results

2.1. PTX-2 Metabolism in Rat and Human S9 Fractions

2.1.1. High Resolution Mass Spectrometry (HRMS) Method for PTX-2 Quantification and the Detection of Metabolites

We first developed a LC–HRMS method for PTX-2 quantification. The chromatographic step was performed as described in the Materials and Methods section. PTX-2 was eluted after the same retention time in both active and inactivated S9 as the standard (Figure 1). The standard solution of PTX-2 was used to establish a linear calibration curve (R^2 = 0.99) between 5 and 100 ng/mL. The limit of detection (LOD) and the limit of quantification (LOQ) were estimated using signal intensities of 5 and 10 ng/mL standards, since no noise level was detected when extracting molecular mass. The LOD was assessed at 0.25 ng/mL and the LOQ at 1.1 ng/mL. Next, we determined the recoveries of PTX-2 following treatment with inactivated S9 fractions. We observed recoveries of 177 ± 2% and 151 ± 5% with inactivated rat S9, while 116 ± 39% and 122 ± 2% recoveries were obtained with inactivated human S9. Since the method proved to be efficient for the detection and quantification of PTX-2, we investigated the loss of PTX-2 in active S9 fractions.

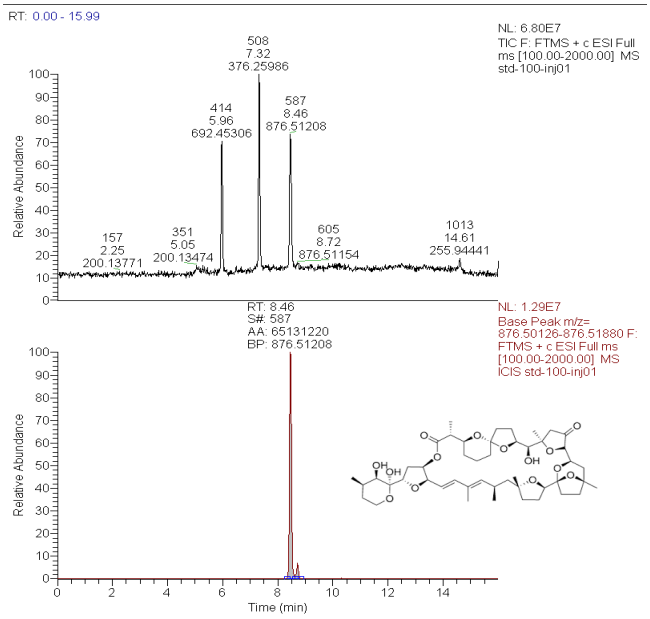

(**a**)

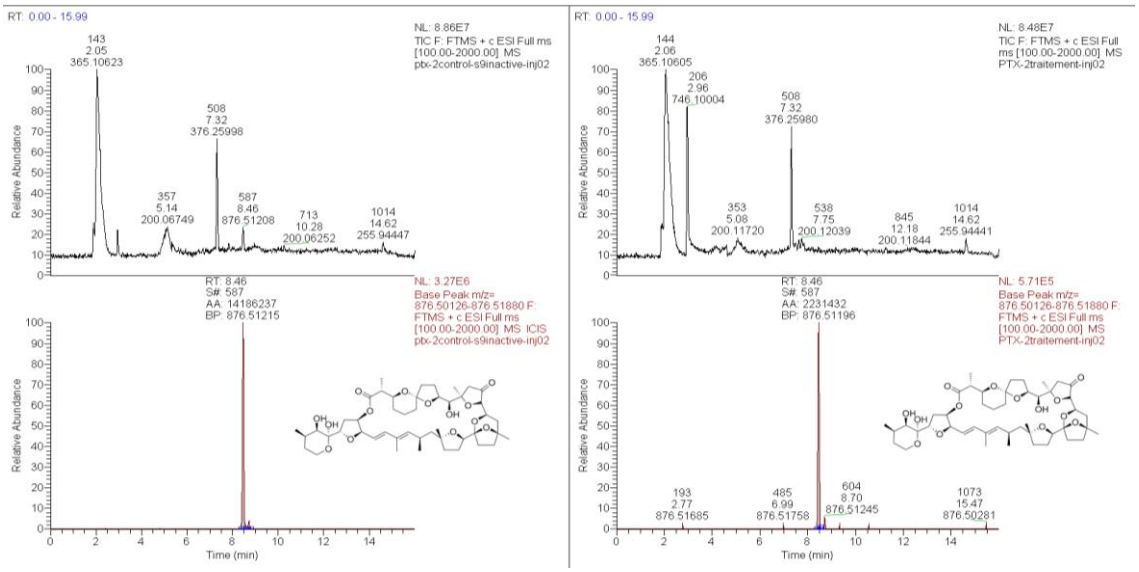

(**b**)

Figure 1. Total Ion Chromatogram (above) and Extracted Ion Chromatogram with extraction window of 5 ppm (below) obtained from the LC–HRMS analysis of PTX-2 in different samples. (**a**) Standard at 100 ng/ml, (**b**) inactivated or active S9.

2.1.2. Loss of PTX-2 and Metabolite Formation in Active S9 Fractions

We observed more than half of the decrease (53 ± 8% and 60 ± 0%) of PTX-2 with active rat S9. Regarding active human S9, while 93 ± 1% of the PTX-2 disappeared in the first assay, only 50 ± 0% of the PTX-2 disappeared in the second assay.

The formation of metabolites was investigated using MetWorks® 1.3.0. SP1. software (Thermo Fisher Scientific, Waltham, MA, USA). Starting from ammonium as the parent adduct mass (*m*/*z* = 876.51), we screened for a wide panel of Phase I reactions based on mass shifts. For both rat and human S9, at least one hydroxylated metabolite could be found in the active S9 samples. The parent compound was also detected. In the first assay with human S9, two additional metabolites corresponding to double and triple hydroxylation were found, but these two metabolites were not

found in the second assay. With both inactivated rat and human S9, only a PTX-2 ammonium adduct could be found (Figure 2a,b).

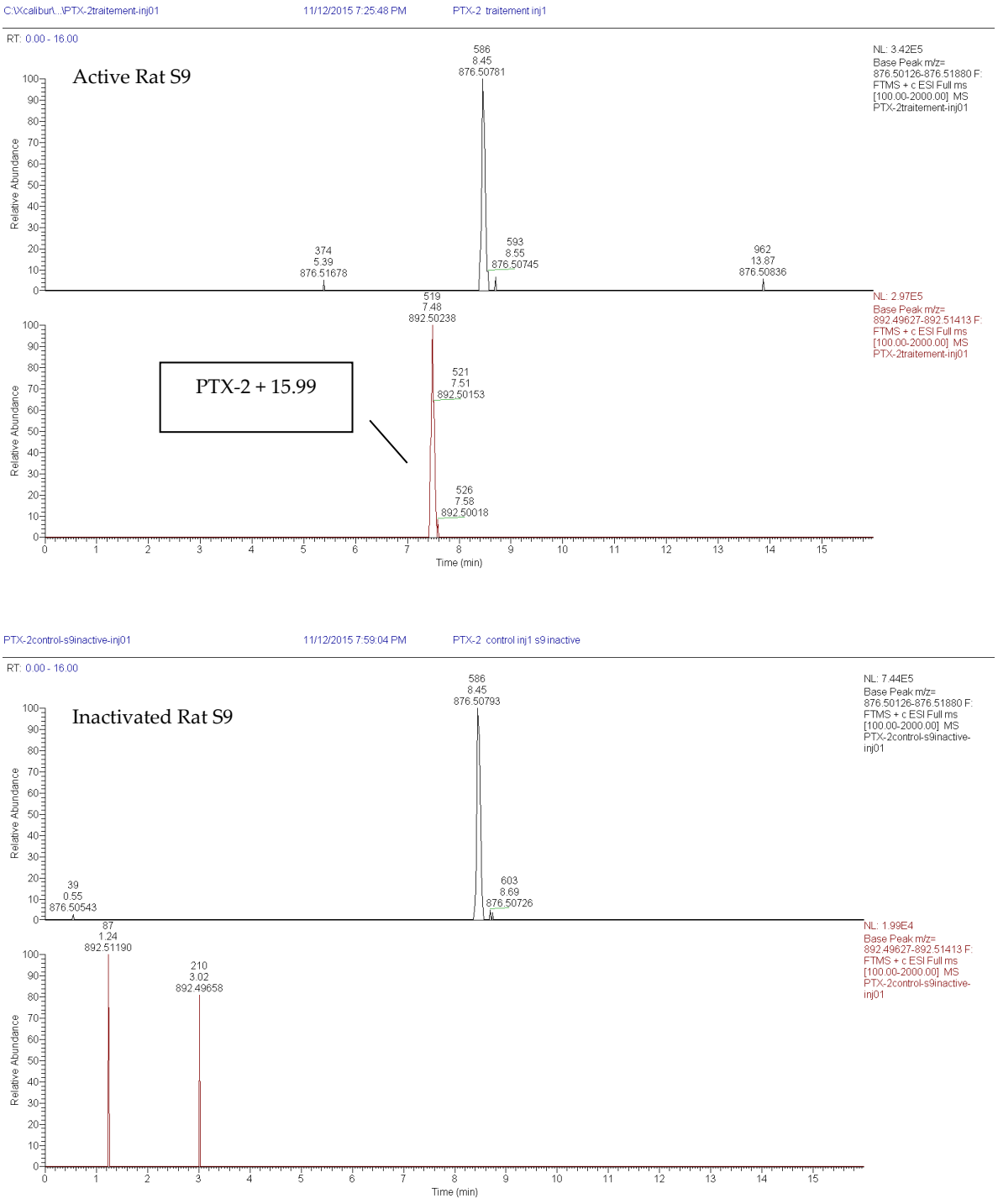

(**a**)

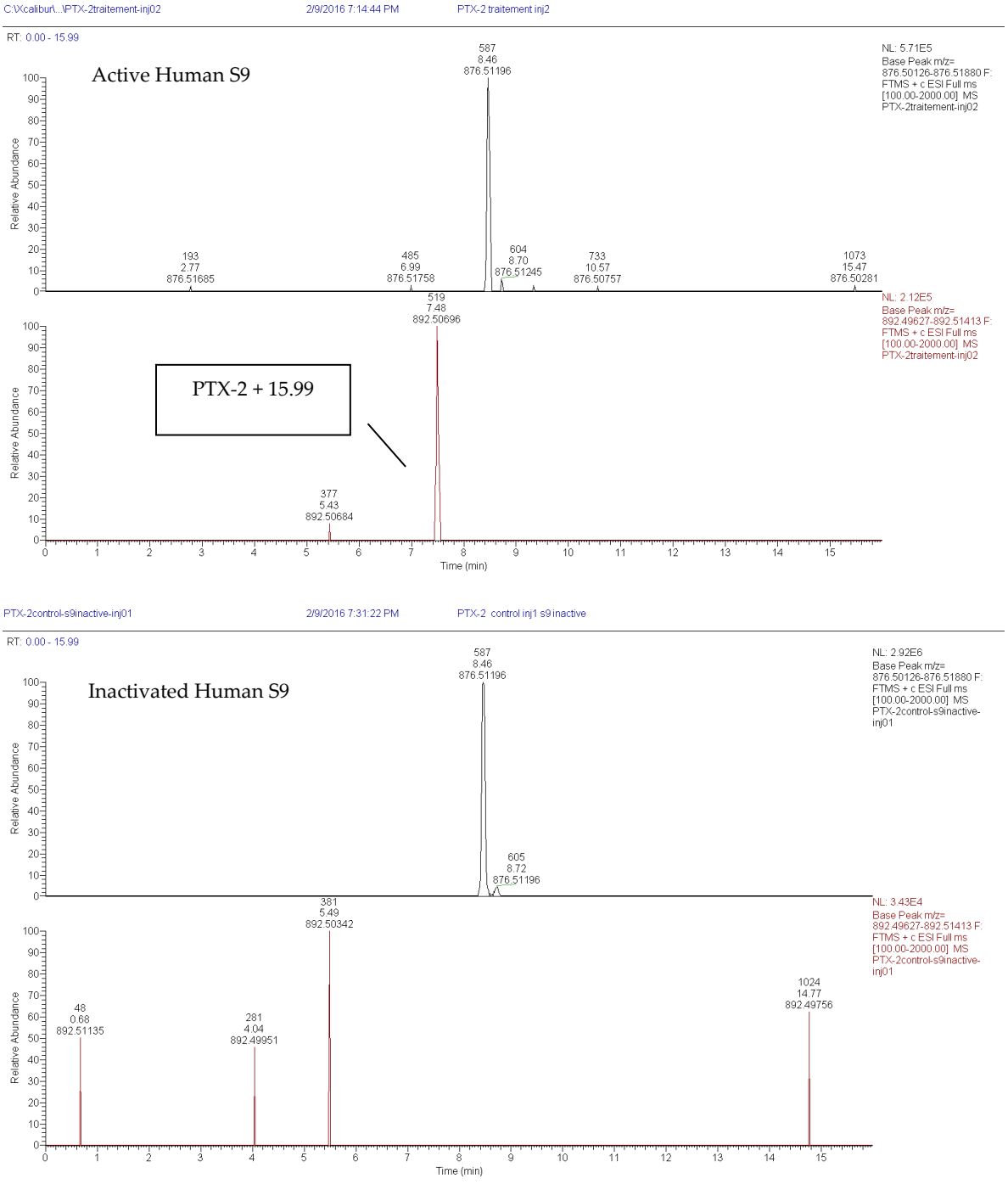

(**b**)

Figure 2. Total ion chromatograms obtained by LC–HRMS analysis. Mass traces of PTX-2 of mass ± 5 ppm and of hydroxylated metabolites are depicted for the treatment with induced rat (**a**) and human (**b**) liver S9.

Since these data strongly suggest a major role for Phase I enzymes in the metabolism of PTX-2, we investigated whether PTX-2 may modulate xenobiotic-metabolizing enzyme (XME) gene expressions in liver cells such as the metabolic competent HepaRG cells.

2.2. Effects of PTX-2 on the Expression of Phase 0, I, II, and III Metabolism Genes in HepaRG Cells by qRT-PCR

In order to determine the sub-toxic concentrations of PTX-2 for qRT-PCR analysis, viability was assessed in HepaRG cells by nuclear cell counting using a High Content Analysis. After 24 h of

treatment, PTX-2 was toxic only for the two highest doses, resulting in a 27% decrease of cell numbers at 128 nM and 42% at 256 nM (see Figure S1). We selected three sub-toxic concentrations of PTX-2, 16, 32, and 64 nM, for an mRNA expression analysis. PTX-2 had almost no effect regarding the Phase 0 influx transporters SLCO, but induced a concentration-dependent effect on both SLC22A1 and SLC22A3 mRNA (1.8-fold and 2.4-fold, respectively) (Table 1). Regarding CYP genes, a concentration-dependent upregulation of CYP1A1, 1A2, 2B6, 2C9, and 2C19 mRNA expression was observed. CYP1A1 and 1A2 mRNA expression were the most induced (18.7-fold and 8.8-fold, respectively). Although some variability was observed between the three independent experiments, induction was obvious when the experimental results were analyzed independently (see Table S1). For Phase II genes, the concentration-dependent induction of SULT1E1 (3.5-fold) and UGT1A1 (2.3-fold) was produced by PTX-2, whereas a concentration-independent induction of UGT1A9 and 2B4 was observed (2.1-fold with 32 nM PTX-2). A slight downregulation was observed for GSTM1 (0.8-fold with 16 and 64 nM PTX-2). Finally, PTX-2 upregulation of all of the Phase III transporters was concentration-dependent, with ABCB1 being the most upregulated (2.1-fold). Omeprazole (50 µM) and rifampicin (10 µM) were used as positive controls for CYP gene upregulation. Rifampicin, a well-known CYP3A4 inducer [18,19], upregulated CYP3A4 substantially (29.7-fold), and CYP2B6 and 2C9 slightly (3.2-fold and 2.1-fold, respectively). Omeprazole, a well-known inducer of the CYP1A family [18–20], greatly upregulated CYP1A1 and 1A2 (over 100-fold), but also CYP3A4 (12.9-fold), and to a lesser extent CYP2B6 (4.7-fold). Considering the potent upregulation of CYP1A1 and 1A2 gene expression by PTX-2, we investigated whether the effect could be detected in CYP1A's proteins and enzymatic activities.

Table 1. Effects of PTX-2 on mRNA expression in HepaRG cells. The cells were treated with three sub-toxic doses of PTX-2 for 24 h. Rifampicin (RIF) (10 µM) and omeprazole (OME) (50 µM) were used as positive controls. The results were obtained from three independent experiments. The figures are the means ± standard deviations (SD) of fold change relative to solvent control. Fold change between 0.9 to 0.5 (light blue) or less than 0.5 (dark blue) depicts gene down-regulation whereas fold change between 1.0 to 2.5 (white), 2.6 to 8 (light red) or greater than 8 (dark red) depicts gene up-regulation. * p <0.05, ** p <0.01, *** p <0.001 after one-way ANOVA followed by Dunnett's post hoc tests.

Metabolism phases	Gene	(nM)						OME		RIF		Gene
		16		32		64						
		Mean	SD	Mean	SD	Mean	SD	Mean	SD	Mean	SD	
Nuclear receptors	AHR	1.0	0.4	1.2	0.6	1.5	0.7	0.8	0.3	0.9	0.3	AHR
	NR1I2	1.3	0.2	1.5	0.6	1.4	0.3	1.0	/	0.7	0.4	NR1I2
Phase 0 influx transporters	SLC22A1	1.4	0.6	1.4	0.2	1.8	1.1	1.3	1.2	1.1	0.3	SLC22A1
	SLC22A3	1.6	0.3	1.8	0.4	2.4 **	0.3	1.0	0.4	1.1	0.5	SLC22A3
	SLCO1A2	0.9	0.6	1.2	1.1	1.1	0.6	0.4	0.3	0.2	0.2	SLCO1A2
	SLCO1B1	1.0	0.2	1.2	0.6	1.0	0.3	0.6	0.1	1.0	0.3	SLCO1B1
Phase I mono-oxygenases	CYP1A1	4.2	2.6	10.1	9.1	18.7	21.8	127.0 ***	67.1	0.4	0.4	CYP1A1
	CYP1A2	4.4	0.6	8.3	2.9	8.8	4.8	245.2 **	160.1	1.4	0.2	CYP1A2
	CYP2B6	1.6	0.5	3.1	2.1	3.5	2.6	8.0	8.0	4.3	2.5	CYP2B6
	CYP2C9	1.2	0.1	1.7	0.5	1.9	0.6	1.4	0.3	2.2 **	0.3	CYP2C9

	CYP2C19	1.3	0.3	1.4	0.2	1.8 *	0.3	1.2	0.2	1.6	0.4	**CYP2C19**
	CYP3A4	1.2	0.2	1.2	0.2	1.3	0.2	13.9 **	6.7	29.2 ***	3.6	**CYP3A4**
	CYP3A5	1.0	0.1	1.1	0.3	1.3	0.3	1.1	0.2	1.5*	0.2	**CYP3A5**
Phase II transferases	**GSTM1**	0.8	0.3	1.0	0.1	0.8	0.1	1.2	0.3	1.0	0.1	**GSTM1**
	NAT1	1.2	0.5	1.2	0.6	1.3	0.5	1.0	0.2	1.0	0.2	**NAT1**
	NAT2	1.1	0.0	1.2	0.1	1.3	0.3	0.8	0.2	0.9	0.3	**NAT2**
	SULT1A1	1.2	0.1	1.2	0.2	1.2	0.2	0.9	0.1	1.0	0.1	**SULT1A1**
	SULT1E1	1.7	1.2	2.4	2.0	3.5	3.4	0.4	0.2	0.7	0.4	**SULT1E1**
	UGT1A1	1.2	0.4	1.8	0.8	2.3	0.8	2.8	1.5	1.7	0.2	**UGT1A1**
	UGT1A9	1.3	0.3	2.1*	0.7	1.8	0.3	1.2	0.1	1.1	0.3	**UGT1A9**
	UGT2B4	1.6	0.6	2.1	0.7	1.7	0.5	1.3	0.2	1.4	0.5	**UGT2B4**
Phase III efflux transporters	**ABCB1**	1.4	0.2	1.9	0.6	2.1*	0.6	1.4	0.5	1.7	0.4	**ABCB1**
	ABCC2	1.2	0.3	1.4	0.4	1.5	0.5	1.2	0.5	1.2	0.2	**ABCC2**
	ABCC3	1.0	0.1	1.3	0.3	1.4	0.3	1.0	0.3	0.9	0.0	**ABCC3**
	ABCG2	1.2	0.3	1.5	0.3	2.0	0.9	2.6	1.4	1.1	0.1	**ABCG2**
			0.4		0.9		2.5		8		250	

x-Fold change compared to solvent control

2.3. Induction of CYP1A2 Proteins in HepaRG Cells

In order to confirm the upregulation of gene expression for proteins, CYP1A2 proteins were quantified after a 24 h treatment with PTX-2 by a high content analysis. As shown in Figure 3a, 64 nM PTX-2 greatly induced CYP1A2 fluorescence in comparison with the MeOH solvent control. PTX-2 caused a dose-dependent induction of CYP1A2 (Figure 3b). Although the two highest concentrations induced some toxicity (27% and 42%), a significant induction was also observed for a lower concentration (64 nM), increasing the CYP1A2 protein level 2-fold. Omeprazole poorly induced CYP1A2 proteins (1.3-fold increase).

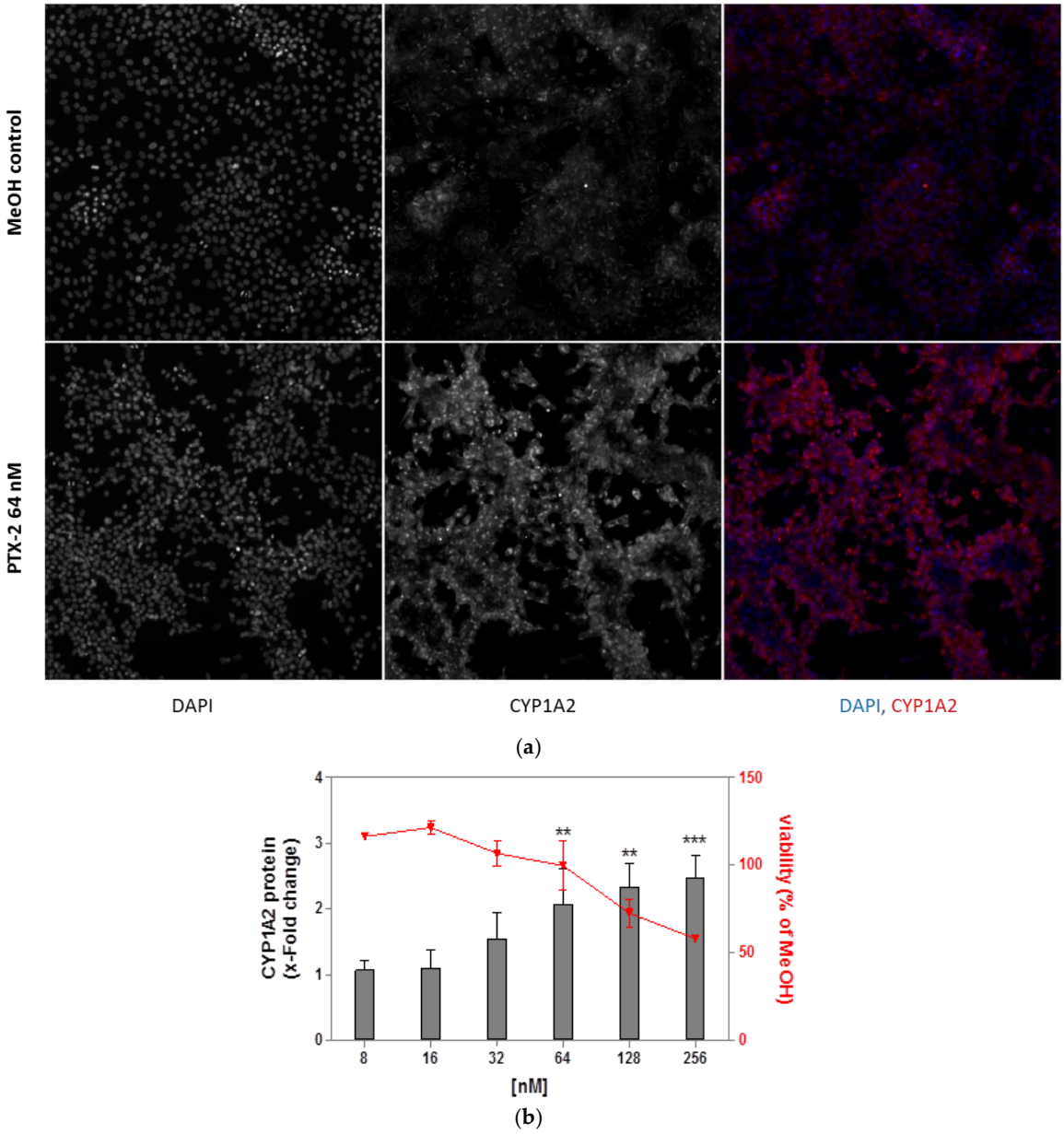

Figure 3. CYP1A2 protein induction after a 24 h treatment with PTX-2 in HepaRG cells. (**a**) Representative images at 10× magnification of CYP1A2 induction in HepaRG control cells (2.57% MeOH) and cells treated with 64 nM PTX-2. CYP1A2 was labeled with a specific antibody, and cell nuclei were stained with DAPI. The images were captured with Arrayscan VTi. Blue: nuclei, Red: CYP1A2; (**b**) CYP1A2 protein induction in HepaRG cells treated with PTX-2 for 24 h. The left Y axis depicts the fold induction of CYP1A2 normalized to solvent control, whereas the right Y axis depicts cell viability. The results were obtained from three independent experiments performed in triplicate (mean ± SD). ** p <0.01, *** p <0.001 after one-way ANOVA followed by Dunnett's post hoc tests.

2.4. CYP1A1 Reporter Gene Assay in HepG2 Cells

In order to confirm the upregulation of CYP1A1 mRNA observed in the HepaRG cells, we investigated the capability of PTX-2 to induce CYP1A1 promoter activity in transfected HepG2 cells. Firefly luciferase values were considerably decreased with PTX-2 (in the range of blank values), suggesting some interference of the toxin with the model (data not shown). In order to elucidate this, PTX-2 and a positive control (a mixture of CITCO and 3-MC) were co-incubated. A substantial decrease in luciferase values was again observed, confirming that this model was inappropriate for investigating PTX-2 induction on CYP1A1 due to obvious interference.

2.5. Induction of CYP1A Proteins in HepaRG Cells

As we could not investigate CYP1A1 induction via reporter gene assay, we performed western blotting targeting both CYP1A1 and CYP1A2 proteins. Western blotting was performed after a 24 h treatment with PTX-2. As shown in Figure 4, omeprazole greatly induced CYP1A2 proteins but slightly induced CYP1A1. CYP1A2 was slightly induced by 32 and 64 nM PTX-2, while 16 and 32 nM PTX-2 slightly induced CYP1A1.

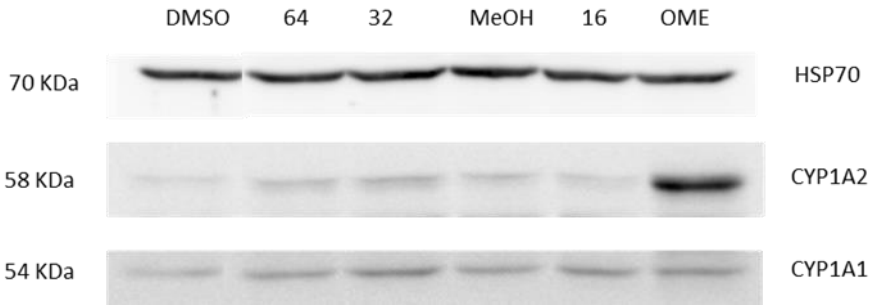

Figure 4. CYP1A induction in HepaRG cells treated with PTX-2. Cells were treated for 24 h with PTX-2 prior to measurement via western blotting (n = 1). Omeprazole (50 μM) was used as a positive control.

2.6. Effects of PTX-2 on CYP1A Activities in HepaRG Cells

As our results suggest an upregulation of CYP1A1 and 1A2 gene expression, we examined whether PTX-2 could induce these CYP enzymatic activities through a ethoxyresorufin-*O*-deethylase (EROD) reaction. 3-methylcholanthrene (5 μM) was used as a positive control. The results are presented in Figure 5. PTX-2 failed to induce EROD activity regardless of the incubation time in HepaRG cells.

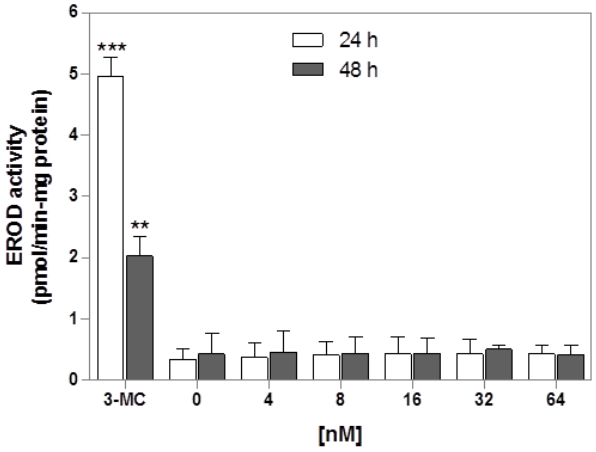

Figure 5. CYP1A activities in HepaRG cells after treatment with PTX-2. Cells were treated for 24 or 48 h with PTX-2 prior to ethoxyresorufin-*O*-deethylase (EROD) activity measurement. The positive control used was 3-methylcholanthrene (5 μM). The results were obtained from two independent experiments performed in triplicate (mean ± SD). ** p <0.01, *** p <0.001 after one-way ANOVA followed by Dunnett's post hoc tests.

2.7. CAR and PXR Transactivation Assay in Transfected HepG2 and HEK-T Cells

In order to assess whether PTX-2 could activate nuclear receptors that regulate drug-metabolizing genes, transactivation assays on the two main xenobiotic-metabolizing regulatory nuclear receptors, CAR and PXR, were conducted in transfected HepG2 and HEK-T cells, respectively. PTX-2 was not toxic in either cell line up to 200 nM in the CTB assay. However, PTX-2 induced morphology changes in HepG2 cells (rounded cells, data not shown), so only PTX-2 concentrations

below 100 nM were used in the transactivation assays. The results are presented in Figure 6. PTX-2 showed a very slightly inhibited CAR transactivation, and no effects regarding PXR.

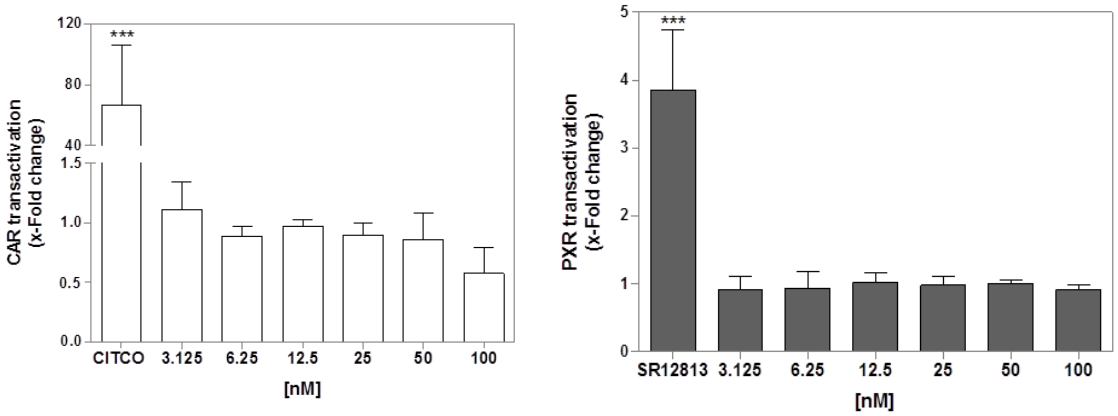

(**a**) (**b**)

Figure 6. Transactivation of CAR (**a**) and PXR (**b**) in HepG2 and HEK-T cells. The cells were transfected with plasmids before incubation with PTX-2 for 24 h. CITCO (10 μM) and SR12813 (10 μM) were used as positive controls. The results were obtained from three independent experiments performed in triplicate (mean ± SD). *** p <0.001 after one-way ANOVA followed by Dunnett's post hoc tests.

2.8. AhR Reporter Gene Assay in HepG2 Cells

In order to investigate the capability of PTX-2 to activate AhR, promoter activity was investigated in transfected HepG2 cells. A large decrease of luciferase values was again observed with PTX-2 as well as with a co-incubation of PTX-2 and the positive control 3-MC (data not shown), again indicating the clear interference of PTX-2 with the model.

3. Discussion

In this study, we showed that PTX-2 is metabolized by rat and human liver S9 fractions, as the PTX-2 amounts decreased simultaneously with the appearance of at least one hydroxylated metabolite. This metabolite was previously described using a rat S9 fraction [13]. However, we did not detect the four other hydroxylated metabolites that were also reported in this publication. We observed two additional metabolites with human S9, but only in the assay where we observed an almost total loss of PTX-2. We cannot exclude that other metabolites may have been produced that we failed to detect, whether because they were too low in quantity, or not stable enough. In fact, Kittler et al. [13] used a different analytical approach (triple quadrupole mass spectrometry), which could explain the difference with our results. We established recoveries of higher than 100%, which could be explained by ion enhancement phenomena during ionization. Matrix effects have been previously observed when analyzing PTX-2 in mussel extracts [21,22]. Regarding the results from the rat S9, we noticed that this matrix strongly affects the recovery rates. To be sure that the products resulted from enzymatic reactions and were not due to any other process, we confirmed that no hydroxylated metabolites were detected with inactivated S9. Concerning the metabolites formed, we did not observe any species difference between rat and human, suggesting that similar Phase I enzymes are probably involved in the PTX-2 metabolism in mammals. Although PTX-2 metabolism has already been investigated, very little information has been published regarding the enzymes and transporters involved in PTX-2 uptake, metabolism, and excretion. Our results on gene expression revealed that PTX-2 could affect the regulation of several XME genes in human HepaRG cells. A pronounced up-regulation of CYP1A1 and 1A2 mRNA was indeed observed, indicating a plausible key role for these two enzymes in the hydroxylation of PTX-2. The upregulation of SULT1E1 and several UGTs suggests that PTX-2 itself or the hydroxylated metabolites formed through the CYP process may be conjugated. The results on transporter gene expression highlighted the possible role of P-gP and ABCG2 in the efflux of PTX-2, as these genes were found to be upregulated.

The induction of CYP1A mRNA could be correlated with the induction of protein levels, since we showed CYP1A2 induction using two different methodologies (immunostaining and western blot), and CYP1A1 induction via western blotting. However, we did not detect any increase of EROD activity in the HepaRG cells (up to 64 nM PTX-2 for 24 h or 48 h). We previously showed that five main CYP activities were not affected after 72 h of treatment with 5 nM PTX-2 [11]. It is possible that the level of increase of CYP1A mRNA had no impact on CYP activities. For instance, Genies et al. [23] showed that 200 nM of B[a]P treatment in HepG2 cells upregulated CYP1A1 mRNA at 6 h (200-fold induction), before decreasing drastically after 14 h of treatment. Despite strong mRNA induction, the EROD measurements at 24 h showed only weak CYP1A1 activity. Therefore, it can be assumed that the nM range of PTX-2 is too weak to cause an increase in CYP1A activities. Further investigations are needed to reveal the underlying mechanisms.

Using transactivation assays, we showed that PTX-2 activated neither CAR nor PXR. A previous study showed that PTX-2 failed to induce PXR translocation in HepG2 cells [11]. These results are in accordance with our data on gene expression, as CYP3A4, known to be primarily under PXR regulation [17], was not upregulated with PTX-2. For AhR, our model was biased by PTX-2 and we could not achieve a conclusion. Still, it is unlikely that PTX-2 would not interfere with AhR, as CYP1A1 and 1A2 gene regulation have been described as being regulated almost exclusively by AhR [14,15]. Another common methodology to study the possible activation of AhR by PTX-2 would be in silico modeling of the quantitative structure-activity relationship (QSAR) based, for instance, on protein X-ray crystallography. Although informative, this technique is a non-cellular model and needs to be confirmed in a cell-based assay.

Guo et al. [24] showed that hydroxylated metabolites of okadaic acid (OA) kept similar Protein Phosphatase 2A inhibition properties as the parent toxin. Besides, bioactivation has been previously reported for OA [25,26]. Using HepG2 transformed cell lines, Hashizume et al. [26] could also pinpoint the role of CYP1A2 in OA bioactivation. In light of this, the question arises as to whether the hydroxylated metabolite(s) of PTX-2 could produce the same effects as PTX-2 itself. In our study on metabolically competent HepaRG cells, PTX-2 toxicity was depicted with concomitant CYP1A2 induction. However, in cell models with no or low CYP1A levels (HEK-T and HepG2), no toxicity was observed, suggesting that the toxicity could be due to the formation of toxic Phase I metabolites. Further investigation is needed to confirm this hypothesis.

No previous study has been conducted to identify the CYP(s) responsible for PTX-2 metabolism. Ferron et al. [11] observed that the toxicity of PTX-2 on HepaRG cells was modified when CYP3A4 was chemically modulated by an inducer or an inhibitor. However, the authors questioned the specificity of the CYP3A4 inducer and inhibitor in such a complex cell model, and suggested that P-gP could also play a role in the toxic responses observed. From our results, we can suggest that PTX-2 is an inducer of its own metabolism, implying that CYP1A1 and CYP1A2 would be responsible for its hydroxylation. Such a phenomenon has already been described for several compounds [27,28]. The use of HepG2 transformed cell lines, as developed by Hashizume et al. [26], would be an appropriate way of confirming this assumption.

The elucidation of the structure of metabolites, as well as further investigation regarding the possible involvement of Phase II metabolism, is also needed to complete the available data on PTX-2.

4. Conclusions

In conclusion, we showed that PTX-2 undergoes Phase I metabolism with human S9 fractions, and at least one hydroxylated metabolite could be found. We also observed that PTX-2 up-regulates both CYP1A1 and 1A2 gene expression and induces CYP1A protein levels in HepaRG cells. No effects on several other CYPs could be observed, which is consistent with the absence of CAR and PXR transactivation after PTX-2 treatment. To our knowledge, this is the first time that such a complete investigation of hepatic xenobiotic metabolism has been assessed for a phycotoxin.

5. Materials and Methods

5.1. Chemicals

PTX-2 standard was purchased from the National Research Council Institute for Marine Biosciences (Halifax, NS, Canada). Omeprazole, rifampicin, 3-methylcholanthrene, SR12813, CITCO, ethoxyresorufin, resorufin, and formate ammonium were purchased from Sigma-Aldrich (St. Louis, MO, USA). Reduced nicotinamide adeninedinucleotide phosphate (NADP+), glucose 6-phosphate (G6P), magnesium chloride hexahydrate, potassium chloride, Na_2HPO_4, and NaH_2PO_4 were purchased from Carl Roth (Karlsruhe, Germany). All of the other chemicals, including acetonitrile (ACN), methanol (MeOH), and dimethyl sulfoxide (DMSO) were of analytical grade and purchased from Fisher Scientific (Leicestershire, UK). Formic acid was purchased from Merck (Darmstadt, Germany). The deionised water was prepared using a Milli-Q system (Millipore, Bedford, MA, USA). The β-naphtoflavone and phenobarbital-induced Sprague Dawley rat and human hepatic S9 fractions were purchased from Biopredic International (Rennes, France).

5.2. S9 Phase I Metabolism

In order to target Phase I metabolism, specific co-factors were added to the S9 fractions: NADPH regenerating system (NADP+ (4 mM) and G6P (5 mM)), KCl (33 mM), $MgCl_2$ (8 mM), and 0.1 M sodium phosphate buffer (Na_2HPO_4 [0.2 M] + NaH_2PO_4 [0.2 M], pH 7.4). An experimental volume of 0.5 mL containing Phase I co-factors (final concentration as described above), S9-fraction (final concentration 2.2 mg/mL), and 50 nM PTX-2 was incubated in a water bath at 37 °C for 3 h. The reaction was then stopped by adding 0.5 mL of ice-cold MeOH. After 20 min centrifugation (14,000 g) at 4 °C, the samples were analyzed or frozen at −80 °C until analysis. For the S9 controls, the same procedure was followed, but the S9 fraction was heat-inactivated for 45 min at 60 °C prior to incubation with the co-factors and PTX-2.

5.3. LC–HRMS Analysis

The metabolism investigation was conducted in two steps: first the decrease of the parent compound was measured via an LC–HRMS quantitative method, and then the formation of metabolites was studied via the metabolite research software MetWorks®. The analyses were conducted on the Thermo Fisher Accela LC (Thermo Fisher, Bremen, Germany) system hyphenated to an LTQ-Orbitrap XL mass spectrometer. The LC elutions were performed on an Agilent Zorbax Eclipse XDB-C18 column (Agilent Technologies, Santa Clara, CA, USA) (150 × 3.0 mm, 3.5 μm). Chromatographic separation was carried out using two mobile phase preparations, consisting of mobile phase (A), 100% water, and mobile phase (B), 5% water and 95% acetonitrile. Both mobile phases contained 2 mM of ammonium formate and 50 mM of formic acid. The gradient conditions were as follows: from 0 to 5 min, ramp up linearly from 98% to 2% of mobile phase A and hold for 7 min, then ramp back over 1 min to initial conditions and hold for 3 min to re-equilibrate the system. The flow rate was set at 0.3 mL min^{-1}, the injection volume was 10 μL, and the column oven was maintained at 25 °C. PTX-2 was quantified using a calibration curve with PTX-2 standards at 0, 5, 10, 25, 50, 75, and 100 ng/mL in MeOH/H_2O (2/3, 1/3). The mass spectrometer was operated with an electrospray ionization probe in positive mode using the following source parameters: sheath gas flow rate: 40 arb; auxiliary gas flow rate: 15 arb; sweep gas flow rate: 2 arb; ion spray voltage: 3.5 kV; capillary temperature: 350 °C; capillary voltage: 30 V; and tube lens: 100 V. The instrument was calibrated using the manufacturer's calibration solution, consisting of three mass calibrators (i.e., caffeine, tetrapeptide MRFA, and Ultramark) to reach mass accuracies in the 1–3 ppm range. The instrument was operated in full-scan mode from m/z 100–1000 at a resolving power of 60,000 (full width at half maximum), allowing PTX-2 detection as ammonium adducts [PTX-2]-NH_4^+ (m/z = 876.51), as well as metabolite formation investigations using MetWorks 1.3.0. SP1. software (Thermo Fisher Scientific, Waltham, MA, USA). The extraction's mass window was set at ±5 ppm. The PTX-2

recoveries were calculated as follows: Ri = (ci × 100)/c0, where ci is the measured concentration of the sample i, and c0 is the initial concentration.

5.4. Cell Culture

5.4.1. HepaRG Cells

HepaRG cells were cultured as previously published in [25,29]. Briefly, HepaRG cells (passages 13–19) were seeded at 30,000 cell/cm^2 in 96-well plates in culture medium (Williams' E Medium with GlutaMAX-I, supplemented with 10% fetal bovine serum, 100 IU/mL penicillin, 100 μg/mL streptomycin, 5 μg/mL bovine insulin, and 50 μM hydrocortisone hemisuccinate). After 2 weeks, the cells were cultured in the same medium supplemented with 1.7% DMSO (differentiation medium) for an additional 2 weeks. The medium was renewed every 2 to 3 days.

5.4.2. HepG2 and HEK-T Cells

The human hepatocellular carcinoma cell line HepG2 and the human embryonic kidney cell line HEK-T were obtained from the European Collection of Cell Cultures (ECACC, Porton Down, UK). The cells were cultured in high glucose Dulbecco's modified Eagle's medium (DMEM, Pan-Biotech GmbH, Aidenbach, Germany), supplemented with 10% fetal calf serum (Pan-Biotech GmbH, Aidenbach, Germany), 100 U/mL penicillin, and 100 g/mL streptomycin (PAA Laboratories GmbH, Pasching, Austria) at 37 °C in a humidified atmosphere containing 5% CO_2. The cells were passaged every 2–4 days (80–90% confluence), and seeded at 100,000 cells/cm^2 and 50,000 cells/cm^2 respectively for HepG2 and for HEK-T cells in 96-well plates.

5.5. Cytotoxicity Assays

Cell viability was assessed in HepaRG cells via the DAPI-mediated staining of nuclei. The cells were treated with different concentrations of PTX-2 for 24 h, and then fixed with 4% paraformaldehyde in Phosphate Buffered Saline (PBS) for 10 min and permeabilized with 0.2% Triton X-100. The nuclei were stained with 1 μg/mL DAPI, and quantified using ArrayScan (see below). Cell viability was determined in HepG2 and HEK-T cells after 24 h of treatment with PTX-2 using the CellTiter-Blue® Cell Viability Assay (Promega, Madison, WI, USA). CellTiter-Blue® reagent was diluted at 1:4 with phosphate buffered saline (PBS), and 20 μL of the diluted reagent was added to each well. The cells were incubated for 2 h at 37 °C, and the fluorescence was measured at 590 nm (excitation at 540 nm).

5.6. Real-Time Quantitative Polymerase Chain Reaction (RT-qPCR) Analysis

The HepaRG cells were seeded in 12-well plates at a density of 20,000 cells/cm^2, and cultured until differentiation as described previously. Following 24 h incubation with PTX-2 or positive controls 50 μM omeprazole and 10 μM rifampicin, the cells were washed twice with Phosphate Buffered Saline (PBS). Total RNA extraction was then performed using the Total RNA isolation NucleoSpin® RNA II kit from Macherey Nagel (Hoerd, France) following the manufacturer's protocol. The RNA concentration and quality were determined by spectrophotometric measurements with BioSpec-nano (Shimadzu Biotech, Marne la Vallée, France). The RNA's integrity was checked through electrophoresis using Experion (Bio-Rad, Marne la Coquette, France). The RNA samples were then reverse transcribed into double strand cDNA using the High Capacity RNA-to-cDNA kit (Applied Biosystems, Foster City, CA, USA) according to the manufacturer's instructions. The sequences of target genes were obtained from the National Center for Biotechnology Information (NCBI) GenBank sequence database [30]. The primers were designed with the Primer designing tool from NCBI [31]. For each gene, at least one primer was designed on the exon–exon junction. All of the primers (see Table S2) were purchased from Sigma-Aldrich (Saint-Louis, MO, USA). Quantitative PCR was performed using a LightCycler® 1536 from Roche (Mannheim, Germany). SYBR Green chemistry was used. The reactions were performed in a total volume of 2 μL containing 1X LightCycler 1536 DNA

Green Master, 1× LightCycler 1536 DNA Master Mix (Roche), 300 nM of each primer, and 0.1 ng of cDNA. Negative quantitative PCR controls of RNase-free water were included in each run for a contamination assessment. The thermal cycling conditions were 94 °C for 15 s, followed by 40 cycles of 15 s at 94 °C, and 30 s at 60 °C with a slow temperature ramp (4.8 °C/s). LightCycler® 1536 software (version 1.1.0.1112; Roche, Basel, Switzerland) was used for the quantitative analysis, and a melting curve analysis was used to check the specificity of each amplicon. The threshold Cqs were calculated from a baseline subtracted curve fit. Calibration curves were established for each gene from a serial dilution of a reference sample (pool of cDNA samples). According to these calibration curves, for each sample, mean relative amounts of mRNA of the target genes were calculated and then normalized to the GAPDH reference gene. The values were presented as fold changes relative to the solvent control.

5.7. CYP1A2 Protein Expression

After 24 h of incubation with PTX-2, the HepaRG cells were fixed with 4% paraformaldehyde in phosphate buffered saline (PBS) for 10 min and permeabilized with 0.2% Triton X-100 for 15 min. The plates were then incubated in blocking solution (PBS with 1% BSA and 0.05% Tween-20) for 30 min before the addition of primary antibodies prepared in blocking solution and filtered with a 0.2 µm syringe filter. The primary and secondary antibodies were purchased from Abcam (Cambridge, UK): mouse monoclonal anti-CYP1A2 S19 (ab22717) and goat anti-mouse IgG H&L DyLight® (Thermo Fisher Scientific, Waltham, MA, USA) 550 (ab96876). The primary antibody (1/1000) was incubated overnight at 5 °C. After washing with PBS + 0.05% Tween 20, the secondary antibody (1/1000) was incubated for 45 min at room temperature. Nuclear DAPI (1 µg/mL) staining was used for automated cell identification by a high content analysis. The plates were scanned with the Thermo Scientific ArrayScan VTI HCS Reader (Thermo Scientific, Waltham, MA, USA), and analyzed using the Target Activation module of the BioApplication software (version: 6.0.1.4021; Thermo Fisher Scientific, Waltham, MA, USA). For each well, 10 fields (10× magnification) were scanned and analyzed for immunofluorescence quantification. Cell numbers were determined by cell counting following DAPI staining. CYP1A2 was quantified in the whole cell, and expressed as a fold increase compared to solvent control cells.

5.8. Western Blot for CYP1A Expression

Extracts from the HepaRG cells were separated using SDS-PAGE. The proteins were transferred to nitrocellulose membranes in a transfer buffer (25 mM Tris, 200 mM glycine, and ethanol 20%). The membranes were blocked in 5% low fat milk in Tris-buffer saline (TBS) (65 mM Tris pH 7.4, 150 mM NaCl) for 1 h at room temperature. The primary antibodies were purchased from Abcam (Cambridge, UK): mouse monoclonal anti-CYP1A2 S19 (ab22717) and rabbit polyclonal anti-CYP1A1 (ab3568), and from Santa Cruz Biotechnology (Dallas, TX, USA): mouse anti-HSC70 (SC-7298). The secondary antibodies were purchased from Dako (Santa Clara, CA, USA): goat anti-mouse (P0447) and goat anti-rabbit (P0448). The membranes were incubated with primary antibodies (1/1000) overnight at 4 °C. After being washed with TBS, appropriate secondary antibodies (1/1000) linked to horseradish peroxidase were incubated for one hour in 5% low-fat milk in TBS at room temperature. The immunocomplexes were visualized with an Immobilon Western Chemiluminescent HRP substrate (Millipore, Billerica, MA, USA), and scanned with a Fujifilm LAS-3000 imager (Fujifilm, Tokyo, Japan).

5.9. EROD Activity

The HepaRG cells were treated for 24 h or 48 h (renewal of PTX-2 after 24 h treatment) with PTX-2 in DMSO and a serum-free medium before the removal of the toxin and incubation with a specific CYP1A substrate. As a positive control, 3-MC (5 µM) was used. The CYP1A1/1A2 activity was monitored through a ethoxyresorufin-O-deethylase (EROD) reaction. The HepaRG cells were incubated with a solution of 2 µM ethoxy-resorufin for 30 min. The supernatants were then collected. The concentration of resorufin was determined by fluorescence measurement (λ ext = 530 nm and λ em = 585 nm). The protein content was measured with the bicinchoninic acid (BCA) assay (Pierce BCA

Assay™ Kit, Thermo Fisher Scientific, Waltham, MA, USA). Activity is expressed as pmol of resorufin min^{-1} mg of $protein^{-1}$.

5.10. CAR and PXR Transactivation Assays

The transactivation assays were conducted as previously described [32]. Briefly, 24 h after seeding, HepG2 cells were transiently transfected using TransIT-LT1 (Mirus Bio, Madison, WI, USA) according to the manufacturer's protocol. For each well, the transfection mixture contained 40 ng pGAL4-(UAS)5-TK-luc, 40 ng pGAL4/DBD-hCAR/LBD(+3aa), and 1 ng pcDNA3-Rluc for the CAR assay. pcDNA3-Rluc was used as an internal control for normalization. Four to six hours after transfection, the cells were incubated with different concentrations of PTX-2 dissolved in serum-free DMEM without a phenol red medium. CAR agonist CITCO (10 μM) was used as positive control. After 24 h, the culture medium was removed and the cells were lysed after addition of 50 μL lysis buffer (100 mM potassium phosphate with 0.2% (*v*/*v*) Triton X-100, pH 7.8) for 15 min on an orbital shaker. After centrifugation (5 min, 2000 *g*) 5 μL of the supernatant was analyzed for luciferase activity as previously described [33]. The PXR transactivation assay was performed in HEK-T cells in the same way as that described for the CAR transactivation assay. The transfection mixture contained 40 ng pGAL4-(UAS)5-TK-luc, 40 ng pGAL4-hPXR-LBD, and 1 ng pcDNA3-Rluc per well. The PXR agonist SR12813 (10 μM) was used as a positive control. The firefly luciferase values were normalized to Renilla luciferase values, and expressed as fold-inductions normalized against solvent control.

5.11. AhR and CYP1A1 Reporter Gene Assays

The AhR and CYP1A1 reporter gene assays were performed in HepG2 cells as described for the CAR transactivation assay, except here no plasmid expressing a chimeric AhR was necessary, AhR basal expression being sufficiently high to measure reporter gene activity. For each well, the transfection mixture contained 80 ng p3xDREC for AhR or 50 ng pT81luc-hCYP1A1 for CYP1A1 and 1 ng pcDNA3-Rluc as an internal control for normalization. Four to six hours after transfection, the cells were incubated with different concentrations of PTX-2 dissolved in serum-free DMEM without a phenol red medium. The AhR agonist 3-Methylcholanthren (5 μM) and a mixture of 3-Methylcholanthren (5 μM) and CITCO (10 μM) for CYP1A1 were used as positive controls. The firefly luciferase values were normalized to Renilla luciferase values and expressed as fold-inductions normalized against solvent control.

5.12. Statistics/Data Analysis

GraphPad Prism 5 (GraphPad Software, Inc., La Jolla, CA, USA) was used for the statistical analyses. The data were compared to the control condition using one-way analysis of variance (ANOVA) followed by Dunnett's post hoc tests. All error bars denote SD. Statistical significance was depicted as follows: * $p < 0.05$, ** $p < 0.01$, *** $p < 0.001$.

Supplementary Materials: Figure S1: Cell viability in HepaRG cells. Following 24 h of treatment with different concentrations of PTX-2, the nuclei were stained with 1 μg/mL DAPI and scored using ArrayScan. The results were obtained from three independent experiments performed in triplicate (mean ± SD), Table S1: Effects of PTX-2 on mRNA expression of CYP1A1, 1A2, 2B6, and SULT1E1 in HepaRG cells. The data represent the means of fold change compared to solvent control, Table S2: Summary of primers used for q-PCR analysis.

Acknowledgments: We would like to thank Patrick Fach and Cédric Woudstra from the IdentyPath platform (Anses Maisons-Alfort) for their excellent support and advices in the qRT-PCR assays. We would like to thank Sophie Rose and Sophie Langouet from IRSET for her help in western blot assay.

Author Contributions: J.A., A.H., V.F., D.H.-P., S.H-P., and L.L.H. conceived and designed the experiments; J.A., A.H., and E.D performed the experiments; J.A., A.H., E.D., and L.L.H. analyzed the data; J.A., E.D., V.F., S.H-P., A.L., and L.L.H. wrote the paper.

Conflicts of Interest: The authors declare no conflict of interest.

References

1. Yasumoto, T.; Murata, M.; Oshima, Y.; Sano, M.; Matsumoto, G.K.; Clardy, J. Diarrhetic shellfish toxins. *Tetrahedron* **1985**, *41*, 1019–1025, doi:10.1016/S0040-4020(01)96469-5.
2. Yasumoto, T.; Murata, M.; Lee, J. Polyether toxins produced by dinoflagellates. In *Mycotoxins andPhycotoxins '88*; Natori, S., Hashimoto, K., Ueno, Y., Eds.; Elsevier: Amsterdam, The Netherlands, 1989; pp. 375–382.
3. Draisci, R.; Lucentini, L.; Giannetti, L.; Boria, P.; Poletti, R. First report of pectenotoxin-2 (PTX-2) in algae (Dinophysis fortii) related to seafood poisoning in Europe. *Toxicon* **1996**, *34*, 923–935.
4. Miles, C.O.; Wilkins, A.L.; Munday, R.; Dines, M.H.; Hawkes, A.D.; Briggs, L.R.; Sandvik, M.; Jensen, D.J.; Cooney, J.M.; Holland, P.T.; et al. Isolation of pectenotoxin-2 from Dinophysis acuta and its conversion to pectenotoxin-2 seco acid, and preliminary assessment of their acute toxicities. *Toxicon* **2004**, *43*, 1–9.
5. Ito, E.; Suzuki, T.; Oshima, Y.; Yasumoto, T. Studies of diarrhetic activity on pectenotoxin-6 in the mouse and rat. *Toxicon* **2008**, *51*, 707–716.
6. Ishige, M.; Satoh, N.; Yasumoto, T. Pathological studies on mice administered with the causative agent of diarrhetic shellfish poisoning (okadaic acid and pectenotoxin-2). *Hokkaidoritsu Eisei Kenkyushoho* **1988**, *38*, 15–18.
7. Terao, K.; Ito, E.; Yanagi, T.; Yasumoto, T. Histopathological studies on experimental marine toxin poisoning. I. Ultrastructural changes in the small intestine and liver of suckling mice induced by dinophysistoxin-1 and pectenotoxin-1. *Toxicon* **1986**, *24*, 1141–1151.
8. Espina, B.; Louzao, M.C.; Ares, I.R.; Cagide, E.; Vieytes, M.R.; Vega, F.V.; Rubiolo, J.A.; Miles, C.O.; Suzuki, T.; Yasumoto, T.; et al. Cytoskeletal toxicity of pectenotoxins in hepatic cells. *Br. J. Pharmacol.* **2008**, *155*, 934–944.
9. Moon, D.-O.; Kim, M.-O.; Kang, S.-H.; Lee, K.-J.; Heo, M.-S.; Choi, K.-S.; Choi, Y.-H.; Kim, G.-Y. Induction of G2/M arrest, endoreduplication, and apoptosis by actin depolymerization agent pextenotoxin-2 in human leukemia cells, involving activation of ERK and JNK. *Biochem. Pharmacol.* **2008**, *76*, 312–321.
10. Kim, M.-O.; Moon, D.-O.; Heo, M.-S.; Lee, J.-D.; Jung, J.H.; Kim, S.-K.; Choi, Y.H.; Kim, G.-Y. Pectenotoxin-2 abolishes constitutively activated NF-κB, leading to suppression of NF-κB related gene products and potentiation of apoptosis. *Cancer Lett.* **2008**, *271*, 25–33.
11. Ferron, P.J.; Hogeveen, K.; De Sousa, G.; Rahmani, R.; Dubreil, E.; Fessard, V.; Le Hegarat, L. Modulation of CYP3A4 activity alters the cytotoxicity of lipophilic phycotoxins in human hepatic HepaRG cells. *Toxicol. In Vitro* **2016**, *33*, 136–146.
12. Yoon, M.Y.; Kim, Y.C. Acute toxicity of pectenotoxin-2 and its effects on hepatic metabolising enzyme system in mice. *Korean J. Toxicol.* **1997**, *13*, 183–186.
13. Kittler, K.; Preiss-Weigert, A.; These, A. Identification Strategy Using Combined Mass Spectrometric Techniques for Elucidation of Phase I and Phase II in Vitro Metabolites of Lipophilic Marine Biotoxins. *Anal. Chem.* **2010**, *82*, 9329–9335.
14. Ramadoss, P.; Marcus, C.; Perdew, G.H. Role of the aryl hydrocarbon receptor in drug metabolism. *Expert Opin. Drug Metab. Toxicol.* **2005**, *1*, 9–21.
15. Beischlag, T.V.; Morales, J.L.; Hollingshead, B.D.; Perdew, G.H. The aryl hydrocarbon receptor complex and the control of gene expression. *Crit. Rev. Eukaryot. Gene Expr.* **2008**, *18*, 207–250.
16. Wang, Y.-M.; Ong, S.S.; Chai, S.C.; Chen, T. Role of CAR and PXR in xenobiotic sensing and metabolism. *Expert Opin. Drug Metab. Toxicol.* **2012**, *8*, 803–817.
17. Omiecinski, C.J.; Vanden Heuvel, J.P.; Perdew, G.H.; Peters, J.M. Xenobiotic Metabolism, Disposition, and Regulation by Receptors: From Biochemical Phenomenon to Predictors of Major Toxicities. *Toxicol. Sci.* **2011**, *120* (Suppl. 1), S49–S75.
18. Nishibe, Y.; Hirata, M. Effect of phenobarbital and other model inducers on cytochrome P450 isoenzymes in primary culture of dog hepatocytes. *Xenobiotica* **1993**, *23*, 681–692.
19. Li, A.P.; Rasmussen, A.; Xu, L.; Kaminski, D.L. Rifampicin induction of lidocaine metabolism in cultured human hepatocytes. *J. Pharmacol. Exp. Ther.* **1995**, *274*, 673–677.
20. Masubuchi, N.; Li, A.P.; Okazaki, O. An evaluation of the cytochrome P450 induction potential of pantoprazole in primary human hepatocytes. *Chem. Biol. Interact.* **1998**, *114*, 1–13.
21. Fux, E.; Rode, D.; Bire, R.; Hess, P. Approaches to the evaluation of matrix effects in the liquid chromatography-mass spectrometry (LC-MS) analysis of three regulated lipophilic toxin groups in mussel matrix (*Mytilus edulis*). *Food Addit. Contam. Part A* **2008**, *25*, 1024–1032.

22. Zendong, Z.; McCarron, P.; Herrenknecht, C.; Sibat, M.; Amzil, Z.; Cole, R.B.; Hess, P. High resolution mass spectrometry for quantitative analysis and untargeted screening of algal toxins in mussels and passive samplers. *J. Chromatogr. A* **2015**, *1416*, 10–21.
23. Genies, C.; Maître, A.; Lefèbvre, E.; Jullien, A.; Chopard-Lallier, M.; Douki, T. The Extreme Variety of Genotoxic Response to Benzo[a]pyrene in Three Different Human Cell Lines from Three Different Organs. *PLoS ONE* **2013**, *8*, e78356. doi:10.1371/journal.pone.0078356
24. Guo, F.; An, T.; Rein, K.S. The algal hepatoxoxin okadaic acid is a substrate for human cytochromes CYP3A4 and CYP3A5. *Toxicon* **2010**, *55*, 325–332.
25. Le Hegarat, L.; Dumont, J.; Josse, R.; Huet, S.; Lanceleur, R.; Mourot, A.; Poul, J.M.; Guguen-Guillouzo, C.; Guillouzo, A.; Fessard, V. Assessment of the genotoxic potential of indirect chemical mutagens in HepaRG cells by the comet and the cytokinesis-block micronucleus assays. *Mutagenesis* **2010**, *25*, 555–560.
26. Hashizume, T.; Yoshitomi, S.; Asahi, S.; Matsumura, S.; Chatani, F.; Oda, H. In vitro micronucleus test in HepG2 transformants expressing a series of human cytochrome P450 isoforms with chemicals requiring metabolic activation. *Mutat. Res. Toxicol. Environ. Mutagen.* **2009**, *677*, 1–7.
27. Berthou, F.; Goasduff, T.; Dreano, Y.; Ménez, J.-F. Caffeine increases its own metabolism through cytochrome P4501A induction in rats. *Life Sci.* **1998**, *57*, 541–549.
28. Aimova, D.; Svobodova, L.; Kotrbova, V.; Mrazova, B.; Hodek, P.; Hudecek, J.; Václavíková, R.; Frei, E.; Stiborová, M. The Anticancer Drug Ellipticine Is a Potent Inducer of Rat Cytochromes P450 1A1 and 1A2, Thereby Modulating Its Own Metabolism. *Drug Metab. Dispos.* **2007**, *35*, 1926–1934.
29. Bazin, E.; Mourot, A.; Humpage, A.R.; Fessard, V. Genotoxicity of a freshwater cyanotoxin, cylindrospermopsin, in two human cell lines: Caco-2 and HepaRG. *Environ. Mol. Mutagen.* **2010**, *51*, 251–259.
30. National Center for Biotechnology Information (NCBI) GenBank sequence database. Available online: http://www.ncbi.nlm.nih.gov/ (accessed on 11 January 2016).
31. National Center for Biotechnology Information (NCBI) Primer designing tool. Available online: http://www.ncbi.nlm.nih.gov/tools/primer-blast/index.cgi?LINK_LOC=BlastHome (accessed on 15 January 2016).
32. Luckert, C.; Hessel, S.; Lampen, A.; Braeuning, A. Utility of an appropriate reporter assay: Heliotrine interferes with GAL4/upstream activation sequence-driven reporter gene systems. *Anal. Biochem.* **2015**, *487*, 45–48.
33. Hampf, M.; Gossen, M. A protocol for combined Photinus and Renilla luciferase quantification compatible with protein assays. *Anal. Biochem.* **2006**, *356*, 94–99.

As shown previously SPX-1 efflux is dose-dependent and reaches about 60% when a high dose is used. Data on *in vitro* intestinal passage (Espiña et al., 2011) showed that a certain amount of SPX-1 is prone to enter blood circulatory system. This was confirmed *in vivo* by Otero et al., 2012 who detected SPX-1 in the blood and urine of mice after oral administration. Thus, the question whether hepatic metabolism leading to detoxification of SPX-1 is occurring has not been much deeply investigated. Therefore, we assessed the hepatic metabolism of SPX-1 using rat and human S9 fractions. The activity of metabolites towards nicotinic receptors was also studied.

Publication #3: Metabolism of the lipophilic phycotoxin 13-desmethylspirolide C in human and rat liver fractions

Article to be submitted in *Toxicology Letters*.

Metabolism of the lipophilic phycotoxin 13-desmethylspirolide C in human and rat liver fractions

Jimmy Alarcan[a], Estelle Dubreil[b], Antoine Huguet[a], Romulo Aráoz[c,d], Françoise Brée[e], Belkacem Bouaita[f], Dominique Hurtaud-Pessel[b], Stefanie Hessel-Pras[g], Alfonso Lampen[g], Valérie Fessard[a] and Ludovic Le Hégarat[a,*]

[a]Toxicology of Contaminants Unit, French Agency for Food, Environmental and Occupational Health & Safety, ANSES, Fougères 35306, France; jimmy.alarcan@anses.fr, antoine.huguet@anses.fr, ludovic.lehegarat@anses.fr, valerie.fessard@anses.fr

[b]Analysis of Residues and Contaminants Unit, French Agency for Food, Environmental and Occupational Health & Safety, ANSES, Fougères 35306, France; estelle.dubreil@anses.fr, dominique.pessel@anses.fr

[c]CNRS, Institut de Neurosciences (Neuro-PSI), UMR9197, 91191 Gif sur Yvette, France

[d]CEA/DRF/JOLIOT/SIMOPRO, Université Paris-Saclay, 91191 Gif sur Yvette, France; Romulo.ARAOZ@cea.fr

[e]Eurosafe, Parc d'Affaires La Bretêche, 35760 Saint Grégoire, France; francoise.bree@eurosafe.fr

[f]Biopredic International, Parc d'Affaires La Bretêche, 35760 Saint Grégoire, France; belkacem.bouaita@biopredic.com

[g]BfR, German Federal Institute for Risk Assessment, Department of Food Safety, Max Dohrn Strasse 8-10, 10589 Berlin, Germany; Stefanie.Hessel-Pras@bfr.bund.de, Alfonso.Lampen@bfr.bund.de

Corresponding author:

Ludovic Le Hégarat

Adress: ANSES, French Agency for Food, Environmental and Occupational Health & Safety, Fougères Laboratory, Toxicology of contaminants Unit, 10B rue Claude Bourgelat, 35306 Fougères, France

Phone: +33-(0)-299-172747.

Fax: +33-(0)-299-947880.

E-mail: ludovic.lehegarat@anses.fr

Abbreviations : α-BgTx: alpha-bungarotoxin; Clint: intrinsic clearance; CYP: cytochrome P450; EFSA: European Food Safety Authority; fm: fraction metabolized; HLM: human liver microsome; ip: intra-peritoneal; LC/HRMS: liquid chromatography/high resolution mass spectrometry; LOD: limit of detection; LOQ: limit of quantification; nAChR: nicotinic acetylcholine receptor; qPCR: quantitative polymerase chain reaction; SPX-1: 13-desmethylspirolide C

Abstract

13-desmethylspirolide C (SPX-1) is a phycotoxin produced by dinoflagellates which can accumulate in shellfish. SPX-1 induces neurotoxic effects in rodents through blockade of nicotinic acetylcholine receptors. As no human intoxication following consumption of contaminated seafood has ever been clearly reported, this toxin is not regulated. Nevertheless shellfish consumers can be exposed to low levels of SPX-1 which are recurrently found in shellfish. In order to follow the behavior of the toxin after ingestion and to establish if it can be detoxified thus explaining the absence of human intoxication, we assessed the metabolism of SPX-1 using external metabolic activation systems. Using rat and human liver S9 fractions, Phase I hydroxylation reactions were first checked before screening both phase I and II reactions. Then, the activity of the resulting metabolites towards nicotinic acetylcholine receptor was undertaken using a receptor-binding assay. Finally, direct participation of specific cytochrome P450 was assessed using a new innovative *in vitro* tool: the CYP1A2-Silensomes™. Our results indicate that SPX-1 is almost completely metabolized with both rat and human liver S9. No conjugated metabolite was detected when S9 assays were run simultaneously with phase I and II cofactors. The receptor-binding assays showed that the metabolites have a decreased affinity towards nicotinic acetylcholine receptors. Finally, we showed that CYP1A2 is playing an important role in SPX-1 biotransformation. Thus, liver first-pass metabolism participates in the detoxification of SPX-1 and therefore harmful effects may occur only in case of high levels contamination.

Keywords: spirolide, metabolism, Silensomes™, CYP, nicotinic acetylcholine receptors

1. Introduction

13-desmethyl spirolide C - (SPX-1) belongs to a particular group of lipophilic marine biotoxins, the cyclic imine toxins (Figure 1). It is mainly produced by dinoflagellates of the species *Alexandrium ostenfeldii* and *A. peruvianum* (Cembella et al., 2000, Touzet et al., 2008). SPX-1 accumulates in shellfish and is recurrently detected during monitoring (Amzil et al., 2007, Picot et al., 2013). Based on occurrence data provided by multiple countries, the EFSA (bulletin #1628) reported that SPX-1 is detected at a typical concentration of 20-50 µg/kg shellfish, but some teams also reported high levels

of contamination (Miles et al., 2010 reported 226 µg/kg shellfish). Currently, there is no regulation on SPX-1 in seafood worldwide including Europe due to lack of scientific evidence between human intoxication and SPX-1 levels in shellfish.

Structurally, it features a unique cyclic imine moiety involved in potent antagonism towards muscle and neuronal nicotinic acetylcholine receptors (nAChRs) (Gill et al., 2003, Bourne et al., 2010, Aráoz et al., 2015). Classified as fast-acting toxin, SPX-1 induces rapid death, between 3 and 20 minutes, after intra-peritoneal injection or gavage to rodents by blocking respiratory muscles (Gill et al., 2003, Munday et al., 2012). Intra peritoneal and oral LD_{50} were estimated to 6.9 and 160 µg/kg b.w, respectively (Munday et al., 2012). Besides, after a single oral administration of 27.9 µg/kg to mice, no clinical effect was reported and only low amounts of SPX-1 were detected in blood and urine (Otero et al., 2012). Additionally, *in vitro* studies on human intestinal barrier model showed that SPX-1 can easily cross the monolayer (Espiña et al., 2011). Taken together, these results may highlight a crucial role of the liver in the biotransformation of SPX-1. Indeed, several hydroxylated metabolites of SPX-1, which are likely produced by cytochrome(s) P450, have been described using human liver microsomes (HLM) (Hui et al., 2012).

In order to better characterize the potential toxicity of SPX-1 to humans in relation with liver metabolism, we proposed to undertake a multi approach-based assessment by i) screening both main phase I and phase II reactions in rat and human liver S9, ii) investigating the receptor-binding activity of S9-generated metabolites using the Torpedo- nAChRs binding assay, iii) studying nuclear receptors and phases 0, I, II and III gene regulation in human HepaRG® cell line, and finally iv) identifying the P450 implicated in the metabolism of SPX-1 using the Silensomes™ technology.

Figure 1. Chemical structure of SPX-1

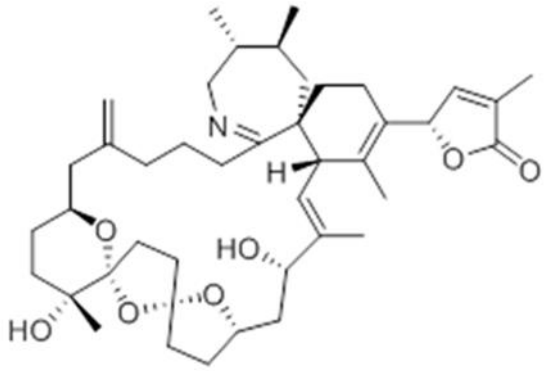

2. Materials and methods

2.1 Chemicals

SPX-1 was purchased from the National Research Council Institute for Marine Biosciences (Halifax, NS Canada). Omeprazole, rifampicin, alamethicin (Trichoderma viride), D-Saccharic acid 1,4-lactone monohydrate (d-saccharolactone), L-glutathione reduced (GSH), uridine 5'-diphosphoglucuronic acid triammonium salt (UDPGA), adenosine 3'-phosphate 5'-phosphosulfate lithium salt hydrate (PAPS) and S-(5'-Adenosyl)-L-methionine p-toluenesulfonate salt (SAM), Streptavidin-HRP and α-BgTx were purchased from Sigma-Aldrich (St. Louis, MO, USA). o-Phenylenediamine (OPD) tablets were

obtained from DAKO (Glostrup, Denmark). Biotin-α-BgTx was obtained from Molecular Probes (Eugene, OR, USA). Reduced nicotinamide adenine dinucleotide phosphate (NADP+), glucose 6-phospate (G6P), magnesium chloride hexahydrate, potassium chloride, Na_2HPO_4, and NaH_2PO_4 were purchased from Carl Roth (Karlsruhe, Germany). All other chemicals including acetonitrile (ACN), methanol (MeOH) and dimethyl sulfoxide (DMSO) were of analytical grade and purchased from Fisher Scientific (Leicestershire, England). Formic acid was purchased from Merck (Darmstadt, Germany). Deionised water was prepared using a Milli-Q system (Millipore, Bedford, MA, USA). β-naphtoflavone and phenobarbital induced Sprague Dawley rat and human hepatic S9 fractions as well as CYP1A2-Silensomes™ were purchased from Biopredic International (Rennes, France).

2.2 Cell culture

HepaRG® cells were cultured as previously published (Le Hegarat et al., 2010). Briefly, HepaRG® cells (passages 13–19) were seeded at 30 000 cell/cm^2 in 96-well (for High Content Analysis) or 12-well plates (for qPCR assays) in culture medium (Williams' medium E with GlutaMAX-I, supplemented with 10% fetal bovine serum, 50 IU/ml penicillin, 50 µg/ml streptomycin, 2 mM L-glutamine, 5 µg/ml bovine insulin, and 50 µM hydrocortisone hemisuccinate). After 2 weeks, the cells were cultured in the same medium supplemented with 1.7% DMSO (differentiation medium) for two additional weeks. The medium was renewed every 2 to 3 days.

2.3 Silensomes™

Silensomes™ are human pooled liver microsomes in which a single CYP has been chemically and irreversibly inactivated using mechanism based inhibitors (Parmentier et al., 2016). It proved to have better predictability for the *fm* evaluation than recombinant CYP towards several drug CYP-mediated metabolic studies (Parmentier et al., 2016).

2.4 S9 phase I metabolism

In order to target phase I metabolism, specific co-factors were added to liver S9 fractions: NADPH regenerating system (4 mM $NADP^+$ and 5mM G6P), KCl (33 mM), $MgCl_2$ (8 mM), and 0.1 M sodium phosphate buffer (0.2 M Na_2HPO_4 + 0.2 M NaH_2PO_4, pH 7.4). An experimental volume of 0.5 mL containing phase I co-factors (final concentration as described above), S9-fraction (final concentration 2.2 mg/mL) and 100 nM SPX-1 were incubated in a water bath at 37 °C for 3 h. The reaction was then stopped by adding 0.5 mL of ice cold MeOH. After 20 min centrifugation (14 000×g) at 4°C, samples were analyzed or stored at -80°C until analysis. For negative metabolic control, the same procedure was followed but S9 fraction was heat-inactivated for 45 min at 60°C prior to incubation with co-factors and SPX-1. Two independent experiments were conducted with the same S9 batches.

2.5 S9 phase I and II metabolism

In order to check if phase II enzymes may be involved in SPX-1 metabolism, several phase II reactions were screened along with phase I: gluruconidation, sulfation, glutathione conjugation and methylation. The procedure was conducted as followed: rat or human liver S9 fractions were first cooled on ice for 15 min with alamethicin (0.025 mg/ml). Then, d-saccharolactone (10 mM), UDPGA (6 mM), GSH (5 mM), PAPS (0,2 mM), SAM (0,1 mM) NADPH regenerating system (4 mM $NADP^+$ and 5mM G6P), KCl (33 mM), $MgCl_2$ (8 mM), and 0.1 M sodium phosphate buffer (0.2 M Na_2HPO_4 + 0.2 M NaH_2PO_4, pH 7.4) were added. An experimental volume of 0.5 mL containing phase I and II co-factors (final concentration as described above), S9-fraction (final concentration 2.2 mg/mL), and 100 nM SPX-1 were incubated in a water bath at 37 °C for 3 h. The reactions were stopped by adding 0.5 mL of ice cold MeOH. After 20 min centrifugation (14 000×g) at 4°C, samples were analyzed or stored at -80°C until analysis. For negative metabolic control, S9 fraction was heat-inactivated for 45 min at

60°C prior to incubation with co-factors and SPX-1. Two independent experiments were conducted with the same S9 batches.

2.6 Purification of *Torpedo* Electrocyte Membranes

Torpedo electrocyte membranes rich in nAChRs were purified from the electric organ of *Torpedo marmorata* as described previously (Hill et al., 1991, Vilariño et al., 2009).

2.7 Microplate receptor-binding assay

Prior to the analysis, the metabolites generated in S9 assays were evaporated at 40°C under a stream of N_2. The dried samples were resuspended in 100 µL methanol. Dilutions of the samples (6 %) were prepared in TBS-BSA (150 mM NaCl, 50 mM Tris-HCl, 0.5% BSA, pH 7.4). The binding activity of SPX-1 and its metabolites was assessed using the non-radioactive microplate receptor-binding assay as described by Aráoz et al (Aráoz et al., 2012). Briefly, 96-well microplate coated with Torpedo-nicotinic acetylcholine receptors was incubated overnight at 4°C with 100 µL of toxin or toxin-derived metabolites samples. Methanol concentration in the samples was 6 %. At this concentration, methanol does not interfere with the binding assay, as the tolerance of the method to methanol is higher (10%) (Rubio et al., 2014). The next day, the microplate was incubated at room temperature for 30 min, after which, a volume of 50 µL biotin-α-bungarotoxin (BgTx) (2.4×10^{-7} M) was added to each well prior to incubation for 30 min at room temperature under constant shaking. The wells were washed thrice with 250 µL washing buffer (TBS containing 0.1% Tween 20), and immediately after, 100 µL of streptavidin-HRP (220 ng/nL protein) was added to each well and further incubated for 30 min. For quantifying the inhibition binding, the wells were washed thrice as described, and 100 µL of freshly prepared peroxidase substrate OPD (as indicated by the supplier) were added to each well. After 5 min, the enzymatic reaction was stopped by adding 100 µL 0.5 M H_2SO_4. The data were recorded using an ELISA reader (CLARIOstar, BMG LABTECH). The optical density obtained at 492 nm (OD492nm) was transformed into an inhibition percentage using:

Inhibition % = 100× (100% signal - signal sample)/(100% signal - 100% inhibition)

where: 100% signal represents the absorption data from wells in which Torpedo membranes were incubated in the absence of toxins/extracts; signal sample is the absorption data of tested samples wells; 100% inhibition, is the absorption data obtained after incubating Torpedo-nAChRs with 1×10^{-5} M α-BgTx. Each sample was tested in triplicate.

2.8 Real time quantitative Polymerase Chain Reaction (RT-qPCR) analysis

For qPCR assays, after 24 h incubation with SPX-1 or positive controls (50 µM omeprazole and 10 µM rifampicin), cells were washed twice with PBS. Total RNA extraction was then performed using the Total RNA isolation NucleoSpin® RNA II kit from Macherey Nagel (Hoerd, France) following the manufacturer's protocol. RNA concentration and quality was determined by spectrophotometric measurements with BioSpec-nano (Shimadzu Biotech, Marne la Vallée, France). RNA integrity was checked through electrophoresis using Experion (Bio-Rad, Marne la Coquette, France). RNA samples were then reverse transcribed into double strand cDNA using the High Capacity RNA-to-cDNA kit (Applied Biosystems, Foster City, CA, USA) according to the manufacturer's instructions. The sequences of target genes were obtained from the National Center for Biotechnology Information (NCBI) GenBank sequence database (http://www.ncbi.nlm.nih.gov/). Primers were designed with the Primer designing tool from NCBI (http://www.ncbi.nlm.nih.gov/tools/primer-blast/index.cgi?LINK_LOC=BlastHome). For each gene, at least one primer was designed on the exon-exon junction. All primers (Supplementary data Table S1) were purchased from Sigma-Aldrich (Saint-Louis, MO, USA). Quantitative PCR was performed using Light Cycler® 1536 from Roche (Mannheim, Germany). SYBR Green chemistry was used. Reactions were performed in a total volume of 2 µl containing 1X Light cycler 1536 DNA Green Master, 1X Light cycler 1536 DNA Master mix (Roche),

300 nM of each primer, and 0.1 ng cDNA. Negative quantitative PCR controls of RNase-free water were included in each run for contamination assessment. The thermal cycling conditions were 94°C for 15 s, followed by 40 cycles of 15 s at 94°C and 30 s at 60°C with a slow ramp temperature (2,2°C/s). Light Cycler® 1536 software (version 1.1.0.1112; Roche, Basel, Switzerland) was used for the quantitative analysis. Melting curve analysis was used to check the specificity of each amplicon. Threshold Cqs were calculated from a baseline subtracted curve fit. Calibration curves were established for each gene from a serial dilution of a reference sample (pool of cDNA samples). According to these calibration curves, for each sample, mean relative amounts of mRNA of the target genes were calculated and then normalized to the GAPDH reference gene. Values were presented as fold change normalized to the solvent control.

2.9 Silensomes™ phase I clearance and CYP investigation

In order to investigate the involvement of CYP1A2 in SPX-1 metabolism, appropriate co-factors were added to CYP1A2-Silensomes™ fractions: NADPH (1 mM), $MgCl_2$ (5 mM), and 0.1 M sodium phosphate buffer (0.2 M Na_2HPO_4 + 0.2 M NaH_2PO_4, pH 7.4). An experimental volume of 0.1 mL containing phase I co-factors (final concentration as described above), Silensomes™ (final concentration 1 mg/mL) and 100 nM SPX-1 were incubated in a water bath at 37 °C for different times. The reaction was then stopped by adding 0.1 mL of ice cold ACN. After 20 min centrifugation (14 000×g) at 4°C, samples were analyzed or stored at -80°C until analysis. Homologous control Silensomes™ were treated following the same procedure. The *in vitro* intrinsic clearances (Cl_{int}) were calculated as follow: Cl_{int} (µL/min/mg) = (slope x V) / P, where slope is the elimination rate constant (min^{-1}) for exponential substrate loss, V is the incubation volume (µL) and P is the microsomal protein amount (mg) in incubation. The fraction metabolized (fm) by CYP was calculated as follow: CYP1A2 fm = [1- (Cl_{int} CYP1A2-Silensomes™/ Cl_{int} Control-Silensomes™)] x 100. Three independent experiments were conducted with the same Silensomes™ batches.

2.10 LC/HRMS analysis

Metabolism investigation was conducted in two steps: the decrease of the parent compound was first measured using LC/HRMS quantitative method and then the formation of metabolites was studied via the metabolite research software MetWorks® 1.3. Analyses were conducted on a Thermo Fisher Accela LC (Thermo Fisher, Bremen, Germany) system hyphenated to an LTQ-Orbitrap XL mass spectrometer. LC elutions were performed on an Agilent Zorbax Eclipse XDB-C18 column (Agilent Technologies, Santa Clara, CA, USA) (150×3.0 mm, 3.5 µm). Chromatographic separation was carried out using two mobile phase preparations consisting of mobile phase (A) 100 % water and mobile phase (B) 5 % water and 95 % acetonitrile. Both mobile phases contained 2 mM formate ammonium and 50 mM formic acid. The gradient conditions were set as follows: from 0 to 5 min ramp linearly from 98 to 2 % of mobile phase A and hold for 7 min, then ramp over 1 min to initial conditions and hold for 3 min to re-equilibrate the system. The flow rate was set at 0.3 mL min^{-1}, the injection volume was 10 µL and the column oven was maintained at 25°C. SPX-1 was quantified using a calibration curve with SPX-1 standards at 0, 5, 10, 25, 50, 75 and 100 ng/ml in MeOH/H_2O (2/3, 1/3). The mass spectrometer was operated with an electrospray ionization probe in positive mode using the following source parameters: sheath gas flow rate: 40 arb; auxiliary gas flow rate: 15 arb; sweep gas flow rate: 2 arb; ion spray voltage: 3.5 kV; capillary temperature: 350°C; capillary voltage: 30 V; and tube lens: 100 V. The instrument was calibrated using the manufacturer's calibration solution consisting of three mass calibrators (i.e. caffeine, tetrapeptide MRFA and Ultramark) to reach mass accuracies in the 1–3 ppm range. The instrument was operated in full-scan mode from m/z 100–1,000 at a resolving power of 60,000 (full width at half maximum) allowing SPX-1 detection as protonated adduct $[M+H]^+$ (m/z = 692.4521) as well as metabolite formation investigations using MetWorks® software (Thermo Fisher Scientific, Waltham, MA, USA). The extraction mass window was set at ± 5 ppm. SPX-1 recoveries were calculated as follow: Ri = (ci x 100)/c0 where ci is the measured concentration of the sample i and c0 is the initial concentration.

2.11 Statistical analysis

GraphPad Prism 5 (GraphPad Software, Inc., La Jolla, CA, USA) was used for the statistical analyses. Data were compared to the control group using one-way ANOVA followed by Dunnett's post hoc tests. All error bars denote standard deviation (SD). Statistical significance was set as follows: *$p < 0.05$, **$p < 0.01$, ***$p < 0.001$.

3. Results

3.1 SPX-1 phase I metabolism in rat and human S9 fractions

First, a quantitative method for SPX-1 dosage using LC-HRMS was developed. SPX-1 eluted at the same retention time in both native and inactivated S9 as compared to standard. A standard solution of SPX-1 was used to establish a linear calibration curve ($R^2 = 0.99$) between 5 and 100 ng/mL toxin. The limits of detection (LOD) and quantification (LOQ) were estimated using signal intensities at 5 and 10 ng/mL SPX-1 standards since there was no signal to noise ratio when extracting the molecular mass. LOD and LOQ values were 0.76 and 3.4 ng/mL respectively. We then determined the recoveries of SPX-1 following treatment with inactivated S9 fractions. We observed a mean recovery of 83 ± 11% with inactivated rat S9 while 61 ± 1% mean recovery was obtained with inactivated human S9 (Supplementary data Table S2).

With native liver S9 fractions, we observed a full loss for rat, 99% ± 2%, and almost full loss for human, 87 ± 18% (supplementary data Table S3).

The detection of metabolites was investigated using MetWorks® software. From $[M+H]^+$ protonated parent ion (m/z = 692.4521), the screening of a wide panel of phase I reactions based on mass shifts was performed. In rat S9, one metabolite with m/z = 708.4470 was found in the two experiments whereas four additional metabolites (m/z = 706.4313, m/z = 722.4263, m/z = 724.4419 and m/z = 724.4576) were only found in the second experiment (Table 1). For human S9, one common metabolite m/z = 722.4263 was found in the two experiments and three additional metabolites were detected only in the second experiment (two peaks for m/z = 708.4470 and m/z = 706.4313) (Table 1). For the double peak, the minor peak featured the same retention times as for rat (5.50 min), whereas the major had a retention time of 5.76 min. Since we observed an extensive metabolism of SPX-1 by phase I enzymes in both rat and human S9, we investigated if phase II enzymes could be implicated in SPX-1 or phase I metabolites conjugation.

Table 1. SPX-1 metabolites detected after incubation with rat or human S9 fractions and phase I co-factors. S9 fractions were incubated for 3 h with specific phase I co-factors and 100 nM of SPX-1. Results were obtained from two independent experiments conducted with the same S9 batches. Retention times in black and green indicate results for rat and human S9 respectively.

Entity	Formula $[M+H]^+$	Accurate m/z	Rt (min)	
			Assay #1	Assay#2
SPX-1	$C_{42}H_{62}NO_7^+$	692.4507	5.73	5.88
M1	$C_{42}H_{60}NO_8^+$	706.4313		5.77/5.76
M2	$C_{42}H_{62}NO_8^+$	708.4470	5.44	5.50/5.50/5.76
M3	$C_{42}H_{60}NO_9^+$	722.4263	5.55	5.44/5.47
M4	$C_{42}H_{62}NO_9^+$	724.4419		5.31
M5	$C_{42}H_{64}NO_9^+$	726.4576		5.33

3.2 SPX-1 phase I and II metabolism in rat and human S9 fractions

We observed a mean recovery of 88 ± 24% with inactivated rat S9 while 87 ± 1% mean recovery was obtained with inactivated human S9 (Supplementary data Table S4). For both native S9 fractions, we observed similar results as the experiments with only phase I co-factors: 97 ± 5% and 100% ± 0% loss of SPX-1 with respectively native rat and human S9 fractions (Supplementary data Table S5). From the protonated ion parent (m/z = 692.4521), the screening of a wide panel of phase I and phase II reactions based on mass shifts was performed. For rat S9, two metabolites were found in the two experiments: the same metabolite as detected only with phase I co-factors (m/z = 708.44701) and a new one with m/z = 678.4000 (Table 2). The first experiment featured also one other metabolite previously described: m/z = 724.4419. The second experiment also featured the previously described metabolites with m/z = 706.4313 and m/z = 726.4576. For human S9, four metabolites were found in the two experiments: three same metabolites as previously detected (two with m/z = 708.4470 and one with m/z = 722.4263) and one with m/z = 678.4000 (Table 2). Retention times for metabolites with m/z = 678.4000 were substantially different between rat and human S9 (5.08 min for rat S9 and 5.33 min for human S9). In the first experiment, a new metabolite with m/z = 788.40381 was detected. In both inactivated rat and human S9, only SPX-1 protonated adduct was detected (data not shown).

Table 2. SPX-1 metabolites detected after incubation with rat or human S9 fractions and phase I and II co-factors. S9 fractions were incubated for 3 h with specific phase I and II co-factors and 100 nM of SPX-1. Results were obtained from two independent experiments conducted with the same S9 fraction batches. Retention times in black and green indicate results for rat and human S9 respectively.

Entity	Formula $[M+H]^+$	Accurate m/z	Rt (min)	
			Assay #1	Assay#2
SPX-1	$C_{42}H_{62}NO_7^+$	692.4507		5.80
M0	$C_{41}H_{60}NO_7^+$	678.4000	5.08/5.33	5.05/5.34
M1	$C_{42}H_{60}NO_8^+$	706.4313		5.72
M2	$C_{42}H_{62}NO_8^+$	708.4470	5.45/5.60/5.76	5.46/5.60/5.76
M3	$C_{42}H_{60}NO_9^+$	722.4263	5.56	5.58
M4	$C_{42}H_{62}NO_9^+$	724.4419	5.29	
M5	$C_{42}H_{64}NO_9^+$	726.4576		5.28
M6	$C_{42}H_{62}NSO_{11}^+$	788.4038	9.25	

3.3 Metabolites activity towards nicotinic acetylcholine receptor

To determine the degree of detoxification of SPX-1 by S9 liver fractions, the affinity of the metabolites was tested with a Torpedo-nAChR-binding assay. Metabolites from rat S9-phase I incubation decreased by ~11% the competitive binding of Biotin-α-bungarotoxin to the receptor, compared to toxin control (Table 3). On the contrary, the metabolites resulting from incubations with rat S9 phases I + II co-factors showed a ~38% decrease of the inhibition binding (Table 3).

In the case of human S9 treatments, the SPX-1 metabolites from phase I incubations inhibited by ~41% the binding of Biotin-α-bungarotoxin towards Torpedo-nAChR when compared to the control (Table 3). Finally, an average decrease of ~21% of the inhibition for SPX-1 metabolites resulting from phase I and II incubations with human S9 was observed compared to the control (Table 3).

Altogether, under our experimental conditions, the metabolites of SPX-1 showed a decreased inhibition-binding activity towards muscle-type nAChR. Our functional results suggest a differential affinity of some metabolites towards the nicotinic receptor.

Table 3. Functional activity of SPX-1 metabolites. Following SPX-1 incubation with rat and human S9, the antagonistic activity of the resulting metabolites was tested against Torpedo-nicotinic acetylcholine using a non-radioactive microplate-receptor binding assay. Data represents the mean ± SD of two independents experiments performed in three replicates.

Treatment	**SPX-1 Ctrl**	**SPX-1 metabolites**	
	Inhibition (%)	Mass (*m*/*z*)	Inhibition (%)
Rat S9 Phase I (assay #2)	49.9 ± 2.7	706.4313, 708.4470, 722.4263, 724.4419, 726.4576	38.7 ± 1.3
Rat S9 Phase I + II (assay #1)	54.4 ± 5.5	678.4000, 708.4470, 724.4419	15.5 ± 1.7
Human S9 Phase I (assay #1)	48.7 ± 7.2	722.4263	7.2 ± 2.0
Human S9 Phase I + II (assay #1)	52.7 ± 5.4	678.4000, 708.4470, 722.4263, 788.4038	33.2 ± 1.0
Human S9 Phase I + II (assay #2)	58.7 ± 6.1	678.4000, 708.4470, 722.4263	37.0 ± 2.1

3.4 Effects of SPX-1 on the expression of nuclear receptors, phase 0, I, II and III metabolism genes in HepaRG cells by qRT-PCR

Gene expression levels were analyzed after 24 h treatment to 33 and 66 nM SPX-1 (percentage of solvent MeOH below 1%). These concentrations were not cytotoxic based on previous study (Ferron et al., 2016). No significant statistical effect regarding nuclear receptors was observed (Table 4). For phase I genes, *CYP1A2* was strongly up regulated at 66 nM SPX-1 (8.5 fold induction) whereas other *CYPs* were not much affected (Table 4). The results on phase II genes showed a slight up-regulation of *NAT1* (1.8 fold induction) at 33 nM SPX-1. Similarly, regarding transporters, an up-regulation of *SLC22A3* (2.0 fold induction) was observed at 66 nM SPX-1. Omeprazole (50 µM) and rifampicin (10 µM) used as positive controls clearly showed an up-regulation for several *CYP* genes. Considering the strong up-regulation of *CYP1A2* gene expression by SPX-1, we investigated if the CYP1A2 could be involved in the metabolism of SPX-1 using CYP1A2-Silensomes™ tool.

Table 4. Effects of SPX-1 on mRNA expression in HepaRG cells. Cells were treated with two concentrations of SPX-1 for 24 h. Rifampicin (10 µM) and omeprazole (50 µM) were used as positive controls. Results were obtained from three independent experiments. Data represents means ± SD of fold change compared to solvent control. *$p < 0.05$, **$p < 0.01$, ***$p < 0.001$ after one-way ANOVA followed by Dunnett's post hoc tests.

Metabolism Phases	Gene	[nM]				OME		RIF		Gene
		33		66						
		Mean	SD	Mean	SD	Mean	SD	Mean	SD	
Nuclear receptors	*AHR*	1.3	0.8	1.2	0.9	0.8	0.3	0.9	0.3	*AHR*
	NR1I2	1.4	0.1	1.3	0.2	1.0	/	0.7	0.4	*NR1I2*
Phase 0 influx transporters	*SLC22A1*	1.8	1.6	1.6	1.1	1.3	1.2	1.1	0.3	*SLC22A1*
	SLC22A3	1.5	0.6	2.0	0.6	1.0	0.4	1.1	0.5	*SLC22A3*
	SLCO1A2	0.8	0.3	0.5	0.5	0.4	0.3	0.2*	0.2	*SLCO1A2*
	SLCO1B1	1.3	0.9	0.9	0.6	0.6	0.1	1.0	0.3	*SLCO1B1*
Phase I mono-oxygenases	*CYP1A1*	1.9	1.2	1.5	1.5	127.0**	67.1	0.4	0.4	*CYP1A1*
	CYP1A2	2.3	1.5	8.5	6.7	245.2**	160.1	1.4	0.2	*CYP1A2*
	CYP2B6	2.1	2.0	2.8	2.9	8.0	8.0	4.3	2.5	*CYP2B6*
	CYP2C9	1.3	0.7	1.3	0.8	1.4	0.3	2.2	0.3	*CYP2C9*
	CYP2C19	1.2	0.5	1.3	0.2	1.2	0.2	1.6	0.4	*CYP2C19*
	CYP3A4	1.1	0.2	1.0	0.2	13.9**	6.7	29.2***	3.6	*CYP3A4*
	CYP3A5	1.1	0.6	1.1	0.6	1.1	0.2	1.5	0.2	*CYP3A5*
Phase II transferases	*GSTM1*	1.0	0.2	1.4	0.5	1.2	0.3	1.0	0.1	*GSTM1*
	NAT1	1.8*	0.5	1.4	0.3	1.0	0.2	1.0	0.2	*NAT1*
	NAT2	1.1	0.4	1.0	0.2	0.8	0.2	0.9	0.3	*NAT2*
	SULT1A1	1.0	0.1	0.9	0.2	0.9	0.1	1.0	0.1	*SULT1A1*
	SULT1E1	1.1	0.4	0.8	0.7	0.4	0.2	0.7	0.4	*SULT1E1*
	UGT1A1	1.7	1.2	2.0	1.9	2.8	1.5	1.7	0.2	*UGT1A1*
	UGT1A9	1.1	0.2	1.1	0.5	1.2	0.1	1.1	0.3	*UGT1A9*
	UGT2B4	1.2	0.2	1.1	0.5	1.3	0.2	1.4	0.5	*UGT2B4*
Phase III efflux transporters	*ABCB1*	1.3	0.4	1.4	0.4	1.4	0.5	1.7	0.4	*ABCB1*
	ABCC2	1.4	0.5	1.3	0.4	1.2	0.5	1.2	0.2	*ABCC2*
	ABCC3	1.1	0.4	1.4	0.8	1.0	0.3	0.9	0.0	*ABCC3*
	ABCG2	1.3	0.5	1.0	0.4	2.6	1.4	1.1	0.1	*ABCG2*

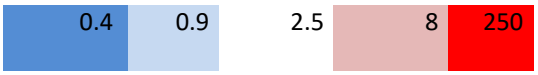

3.5 SPX-1 phase I metabolism using CYP1A2-Silensomes™

CYP1A2-Silensomes™ was incubated with 100 nM of SPX-1. Depletion of SPX-1 throughout time is shown in Figure 2. With control-Silensomes™ SPX-1 was not detected anymore after 15 min. A slower depletion was observed when CYP1A2 was inhibited. From the depletion curves, we estimated the *in vitro* intrinsic clearance (Cl_{int}) which was two-fold lower with CYP1A2-Silensomes™ (159.1 ± 12.2 $\mu L \times min^{-1} \times mg^{-1}$) than in control (303.4 ± 21.5 $\mu L \times min^{-1} \times mg^{-1}$). From these data, the CYP1A2 *fm* was evaluated to 48%.

Figure 2. SPX-1 kinetics with CYP1A2-Silensomes™. 100 nM SPX-1 was incubated with co-factors and microsomes for different times. Results were obtained from three independent experiments performed in triplicate and conducted with the same Silensomes® batches. Data represents means ± SD.

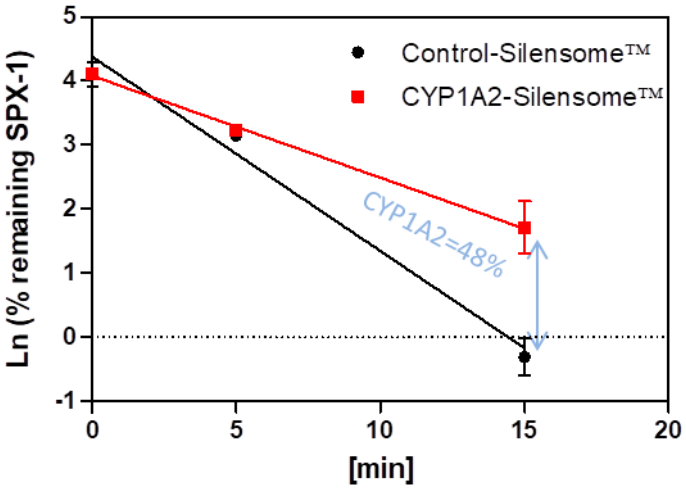

The detection of the metabolites was also investigated as described above. For both homologous control Silensomes™ and CYP1A2-Silensomes™ five metabolites were found (Figure 3). One hydroxyl metabolite (m/z = 708.4470) could be detected but disappeared throughout time. The major metabolite was the same as previously observed in human S9 assays with a mass corresponding to the conversion of a methyl into a carboxylic acid (m/z = 722.4263).

Figure 3. Metabolites kinetics in CYP1A2-Silensomes™ and its respective control. Results were obtained from three independent experiments performed in triplicate. Data represents means ± SD.

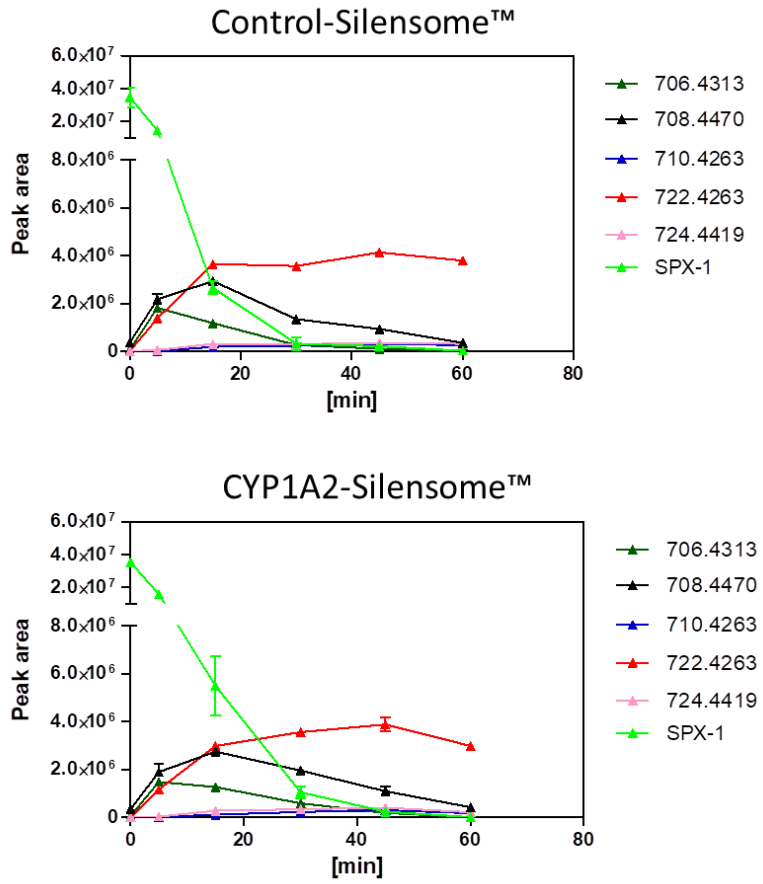

4. Discussion

In this study, we first assessed the metabolism of SPX-1 in rat and human liver S9 as well as the toxicity of the metabolites before undertaking a preliminary investigation on the involved pathways.

Using human liver S9 fractions, we observed a full depletion of SPX-1 simultaneously to the formation of multiple metabolites. We detected five metabolites with the same accurate masses as described with HLM (Hui et al., 2012). Our unability to detect the other ones may be related to the lower concentration of toxin used in our experiments, 100 nM compared to 10 µM used by Hui and collaborators. The main metabolites were successfully detected in the two experiments, but some minor metabolites were only detected in one experiment. This is likely the result of analytical discrepancies, the sensitivity can indeed slightly vary from one run to another. One phase II metabolite was detected but needs to be confirmed. Using rat S9, a similar depletion of SPX-1 was observed. The same four metabolites were detected in rat and humans. However, different retention times were found between rat and human S9 for several metabolites. Especially, the major oxygenated metabolite found with human S9 has a different retention time compared to the one found with rat S9. This may indicate that the biotransformation occurred on a different site of the SPX-1, meaning that the metabolites could be isomers. As isomers can display great differences in pharmacokinetics and pharmacodynamics (Chhabra et al., 2013), if it turns out that metabolites from rat S9 are isomers of those produced with the human S9, additional studies will be required to study the toxic potential.

We demonstrated that SPX-1 was completely transformed into different metabolites by rat and human liver fractions. Then, it is important to determine if the metabolic process could lead to detoxification or bioactivation by studying the capacity of the metabolites to inhibit muscle nicotinic acetylcholine receptors as the parent compound (Aráoz et al., 2015). Although it is difficult to draw conclusions for each single metabolite since the samples contained various mixtures of metabolites, it appears that the metabolites produced by both rat and human liver S9 show a decreased affinity for nicotinic acetylcholine receptors. When calculating the mean of inhibitions from both experimental conditions (phase I and phase I+II), the rat metabolites show higher affinity than human metabolites. However, to get a clearer view, it should be further studied by assessing the activity of each single metabolite on nAChR as well as on other cellular targets. Since rat and human liver S9 featured a similar pattern of metabolites, this indicates that rat is likely to be a suitable model for in vivo experiments.

We confirmed that SPX-1 undergoes a large biotransformation process by liver enzymes and then we aimed at getting a closer look on the pathways involved by investigating the modulation by SPX-1 of a panel of xenobiotics metabolism-associated genes expression in human HepaRG® cells. We observed that SPX-1 particularly up-regulated *CYP1A2*, after 24 h of treatment. In the human liver, CYP1A2 plays an important role in xenobiotic metabolism (about 10-20% of drugs are substrates of CYP1A2) (Omiecinski et al., 2011). Besides detoxification reactions, CYP1A2 is also known to bioactivate some xenobiotics such as 1-nitropyrene or aflatoxin B1 (Yamazaki et al., 2000, Van Vleet et al., 2002). To point out if this enzyme is implied in SPX-1 metabolism, we used the innovative Silensomes™ tool. The intrinsic clearance found in the control classifies SPX-1 in the category of “high intrinsic clearance compounds” according to Nassar et al., 2009. This concurs with the results of Hui et al., 2012 who observed as well a high intrinsic clearance of SPX-1 within their experimental conditions. We found that the contribution of CYP1A2 was estimated to 48%, meaning that other(s) xenobiotic-metabolizing enzyme(s) can likely participate in SPX-1 metabolism.

It is likely that the high rate of SPX-1 metabolisation may explain why no human intoxication related to SPX-1 shellfish contamination was reported so far. Similarly, Otero et al. concluded that a low oral dose of SPX-1 was not toxic to mice. However, saturation of the enzymatic pathway, competition with other compounds as well as genetic variability can provoke a limited detoxification by liver, thus affecting the response to SPX-1. Therefore, some sensitive populations to SPX-1 cannot be excluded.

In conclusion, we showed that SPX-1 undergoes extensive phase I metabolism using liver S9 fraction leading to the formation of several metabolites. If we clearly showed that CYP1A2 was involved in the biotransformation of the toxin, other XMEs are expected to intervene. The metabolites formed were less potent when considering the response towards the nicotinic acetylcholine receptor assay, indicating that hepatic metabolism participates in the detoxification of SPX-1.

Conflict of interest

The authors declare no conflict of interest in the content of this work.

Acknowledgments

We would like to thank Jean-Michel Delmas from the ARC unit for his excellent support and advices on Orbitrap use. We would like to thank Patrick Fach and Cédric Woudstra from the IdentyPath platform (Anses Maisons-Alfort) for their excellent support and advices on qRT-PCR assays. We would like to thank Abdelhafidh Belakermi from Bioprédic International for his help on the Silensomes™ assays.

Funding information

This research did not receive any specific grant from funding agencies in the public, commercial, or not-for-profit sectors.

References

Amzil Z, Sibat M, Royer F, Masson N, Abadie E. (2007). Report on the first detection of pectenotoxin-2, spirolide-A and their derivatives in French shellfish. Mar Drugs. 5(4), 168–179.

Aráoz, R., Ramos, S., Pelissier, F., Guérineau, V., Benoit, E., Vilariño, N., Botana, L.M., Zakarian, A. and Molgó, J. (2012). Coupling the Torpedo microplate-receptor binding assay with mass spectrometry to detect cyclic imine neurotoxins. Anal Chem. 84(23), 10445-10453.

Aráoz R, Ouanounou G, Iorga BI, Goudet A, Alili D, Amar M, et al. (2015). The Neurotoxic Effect of 13,19-Didesmethyl and 13-Desmethyl Spirolide C Phycotoxins Is Mainly Mediated by Nicotinic Rather Than Muscarinic Acetylcholine Receptors. Toxicol Sci. 147(1), 156–67.

Bourne, Y., Radic, Z., Aráoz, R., Talley, T. T., Benoit, E., Servent, D., Taylor, P., Molgó, J., and Marchot, P. (2010). Structural determinants in phycotoxins and AChBP conferring high affinity binding and nicotinic AChR antagonism. Proc. Natl. Acad. Sci. USA 107, 6076–6081.

Cembella, A.D., Lewis, N.I., Quilliam, M.A., (2000). The marine dinoflagellate Alexandriumostenfeldii (Dinophyceae) as the causative organism of spirolide shellfish toxins. Phycologia 39, 67–74.

Chhabra N, Aseri ML, Padmanabhan D. (2013). A review of drug isomerism and its significance. Int J Appl Basic Med Res. 3,16–18.

EFSA Panel on Contaminants in the Food Chain (CONTAM); Scientific Opinion on marine biotoxins in shellfish – Cyclic imines (spirolides, gymnodimines, pinnatoxins and pteriatoxins). EFSA Journal 2010; 8(6):1628. [39 pp.]. doi:10.2903/j.efsa.2010.1628. Available online: www.efsa.europa.eu

Espiña B, Otero P, Louzao MC, Alfonso A, Botana LM. (2011). 13-Desmethyl spirolide-c and 13,19-didesmethyl spirolide-c trans-epithelial permeabilities: Human intestinal permeability modelling. Toxicology 287(1–3), 69–75.

Gill S, Murphy M, Clausen J, Richard D, Quilliam M, MacKinnon S, et al. (2003). Neural Injury Biomarkers of Novel Shellfish Toxins, Spirolides: A Pilot Study Using Immunochemical and Transcriptional Analysis. NeuroToxicology 24(4–5), 593–604.

Hill J.A., Jr., Nghiem H.O., Changeux J.P. Serine-specific phosphorylation of nicotinic receptor associated 43 K protein. Biochemistry. 1991;30:5579–5585

Hui JPM, Stuart Grossert J, Cutler MJ, Melanson JE. (2012). Strategic identification of in vitro metabolites of 13-desmethyl spirolide C using liquid chromatography/high-resolution mass spectrometry: Identification of in vitro metabolites of 13-desmethyl spirolide C. Rapid Commun Mass Spectrom. 26(3), 345–54.

Le Hegarat, L., Dumont, J., Josse, R., Huet, S., Lanceleur, R., Mourot, A., Poul, J.-M., Guguen-Guillouzo, C., Guillouzo, A., and Fessard, V. (2010). Assessment of the genotoxic potential of indirect chemical mutagens in HepaRG cells by the comet and the cytokinesis-block micronucleus assays. Mutagenesis 25, 555–560.

Miles CO, Rundberget T, Sandvik M, Aasen JAB and Selwood AI, 2010. The presence of pinnatoxins in Norwegian mussels. Report 07b - 2010, Veterinærinstituttet, National Veterinary Institute. Available from http://www.vetinst.no/eng/Research/Publications/Report-Series/Rapportserie-2010/7b-2010-The-presence-of-pinnatoxins-in-Norwegian-mussels.

Munday R, Quilliam MA, LeBlanc P, Lewis N, Gallant P, Sperker SA, Ewart HS, MacKinnon SL. (2012). Investigations into the toxicology of spirolides, a group of marine phycotoxins. Toxins. 4(1), 1-14.

A. F.Nassar, P. F.Hollenberg, J. Scatina. (2009). Drug Metabolism Handbook: Concepts and Applications. JohnWiley, Chichester.

Omiecinski CJ, Vanden Heuvel JP, Perdew GH, Peters JM. (2011). Xenobiotic Metabolism, Disposition, and Regulation by Receptors: From Biochemical Phenomenon to Predictors of Major Toxicities. Toxicol Sci. 120(Supplement 1), S49–75.

Otero P, Alfonso A, Rodríguez P, Rubiolo JA, Cifuentes JM, Bermúdez R, et al. (2012). Pharmacokinetic and toxicological data of spirolides after oral and intraperitoneal administration. Food Chem Toxicol. 50(2), 232–7.

Parmentier Y, Pothier C, Delmas A, Caradec F, Trancart M-M, Guillet F, et al. (2016). Direct and quantitative evaluation of the human CYP3A4 contribution (f m) to drug clearance using the in vitro SILENSOMES model. Xenobiotica 3, 1–14.

Picot C, Limon G, Durand G, Parent-Massin D, Roudot AC. (2013). Probabilistic dietary exposure to phycotoxins in a recreational shellfish harvester subpopulation (France). J Expo Sci Environ Epidemiol. 23(4), 435-441.

Rubio, F., Kamp, L., Carpino, J., Faltin, E., Loftin, K., Molgó, J. and Aráoz, R. (2014). Colorimetric microtiter plate receptor-binding assay for the detection of freshwater and marine neurotoxins targeting the nicotinic acetylcholine receptors. Toxicon 91, 45-56

Touzet, N., Franco, J.M., Raine, R., (2008). Morphogenetic diversity and biotoxin composition of Alexandrium (dinophyceae) in Irish coastal waters. Harmful Algae 7, 782-797.

Van Vleet TR, Mace K, Coulombe Jr RA. (2002). Comparative Aflatoxin B1 Activation and Cytotoxicity in Human Bronchial Cells Expressing Human CYPs 1A2 and 3A4. ADVS Fac Publ.16.

Vilariño, N., Fonfría, E.S., Aráoz, R., Molgó, J. and Botana, L.M. (2009). Detection of gymnodimine-A and 13-desmethyl C spirolide phycotoxins by fluorescence polarization. Anal Chem. 81, 2708-2714.

Yamazaki H, Hatanaka N, Kizu R, Hayakawa K, Shimada N, Guengerich FP, et al. (2000). Bioactivation of diesel exhaust particle extracts and their major nitrated polycyclic aromatic hydrocarbon components, 1-nitropyrene and dinitropyrenes, by human cytochromes P450 1A1, 1A2, and 1B1. Mutat Res Toxicol Environ Mutagen. 472(1), 129–138.

Supplementary Data Description

Table S1. Summary of primers used for q-PCR analysis.

Gene	Sequence (5' to 3')	Gene	Sequence (5' to 3')
AHR	F: TAGGGTTTCAGCAGTCTGATGTC R: CTACTGTCTGGGGGAGACCA	*SULT1E1*	F: ACAGGATCAACTAAACAGTGTACCA R: ATCTGGTCTTGCCTGGAACG
NR1I2	F: AGACACTGCAGGTGGCTTC R: TGGGGAGAAGAGGGAGATGG	*UGT1A1*	F: CTGCCTTCACCAAAATCCACTATC R: CACAGGACTGTCTGAGGGATTT
CYP1A1	F: ACCCTGAAGGTGACAGTTCC R: TCTTGGAGGTGGCTGAGGTA	*UGT1A9*	F: CGGAGTATGATCTCTACAGCCAC R: TTCAAATTCCATAGGCAACGGC
CYP1A2	F: CTTCGCTACCTGCCTAACCC R: CCCGGACACTGTTCTTGTCA	*UGT2B4*	F: GAAGTTCTAGGAAGACCCACTACG R: GGGTGAGGAAATTGAAAATCCCAG
CYP2B6	F: TTCGGCGATTCTCTGTGACC R: ATGAGGGCCCCCTTGGAT	*ABCB1*	F: CAGCTGTTGTCTTTGGTGCC R: CCAATGTGTTCGGCATTAGGC
CYP2C9	F: AAATGGAGAAGGAAAAGCACAACC R: TCAACTGCAGTGTTTTCCAAGC	*ABCC2*	F: GTGTGGATTCCCTTGGGCTT R: GAAGAAAACCAACGAATACCTGCTT
CYP2C19	F: CCTGGAACGCATGGTGGT R: TCCATTGCTGAAAACGATTCCAAAT	*ABCC3*	F: CCAACTCAGTCAAACGTGCG R: ACCTAGGTTCTGCCAGAGGA
CYP3A4	F: TCACAAACCGGAGGCCTTTT R: TGGTGAAGGTTGGAGACAGC	*ABCG2*	F: AGTTCTCAGCAGCTCTTCGG R: TTCCAACCTTGGAGTCTGCC
CYP3A5	F: GCCCAATAAGGCACCACCTA R: CCACCATTGACCCTTTGGGA	*SLC22A1*	F: TGTCAAATTTGTTGGCGGGG R: TTTAACCAGTGCAGGTCAGGT
GSTM1	F: GGGGGACGCTCCTGATTATG R: GGGCAGATTGGGAAAGTCCA	*SLC22A3*	F: GCATTGCTAAGTGCAATGGGA R: GCTTGTGAACCAAGCAAACATAAG
NAT1	F: ACTAAGAAAGGGGATCATGGACATT R: ACAGCTCGGATCTGGTGTTG	*SLCO1A2*	F: GCACAAGAGTATTTGCTGGCAT R: CGGCAATCCGAGGTAGATGT
NAT2	F: ACAGACCTTGGAAGCAAGAGG R: CTTCAATGTCCATGATCCCTTTGG	*SLCO1B1*	F: TCCACATCATTTTCAAGGGTCTACT R: TGCTTCATCCATGACACTTCCAT
SULT1A1	F: TCGGAGAAGTGTCCTACGGAT R: CCACGAAGTCCACGGTCTC	*GAPDH*	F: GTCAAGGCTGAGAACGGGAA R: AAATGAGCCCCAGCCTTCTC

Table S2. SPX-1 recovery after incubation with rat and human inactivated S9 fractions. S9 fractions were heat-inactivated for 45 min before a 3 hour-incubation with specific phase I co-factors and 100 nM of SPX-1. Results were obtained from two independent experiments conducted with the same S9 batches.

Assay	Inactivated Rat S9	Inactivated Human S9
#1	90 ± 1%	61 ± 1%
#2	75 ± 5%	60 ± 0%

Table S3. SPX-1 depletion after incubation with rat and human S9 fractions. S9 fractions were incubated for 3 h with specific phase I co-factors and 100 nM of SPX-1. Results were obtained from two independent experiments conducted with the same S9 batches.

Assay	Native Rat S9	Native Human S9
#1	97 ± 0%	100 ± 0%
#2	100 ± 0%	74 ± 4%

Table S4. SPX-1 recovery after incubation with rat and human inactivated S9 fractions. S9 fractions were heat-inactivated for 45 min before a 3 hour-incubation with specific phase I and II co-factors and 100 nM of SPX-1. Results were obtained from two independent experiments conducted with the same S9 batches.

Assay	Inactivated Rat S9	Inactivated Human S9
#1	71 ± 3%	86 ± 2%
#2	105 ± 5%	88 ± 1%

Table S5. SPX-1 depletion after incubation with rat and human S9 fractions. S9 fractions were incubated for 3 h with specific phase I and II co-factors and 100 nM of SPX-1. Results were obtained from two independent experiments conducted with the same S9 batches.

Assay	Native Rat S9	Native Human S9
#1	100 ± 0%	100 ± 0%
#2	93 ± 1%	100 ± 0%

Several *in vitro* studies have investigated the intestinal absorption of OA as well as its hepatic metabolism. The transporters OATP1B3 and P-gp have been shown to be involved in OA influx and excretion respectively (Ikema et al., 2015, Ehlers et al., 2014). Hydroxylated metabolites were described using CYP supersomes, hepatic cells or S9 fractions (Guo et al., 2010, Kittler et al., 2010, Kolrep et al., 2017). The interaction of OA with nuclear receptors such as PXR has been studied but conflicting results were reported (Ding and Staudinger 2005, Ferron et al., 2016). Besides, OA is an inflammation inducer and inflammation processes are known to interfere with metabolism leading to a decrease in drug metabolism capacity (Gu et al., 2006). Thus, in this following work, we aimed assessing if metabolism and inflammation pathways can be linked together in the OA toxic response.

Preliminary results: Modulation of CYP3A4 and P-gp by okadaic acid and its associated mechanism: PXR inhibition and possible role of inflammation

In this section, we present the preliminary results obtained from our investigation on a possible interplay between xenobiotic metabolism and inflammation. Although the results are presented using the structure of a research article, complementary studies are necessary before submitting this work.

1. Introduction

Okadaic acid is one of the best known marine biotoxins produced by phytoplanktonic species (The EFSA journal 2008, Reguera et al., 2014). Belonging to the group of diarrhetic shellfish poisoning (DSP), OA has been reported to cause a wide panel of gastro-intestinal symptoms in humans, such as diarrhea, nausea, abdominal pain or vomiting (Valdiglesias et al., 2013). OA is a potent inhibitor of protein phosphatase 2A (PP2A) and to a lesser extent of PP1 (Takai et al., 1992). It was previously shown that OA was cytotoxic in human metabolic competent liver HepaRG cells inducing apoptosis and DNA damage (Ferron et al., 2016). Regarding hepatic metabolism, the formation of several hydroxylated metabolites using CYP recombinants, rat liver S9 as well as HepaRG cells supernatants has been described (Kittler et al., 2010, Guo et al., 2010, Kittler et al., 2014). Besides, the formed hydroxylated metabolites were shown to possess a remaining PP2A inhibitory activity (Guo et al., 2010). Moreover, CYP3A4 inhibition by ketoconazole highly increased the cytotoxicity of OA on HepaRG cells suggesting the implication of phase I metabolism in OA detoxification (Ferron et al., 2016, Kittler et al., 2014). Although it was demonstrated that OA activated PXR-dependent transcriptional activity in HepG2 cells, the toxin failed inducing CYP activities in HepaRG cells (Ferron et al., 2016).

Taken together these data suggest that phase I metabolism, especially CYP3A4, participates in reducing the toxicity of OA. Besides, P-gp was found to actively contribute in OA efflux in Caco-2 cells (Ehlers et al., 2014). However, the involvement of other efflux transporters in OA kinetics remains unknown. Besides, if OA can regulate its own metabolism remains unknown as well. In fact, the expression of phase 0, I, II and III metabolism proteins is orchestrated by several transcription factors (AhR, NRF-2, PXR, CAR) that recognize xenobiotics as ligands (Ramadoss et al., 2005, Beischlag et al., 2008, Wang et al., 2012, Omiecinski et al., 2011). These regulatory processes enable activating cellular detoxification and cell protection from xenobiotics effects (Omiecinski et al., 2011). Inflammation is also a process known to have impact on CYP regulation. Indeed, it has been shown *in*

vitro that NF-κB could inhibit cyp3a4 through interactions with RXR complex (Gu et al., 2006). Pro-inflammation cytokines are also known to decrease drug metabolism (Monshouwer et al., 1996). Regarding inflammatory effects, OA was shown to induce nuclear translocation of NF-κB in intestinal Caco-2 cells (Ferron et al., 2014).
In this study we aimed assessing the role of P-gp in the toxicity of OA using a multi parametric approach and also the correlation between the effects of OA on drug metabolism and inflammation. In this purpose, we investigated the capability of OA i) to modulate gene expression of a panel of phase I enzymes (CYP) and phase III transporters as well as key inflammation mediators in the human hepatic HepaRG cell line using qPCR, ii) to activate nuclear receptors PXR and RXRα in HEK-T transfected cell lines using trans-activation assays.

2. Materials and Methods

2.1. Chemicals

OA standard was purchased from the National Research Council Institute for Marine Biosciences (Halifax, NS Canada). Ketoconazole, verapamil, SR12813, CD2608, dexamethasone and indomethacine were purchased from Sigma-Aldrich (St. Louis, MO, USA). All other chemicals including methanol (MeOH) and dimethyl sulfoxide (DMSO) were of analytical grade and purchased from Fisher Scientific (Leicestershire, England). Deionised water was prepared using a Milli-Q system (Millipore, Bedford, MA, USA).

2.2. Cell culture

2.2.1. HepaRG cells

HepaRG cells were cultured as previously published (Le Hégarat et al., 2010). Briefly, HepaRG cells (passages 13–19) were seeded at 30,000 cells/cm^2 in 96-well plates in culture medium (Williams' medium E with GlutaMAX-I, supplemented with 10% fetal bovine serum, 100 IU/ml penicillin, 100 µg/ml streptomycin, 5 µg/ml bovine insulin, and 50 µM hydrocortisone hemisuccinate). After 2 weeks, the cells were cultured in the same medium supplemented with 1.7% DMSO (differentiation medium) for an additional two weeks. The medium was renewed every 2 to 3 days.

2.2.2. HEK-T cells

The human embryonic kidney cell line HEK-T was obtained from the European Collection of Cell Cultures (ECACC, Porton Down, UK). The cells were cultured in high glucose Dulbecco's modified Eagle's medium (DMEM, Pan-Biotech GmbH, Aidenbach, Germany) supplemented with 10% fetal calf serum (Pan-Biotech GmbH, Aidenbach, Germany), 100 U/ml penicillin and 100 g/ml streptomycin (PAA Laboratories GmbH, Pasching, Austria). The cells were passaged every 2–4 days (80–90% confluence) and seeded at 50,000 cells/cm^2 in 96-well plates.

2.3. Cytotoxicity assays

Cell viability was assessed in HepaRG cells via DAPI-staining of nuclei. The cells were treated with different concentrations of OA with or without ketoconazole (10 µM) or verapamil (50 µM) for 24 h, and then fixed with 4% paraformaldehyde in Phosphate Buffered Saline (PBS) for 10 min and permeabilized with 0.2% Triton X-100. The nuclei were stained with 1 µg/ml DAPI, and quantified using ArrayScan (see below). Cell viability was determined in HEK-T cells after 24 h treatment with OA using the CellTiter-Blue® Cell Viability Assay (Promega, Madison, WI, USA). CellTiter-Blue® reagent was diluted 1:4 with PBS, and 20 µl of the diluted reagent were added to each well. The cells were incubated for 2 h at 37°C, and the fluorescence was measured at 590 nm (excitation at 540 nm) using an Infinite M200 microplate reader (Tecan).

2.4. Real time quantitative Polymerase Chain Reaction (RT-qPCR) analysis

HepaRG cells were seeded in 12-well plates at a density of 20,000 cells/cm^2 and cultured until differentiation as described previously. Following 24 h incubation with OA, cells were washed twice with Phosphate Buffered Saline (PBS). Total RNA extraction was then performed using the Total RNA isolation NucleoSpin® RNA II kit from Macherey Nagel (Hoerd, France) following the manufacturer's protocol. The RNA concentration and quality were determined by spectrophotometric measurements with a BioSpec-nano (Shimadzu Biotech, Marne la Vallée, France). The RNA´s integrity was checked through electrophoresis using an Experion (Bio-Rad, Marne la Coquette, France). The RNA samples were then reverse transcribed into double strand cDNA using the High Capacity RNA-to-cDNA kit (Applied Biosystems, Foster city, CA, USA) according to the manufacturer's instructions. The sequences of target genes were obtained from the National Center for Biotechnology Information (NCBI) GenBank sequence database. The primers were designed with the Primer designing tool from NCBI. For each gene, at least one primer was designed on the exon-exon junction. All primers (see Table S1) were purchased from Sigma-Aldrich (Saint-Louis, MO, USA). Quantitative PCR was performed using Light Cycler® 1536 from Roche (Mannheim, Germany). SYBR Green chemistry was used. The reactions were performed in a total volume of 2 µl containing 1X LightCycler 1536 DNA Green Master, 1X LightCycler 1536 DNA Master mix (Roche), 300 nM each primer, and 0.1 ng cDNA. Negative quantitative PCR controls of RNase-free water were included in each run for contamination assessment. The thermal cycling conditions were 94°C for 15 s, followed by 40 cycles of 15 s at 94°C, and 30 s at 60°C with a slow temperature ramp (4.8°C/s). LightCycler® 1536 software (version 1.1.0.1112; Roche, Basel, Switzerland) was used for the quantitative analysis, and a melting curve analysis was used to check the specificity of each amplicon. The threshold Cqs were calculated from a baseline subtracted curve fit. Calibration curves were established for each gene from a serial dilution of a reference sample (pool of cDNA samples). According to these calibration curves, for each sample, mean relative amounts of mRNA of the target genes were calculated and then normalized to the GAPDH reference gene. The values were presented as fold change regarding the solvent control.

2.5. H2AX protein expression

After 24 h incubation of OA with or without ketoconazole (10 µM) or verapamil (50 µM), the HepaRG cells were fixed with 4% paraformaldehyde in PBS for 10 min and permeabilized with 0.2% Triton X-100 for 15 min. The plates were then incubated in blocking solution (PBS with 1% BSA and 0.05% Tween-20) for 30 min before the addition of primary antibodies prepared in blocking solution and filtered with a 0.2 µm syringe filter. The primary and secondary antibodies were purchased from Abcam (Cambridge, UK): mouse monoclonal anti ɣH2AX ser139 (ab2893) and goat anti-mouse IgG H&L DyLight® (Thermo Fisher Scientific, Waltham, MA, USA) 550 (ab96876). The primary antibody (1/1000) was incubated for 1.5 h at room temperature. After washing with PBS + 0.05% Tween 20, the secondary antibody (1/1000) was incubated for 45 min at room temperature. Nuclear DAPI (1 µg/mL) staining was used for automated cell identification by high content analysis. The plates were scanned with the Thermo Scientific ArrayScan VTI HCS Reader (Thermo Scientific, Waltham, MA, USA), and analyzed using the Target Activation module of the BioApplication software (version: 6.0.1.4021; Thermo Fisher Scientific, Waltham, MA, USA). For each well, 10 fields (10× magnification) were scanned and analyzed for immunofluorescence quantification. Cell numbers were determined by DAPI staining. H2AX was quantified in the nuclei, and expressed as a fold increase compared to solvent control cells.

2.6. PXR and RXRα transactivation assay

Transactivation assays were conducted as previously described (Luckert et al., 2015). Briefly, 24 h after seeding, HEK-T cells were transiently transfected using TransIT-LT1 (Mirus Bio, Madison, WI, USA) according to the manufacturer's protocol. For each well the transfection mixture contained 40 ng pGAL4-(UAS)5-TK-luc, 40 ng pGAL4-hPXR-LBD and 1 ng pcDNA3-Rluc for PXR assay and 40 ng pGAL4-(UAS)5-TK-luc, 40 ng pCMX-GAL4-hRXRα and 1 ng pcDNA3-Rluc for RXRα assay. pcDNA3-Rluc

was used as an internal control for normalization. Four to six hours after transfection the cells were incubated with different concentrations of OA dissolved in culture medium (0.1 % MeOH). PXR agonist SR12813 (10 µM) and RXRα agonist CD2608 (100 nM) were used as positive controls. After 24 h the culture medium was removed and the cells were lysed after addition of 50 µl lysis buffer (100 mM potassium phosphate with 0.2% (v/v) Triton X-100, pH 7.8) for 15 min on an orbital shaker. After centrifugation (5 min, 2000×g) 5 µl of the supernatant was analyzed for luciferase activity as previously described (Hampf and Gossen, 2006). Firefly luciferase values were normalized to Renilla luciferase values and expressed as fold-induction normalized against solvent control.

2.7. Statistics/Data analysis

GraphPad Prism 5 (GraphPad Software, Inc., La Jolla, CA, USA) was used for the statistical analyses. The data were compared to the control condition using one-way analysis of variance (ANOVA) followed by Dunnett's post hoc tests. All error bars denote SD. Statistical significance was depicted as follows: * $p < 0.05$, ** $p < 0.01$, *** $p < 0.001$.

3. Results

3.1. Modulation of OA toxicity by P-gp in HepaRG cells

In order to assess the possible role of P-gp in the modulation of OA toxicity, we used a specific inhibitor, namely verapamil. Ketoconazole, a CYP3A4 inhibitor an also to a less extent a P-gp inhibitor, was also used. The inhibition of CYP3A4 or P-gp resulted in higher cytotoxicity (Figure 1a). P-gp inhibition led to the highest decrease of cell count as shown by IC_{50} values summarized in Table 1. For the phosphorylation of histone H2AX, the inhibition of CYP3A4 or P-gp only led to higher genotoxic responses at very toxic concentrations (Figure 1b).

(a)

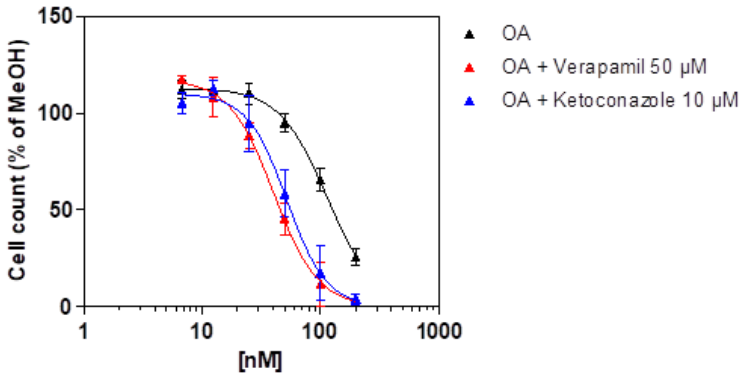

(**b**)

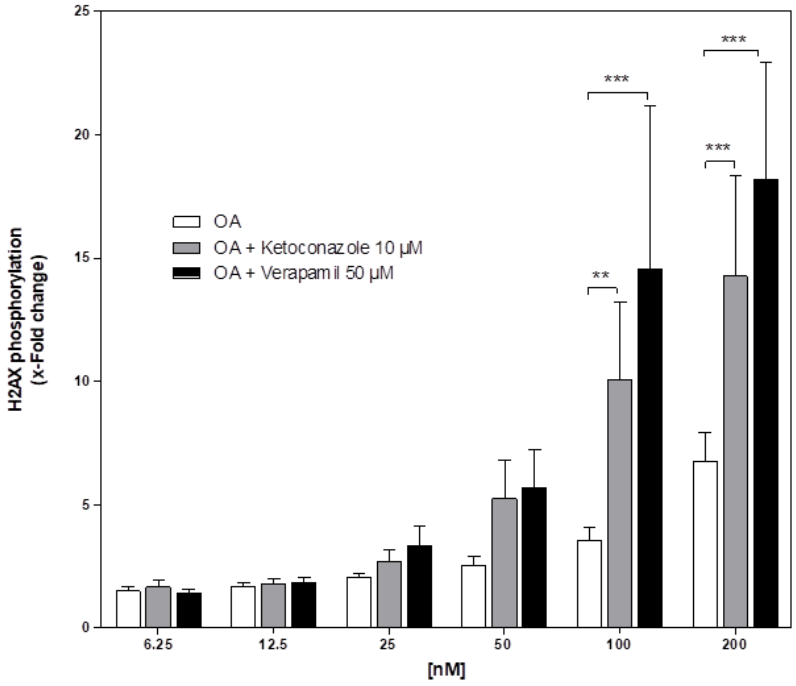

Figure 1. Effects of P-gp and CYP3A4 inhibitors on the toxicity of OA. (a) depicts cell count, measured as number of DAPI-stained nuclei. (b) depicts phosphorylation of H2AX, measured by immunofluorescence. Results were obtained from three independent experiments. Data represent means ± SD normalized to solvent control.

Table 1. Effects of P-gp and CYP3A4 inhibitors on cell count. IC_{50} were calculated using GraphPad Prism 5. Results were obtained from three independent experiments.

Experimental condition	IC_{50} (nM)
OA	114.5
OA + ketoconazole	52.4
OA + verapamil	40.5

Since these data confirm the role of CYP3A4 and P-gp in the metabolism of OA, the relationship between metabolism and inflammation in the HepaRG competent metabolic hepatic cell line was investigated through transcripts levels.

3.2. Effects of OA on the expression of phase I and III metabolism and inflammation genes in HepaRG cells by qRT-PCR

Based on previous results, we selected three subtoxic concentrations of OA: 12.5, 25 and 50 nM, for mRNA expression analysis. Only fold inductions ≤ 0.5 and ≥ 1.5 and statistically significant were considered (Table 2). For the transporters, down-regulation was observed with influx transporters genes: concentration-dependent for *SLCO1A2* (0.01 fold at 50 nM) or non concentration-dependent for *SLC22A1* and *SLCO1B1* (0.41 fold and 0.19 fold respectively at 25 nM). Regarding efflux transporters genes, OA induced in a concentration-dependent way *ABCB1* (3.09 fold at 50 nM) and *ABCG2* (2.38 fold at 50 nM) whereas a concentration-dependent down-regulation of *ABCC3* was observed (0.16 fold at 50 nM). Concerning the metabolic enzymes, a down-regulation was observed for *CYP1A1* (0.14 fold at 12.5 nM), *2C9* (0.28 fold at 25 nM), and *3A5* (0.23 fold at 25 nM) but not

concentration-related. On the contrary, *CYP2C19* and *3A4* were down-regulated in a concentration-dependent way (0.38 fold at 12.5 nM and 0.09 fold at 50 nM, respectively). Results on transferases genes show a concentration-dependent down-regulation of *GSTM1* (0.21 fold at 50 nM), *NAT2* (0.27 fold at 50 nM), *SULT1A1* (0.09 fold at 50 nM), *SULT1E1* (0.03 fold at 50 nM), *UGT1A9* (0.22 fold at 50 nM) and *UGT2B4* (0.03 fold at 50 nM). Regarding inflammation genes, OA up-regulated *IL6* (15.74 fold at 50 nM), *IL8* (12.60 fold at 50 nM) and *NFKB3* (2.25 fold at 50 nM) in a concentration-dependent manner. Some genes were also regulated but without statistical significance: *AHR* (2.60 fold at 50 nM), *NR1I2* (0.29 fold at 50 nM), *CYP2B6* (0.45 fold at 25 nM), *COX1* (3.19 fold at 12.5 nM) and *COX2* (21.63 fold at 50 nM). Considering the potent down-regulation of many drug metabolism genes (especially *CYP3A4*) by OA, we investigated the effects of OA on the regulatory nuclear receptors PXR and RXRα.

Table 2. Effects of OA on mRNA expression of metabolism and inflammation genes in HepaRG cells. The cells were treated with three sub-toxic doses of OA for 24 h. The results were obtained from three independent experiments. The figures are the means ± standard deviations (SD) of fold change relative to solvent control. Fold change between 0.9 and 0.5 (light blue), 0.5 and 0.2 (blue) or less than 0.2 (dark blue) depicts gene down-regulation whereas fold change between 1.0 to 1.5 (white), 1.6 to 2.5 (light red), 2.6 to 8 (red) or greater than 8 (dark red) depicts gene up-regulation. * $p < 0.05$, ** $p < 0.01$, *** $p < 0.001$ after one-way ANOVA followed by Dunnett's post hoc tests.

Pathway	Gene	(nM)					
		12.5		25		50	
		Mean	SD	Mean	SD	Mean	SD
Nuclear receptors	*AHR*	1.01	0.34	1.73	1.02	2.60	0.90
	NR1I2	0.42	0.02	0.35	0.07	0.29	0.41
Phase 0 influx transporters	*SLC22A1*	0.46*	0.30	0.41*	0.27	0.55	0.18
	SLC22A3	0.70	0.13	0.83	0.14	1.14	0.50
	SLCO1A2	0.50	0.56	0.26	0.31	0.01*	0.01
	SLCO1B1	0.36***	0.15	0.19***	0.01	0.24***	0.04
Phase I CYP	*CYP1A1*	0.14*	0.06	0.41	0.29	0.27*	0.48
	CYP1A2	1.28	1.66	1.42	0.74	0.71	0.62
	CYP2B6	0.59	0.23	0.45	0.14	0.98	0.95
	CYP2C9	0.38***	0.14	0.28***	0.11	0.40***	0.14
	CYP2C19	0.38***	0.05	0.41***	0.15	0.60**	0.16
	CYP3A4	0.12***	0.01	0.06***	0.02	0.09***	0.01
	CYP3A5	0.25***	0.04	0.23***	0.04	0.43***	0.11
Phase II	*GSTM1*	0.41**	0.04	0.26***	0.06	0.21***	0.28

transferases	***NAT1***	0.76	0.14	0.92	0.11	1.90	0.94
	NAT2	0.46***	0.11	0.33***	0.04	0.27***	0.08
	SULT1A1	0.36***	0.04	0.19***	0.03	0.09***	0.04
	SULT1E1	0.66	0.45	0.29*	0.29	0.03**	0.04
	UGT1A1	0.74	0.47	0.67	0.42	0.77	0.36
	UGT1A9	0.36***	0.03	0.24***	0.02	0.22***	0.04
	UGT2B4	0.23***	0.06	0.11***	0.04	0.03***	0.02
Phase III efflux transporters	***ABCB1***	0.89	0.19	1.52	0.40	3.09**	0.81
	ABCC2	0.61	0.19	0.72	0.16	0.97	0.24
	ABCC3	0.34***	0.09	0.21***	0.07	0.16***	0.06
	ABCG2	1.08	0.52	1.28	0.33	2.38**	0.25
Inflammation	***COX1***	3.19	1.83	1.90	1.36	2.80	2.07
	COX2	3.85	2.54	6.84	6.28	21.63	19.61
	IL6	1.40	0.44	4.68	2.56	15.74*	10.95
	IL8	0.93	0.29	2.32	0.79	12.60**	5.04
	NFKB1	0.96	0.17	1.20	0.11	1.44*	0.18
	NFKB3	0.93	0.12	1.17	0.31	2.25**	0.51
	0.2	0.5	0.9	1.5	2.5	8	25

x-Fold change compared to solvent control

3.3. PXR and RXRα transactivation assay in transfected HEK-T cells

3.3.1. Effects of OA on PXR and RXRα

In order to assess if OA can activate nuclear receptors that regulate drug-metabolizing genes, a transactivation assay on PXR and RXRα was conducted in transfected HEK-T cells. OA exerted a dose-dependent toxicity on HEK-T cells detected by the CTB assay (Figure S1). Consequently, only concentrations up to 50 nM were used in the transactivation assays. Results are presented in Figure 2. OA inhibited greatly both PXR and RXRα transactivation in a dose-dependent way.

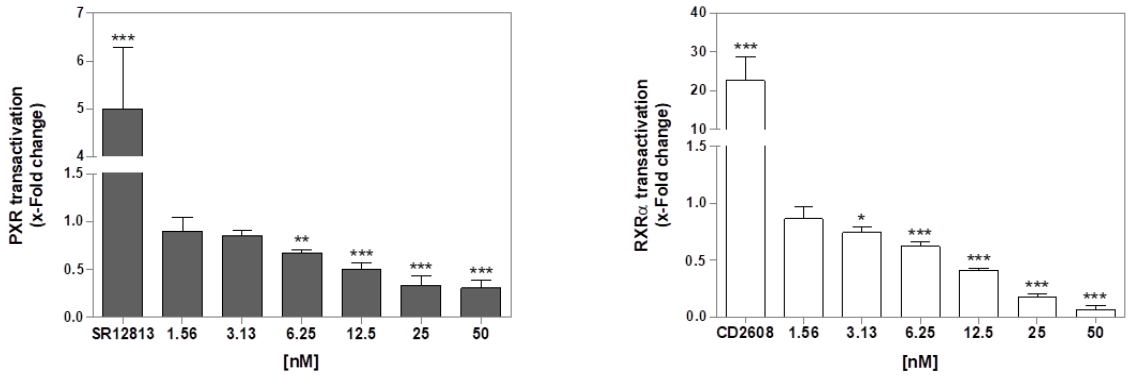

(**a**) (**b**)

Figure 2. Transactivation of PXR (a) and RXRα (b) in HEK-T cells. The cells were transfected with plasmids before incubation with OA for 24 h. SR12813 (10 µM) and CD2608 (100 nM) were used as positive controls. Results were obtained from three independent experiments performed in triplicate (mean ± SD). *p < 0.05, **p < 0.01, ***p < 0.001 after one-way ANOVA followed by Dunnett's post hoc tests.

In order to confirm the effects observed on both PXR and RXRα, we co-incubated OA with their respective positive controls. Results are presented in Figure 3. The co-incubation of OA and positive control resulted as well in the inhibition of both PXR and RXRα transactivation in a dose-dependent way.

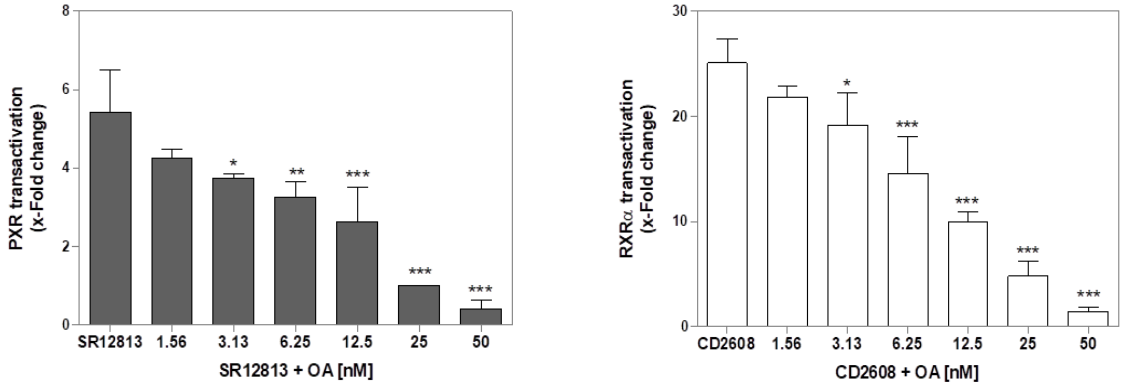

(**a**) (**b**)

Figure 3. Transactivation of PXR (a) and RXRα (b) in HEK-T cells. The cells were transfected with plasmids before co-incubation of OA and the corresponding positive control (10 µM SR12813 and 100 nM CD2608) for 24 h. Results were obtained from three independent experiments performed in triplicate (mean ± SD). *p < 0.05, **p < 0.01, ***p < 0.001 after one-way ANOVA followed by Dunnett's post hoc tests.

OA was shown to inhibit both PXR and RXRα which are known to control CYP3A gene regulation. As we previously observed not only down regulation of CYP3A gene expression but also up regulation of pro-inflammatory genes, we investigated if inflammation could modulate OA responses towards PXR and RXRα.

3.3.2. Modulation of PXR and RXRα OA-mediated inhibition by inflammation inhibitors

We used two inflammation inhibitors, dexamethasone and indomethacin. After 1 h of pre-treatment with the inflammation inhibitor, OA and the inhibitor were co-incubated for 24 h. The

co-incubation of OA and dexamethasone slightly reduced PXR transactivation (Figure 4a) in a concentration-dependent way but with no statistical significance. However treatment with indomethacine resulted in the inhibition of PXR in a concentration-dependent way (Figure 4b). The co-incubation of OA and dexamethasone or indomethacine inhibited the RXRα transactivation in a concentration-dependent way (Figure 5a and 5b).

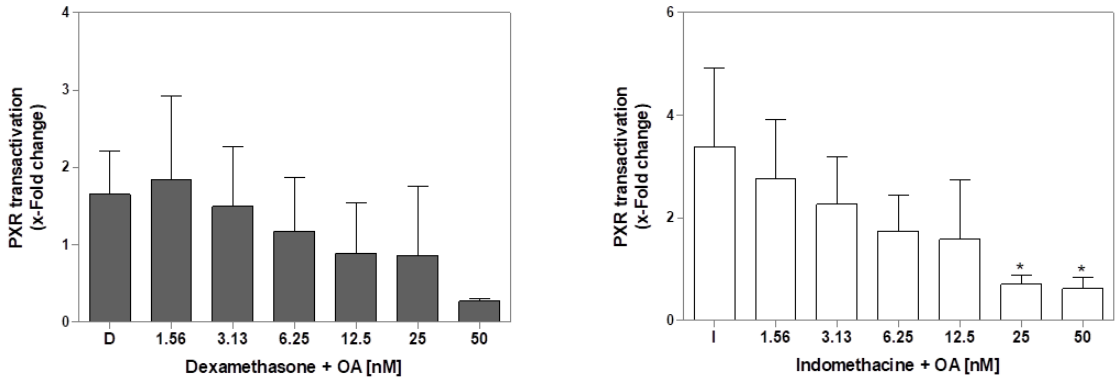

(**a**) (**b**)

Figure 4. Transactivation of PXR in HEK-T cells. The cells were transfected with plasmids before co-incubation of OA with dexamethasone (20 µM) (a) or indomethacine (50 µM) (b) for 24 h. Results were obtained from three independent experiments performed in triplicate (mean ± SD). *p < 0.05, **p < 0.01, ***p < 0.001 after one-way ANOVA followed by Dunnett's post hoc tests.

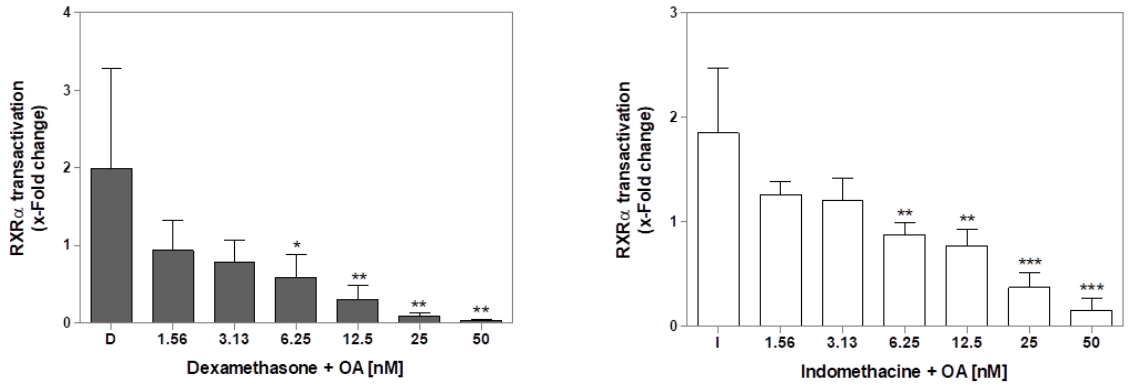

(**a**) (**b**)

Figure 5. Transactivation of RXRα in HEK-T cells. Cells were transfected with plasmids before co-incubation of OA with dexamethasone (20 µM) (a) or indomethacine (50 µM) (b) for 24 h. Results were obtained from three independent experiments performed in triplicate (mean ± SD). *p < 0.05, **p < 0.01, ***p < 0.001 after one-way ANOVA followed by Dunnett's post hoc tests.

4. Discussion

In this study, we first showed that P-gp plays a key role in OA toxicity. It may even play a role as important as CYP3A4 since P-gp inhibition led to equal or even slightly higher toxic responses. These findings confirm the results given by Chambers et al., 1993 who showed that overexpressing P-gp human KB-V1 cells were less sensitive to OA cytotoxicity than the parental KB-3 cells. However, of the link between other efflux transporters and OA toxicity has been neglected up to now.

Our results revealed that OA can affect the regulation of numerous metabolism genes in human liver HepaRG cells. A global down-regulation of CYP mRNA was indeed observed, *CYP3A4* being the most strongly down-regulated. Results on transporters genes expression confirmed the role of *P-gp* and pointed out the possible role of *ABCG2* in the efflux of OA as these two genes were found to be up-regulated, which will both favor OA excretion. A possible explanation that the expression of most of the drug metabolism genes was decreased is the implication of pro-inflammatory pathways. Indeed, it has been shown that inflammatory mediators can repress drug metabolism whether by targeting regulatory nuclear receoptors or by direct inactivation of the xenobiotic-metabolizing enzymes (Monshouwer et al., 1996, Gu et al., 2006). Here, we showed that OA greatly up-regulated some key inflammatory genes such as *COX2* and *IL6*/*IL8*.

Moreover, using transactivation assays, we showed that OA inhibited both PXR and RXRα. This inhibition was further confirmed when OA and the positive controls were co-incubated. These results are in accordance with the OA-mediated down regulation of the CYP3A4 gene expression, known to be primarily under PXR regulation (Wang et al., 2012). However, other studies showed that OA activates Ciona intestinalis orthologue or human PXR-dependent transcriptional activity in HepG2 cells (Fidler et al., 2012, Ferron et al., 2016). This opposite effect could be due to the localization of the nuclear receptors. Indeed, PXR was shown to be localized in the nucleus of immortalized cell lines (Saradhi et al., 2005) while being localized in the cytoplasm in primary hepatocytes or *in vivo* (Mackowiak and Wang, 2016). Transactivation assays were performed in transfected HEK-T cells which originate from normal human embryonic kidney cells, assuming that nuclear receptors would localize in the cellular cytoplasm.

Activation of PXR can be mediated through direct or indirect mechanism (Mackowiak and Wang 2016). Since we observed the inhibition of PXR and RXRα transactivation, OA would rather be categorized as an inverse agonist. Nevertheless, concluding to the inverse agonist effect of OA towards the PXR and RXRα receptors would need additional experiments to investigate the interaction of OA with the receptor ligand binding domain using for instance *in silico* modelling such as quantitative structure-activity relationship (QSAR) or *in vitro* assays such as protein X-ray crystallography. However, the fact that OA was able to reverse the SR12813-mediated transactivation of PXR or RXRα while being in the nanomolar range suggests rather an indirect mechanism.

Since OA up-regulated some key inflammatory genes, we wanted to explore if PXR/RXRα could be inhibited through inflammation pathway induction. For this purpose, we used two well-known inflammation inhibitors. Indomethacin was shown to be an inhibitor of cyclooxygenase proteins (Kurumbail et al., 1996) which are responsible for prostaglandins synthesis. Our results did not conclude that the cyclooxygenase pathway was involved in OA-mediated PXR/RXRα inhibition. Dexamethasone belongs to the family of glucocorticoid drugs which anti-inflammatory effects are supposed to be mediated by inhibition of transcription factors such as NF-κB or AP-1 (Barnes 1998, Stahn et al., 2007). Dexamethasone was indeed shown to interfere with NF-κB (Chang et al., 1997, Crinelli et al., 2000) and led to the inhibition of several pro-inflammatory mediators such as TNF-α (Crinelli et al., 2000). Our results may suggest a role of inflammation in the inhibition of PXR mediated by OA.

5. Conclusions

In conclusion, although suggested in several other studies, we confirmed that P-gp plays a key role in the modulation of OA toxicity. We also showed that OA down-regulates the expression of several main CYPs, especially the *3A4* gene, and up-regulates genes involved in the inflammation pathways such as *COX2* and *IL6*/*IL8*. Transactivation assays showed that OA inhibits both PXR and RXRα and that inflammation may be implicated since the inhibition of PXR was partially reversed by inflammation inhibitor dexamethasone.

6. Additional assays

One question to be answered is whether OA can bind to the ligand binding pocket of PXR and RXRα or if the inhibitions we reported was triggered by an indirect mechanism. To our knowledge, no crystallography data exist to support a direct binding of OA. However, QSAR modeling approach may appear as a more convenient way to address this issue. Regarding a possible role of inflammation, it could be interesting to check both CYP activity and cytokines (for instance IL-8) release after 24 h or 48 h treatment of OA with or without inflammation inhibitors in HepaRG cells.

Supplementary Materials:

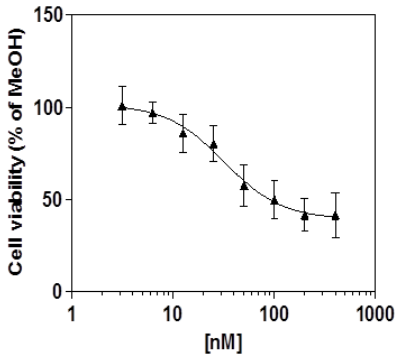

Figure S1. Cell viability response of OA in HEK-T cells. Following 24 h of treatment with different concentrations of OA, cells were incubated with 20 µl of CellTiter-Blue® reagent for 2 h at 37°C. Fluorescence was then measured at 590 nm (excitation at 540 nm). Results were obtained from three independent experiments performed in triplicate (mean ± SD).

Table S1. Summary of primers used for q-PCR analysis.

Gene		Sequence (5' to 3')	Gene		Sequence (5' to 3')
AHR	F:	TAGGGTTTCAGCAGTCTGATGTC	*UGT2B4*	F:	GAAGTTCTAGGAAGACCCACTACG
	R:	CTACTGTCTGGGGGAGACCA		R:	GGGTGAGGAAATTGAAAATCCCAG
NR1I2	F:	AGACACTGCAGGTGGCTTC	*ABCB1*	F:	CAGCTGTTGTCTTTGGTGCC
	R:	TGGGGAGAAGAGGGAGATGG		R:	CCAATGTGTTCGGCATTAGGC
CYP1A1	F:	ACCCTGAAGGTGACAGTTCC	*ABCC2*	F:	GTGTGGATTCCCTTGGGCTT
	R:	TCTTGGAGGTGGCTGAGGTA		R:	GAAGAAAACCAACGAATACCTGCTT
CYP1A2	F:	CTTCGCTACCTGCCTAACCC	*ABCC3*	F:	CCAACTCAGTCAAACGTGCG
	R:	CCCGGACACTGTTCTTGTCA		R:	ACCTAGGTTCTGCCAGAGGA
CYP2B6	F:	TTCGGCGATTCTCTGTGACC	*ABCG2*	F:	AGTTCTCAGCAGCTCTTCGG
	R:	ATGAGGGCCCCCTTGGAT		R:	TTCCAACCTTGGAGTCTGCC
CYP2C9	F:	AAATGGAGAAGGAAAAGCACAACC	*SLC22A1*	F:	TGTCAAATTTGTTGGCGGGG
	R:	TCAACTGCAGTGTTTTCCAAGC		R:	TTTAACCAGTGCAGGTCAGGT
CYP2C19	F:	CCTGGAACGCATGGTGGT	*SLC22A3*	F:	GCATTGCTAAGTGCAATGGGA
	R:	TCCATTGCTGAAAACGATTCCAAAT		R:	GCTTGTGAACCAAGCAAACATAAG
CYP3A4	F:	TCACAAACCGGAGGCCTTTT	*SLCO1A2*	F:	GCACAAGAGTATTTGCTGGCAT
	R:	TGGTGAAGGTTGGAGACAGC		R:	CGGCAATCCGAGGTAGATGT
CYP3A5	F:	GCCCAATAAGGCACCACCTA	*SLCO1B1*	F:	TCCACATCATTTTCAAGGGTCTACT
	R:	CCACCATTGACCCTTTGGGA		R:	TGCTTCATCCATGACACTTCCAT
GSTM1	F:	GGGGGACGCTCCTGATTATG	*COX1*	F:	TCCAGGAGCTCGTAGGAGAG

	R: GGGCAGATTGGGAAAGTCCA		R: CCTTGAGGGAAAAGGGAGCC
NAT1	F: ACTAAGAAAGGGGATCATGGACATT R: ACAGCTCGGATCTGGTGTTG	*COX2*	F: GAAAACTGCTCAACACCGGAAT R: TGTAGTGCACTGTGTTTGGAGT
NAT2	F: ACAGACCTTGGAAGCAAGAGG R: CTTCAATGTCCATGATCCCTTTGG	*IL6*	F: AGAGGCACTGGCAGAAAACA R: ACCAGGCAAGTCTCCTCATTG
SULT1A1	F: TCGGAGAAGTGTCCTACGGAT R: CCACGAAGTCCACGGTCTC	*IL8*	F: GGAGAAGTTTTTGAAGAGGGCTG R: TGCTTGAAGTTTCACTGGCATC
SULT1E1	F: ACAGGATCAACTAAACAGTGTACCA R: ATCTGGTCTTGCCTGGAACG	*NFKB1*	F: GCCACCCGGCTTCAGAAT R: TGAAGGTATGGGCCATCTGC
UGT1A1	F: CTGCCTTCACCAAAATCCACTATC R: CACAGGACTGTCTGAGGGATTT	*NFKB3*	F: CGGCCATGGACGAACTGT R: TGATCTCCACATAGGGGCCA
UGT1A9	F: CGGAGTATGATCTCTACAGCCAC R: TTCAAATTCCATAGGCAACGGC	*GAPDH*	F: GTCAAGGCTGAGAACGGGAA R: AAATGAGCCCCAGCCTTCTC

Acknowledgments: We would like to thank Patrick Fach and Cédric Woudstra from the IdentyPath platform for their excellent support and advices for the qRT-PCR assays.

References

Barnes P. J. Anti-inflammatory actions of glucocorticoids: molecular mechanisms. Clinical Science (London, England) 1998;94(6):557–5722.

Beischlag TV, Morales JL, Hollingshead BD, Perdew GH. The aryl hydrocarbon receptor complex and the control of gene expression. Crit Rev Eukaryot Gene Expr [Internet]. 2008.

Chang CK, Llanes S, Schumer W. Effect of dexamethasone on NF-κB activation, tumor necrosis factor formation, and glucose dyshomeostasis in septic rats. J Surg Res. 1997;72:141–145.

Crinelli R., Antonelli A., Bianchi M., Gentilini L., Scaramucci S., Magnani M. (2000). Selective inhibition of NF-κB activation and TNF-α production in macrophages by red blood cell-mediated delivery of dexamethasone. Blood Cells Mol. Dis. 26, 211–222.

Ehlers A, These A, Hessel S, Preiss-Weigert A, Lampen A. Active elimination of the marine biotoxin okadaic acid by P-glycoprotein through an in vitro gastrointestinal barrier. Toxicol Lett. 2014 Mar;225(2):311–7.

Ferron P-J, Hogeveen K, Fessard V, Hégarat L. Comparative Analysis of the Cytotoxic Effects of Okadaic Acid-Group Toxins on Human Intestinal Cell Lines. Mar Drugs. 2014 Aug 21;12(8):4616–34.

Ferron PJ, Hogeveen K, De Sousa G, Rahmani R, Dubreil E, Fessard V, et al. Modulation of CYP3A4 activity alters the cytotoxicity of lipophilic phycotoxins in human hepatic HepaRG cells. Toxicol In Vitro. 2016 Jun;33:136–46.

Gu X., Ke S., Liu D., Sheng T., Thomas P. E., Rabson A. B., et al. (2006). Role of NF-kappaB in regulation of PXR-mediated gene expression: a mechanism for the suppression of cytochrome P-450 3A4 by proinflammatory agents. J. Biol. Chem. 281 17882–17889.

Guo F, An T, Rein KS. The algal hepatoxoxin okadaic acid is a substrate for human cytochromes CYP3A4 and CYP3A5. Toxicon. 2010 Feb;55(2–3):325–32.

Hampf M, Gossen M. A protocol for combined Photinus and Renilla luciferase quantification compatible with protein assays. Anal Biochem. 2006 Sep;356(1):94–9.

Kittler K, Preiss-Weigert A, These A. Identification Strategy Using Combined Mass Spectrometric Techniques for Elucidation of Phase I and Phase II in Vitro Metabolites of Lipophilic Marine Biotoxins. Anal Chem. 2010 Nov 15;82(22):9329–35.

Kittler K, Fessard V, Maul R, Hurtaud-Pessel D. CYP3A4 activity reduces the cytotoxic effects of okadaic acid in HepaRG cells. Arch Toxicol. 2014;88(8):1519–1526.

Kurumbail GR, Stevens MA, Gierse KJ, Mc Donald JJ, Stegeman AR, Pak YJ, Gildehaus D, Miyashiro MJ, Pennung DT (1996) Structural basis for selective inhibition of cyclooxygenase-2 by anti-inflammatory agents. Nature 384:644–648.

Le Hegarat L, Dumont J, Josse R, Huet S, Lanceleur R, Mourot A, et al. Assessment of the genotoxic potential of indirect chemical mutagens in HepaRG cells by the comet and the cytokinesis-block micronucleus assays. Mutagenesis. 2010 Nov 1;25(6):555–60.

Luckert C, Hessel S, Lampen A, Braeuning A. Utility of an appropriate reporter assay: Heliotrine interferes with GAL4/upstream activation sequence-driven reporter gene systems. Anal Biochem. 2015 Oct;487:45–8.

Mackowiak B, Wang H. Mechanisms of xenobiotic receptor activation: Direct vs. indirect. Biochim Biophys Acta. 2016 Sep;1859(9):1130-40.

Monshouwer M, Witkamp RF, Nujmeijer SM, Van Amsterdam JG, Van Miert a S. Suppression of cytochrome P450- and UDP glucuronosyl transferase-dependent enzyme activities by proinflammatory cytokines and possible role of nitric oxide in primary cultures of pig hepatocytes. Toxicology and applied pharmacology. 1996;137:237–244.

Omiecinski CJ, Vanden Heuvel JP, Perdew GH, Peters JM. Xenobiotic Metabolism, Disposition, and Regulation by Receptors: From Biochemical Phenomenon to Predictors of Major Toxicities. Toxicol Sci. 2011 Mar 1;120(Supplement 1):S49–75.

Opinion of the Scientific Panel on Contaminants in the Food chain on a request from the European Commission on marine biotoxins in shellfish – okadaic acid and analogues, The EFSA Journal (2008) Journal number, 589, 1-62.

Ramadoss P, Marcus C, Perdew GH. Role of the aryl hydrocarbon receptor in drug metabolism. Expert Opin Drug Metab Toxicol. 2005;1(1):9–21.

Reguera B, Riobó P, Rodríguez F, Díaz P, Pizarro G, Paz B, et al. Dinophysis Toxins: Causative Organisms, Distribution and Fate in Shellfish. Mar Drugs. 2014 Jan 20;12(1):394–461.

M. Saradhi, A. Sengupta, G.Mukhopadhyay, R.K. Tyagi, Pregnane and xenobiotic receptor (PXR/SXR) resides predominantly in the nuclear compartment of the interphase cell and associates with the condensed chromosomes during mitosis, Biochim. Biophys. Acta (BBA) - Mol. Cell Res. 1746 (2005) 85–94.

Stahn C, Löwenberg M, Hommes DW, Buttgereit F. Molecular mechanisms of glucocorticoid action and selective glucocorticoid receptor agonists. Mol Cell Endocrinol. 2007;275:71–78.

Takai, A., Murata, M., Torigoe, K., Isobe, M., Mieskes, G., and Yasumoto, T. (1992). Inhibitory effect of okadaic acid derivatives on protein phosphatases. A study on structure-affinity relationship. Biochem. J. 284 (Pt 2), 539–544.

Valdiglesias V, Prego-Faraldo M, Pásaro E, Méndez J, Laffon B. Okadaic Acid: More than a Diarrheic Toxin. Mar Drugs. 2013 Oct 31;11(11):4328–49.

Wang Y-M, Ong SS, Chai SC, Chen T. Role of CAR and PXR in xenobiotic sensing and metabolism. Expert Opin Drug Metab Toxicol. 2012 Jul;8(7):803–17.

Investigations on YTX were hampered by many obstacles: i) YTX passage could not be investigated due to the binding of the toxin to the membrane of the Transwell; ii) YTX metabolism assessment with S9 fractions was abandoned due to analytical issues and iii) transactivation assays suffered of interferences. In the following section, we present our data on transcriptomic analysis.

Preliminary results: Effects of yessotoxin on mRNA expression in human hepatic HepaRG cells

In this section, we present the preliminary results obtained from our investigation on the molecular mode of action of YTX. Although the results are presented using the structure of a research article, complementary studies are necessary before submitting this work.

1. Introduction (750 words)

Marine biotoxins are secondary metabolites produced by a restricted variety of phytoplankton species (Visciano et al., 2016). Due to potential human acute intoxications, regulatory limits have been set to protect consumers (EFSA report 2009). Even if no human intoxication has been reported with YTX (Figure 1), *in vivo* studies have described a potent toxicity in rodents after intra-peritoneal administration (Tubaro et al., 2003, Aune et al., 2008). Following oral exposure, no acute toxicity was reported but ultrastructural changes or cell death was observed in cardiomyocytes (Tubaro et al., 2008, Ferreiro et al., 2017). Many studies also claimed *in vitro* toxicity. In fact, YTX was shown to target multiple pathways depending on the cellular model employed (Alfonso et al., 2016). It has been shown to interfere with autophagy (Fernandez et al., 2015), to induce apoptosis (Korsnes et al., 2011), to depolymerize the actin microfilaments (Franchini et al., 2010, Perez-Gomez et al., 2006) and to increase cytosolic calcium (Pang et al., 2014). The mechanism of action is still unknown but Pazos et al., 2006 showed a direct interaction between YTX and some phosphodiesterases (PDEs).

Besides, almost no information is available on the behavior of YTX after ingestion by humans and especially on its metabolism mainly expected in liver. Using rat S9 liver fractions, Kittler et al., 2010 described only one mono-oxygenated metabolite, but indicated that more metabolites were expected. Moreover YTX was shown to induce toxic effects on several hepatic cell lines suh as HL7702 cells (Pang et al., 2012), Bel7402 cells (Pang et al., 2014) and HepG2 cells (Young et al 2009). While no apoptotic effect (activation of caspase-3) was observed in the metabolic competent hepatic cell line HepaRG (Ferron et al., 2016), apoptosis was observed in low-metabolically competent HL7702 cells (Pang et al., 2012), suggesting a role of detoxification.

Therefore, in this study we undertook a transcriptomic analysis to decipher the effects of YTX towards an extended panel of genes (nuclear receptors, metabolism, inflammation, oxidative stress and autophagy) on human HepaRG cells. These cells differentiate into hepatocytes (Gripon et al., 2002) with a similar expression pattern as primary human hepatocytes including major CYP enzymes, phase II activities, membrane transporters as well as key nuclear factors (PXR, CAR, AhR) (Antherieu et al., 2010).

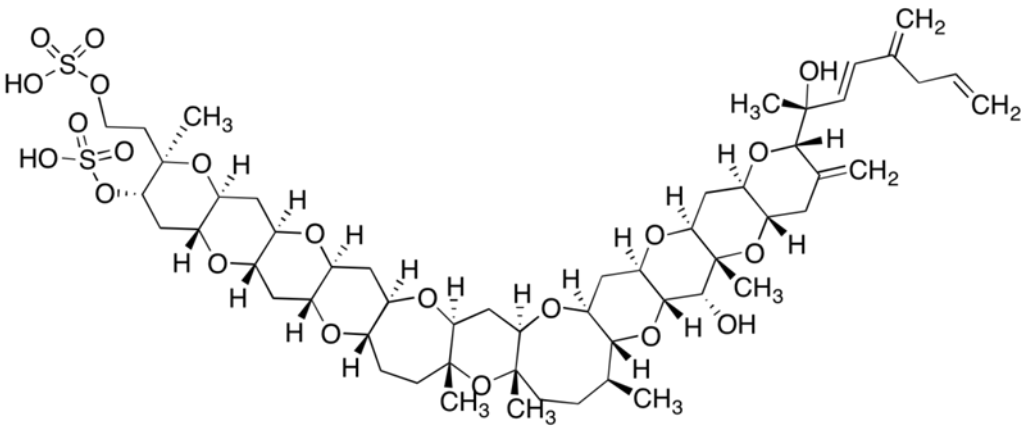

Fig. 1 Structure of YTX

2. Materials and methods

2.1 Chemicals

YTX standard was purchased from the National Research Council Institute for Marine Biosciences (Halifax, NS Canada). MTT was purchased from Sigma-Aldrich (St. Louis, MO, USA). All other chemicals including propan-2-ol, ethanol (EtOH), methanol (MeOH) and dimethyl sulfoxide (DMSO) were of analytical grade and purchased from Fisher Scientific (Leicestershire, England). Deionised water was prepared using a Milli-Q system (Millipore, Bedford, MA, USA).

2.2 Cell culture

HepaRG cells were cultured as previously published (Le Hégarat et al., 2010). Briefly, HepaRG cells (passages 13–19) were seeded at 30,000 cells/cm^2 in 96-well plates in culture medium (Williams' E Medium with GlutaMAX-I, supplemented with 10% fetal bovine serum, 100 IU/ml penicillin, 100 µg/ml streptomycin, 5 µg/ml bovine insulin, and 50 µM hydrocortisone hemisuccinate). After 2 weeks, the cells were cultured in the same medium supplemented with 1.7% DMSO (differentiation medium) for an additional 2 weeks. The medium was renewed every 2 to 3 days.

2.3 Cytotoxicity assays

2.3.1 DAPI

Cell viability was assessed in HepaRG cells via DAPI staining of the nuclei. After treatment with YTX, the cells were fixed with 4% paraformaldehyde in Phosphate Buffered Saline (PBS) for 10 min and permeabilized with 0.2% Triton X-100. The nuclei were stained with 1 µg/ml DAPI, and scored using the Thermo Scientific ArrayScan VTI HCS Reader (Thermo Scientific, Waltham, USA).

2.3.2 MTT assay

Following 24 h treatment with YTX, MTT (5 mg/ml) was added to each well and incubated 1 h at 37°C. The medium was then replaced with 130 µl of solubilization solution (0.7% SDS in Propan-2-ol) and the plate was maintained under shaking for 30 min before measurement. Absorbance was read

at 570 nm using an Infinite M200 microplate reader (Tecan), and viability was calculated as the percentage of mean absorbance to the solvent control condition.

2.4 Real-Time Quantitative Polymerase Chain Reaction (RT-qPCR) Analysis

The HepaRG cells were seeded in 12-well plates at a density of 20,000 cells/cm^2, and cultured until differentiation as described previously. Following 24 h incubation with YTX or positive controls (50 µM omeprazole and 10 µM rifampicin), the cells were washed twice with Phosphate Buffered Saline (PBS). Total RNA extraction was then performed using the Total RNA isolation NucleoSpin® RNA II kit from Macherey Nagel (Hoerd, France) following the manufacturer's protocol. The RNA concentration and quality were determined by spectrophotometric measurements with a BioSpec-nano (Shimadzu Biotech, Marne la Vallée, France). The RNA's integrity was checked by electrophoresis using an Experion (Bio-Rad, Marne la Coquette, France). The RNA samples were then reverse transcribed into double strand cDNA using the High Capacity RNA-to-cDNA kit (Applied Biosystems, Foster City, CA, USA) according to the manufacturer's instructions. The sequences of target genes were obtained from the National Center for Biotechnology Information (NCBI) GenBank sequence database (http://www.ncbi.nlm.nih.gov/). Primers were designed with the Primer designing tool from NCBI (http://www.ncbi.nlm.nih.gov/tools/primer-blast/index.cgi?LINK_LOC=BlastHome). For each gene, at least one primer was designed on the exon-exon junction. All primers (Supplementary data Table S1) were purchased from Sigma-Aldrich (Saint-Louis, MO, USA). Quantitative PCR was performed using Light Cycler® 1536 from Roche (Mannheim, Germany). SYBR Green chemistry was used. Reactions were performed in a total volume of 2 µl containing 1X Light cycler 1536 DNA Green Master, 1X Light cycler 1536 DNA Master mix (Roche), 300 nM of each primer, and 0.1 ng cDNA. Negative quantitative PCR controls of RNase-free water were included in each run for contamination assessment. The thermal cycling conditions were 94°C for 15 s, followed by 40 cycles of 15 s at 94°C and 30 s at 60°C with a slow ramp temperature (2.2°C/s). The Light Cycler® 1536 software (version 1.1.0.1112; Roche, Basel, Switzerland) was used for quantitative analysis. The analysis of the melting curves was used to check the specificity of each amplicon. Threshold Cqs were calculated from a baseline subtracted curve fit. Calibration curves were established for each gene from a serial dilution of a reference sample (pool of cDNA samples). According to these calibration curves, for each sample, mean relative amounts of mRNA of the target genes were calculated and then normalized to the GAPDH reference gene. Values were presented as fold change normalized to the solvent control.

2.5 Statistics/Data analysis

GraphPad Prism 5 (GraphPad Software, Inc., La Jolla, CA, USA) was used for the statistical analyses. The data were compared to the control condition using one-way analysis of variance (ANOVA) followed by Dunnett's post hoc tests. Statistical significance was depicted as follows: * $p < 0.05$, ** $p < 0.01$, *** $p < 0.001$.

3. Results

3.1 Cytotoxicity

After 24 h treatment, YTX had no effect regarding cell count (DAPI staining) and was only slightly toxic in the MTT assay (10 % cytotoxicity at 100 nM) (Figure 2). Based on these results, we selected

two low concentrations (15 and 30 nM) and one high concentration (120 nM) for mRNA expression analysis.

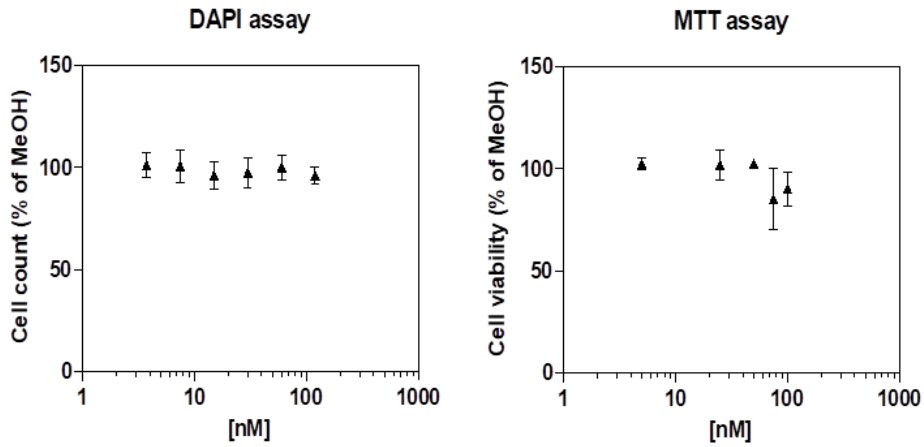

Fig. 2 Cell viability in HepaRG cells. Following 24 h of treatment with different concentrations of YTX, cytotoxicity was measured using DAPI staining or MTT assay. Results were obtained from three independent experiments performed in triplicate (mean ± SD).

3.2 Effects of YTX on the expression of a panel of 45 genes in HepaRG cells by qRT-PCR

Only fold inductions ≤ 0.5 and ≥ 1.5 and statistically significant were considered (Table 1).

3.2.1 Nuclear receptors

Only the two lowest concentrations of YTX induced a potent down-regulation of PXR gene expression (0.4 and 0.5 fold). No effect was detected on the others nuclear receptors genes expression as well as with the highest concentration.

3.2.2 Influx transporters

No effects were reported on influx transporters. A down-regulation without statistical significance was observed for *SLC22A1* at the highest concentration (0.5 fold induction).

3.2.3 CYP

The results for *CYP* showed that YTX down-regulated *CYP1A1* gene expression only at 15 nM (0.4 fold) while *CYP1A2* was up-regulated at the low concentrations (2.6 and 5.4 fold induction) but not at the high concentration. *CYP2B6* was down-regulated only at the high concentration (0.3 fold). *CYP2C9* and *2C19* were down-regulated for all three concentrations (between 0.3 and 0.5 fold). A dose-dependent up-regulation was observed for *CYP3A4* (2.4 fold induction for the high dose).

3.2.4 Transferases

Our data on Phase II genes show a down-regulation for many of them: *SULT1A1* (0.5 fold at 30 nM), *SULT1E1* (0.1 fold at 30 and 120 nM), *UGT1A1* (0.5 fold at 120 nM) and *UGT2B4* (0.4 fold at 15 and 30

nM). On the contrary, YTX induced a dose-dependent up-regulation of *GSTM1* (2.3 fold induction for the high dose).

3.2.5 Efflux transporters

No effects were reported on efflux transporters. A down-regulation without statistical significance was observed for *ABCC3* at the highest concentration (0.4 fold induction).

3.2.6 Inflammation

Low doses of YTX up-regulated *COX2* (5.3 fold induction), *IL6* (8.1 fold induction), *IL8* (15.9 fold induction) and to a lesser extent *NFKB1* (2.3 fold induction). These up-regulations were substantially diminished at the high dose. *COX1* was down-regulated only at 15 nM (0.5 fold).

3.2.7 Oxidative stress

The results on oxidative stress showed an up-regulation of *HMOX1* (2.9 fold induction at 30 nM) and *SOD2* (2.7 fold induction at 30 nM), with stronger effects at low concentrations. A down-regulation of *CAT* was only observed at 15 nM (0.4 fold), higher concentrations leading rather to a slight down-regulation (0.7 fold).

3.2.8 Autophagy

A dose-independent up-regulation for *DRAM1* (2.3 fold induction at 30 nM) was reported.

Table 1 Effects of YTX on mRNA expression in HepaRG cells. The cells were treated with two low (15 and 30 µM, n= 3) and one high (120 µM, n=2) concentrations of YTX for 24 h. Rifampicin (RIF) (10 µM) and omeprazole (OME) (50 µM) were used as positive controls. Results were presented as mean ± SD of fold change relative to the solvent control. A fold change between 0.9 and 0.5 (light blue), 0.5 and 0.2 (average blue) or less than 0.2 (dark blue) depicts gene down-regulation whereas a fold change between 1.5 to 2 (light red), 2 to 5 (average red) or greater than 5 (dark red) depicts gene up-regulation. * $p < 0.05$, ** $p < 0.01$, *** $p < 0.001$ after one-way ANOVA followed by Dunnett's post hoc tests.

Pathway	Gene	(nM)					
		15		30		120	
		Mean	SD	Mean	SD	Mean	SD
Nuclear receptors	***AHR***	1.1	0.7	1.2	0.5	0.7	0.5
	NR1I2	0.4**	0.1	0.5**	0.1	0.7	0.3
	PPARA	0.8	0.1	0.9	0.4	0.8	0.1
	RXRA	0.8	0.4	1.1	1.0	0.8	0.4

Phase 0 influx transporters	*SLC22A1*	0.7	0.6	0.9	0.7	0.5	0.2
	SLC22A3	1.3	0.9	1.7	0.9	0.8	0.6
	SLCO1A2	0.6	0.7	0.6	0.6	/	/
	SLCO1B1	0.8	0.6	1.0	0.3	0.7	0.4
Phase I CYP	*CYP1A1*	0.4	0.5	1.1	0.9	1.4	1.2
	CYP1A2	2.6	2.2	5.4	6.6	1.2	1.4
	CYP2B6	1.1	1.4	1.1	1.2	0.3	0.2
	CYP2C9	0.3**	0.1	0.4**	0.2	0.4**	0.1
	CYP2C19	0.5*	0.3	0.5	0.1	0.5	0.2
	CYP3A4	1.2	0.4	1.4	0.4	2.4	1.4
	CYP3A5	0.8	0.5	0.8	0.3	0.9	0.1
Phase II transferases	*GSTM1*	1.0	0.2	1.5	0.9	2.3	0.8
	NAT1	0.7*	0.1	0.7*	0.2	0.7	0.1
	NAT2	0.6*	0.1	0.7	0.2	0.8	0.1
	SULT1A1	0.5**	0.1	0.5**	0.0	0.7	0.3
	SULT1E1	0.2***	0.1	0.1***	0.1	0.1***	0.0
	UGT1A1	0.8	0.6	1.1	0.6	0.5	0.2
	UGT1A9	0.9	0.1	0.9	0.3	0.8	0.2
	UGT2B4	0.4***	0.1	0.4***	0.1	0.5**	0.2
Phase III efflux transporters	*ABCB1*	0.8	0.2	1.0	0.3	1.0	0.4
	ABCC2	0.8	0.4	0.8	0.4	0.8	0.1
	ABCC3	0.7	0.3	0.7	0.3	0.4	0.1
	ABCG2	0.8	0.4	1.0	0.1	1.1	0.7
Inflammation	*COX1*	0.5	0.3	1.1	1.0	/	/
	COX2	5.3	2.3	5.0	2.7	2.7	2.2
	IL6	8.1	9.4	6.1	2.2	1.3	0.3
	IL8	12.8	10.5	15.9	7.0	3.4	2.9
	NFKB1	1.7	0.4	2.3**	0.5	1.2	0.2
	NFKB3	1.3	1.1	1.6	0.8	0.9	0.5

Oxidative stress	*CAT*	0.4***	0.1	0.6**	0.1	0.7*	0.2
	HMOX1	2.4*	0.4	2.9**	0.6	1.7	0.5
	MAPK1	1.1	0.4	1.3	0.3	0.8	0.1
	NFE2L2	1.2	0.4	1.4	0.2	0.9	0.4
	PRDX1	0.8	0.3	0.8	0.1	0.7	0.1
	SOD1	0.8	0.3	0.8	0.1	0.7	0.1
	SOD2	2.4*	0.7	2.7*	0.7	1.6	0.5
Autophagy	*ATG10*	0.8	0.2	0.8	0.0	0.6*	0.2
	DRAM1	1.7	0.2	2.3*	0.3	1.9	1.0
	GABARAP	1.0	0.1	1.0	0.1	1.0	0.1
	HSP90AA1	1.0	0.5	1.3	0.4	0.8	0.1
	MTOR	0.9	0.4	0.9	0.5	0.8	0.0

0.2	0.5	0.9	1.5	2	5	20

x-Fold change compared to solvent control

4. Discussion (1500 words)

In this study, we investigated the effects of YTX in HepaRG cells, a metabolic competent human liver cell line using a transcriptomic approach. As the role of xenobiotic-metabolism genes in YTX fate is barely known, we investigated several genes related to metabolism as well as inflammation and oxidative stress.

Our study revealed that YTX was able to drastically modulate the mRNA levels of many genes even in the nanomolar range. While xenobiotic metabolism genes were globally rather down-regulated, inflammation genes were up-regulated. We observed down-regulations for several CYP, transferases and transporters in agreement with the observed down-regulation of PXR gene expression *NR1I2*. Indeed, PXR is known to regulate the transcription of many xenobiotic-metabolizing enzymes (Omiecinski et al., 2011). Up-regulations of *COX2*, *IL6* and *IL8* are consistent with the up-regulation of *NFKB1* and *NFKB3*. NF-κB regulates, among many target genes, IL-6 and -8 expression (Roebuck 1999). Moreover, it is well established that inflammation can decrease drug metabolism. Indeed, NF-κB was shown to disrupt the association of the PXR-RXRα complex with DNA, thus inhibiting the transactivation activity (Gu et al., 2009). Moreover, CYP and UGT activities were shown to be decreased by cytokines such as TNF-α, IL-1 or IL-6 (Monshouwer et al., 1996). It should be then further investigated whether YTX can decrease drug metabolism via the induction of inflammatory processes, especially knowing that YTX can trigger *in vitro* the release of TNF-α and IL-2 (Alfonso et al., 2003, Orsi et al., 2010).

Besides, our transcriptomic analysis highlighted some effects on other key genes. *CYP1A2* was the only CYP gene to be up-regulated at low concentration. CYP1A2 is known to catalyze the biotransformation of planar molecules, for instance polycyclic aromatic hydrocarbons (Pelkonen et al., 2008). YTX features a ladder-like skeleton of polycyclic polyethers that makes it a good candidate as CYP1A2 substrate. *SULT1E1* was surprisingly down-regulated to a huge extent. SULT1E1 enzyme catalyzes the transfer of a sulfate group to its substrate (Masahito et al., 2017). No information is available on a possible sulfate metabolite. In fact, YTX already presents two sulfates group at one of its extremities. It is unknown if these two sulfate groups play any particular role in YTX toxic effects.

YTX effects on oxidative stress were not so clear. Whereas key genes such as *HMOX1* were up-regulated, likely indicating the induction of oxidative damage, the gene expression of catalase (*CAT)*, an important enzyme in cell protection from hydrogen peroxide (Chelikani et al., 2004), was down-regulated. Concerning the family of superoxide dismutases, *SOD1,* located in the cytoplasm (Sheng et al., 2014), was barely affected while the mitochondrial *SOD2* (Sheng et al., 2014) was potently up-regulated, indicating mitochondria as a possible target of YTX effects. Consistently, YTX was previously reported to induce changes in the mitochondrial membrane potential and to open the permeability transition pore in hepatic cells (Bianchi et al., 2004).

In this study, we assessed the transcriptomic effects of YTX in hepatic HepaRG cells. Our findings suggest that YTX modulates the expression of many genes involved in drug metabolism as well as on several toxicity pathways including inflammation, oxidative stress and autophagy. Further investigation is required to correlate YTX-induced mRNA changes at the protein level.

5. Additional assays

To complete our mRNA data, several assays are planned to check if the modulations reported at the transciptomic level can be confirmed at the proteomic level. Regarding CYP, EROD assay can be performed to assess a possible induction of CYP1A activity following 24 h or 48 h treatment of YTX in HepaRG cells. Regarding inflammation, release of IL-6 and IL-8 by ELISA following 24 h or 48 h treatment with YTX on HepaRG cells is planned. To confirm the down-regulation of *SULT1E1*, western blot can be performed. Finally, possible YTX-mediated oxidative stress can be assessed using DCFH-DA probe (ROS production) and HMOX1 quantification.

References

Alexander, J., Benford, D., Boobis, A., Ceccatelli, S., Cravedi, J.-P., Di, A., Domenico, D.D., Dogliotti, E., Edler, L., Farmer, P., et al. (2009). Marine biotoxins in shellfish–Summary on regulated marine biotoxins Scientific Opinion of the Panel on Contaminants in the Food Chain. EFSA J 1306, 1–23.

Alfonso, A.; de la Rosa, L.A.; Vieytes, M.R.; Yasumoto, T.; Botana, L.M. Yessotoxin a novel phycotoxin, activates phosphodiesterase activity. Effect of yessotoxin on cAMP levels in human lymphocytes. Biochem. Pharmacol. 2003, 65, 193–208.

Alfonso A, Vieytes MR, Botana LM. Yessotoxin, a Promising Therapeutic Tool. Mar Drugs. 2016;14(2).

Antherieu, S., Chesne, C., Li, R., Camus, S., Lahoz, A., Picazo, L., Turpeinen, M., Tolonen, A., Uusitalo, J., Guguen-Guillouzo, C., et al. (2010). Stable Expression, Activity, and Inducibility of Cytochromes P450 in Differentiated HepaRG Cells. Drug Metab. Dispos. 38, 516–525.

Aune T., Aasen J.A.B., Miles C.O., Larsen S. Effect of mouse strain and gender on LD50 of yessotoxin. Toxicon. 2008;52:535–540.

Bianchi, C.; Fato, R.; Angelin, A.; Trombetti, F.; Ventrella, V.; Borgatti, A.R.; Fattorusso, E.; Ciminiello, P.; Bernardi, P.; Lenaz, G.; et al. Yessotoxin, a shellfish biotoxin, is a potent inducer of the permeability transition in isolated mitochondria and intact cells. Biochim. Biophys. Acta 2004, 1656, 139–147.

Chelikani P, Fita I, Loewen PD. Diversity of structures and properties among catalases. Cell Mol Life Sci. 2004; 61: 192–208.

Fernández-Araujo A, Alfonso A, Vieytes MR, Botana LM. Key role of phosphodiesterase 4A (PDE4A) in autophagy triggered by yessotoxin. Toxicology. 2015 Mar;329:60–72.

Ferron, P.J., Hogeveen, K., De Sousa, G., Rahmani, R., Dubreil, E., Fessard, V., and Le Hegarat, L. (2016). Modulation of CYP3A4 activity alters the cytotoxicity of lipophilic phycotoxins in human hepatic HepaRG cells. Toxicol. In Vitro 33, 136–146.

Ferron P-J, Dumazeau K, Beaulieu J-F, Le Hégarat L, Fessard V. Combined Effects of Lipophilic Phycotoxins (Okadaic Acid, Azapsiracid-1 and Yessotoxin) on Human Intestinal Cells Models. Toxins. 2016 Feb 19;8(2):50.

Franchini A., Malagoli D., Ottaviani E. Targets and effects of yessotoxin, okadaic acid and palytoxin: A differential review. Mar. Drugs. 2010;8:658–677.

Gripon, P., Rumin, S., Urban, S., Le Seyec, J., Glaise, D., Cannie, I., Guyomard, C., Lucas, J., Trepo, C., and Guguen-Guillouzo, C. (2002). Infection of a human hepatoma cell line by hepatitis B virus. Proc. Natl. Acad. Sci. 99, 15655–15660.

Gu X, Ke S, Liu D, Sheng T, Thomas PE, Rabson AB, et al. Role of NF-κB in Regulation of PXR-mediated Gene Expression: a mechanism for the suppression of cytochrome p-450 3a4 by proinflammatory agents. J Biol Chem. 2006;281:17882–9.

Kittler, K.; Preiss-Weigert, A.; These, A. Identification Strategy Using Combined Mass Spectrometric Techniques for Elucidation of Phase I and Phase II in Vitro Metabolites of Lipophilic Marine Biotoxins. Anal. Chem. 2010, 82, 9329–9335.

Korsnes M.S., Espenes A. Yessotoxin as an apoptotic inducer. Toxicon. 2011;57:947–958.

Le Hegarat, L., Dumont, J., Josse, R., Huet, S., Lanceleur, R., Mourot, A., Poul, J.-M., Guguen-Guillouzo, C., Guillouzo, A., Fessard, V., 2010. Assessment of the genotoxic potential of indirect chemical mutagens in HepaRG cells by the comet and the cytokinesis-block micronucleus assays. Mutagenesis 25, 555–560.

Masahito Suiko, Katsuhisa Kurogi, Takuyu Hashiguchi, Yoichi Sakakibara & Ming-Cheh Liu (2017) Updated perspectives on the cytosolic sulfotransferases (SULTs) and SULT-mediated sulfation, Bioscience, Biotechnology, and Biochemistry, 81:1, 63-72.

Monshouwer M, Witkamp RF, Nujmeijer SM, Van Amsterdam JG, Van Miert AS. Suppression of cytochrome P450- and UDP glucuronosyl transferase-dependent enzyme activities by proinflammatory cytokines and possible role of nitric oxide in primary cultures of pig hepatocytes. Toxicol Appl Pharmacol. 1996;137(2):237–244.

Omiecinski, C.J.; Vanden Heuvel, J.P.; Perdew, G.H.; Peters, J.M. Xenobiotic Metabolism, Disposition, and Regulation by Receptors: From Biochemical Phenomenon to Predictors of Major Toxicities. Toxicol. Sci. 2011, 120 (Suppl. 1), S49–S75.

Orsi, C.F.; Colombari, B.; Callegari, F.; Todaro, A.M.; Ardizzoni, A.; Rossini, G.P.; Blasi, E.; Peppoloni, S. Yessotoxin inhibits phagocytic activity of macrophages. Toxicon 2010, 55, 265–273.

Pang M., Qu P., Gao C.L., Wang Z.L. Yessotoxin induces apoptosis in HL7702 human liver cells. Mol. Med. Rep. 2012;5:211–216.

Pang M., Qu P., Gao C.L., Tang X., Wang Z.L. Effect of yessotoxin on cytosolic calcium levels in human hepatocellular carcinoma cells. Biomed. Rep. 2014;2:93–96.

Pazos M., Alfonso A., Vieytes M., Yasumoto T., Botana L. Study of the interaction between different phosphodiesterases and yessotoxin using a resonant mirror biosensor. Chem. Res. Toxicol. 2006;19:794–800.

Pelkonen O, Turpeinen M, Hakkola J, Honkakoski P, Hukkanen J, Raunio H. Inhibition and induction of human cytochrome P450 enzymes: current status. Arch Toxicol. 2008;82:667–715.

Perez-Gomez A., Ferrero-Gutierrez A., Novelli A., Franco J., Paz B., Fernandez-Sanchez M.T. Potent neurotoxic action of the shellfish biotoxin yessotoxin on cultured cerebellar neurons. Toxicol. Sci. 2006;90:168–177.

Roebuck KA. (1999). Regulation of interleukin-8 gene expression. J Interferon Cytokine Res. 19(5):429-38.

Sheng Y., Abreu I. A., Cabelli D. E., Maroney M. J., Miller A. F., Teixeira M., et al. (2014). Superoxide dismutases and superoxide reductases. Chem. Rev. 114 3854–3918.

Tubaro A, Sosa S, Carbonatto M, Altinier G, Vita F, Melato M, et al. Oral and intraperitoneal acute toxicity studies of yessotoxin and homoyessotoxins in mice. Toxicon. 2003;41(7):783–92.

Visciano P., Schirone M., Berti M., Milandri A., Tofalo R., Suzzi G. (2016). Marine biotoxins: occurrence, toxicity, regulatory limits and reference methods. Front. Microbiol. 7:1051.

Young C., Truman P., Boucher M., Keyzers R., Northcote P., Jordan W.T. The algal metabolite yessotoxin affects heterogeneus nuclear ribonucleoproteins in HepG2 cells. Proteomics. 2009;9:2529–2542.

Supplementary data: Table S1 Summary of primers used for q-PCR analysis.

Gene	Sequence (5' to 3')	Gene	Sequence (5' to 3')
AHR	F: TAGGGTTTCAGCAGTCTGATGTC R: CTACTGTCTGGGGGAGACCA	*SLC22A1*	F: TGTCAAATTTGTTGGCGGGG R: TTTAACCAGTGCAGGTCAGGT
NR1I2	F: AGACACTGCAGGTGGCTTC R: TGGGGAGAAGAGGGAGATGG	*SLC22A3*	F: GCATTGCTAAGTGCAATGGGA R: GCTTGTGAACCAAGCAAACATAAG
PPARA	F: TCGGCGAGGATAGTTCTGGA R: TGAAAGCGTGTCCGTGATGA	*SLCO1A2*	F: GCACAAGAGTATTTGCTGGCAT R: CGGCAATCCGAGGTAGATGT
RXRA	F: TCCTGCCGCTCGATTTCTC R: GGAGCTCAGGGTGCTGATG	*SLCO1B1*	F: TCCACATCATTTTCAAGGGTCTACT R: TGCTTCATCCATGACACTTCCAT
CYP1A1	F: ACCCTGAAGGTGACAGTTCC R: TCTTGGAGGTGGCTGAGGTA	*COX1*	F: TCCAGGAGCTCGTAGGAGAG R: CCTTGAGGGAAAAGGGAGCC
CYP1A2	F: CTTCGCTACCTGCCTAACCC R: CCCGGACACTGTTCTTGTCA	*COX2*	F: GAAAACTGCTCAACACCGGAAT R: TGTAGTGCACTGTGTTTGGAGT
CYP2B6	F: TTCGGCGATTCTCTGTGACC R: ATGAGGGCCCCCTTGGAT	*IL6*	F: AGAGGCACTGGCAGAAAACA R: ACCAGGCAAGTCTCCTCATTG
CYP2C9	F: AAATGGAGAAGGAAAAGCACAACC R: TCAACTGCAGTGTTTTCCAAGC	*IL8*	F: GGAGAAGTTTTTGAAGAGGGCTG R: TGCTTGAAGTTTCACTGGCATC
CYP2C19	F: CCTGGAACGCATGGTGGT R: TCCATTGCTGAAAACGATTCCAAAT	*NFKB1*	F: GCCACCCGGCTTCAGAAT R: TGAAGGTATGGGCCATCTGC
CYP3A4	F: TCACAAACCGGAGGCCTTTT R: TGGTGAAGGTTGGAGACAGC	*NFKB3*	F: CGGCCATGGACGAACTGT R: TGATCTCCACATAGGGGCCA
CYP3A5	F: GCCCAATAAGGCACCACCTA R: CCACCATTGACCCTTTGGGA	*CAT*	F: CCTGTGAACTGTCCCTACCG R: ATTTGGAGCACCACCCTGATT
GSTM1	F: GGGGGACGCTCCTGATTATG R: GGGCAGATTGGGAAAGTCCA	*HMOX1*	F: CTGCTCAACATCCAGCTCTTTG R: ATCTTGCACTTTGTTGCTGGC
NAT1	F: ACTAAGAAAGGGGATCATGGACATT R: ACAGCTCGGATCTGGTGTTG	*MAPK1*	F: GCATGGTGTGCTCTGCTTATG R: AGGGTTCTCTGGCAGTAGGT
NAT2	F: ACAGACCTTGGAAGCAAGAGG R: CTTCAATGTCCATGATCCCTTTGG	*NFE2L2*	F: ATCCATTCCTGAGTTACAGTGTCTT R: TGGCTTCTGGACTTGGAACC
SULT1A1	F: TCGGAGAAGTGTCCTACGGAT R: CCACGAAGTCCACGGTCTC	*PRDX1*	F: TTGGTATCAGACCCGAAGCG R: AAAGGCCCCTGAACGAGATG
SULT1E1	F: ACAGGATCAACTAAACAGTGTACCA R: ATCTGGTCTTGCCTGGAACG	*SOD1*	F: TGGTTTGCGTCGTAGTCTCC R: TGGTCCATTACTTTCCTTCTGCT
UGT1A1	F: CTGCCTTCACCAAAATCCACTATC R: CACAGGACTGTCTGAGGGATTT	*SOD2*	F: TTGGGGTTGGCTTGGTTTCA R: GGAATAAGGCCTGTTGTTCCTTG
UGT1A9	F: CGGAGTATGATCTCTACAGCCAC R: TTCAAATTCCATAGGCAACGGC	*ATG10*	F: AGGGCAAGCTTTTTAGATGGGA R: TAGTGTCCCATGGTCCCTGT
UGT2B4	F: GAAGTTCTAGGAAGACCCACTACG R: GGGTGAGGAAATTGAAAATCCCAG	*DRAM1*	F: TCAACCCCTTCCTCCCGTAT R: CGTGGCTGCACCAAGAAATG
ABCB1	F: CAGCTGTTGTCTTTGGTGCC R: CCAATGTGTTCGGCATTAGGC	*GABARAP*	F: GGGTGCCGGTGATAGTAGAAAA R: AGCTCGGAGATGAATTCGCTT
ABCC2	F: GTGTGGATTCCCTTGGGCTT R: GAAGAAAACCAACGAATACCTGCTT	*HSP90AA1*	F: ATGAGCAGTACGCTTGGGAG R: CCATAGGTTCACCTGTGTCTGT
ABCC3	F: CCAACTCAGTCAAACGTGCG R: ACCTAGGTTCTGCCAGAGGA	*MTOR*	F: AAGCCGCGCGAACCTC R: TGGCCCTGGTTTCCTCATTC
ABCG2	F: AGTTCTCAGCAGCTCTTCGG R: TTCCAACCTTGGAGTCTGCC	*GAPDH*	F: GTCAAGGCTGAGAACGGGAA R: AAATGAGCCCCAGCCTTCTC

"Mixture effects" axis

Publication #4: *In vitro* assessment of binary mixtures effects of phycotoxins in human intestinal Caco-2 cells

Article to be submitted in *Toxicological Sciences* or *Archives of Toxicology*.

***In vitro* assessment of binary mixture effects of phycotoxins in human intestinal Caco-2 cells**

Jimmy Alarcan[1], Sabrina Barbé[1], Benjamin Kopp[1], Stefanie Hessel-Pras[2], Alfonso Lampen[2], Valérie Fessard[1] and Ludovic Le Hégarat[1,*]

[1] Toxicology of Contaminants Unit, French Agency for Food, Environmental and Occupational Health & Safety, ANSES, 10B rue Claude Bourgelat, Fougères 35300, France; jimmy.alarcan@anses.fr; sabrina.barbe.53@gmail.com; benjamin.kopp@anses.fr; valerie.fessard@anses.fr; ludovic.lehegarat@anses.fr

[2] German Federal Institute for Risk Assessment, Department of Food Safety, Max-Dohrn-Straße 8-10, 10589 Berlin, Germany; Stefanie.Hessel-Pras@bfr.bund.de (S.H-P.); Alfonso.Lampen@bfr.bund.de (A.L.)

* Correspondence: ludovic.lehegarat@anses.fr; Tel.: +33-02-99-17-27-47

Abstract (150-250 words)

Lipophilic phycotoxins are secondary metabolites produced by phytoplanktonic species. They accumulate in filtering shellfish and can cause human intoxications. Humans could be exposed simultaneously to several phycotoxins but toxicological effects of phycotoxin mixtures on human health are largely unknown. Published data on phycotoxins co-exposure suggested that okadaic acid (OA) could be simultaneously found with pectenetoxin-2 (PTX-2), yessotoxin (YTX) or spirolide-1 (SPX-1). Therefore, the aim of this study was to examine the effects of three binary mixtures OA/PTX-2, OA/YTX and OA/SPX-1 on the human intestinal Caco-2 cells using high-content analysis approach. A multi-parametric approach was used: cell viability (cell count), oxidative stress (ROS formation), inflammation (Interleukine-8), and DNA damage (γ-H2AX) were simultaneously assessed. We first investigated the effects of each toxin in single condition and we observed that OA induced cytotoxicity, DNA breaks and IL-8 release. PTX-2 only induced slightly DNA strand-breaks, whereas SPX-1 and YTX showed a negative response for all endpoints. The addition of another toxin to OA resulted in antagonistic effects at low concentrations but additive or synergistic effects with increases concentrations. Due to noticeable combined effects on some key toxicity pathways, more attention should be paid on possible human health with phycotoxin found in mixtures.

Keywords: phycotoxins, mixtures, antagonism, genotoxicity, inflammation

Abbreviations:

ABC: ATP-binding cassette transporter

CYP: cytochrome P450

DSP: diarrhetic shellfish poisoning

EFSA: European Food Safety Authority

IL-8: interleukine 8

OA: okadaïc acid

P-gp: P-glycoprotein

PP2A: protein phosphatase 2A

PTX-2: pectenotoxin-2

PXR: pregnane x receptor

ROS: reactive oxygen species

SPX-1: spirolide-1

YTX: yessotoxin

1. Introduction (750 words)

Marine biotoxins are secondary metabolites produced by specific phytoplanktonic species (Visciano et al., 2016). Regulatory limits were set to protect consumers (EFSA report 2009) from their potential harm as they can contaminate shellfish and be responsible for foodborne diseases. However, in the absence of human intoxications, no regulatory limits have been established for the group of cyclic imines although they are frequently detected in shellfish and can be very toxic *in vivo* (Munday et al., 2012). Regarding mixtures, the EFSA opinion only stated in case of toxin analogues with established toxicity equivalent factors (TEFs). Due to the lack of studies regarding deleterious effects when different groups of toxins are combined, the impact of toxins co-occurrence on toxicity and therefore on regulation limits needs to be more deeply investigated.

Among lipophilic toxins, several main families have been described: okadaic acid and dinophysistoxins (DTXs), pectenotoxins (PTXs), yessotoxins (YTXs) and finally cyclic imines (including spirolides, pinnatoxines, pteriatioxines and gymnodimines). OA and DTXs are responsible for diarrhetic shellfish poisoning (DSP), characterized by diarrhea, nausea, abdominal pain or vomiting (Valdiglesias et al., 2013). The OA group acts through the inhibition of protein phosphatase 2A (PP2A) and to a lesser extent PP1 (Takai et al., 1992). The group of PTXs, whose main representative is PTX-2, is not anymore included in the DSP toxins since its implication in gastro-intestinal symptoms is not clear (Ito et al., 2008). At cellular level, PTX-2 provoques actin depolarization leading to cytoskeleton disruption (Alligham et al., 2007). The group of YTXs has no recorded effects in humans but has been frequently found concomitantly to OA in shellfish (Alarcan et al., 2018). YTX displays *in vitro* toxicity,

for instance apoptosis or perturbation of calcium flux (Tubaro et al., 2008). Its mechanism of action is still unknown but some studies suggest a possible connection with autophagy (Fernandez et al., 2015). Finally, potent neurological effects in mice have been reported for the group of cyclic imines (Munday et al., 2012). SPX-1 is a selective inhibitor of nicotinic acetylcholine receptors (Araoz et al., 2015).

As for any other food contaminant, the small intestine is one of the first organs in contact with phycotoxins following ingestion. Mixture effects on intestinal cells have been investigated in proliferative human intestinal Caco-2 and HIEC cells (Ferron et al., 2016). Binary combinations of AZA-1/OA and YTX/OA depicted an increasing antagonism effect on viability when toxin concentrations increased whereas AZA-1/YTX mixtures showed synergism with a dose-dependent increase. In this study, we completed these data by assessing a panel of different toxicity endpoints (cell viability, oxidative stress, inflammation and DNA strand breaks) on the human Caco-2 cell line following treatment with lipophilic toxins (OA, PTX-2, YTX and SPX-1) alone or in binary combinations.

2. Materials and methods

2.1 Establishment of mixtures

The choice of relevant mixtures was based on the review that we recently published (Alarcan et al., 2018). Briefly, we retrieved published data reporting shellfish contamination with mixtures of lipophilic phycoctoxins and we established the main occurring mixtures. OA was predominantly found as the main toxin. The most data were reported for America and Europe. The median value ratio for the combination OA/YTX was around 3.5. For the combination OA/SPX-1, it reached 11.5, but this combination was only reported in Europe. The median value ratio for the combination OA/PTX-2 was found to be superior to 10. Three main binary mixtures were then selected with the following ratios: 3:1 for OA/PTX-2 and OA/YTX and 9:1 for OA/SPX-1. We decided to investigate a 3:1 ratio for OA/PTX-2 instead of a high ratio to reflect a high binary contamination scenario that was often reported and represents a higher concern.

2.2 Chemicals

Toxins standards were purchased from the National Research Council Institute for Marine Biosciences (Halifax, NS Canada). DCFH-DA, menadione, potassium bromate ($KBrO_3$), methyl methanesulfonate, TnFα were purchased from Sigma-Aldrich (St. Louis, MO, USA). Primary IL-8 antibody (M801), biotin-conjugated human IL-8 (M802B), HRP-Conjugated Streptavidin (N100), 3,3',5,5'-tetramethylbenzidine (TMB) were obtained from Thermofisher scientific. All other chemicals including ethanol (EtOH), methanol (MeOH) and dimethyl sulfoxide (DMSO) were of analytical grade and purchased from Fisher Scientific (Leicestershire, England). Deionised water was prepared using a Milli-Q system (Millipore, Bedford, MA, USA).

2.3 Cell culture

Caco-2 cells were obtained from the European Collection of Cell Cultures (Porton Down, UK). Cells (passages 30–38) were seeded at 10,000 cells/cm^2 in 96-well plates in culture medium (Dulbecco's modified Eagle's medium, supplemented with 10% fetal bovine serum, 100 IU/ml penicillin and 100 µg/ml streptomycin). Cells were cultured for 3 weeks with renewal of medium every 2 to 3 days.

2.4 Measurement of ROS production

ROS were measured using DCFH-DA probe. Caco-2 cells were pre-treated 30 min with 25 µM DCFH-DA before withdrawal and addition of medium without serum containing the toxins for 24 h at 37°C. Fluorescence was measured at λ ext = 485 nm and λ em = 520 nm using a Fluostar Omega microplate reader (BMG Labtek).

2.5 Cell viability and DNA strand breaks

After 24 h treatment with toxins, Caco-2 cells were fixed with 4% paraformaldehyde in phosphate buffered saline (PBS) for 10 min and permeabilized with 0.2% Triton X-100 for 15 min. Plates were then incubated in blocking solution (PBS with 1% BSA and 0.05% Tween-20) for 30 min before the addition of primary antibody prepared in blocking solution and filtered with a 0.2 µm syringe filter. The primary and secondary antibodies were purchased from Abcam (Cambridge, UK): mouse monoclonal anti γH2AX S19 (ab26350) and goat pAb to Ms IgG Alexa Fluor® 647 (ab150115). The primary antibody (1/1000) was incubated 1.5 h at room temperature. After washing with PBS + 0.05% Tween20, the secondary antibody (1/1000) was incubated for 45 min at room temperature. Nuclear DAPI (1 µg/mL) staining was used for automated cell identification by high content analysis. Plates were scanned with the Thermo Scientific ArrayScan VTI HCS Reader (Thermo Scientific, Waltham, USA) and analyzed using the Target Activation module of the BioApplication software. For each well, 10 fields (10X magnification) were scanned and analyzed for immunofluorescence quantification. Cell numbers were determined by cell counting from DAPI staining. γ-H2AX was quantified in the nuclei and expressed as fold increase compared to solvent control.

2.6 IL-8 release by ELISA

After treatment with toxins, cells supernatants were collected and analyzed for IL-8 release. Samples were transferred to 96-well microplates coated overnight at 4°C with human recombinant IL-8 primary antibody (1 µg/ml). Following addition of the biotin-conjugated human IL-8 antibody (0.1 µg/ml) for 1 h, streptavidin peroxidase (1:10000) was added for 45 min. After washing with PBS + 0.05% Tween20, 3,3',5,5'-tetramethylbenzidine (TMB) solution was added to initiate colorimetric reaction. The reaction was stopped by H_2SO_4 (1 M) and absorbance was measured at 405 nm using a Fluostar Omega microplate reader (BMG Labtek).

2.7 Statistics/Data analysis

GraphPad Prism 5 (GraphPad Software, Inc) was used for statistical analyses. Data were compared to control condition using two-way ANOVA followed by Bonferroni's post hoc tests. All error bars denote standard error of the mean (SEM). Symbols *, **, ***, **** indicate statistical significance between toxin and solvent control respectively ($p < 0.05$, $p < 0.01$, $p < 0.001$, $p < 0.0001$ respectively).

2.8 Interactions analysis using theoretical additivity method

Theoretical additivity method was used as described by Weber et al., (2005). This method compares theoretical predicted values calculated from the results of each individual compound to the measured values obtained with mixtures. In our study, using binary phycotoxin combinations, the predicted mixture effect value was calculated as follows:

Mix(A+B)predicted value = (mean value A + mean value B) – mean value solvent control

For data expressed as fold change compared to solvent control, mean value solvent control = 1. Mix(A+B)predicted value < , = and > Mix(A+B)measured value indicates respectively synergism, additivity and antagonism.

For cell viability analysis, the mean value for the solvent control was set to 100.

Mix(A+B)predicted value < , = and > Mix(A+B)measured value indicates respectively antagonism, additivity and synergism.

The theoretical additivity method was applied to all data sets.

2.9 Interactions analysis using Chou-Talalay method

The Chou-Talalay method (Chou and Talalay 1984) was also used to analyze the interactions between toxins. For each endpoint, the dose-response relationships for the individual toxins and for the binary combinations were modeled using the median-effect equation of the mass action law (Chou 2006):

$fa/fu = (D/D_m)^m$

where D is the dose of the toxin, D_m is the median-effect dose, fa is the fraction affected by D, fu is the fraction unaffected (fu = 1 − fa) and m is the coefficient signifying the shape of the dose–effect relationship (m = 1, m > 1, and m < 1 indicate hyperbolic, sigmoidal and flat sigmoidal dose–effect curves, respectively).

Interactions between toxins were analyzed using the combination index method (Chou 2006):

$(CI)_x = (D)_1/(D_x)_1 + (D)_2/(D_x)_2$

where $(CI)_x$ is the combination index at x% effect, $(D)_1$ and $(D)_2$ are the doses of toxins that exert x% effect in binary combination, $(D_x)_1$ and $(D_x)_2$ are the doses of each toxin alone that exerts x% effect. CI < 1, =1 and >1 indicate respectively synergism, additive effect and antagonism.

Interaction analysis was performed using CompuSyn software, version 3.01 (ComboSyn Inc., Paramus, NJ, USA). Since Chou-Talalay method is only applicable with sigmoidal dose-response data sets, not all data could be analyzed. Raw data from ROS production, IL-8 release and γ-H2AX phosphorylation, originally expressed as fold change compared to solvent control, were processed to obtain data suitable for Chou-Talalay analysis, i.e. comprised between 0.01 and 0.99. For each experiment (phycotoxin doses tested individually or in mixture for one endpoint), the condition showing the highest effect was attributed the value of 0.99 (Amax). All other conditions were then normalized to the Amax. This data processing was described previously by Alassane-Kpembi et al., (2017).

3. Results

3.1 Toxic effects following OA/PTX-2 mixtures treatment in Caco-2 cells

3.1.1 PTX-2 exacerbates the cytotoxicity effect of OA in Caco-2 cells

PTX-2, alone, was slightly toxic for Caco-2 cells, whereas OA showed a potent and concentration-dependent toxicity (IC_{50} = 110.2 nM) (Fig. 1a). Binary OA/PTX-2 mixture induced high cytotoxicity

effect in Caco-2 cells, with a decrease of 80% of cells numbers from 150/50 nM ratio (Fig. 1a), indicating that the addition of PTX-2 increased the cytotoxicity of OA.

3.1.2 PTX-2 decreases ROS production induced by OA

Alone, PTX-2 did not induce ROS production after 24 h treatment whereas OA increased ROS production without being significant (Fig. 1b). We observed that low concentrations of OA/PTX-2 reduced the level of ROS production compared to OA alone (Fig. 1b).

3.1.3 PTX-2 decreases IL-8 production induced by OA only at low concentrations

Only OA hightly induced IL-8 release in Caco-2 cells (Fig. 1c). For low concentrations (conditions A and B), the mixtures resulted in a reduction of IL-8 release compared to OA alone, whereas at higher concentrations (from 75/25 nM) PTX-2 did not decrease IL-8 production induced by OA (Fig. 1c).

3.1.3 PTX-2 decreases γ-H2AX phosphorylation induced by OA only at low concentrations

PTX-2 alone slightly induced the phosphorylation of γ-H2AX (1.8-fold) whereas OA greatly induced a concentration-dependent phosphorylation of γ-H2AX even at the lowest concentration 18.75 nM (Fig. 1d). For low concentrations (conditions A and B), the mixtures resulted in a reduced phosphorylation of γ-H2AX compared to that of OA alone (Fig. 1d). This protective mixture effect is remarkably shown in Fig. 2 where the value for γ-H2AX was considerably lowered in mixture condition compared to OA alone.

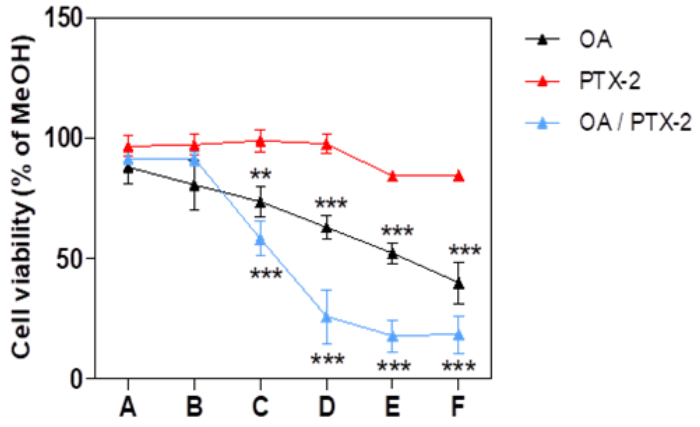

(**a**)

nM	solo		mixtures
	OA	**PTX-2**	**OA/PTX-2**
A	18.75	6.25	18.75/6.25
B	37.5	12.5	37.5/12.5
C	75	25	75/25
D	150	50	150/50
E	300	100	300/100
F	600	200	600/200

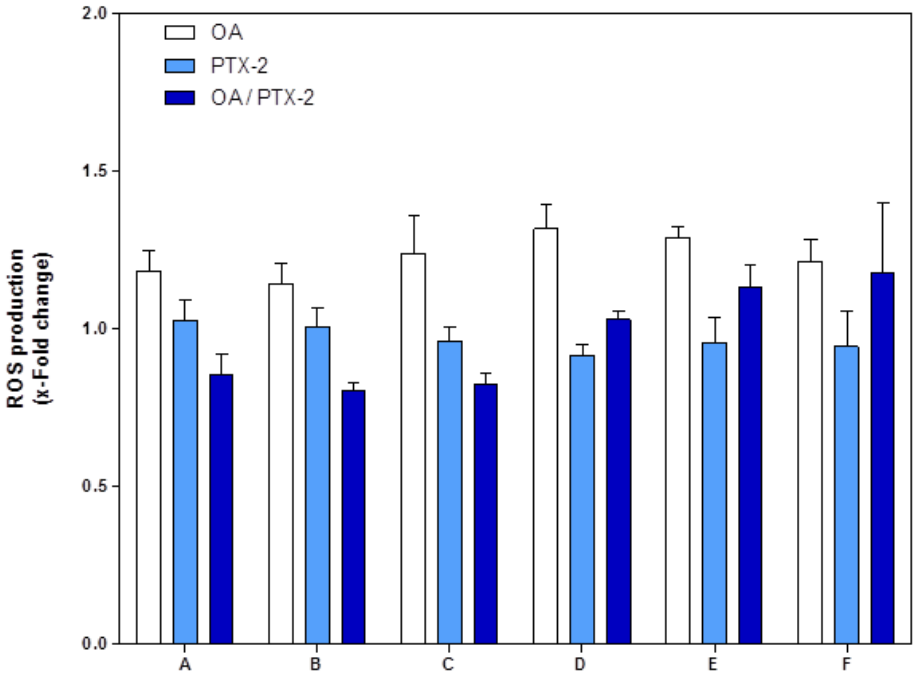
OA
PTX-2
OA / PTX-2
ROS production
(x-Fold change)
2.0
1.5
1.0
0.5
0.0
A
B
C
D
E
F

(b)

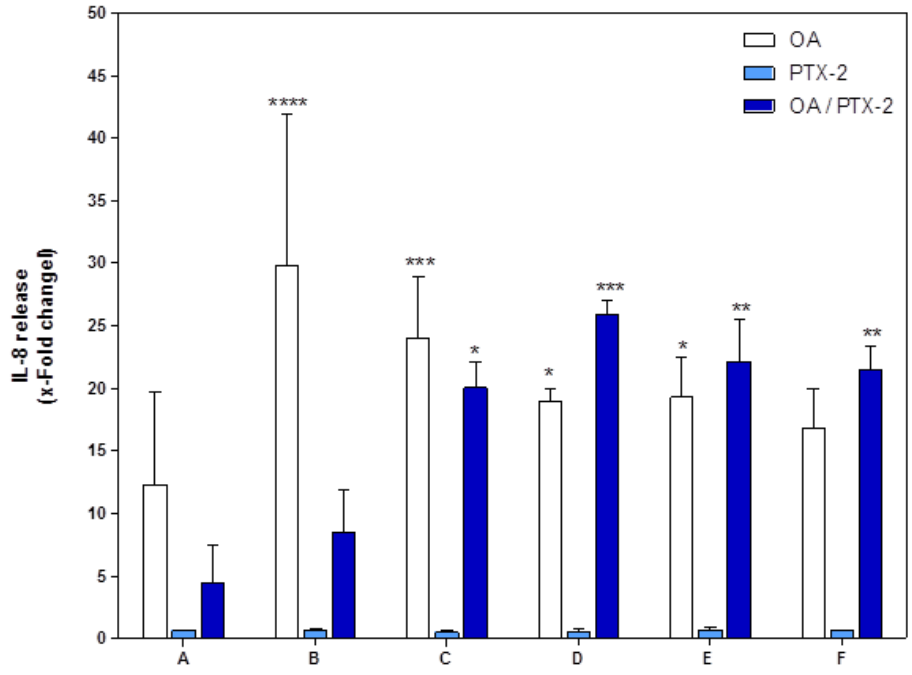
OA
PTX-2
OA / PTX-2
IL-8 release
(x-Fold change)
50
45
40
35
30
25
20
15
10
5
0
****
***
*
*
***
*
**
**
A
B
C
D
E
F

(c)

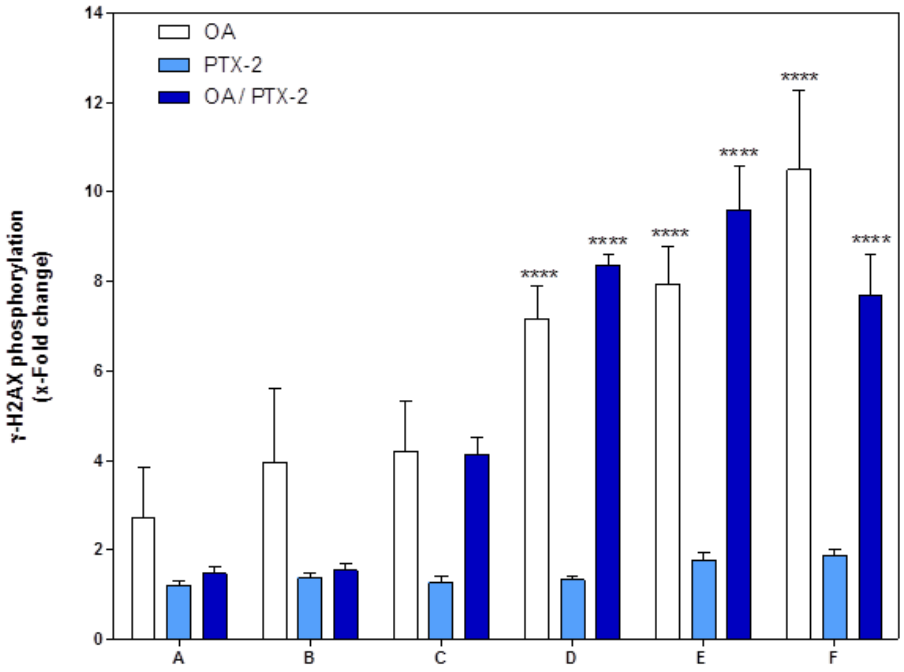

(d)

Fig. 1 Effects of OA/PTX-2 mixtures on a panel of toxicity endpoints in differentiated Caco-2 cells. Cells were pre-treated with the ROS probe DCFH-DA (25 µM) for 30 min before incubation with toxins for 24 h. After fluorometric measurement of ROS production, cell media were collected for IL-8 dosage while cells were fixed for DAPI and γ-H2AX immunostaining. (a) depicts cell viability, (b) depicts ROS production, (c) depicts IL-8 release and (d) depicts phosphorylation of γ-H2AX. Results were obtained from three independent experiments. Data represents means ± SEM of fold change compared to solvent control (4.1% MeOH/0.3% EtOH). *, **, ***, **** indicate statistical significance between toxin and solvent control respectively ($p < 0.05$, $p < 0.01$, $p < 0.001$, $p < 0.0001$ respectively) after two-way ANOVA followed by Bonferroni's post hoc tests.

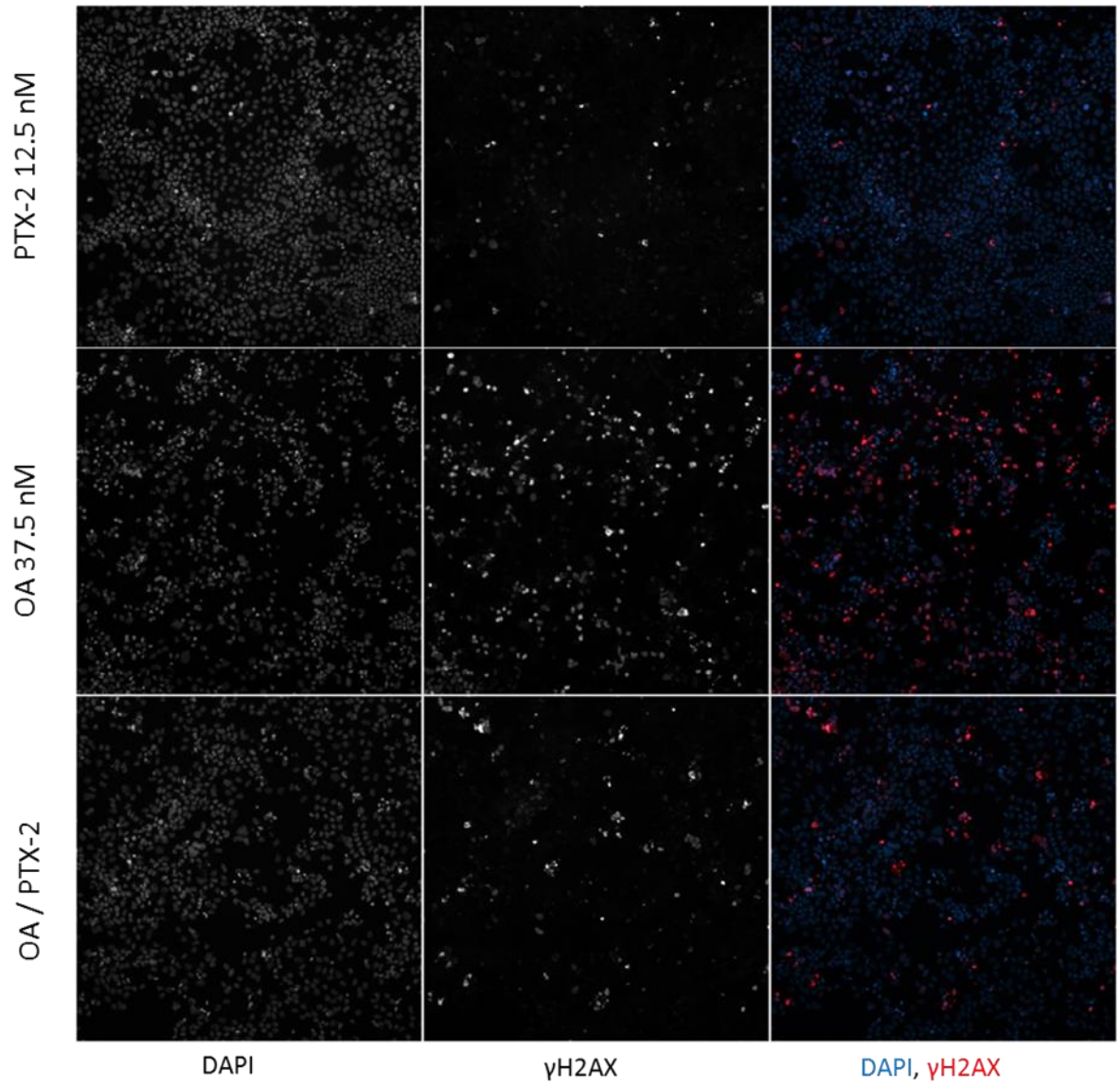

Fig. 2 Representative images (10X magnification) of DNA damage induced by OA and PTX-2 alone and in mixture. Cells were incubated with toxins for 24 h. Cells were labeled with antibodies against γ-H2AX. The nuclei of the cells were stained with DAPI and images were captured with an Arrayscan VTi.

3.2 Toxic effects following OA/SPX-1 mixtures treatment in Caco-2 cells

3.2.1 SPX-1 reduces the cytotoxicity effect of OA in Caco-2 cells at low concentration

SPX-1 was not toxic for Caco-2 cells in our tested range concentration. In mixture condition, a lower toxicity was depicted for 37.5/4.2 and 75/8.3 nM (Fig. 3a).

3.2.2 SPX-1 decreases ROS production, IL-8 release and γ-H2AX phosphorylation induced by OA at low concentrations

Whereas SPX-1 failed to induce any toxic effects in Caco-2 cells, SPX-1 decreased the biological effect of OA at conditions A and B on ROS production, IL-8 release and phosphorylation of γ-*H2AX* (Fig. 3b, 3c and 3d). This protective mixture effect is remarkably shown in Fig. 4 where the value for γ-H2AX was considerably lowered in mixture condition compared to OA alone. However, when the concentration of SPX-1 was increased, this inhibition effect was not observed. For IL-8 release, we rather showed a slight increase compared to OA alone.

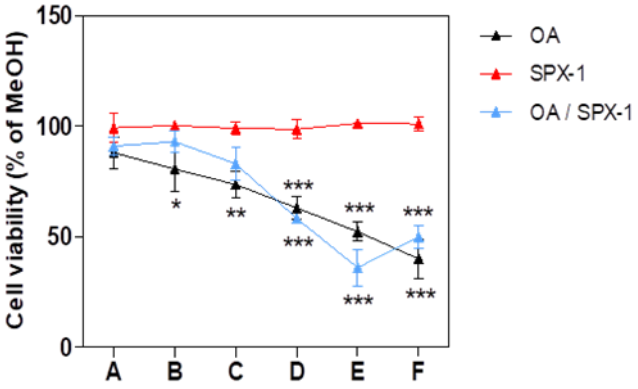

(a)

nM	solo		mixtures
	OA	**SPX-1**	**OA/SPX-1**
A	18.75	2.1	18.75/2.1
B	37.5	4.2	37.5/4.2
C	75	8.3	75/8.3
D	150	16.7	150/16.7
E	300	33.4	300/33.4
F	600	66.7	600/66.7

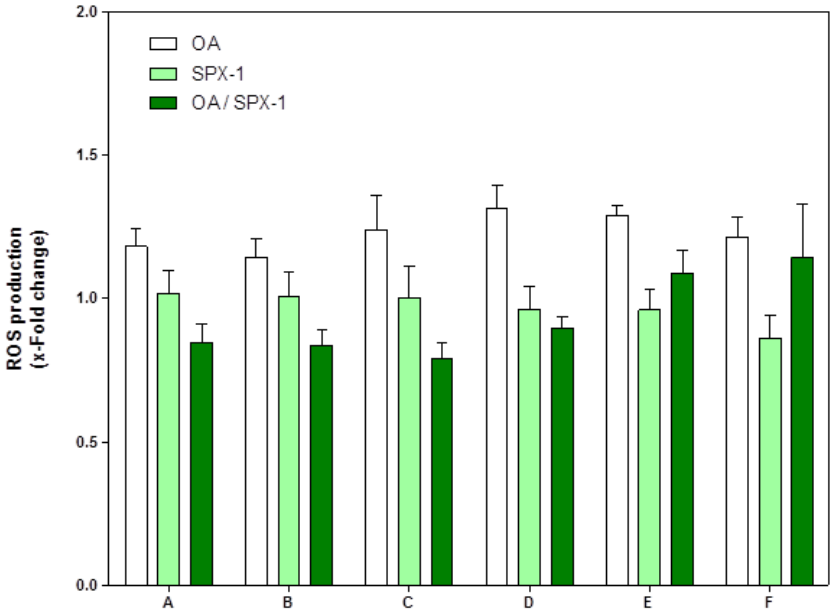

(b)

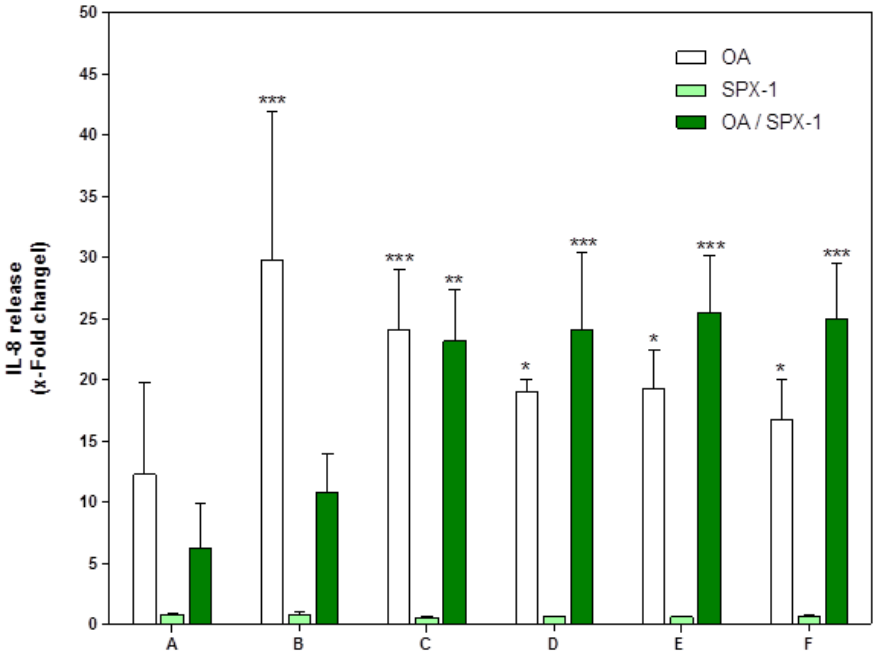

(c)

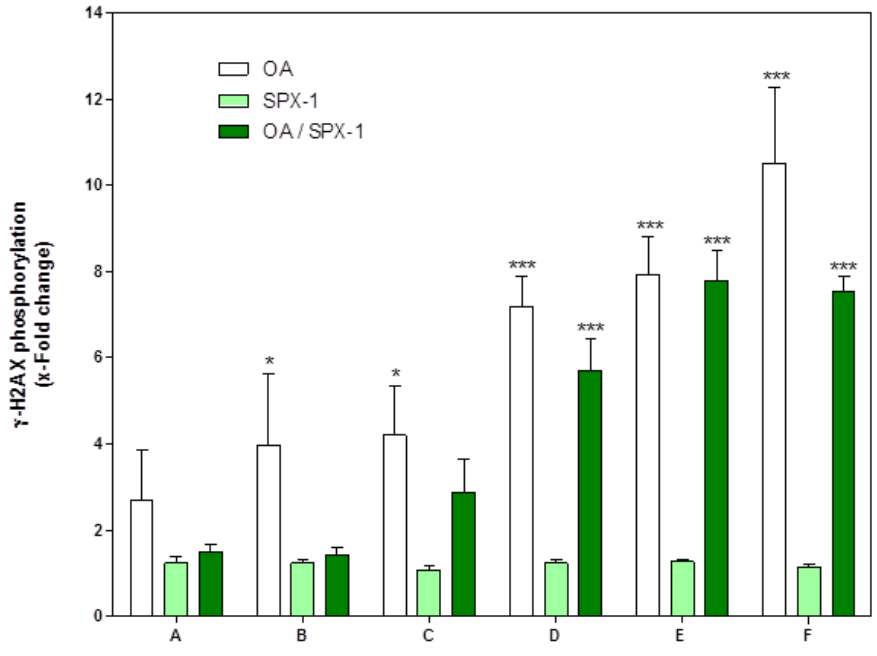

(d)

Fig. 3 Effects of OA/SPX-1 mixtures on a panel of toxicity endpoints in differentiated Caco-2 cells. Cells were pre-treated with the ROS probe DCFH-DA (25 µM) for 30 min before incubation with toxins for 24 h. After fluorometric measurement of ROS production, cell media were collected for IL-8 dosage and cells were fixed for DAPI and γ-H2AX immunostaining. (a) depicts cell viability, (b) depicts ROS production, (c) depicts IL-8 release and (d) depicts phosphorylation of γ-H2AX. Results were

obtained from three independent experiments. Data represents means ± SEM of fold change compared to solvent control (4.1% MeOH/0.3% EtOH). *, **, *** indicate statistical significance between toxin and solvent control respectively ($p < 0.05$, $p < 0.01$, $p < 0.001$ respectively) after two-way ANOVA followed by Bonferroni's post hoc tests.

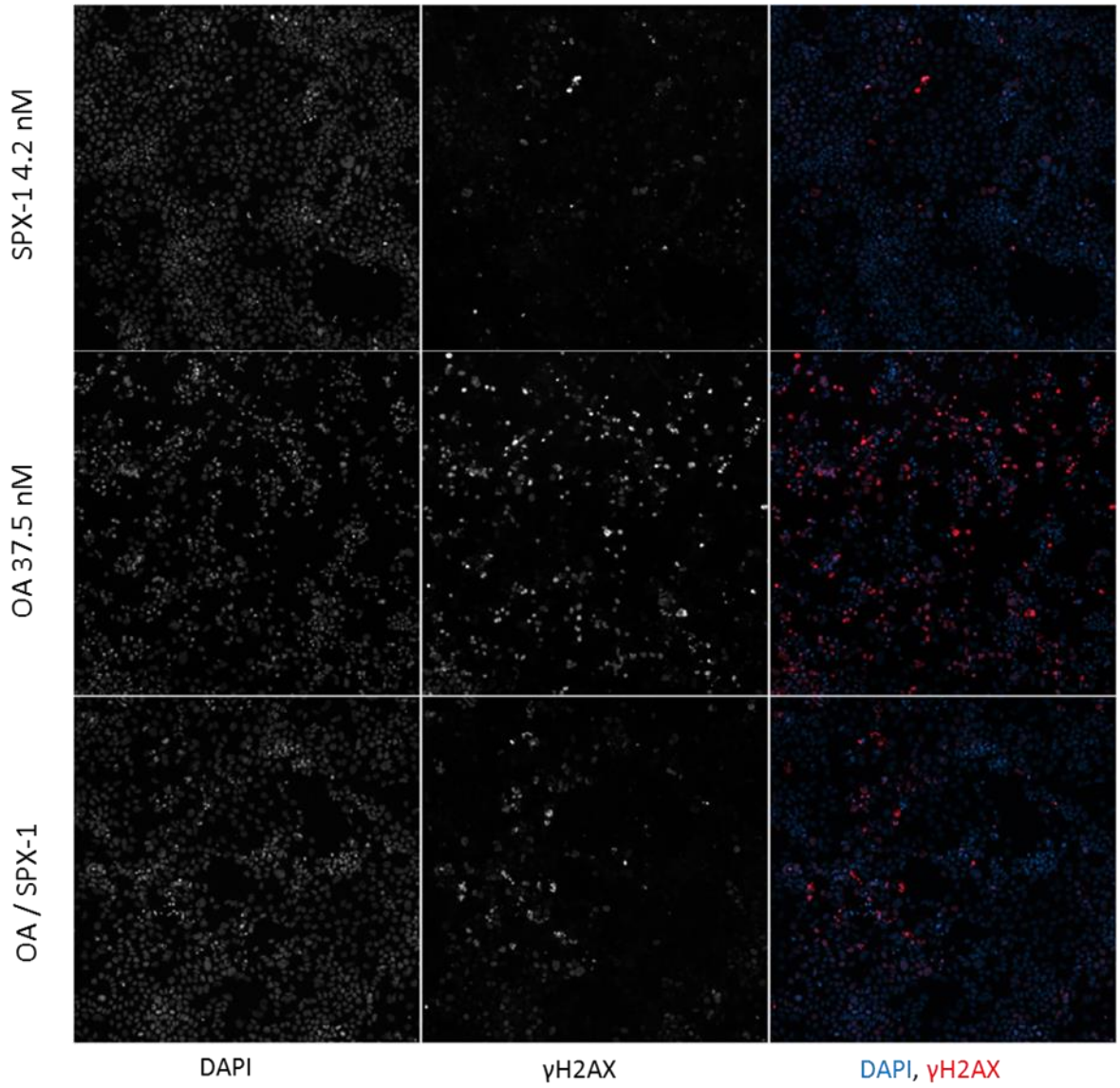

Fig. 4 Representative images (10X magnification) of DNA damage induced by OA and SPX-1 alone and in mixture in differentiated Caco2 cells. Cells were incubated with toxins for 24 h. Cells were labeled with antibodies against γ-H2AX. The nuclei of the cells were stained with DAPI and images were captured with an Arrayscan VTi.

3.3 Toxic effects following OA/YTX mixtures treatment in Caco-2 cells

3.3.1 YTX reduces the cytotoxicity effect of OA in Caco-2 cells at low concentration

YTX was not toxic for Caco-2 cells in our tested range concentration. In mixture conditions, a lower toxicity was depicted for 18.75/6.25 and 37.5/12.5 nM (Fig. 5a).

3.3.2 YTX decreases ROS production and γ-H2AX phosphorylation induced by OA at low concentrations

Whereas YTX failed to induce any toxic effects in Caco-2 cells, YTX decreased the biological effect of OA at conditions A and B on ROS production and phosphorylation of γ-H2AX (Fig. 5b and 5d). This protective mixture effect is remarkably shown in Fig. 6 where the value for γ-H2AX was considerably lowered in mixture condition compared to OA alone. However, when the concentration of YTX was increased, this inhibition effect was not observed.

3.3.3 YTX increases IL-8 release induced by OA at high concentrations

If YTX failed to induce IL-8 release in Caco-2 cells, high concentration of YTX in mixture led to an increase of IL-8 release induced by OA (Fig. 5c).

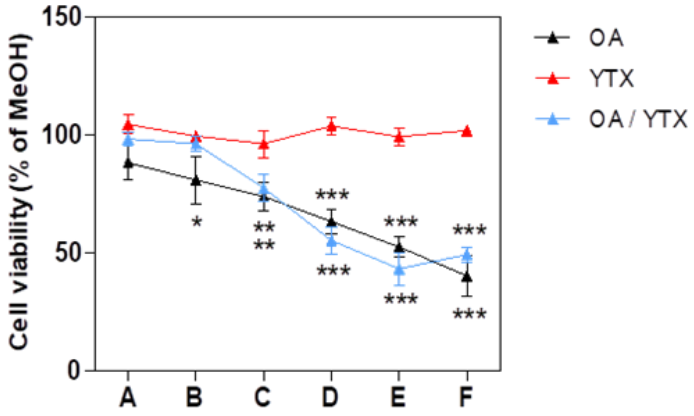

(a)

nM	solo		mixtures
	OA	**YTX**	**OA/YTX**
A	18.75	6.25	18.75/6.25
B	37.5	12.5	37.5/12.5
C	75	25	75/25
D	150	50	150/50
E	300	100	300/100
F	600	200	600/200

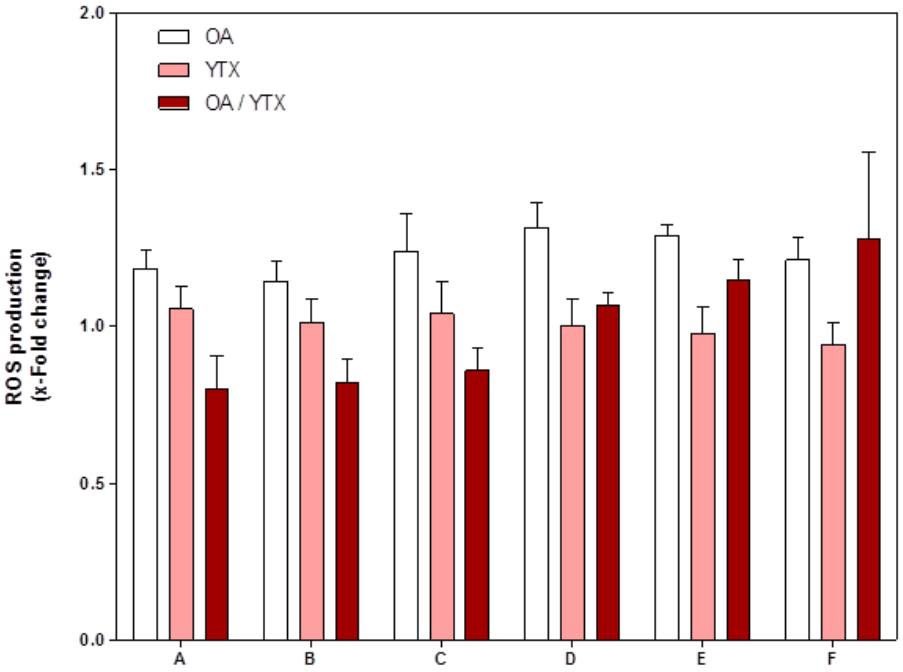
OA
YTX
OA / YTX
ROS production
(x-Fold change)
2.0
1.5
1.0
0.5
0.0
A
B
C
D
E
F

(b)

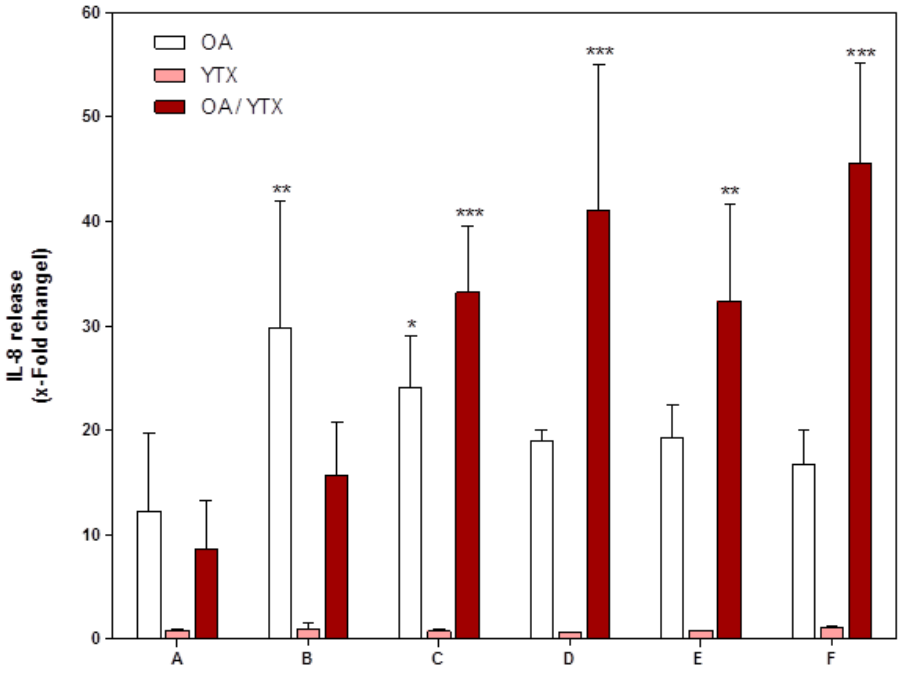
OA
YTX
OA / YTX
IL-8 release
(x-Fold changel)
60
50
40
30
20
10
0
**
*
***
***
**
***
A
B
C
D
E
F

(c)

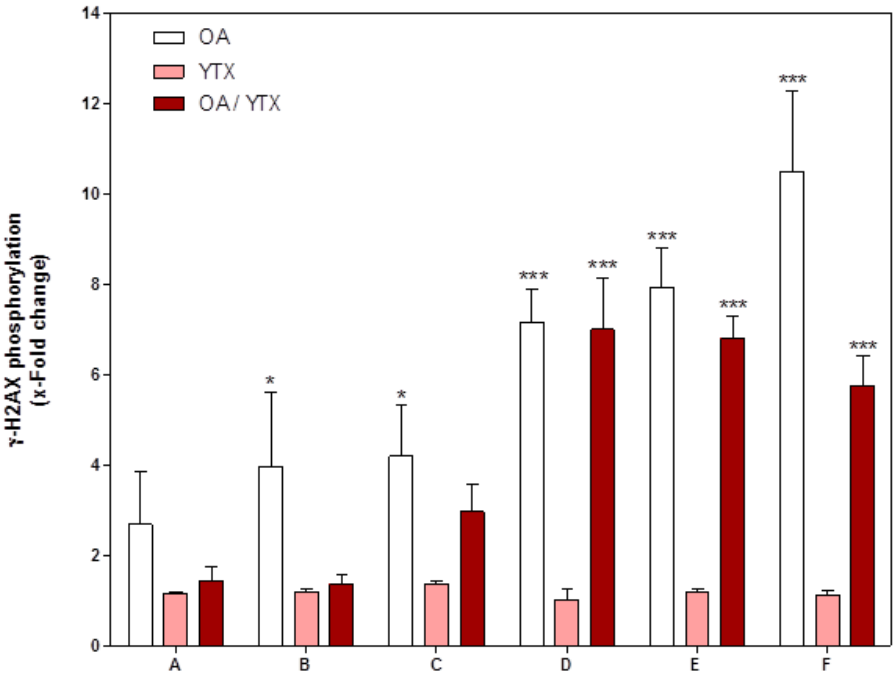

(d)

Fig. 5 Effects of OA/YTX mixtures on a panel of toxicity endpoints in differentiated Caco-2 cells. Cells were pre-treated with ROS probe DCFH-DA (25 µM) for 30 min before incubation with toxins for 24 h. After fluorometric measurement of ROS production, cell media were collected for IL-8 dosage and cells fixed for DAPI and γ-H2AX immunostaining. (a) depicts cell viability, (b) depicts ROS production, (c) depicts IL-8 release and (d) depicts phosphorylation of γ-H2AX. Results were obtained from three independent experiments. Data represents means ± SEM of fold change compared to solvent control (4.1% MeOH/0.3% EtOH). *, **, *** indicate statistical significance between toxin and solvent control respectively ($p < 0.05$, $p < 0.01$, $p < 0.001$ respectively) after two-way ANOVA followed by Bonferroni's post hoc tests.

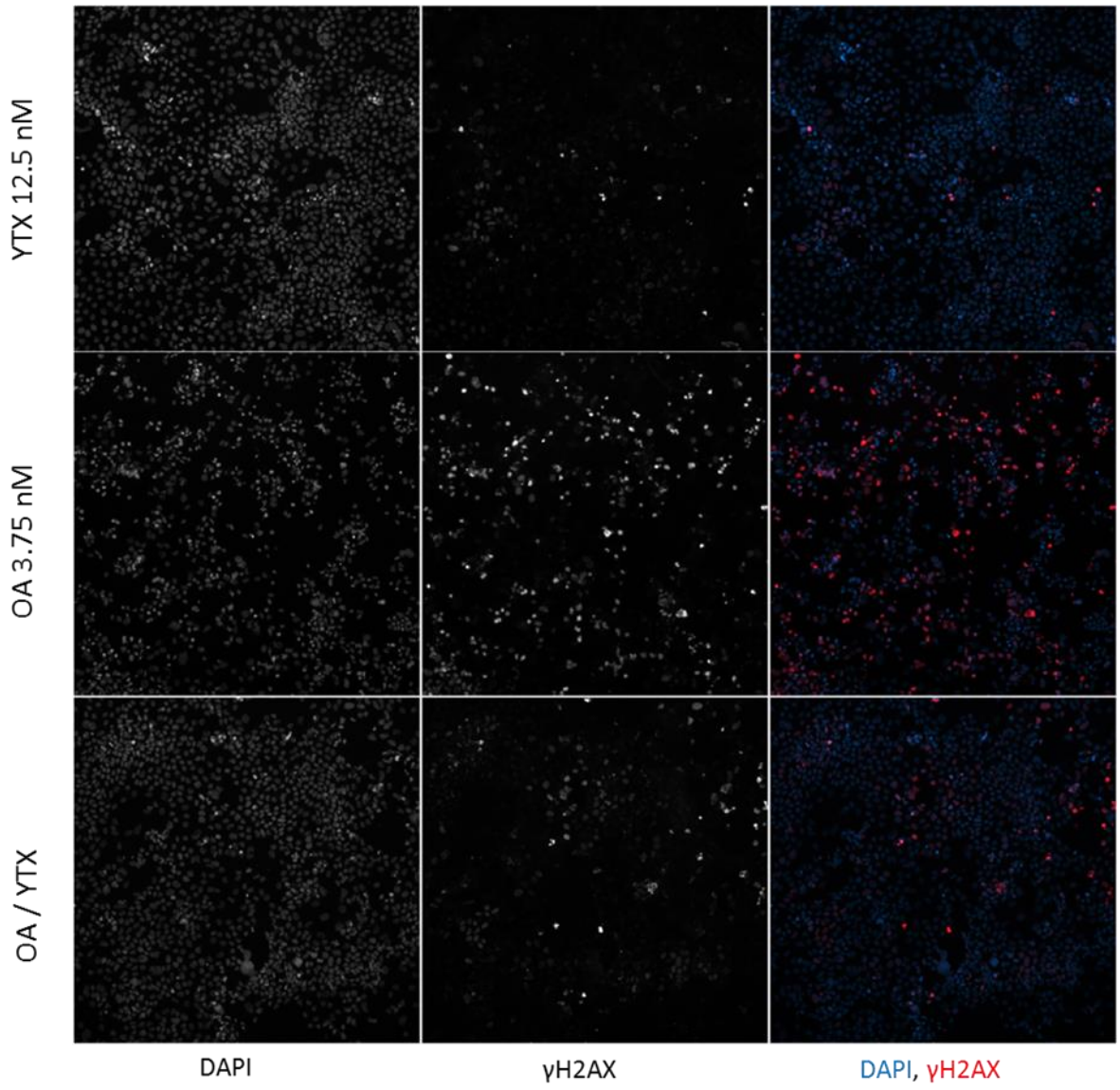

Fig. 6 Representative images (10X magnification) of DNA damage induced by OA and YTX alone and mixture. Cells were incubated with toxins for 24 h. Cells were labeled with antibodies against γ-H2AX. The nuclei of the cells were stained with DAPI and images were captured with an Arrayscan VTi.

3.4 Interactions analysis using theoretical additivity method

The table 1 sums the results of the predictions for OA/PTX-2, OA/SPX-1 and OA/YTX mixtures. Regarding cytotoxicity, OA/PTX-2 mixture showed antagonism at low concentrations and synergism with higher concentrations. ROS measurement depicted antagonism for all concentrations except the two highest where additivity was observed. Antagonism towards IL-8 release was found for low concentrations, followed by additivity for the 75/25 nM and synergism at higher concentrations. For γ-H2AX phosphorylation, antagonism was found for low concentrations, followed by additivity for other concentrations. For OA/SPX-1 mixture, antagonism was observed at low concentrations and rather additivity or synergism for higher concentrations. ROS and γ-H2AX measurements showed antagonism. Antagonism towards IL-8 release was depicted for low concentrations, followed by additivity for the 75/8.3 nM and synergism at higher concentrations. Regarding cytotoxicity and ROS production, OA/YTX mixture showed antagonism at low concentrations and additivity at higher concentrations. Antagonism towards IL-8 release was obtained for low concentrations, followed by a potent synergism at higher concentrations. Data for γ-H2AX phosphorylation showed antagonism.

Table 1 Analysis of OA/PTX-2, OA/SPX-1 and OA/YTX mixtures using theoretical additivity method on a panel of toxicity endpoints in differentiated Caco-2 cells.

		Cytotox	**ROS**	**IL-8**	**γ-H2AX**
OA/PTX-2 (nM)	18.75/6.25	AN	AN	AN	AN
	37.5/12.5	AN	AN	AN	AN
	75/25	SYN	AN	AD	AD
	150/50	SYN	AN	SYN	AD
	300/100	SYN	AD	SYN	AD
	600/200	SYN	AD	SYN	AN
OA/SPX-1 (nM)	18.75/2.1	AN	AN	AN	AN
	37.5/4.2	AN	AN	AN	AN
	75/8.3	AN	AN	AD	AN
	150/16.7	AD	AN	SYN	AN
	300/33.4	SYN	AN	SYN	AN
	600/66.7	AN	AD	SYN	AN
OA/YTX (nM)	18.75/6.25	AN	AN	AN	AN
	37.5/12.5	AN	AN	AN	AN
	75/25	AN	AN	SYN	AN
	150/50	AD	AN	SYN	AD
	300/100	AD	AD	SYN	AN
	600/200	AD	AD	SYN	AN

AD: additivity; AN:antagonism; SYN: synergism

3.5 Interactions analysis using the Chou-Talalay method

In order to run a mixture analysis according to the Chou-Talalay method using CompuSyn software, it is necessary that both toxins alone and mixtures data follow conformity to the mass-action law principle. Among all our data, only one mixture (OA/PTX-2) and two sets (cytotoxicity and DNA damage) featured data suitable for such analysis. The figure 7 depicts CI-Fa plots where the type of interaction according to the fraction affected (x% effect observed) is indicated. The table 2 shows the type of interaction according to the ratio concentration. Towards cytotoxicity, OA/PTX-2 mixture displayed synergism for Fa≥0.35. For Fa<0.35, the type of interaction is not clear since points display both CI> and <1 associated with a large variability for the modelisation (Fig. 7a). The table 1 shows that OA/PTX-2 mixture displayed strong or very strong antagonism for the two low concentrations, and synergism or strong synergism for all other concentrations. Regarding phosphorylation of γ-H2AX, the modelisation showed antagonism for Fa up to 0.7. For higher Fa, the type of interaction is not clear since points display both CI> and <1 associated with a large variability for the modelisation (Fig. 7b). Very strong antagonism for the two low concentrations followed by antagonism, moderate synergism or synergism and strong antagonism for all other concentrations were displayed (Table 1).

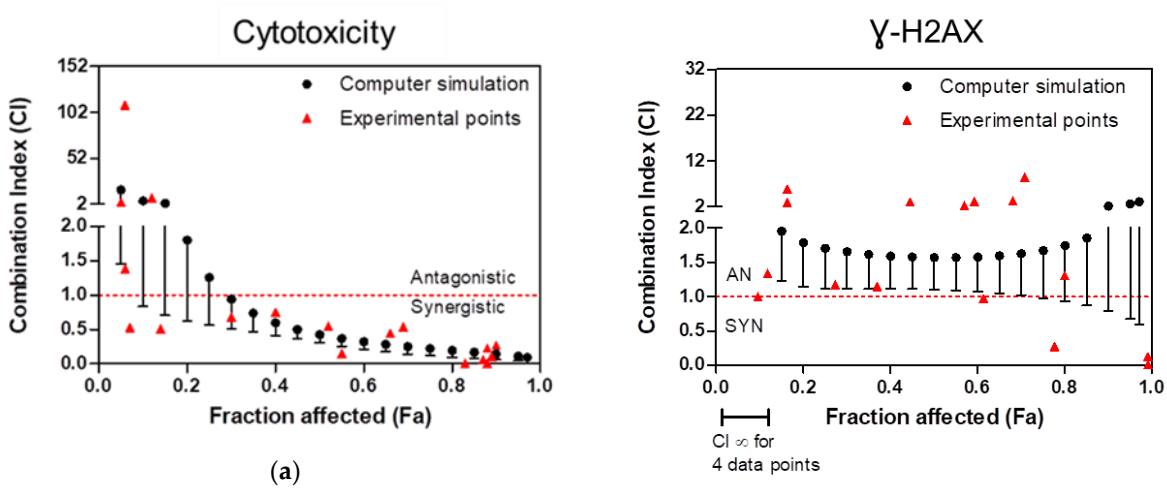

Fig. 7 Analysis of OA/PTX-2 mixtures using the Chou-Talalay method on a panel of toxicity endpoints in differentiated Caco-2 cells. Combination index-Fraction affected (CI-Fa) plots for experimental points and computer simulations are depicted for cytoxicity (a) and phosphorylation of γ-H2AX (b). CI <1, =1 and >1 indicate respectively synergism, additive effect and antagonism. Data represents means ± SEM from three independent experiments.

Table 2 Analysis of OA/PTX-2 mixture using the Chou-Talalay method on a panel of toxicity endpoints in differentiated Caco-2 cells. Combination index according to the concentration ratios are depicted for cytoxicity and phosphorylation of γ-H2AX. CI <1, =1 and >1 indicate respectively synergism, additive effect and antagonism. Data represents means ± SEM from three independent experiments.

OA/PTX-2 (nM)	Cytotoxicity	γ-H2AX
A: 18.75/6.25	3.55 ± 2.6	34.98 ± 33.0
B: 37.5/12.5	38.26 ± 36.0	1883.09 ± 1879.5
C: 75/25	0.53 ± 0.2	1.77 ± 0.6
D: 150/50	0.21 ± 0.2	0.85 ± 0.3
E: 300/100	0.19 ± 0.2	0.77 ± 0.7
F: 600/200	0.39 ± 0.1	4.91 ± 1.7

Very strong antagonism, strong antagonism, antagonism, moderate synergism, synergism, strong synergism

The table 3 sums the results of the characterization of mixtures interaction for OA/PTX-2 combination. Both methods gave similar conclusions except for γ-H2AX where discrepancies were highlighted. For instance, theoretical additivity method described additivity while Chou-Talalay method described antagonism or synergism.

Table 3 Summary of the interactions depicted for OA/PTX-2 mixtures on a panel of toxicity endpoints in differentiated Caco-2 cells. Red colour indicates different effects between the two methods.

OA/PTX-2		Cytotoxicity		γ-H2AX	
	(nM)	TA	CT	TA	CT
A	18.75/6.25	AN	AN	AN	AN
B	37.5/12.5	AN	AN	AN	AN
C	75/25	SYN	SYN	**AD**	**AN**
D	150/50	SYN	SYN	**AD**	**SYN**
E	300/100	SYN	SYN	**AD**	**SYN**
F	600/200	SYN	SYN	AN	AN

TA: theoretical additivity method; CT: Chou-Talalay method; AD: additivity; AN: antagonism; SYN: synergism

4. Discussion (1500 words)

In this study, we investigated the possible effects of binary combinations of lipophilic phycotoxins on a variety of toxicity endpoints in a human intestinal cell model. Based on our review (Alarcan et al., 2018), three main mixtures, all of them featuring OA as the major constituent and reflecting realistic exposure scenarios were tested.

Our study revealed that OA was cytotoxic, induced DNA breaks and triggered release of IL-8 on differentiated Caco-2 cells, similarly to the effects reported on proliferative Caco-2 cells by Ferron et al., (2014). PTX-2 did not affect viability and only induced slightly DNA breaks at the highest concentrations. SPX-1 and YTX did not induce any effect on all tested endpoints. Irrespective of the phycotoxin, no ROS production was detected which may be linked to kinetics as ROS can also occur after a short time of treatment (Belyaeva et al., 2006; Shahraki et al., 2014).

So far, only few studies have been undertaken with phycotoxins mixtures. No combined effects were reported in rodents except in the level of toxins distributed to few internal organs where a reduced uptake was reported (Aasen et al., 2011; Sosa et al., 2013). However, *in vitro* investigation revealed that mixtures of phycotoxins had combined effects in Caco-2 cells (Ferron et al., 2016). Particularly, mixtures of OA and YTX showed a panel of responses from antagonism to additivity depending on the molar ratios towards cell viability (NRU assay). Here, we also reported antagonism or additive effects for mixtures of OA/YTX towars cell viability. More globally, we showed rather antagonistic effects at low concentrations and strong synergistic effects in some cases at higher concentrations. Interestingly, in some cases, mixture effects were different for the same ratio concentration according to the endpoint investigated. For instance, if OA/YTX mixtures were additive regarding cell viability, synergism was shown for IL-8 release and antagonism was depicted for the phosphorylation of γ-H2AX.

Our study revealed that only OA provoked IL-8 release in solo condition. However we observed greater combined effect at high concentrations with OA/YTX mixtures, meaning that YTX may exert potentiation towards OA. Similarly, considering the very low level effect induced by PTX-2 alone, but the combined effect at high concentrations when in mixture with OA, it seems that PTX-2 could potentiate the effects of OA. However, it remains difficult to reach a clear conclusion since currently no mathematical models for testing potentiation exist.

Two different mathematical methods were employed to assess the combined effects of phycotoxins in the mixtures. The theoretical additivity method is an additivity model that allows predictions of additive effects whereas Chou-Talalay method provides a quantitative analysis of drugs interactions. If the theoretical additivity method is easy to handle, fast and applicable to all kind of data, only limited information is provided. The Chou-Talalay method is a powerful tool which offers quantitative definition for additivity and the type of interaction (synergism or antagonism) in chemical mixtures but is not suitable when one drug is not exerting any effect (Chou, 2010). We showed many deviations from the predicted additivity for almost all the combinations and all the endpoints tested, meaning that the phycotoxins tested are able to interact and to modulate their toxic effects. This was confirmed for OA/PTX-2 mixture regarding cytotoxicity as Chou-Talalay analysis revealed antagonistic effects at low concentrations and synergistic effects at high concentrations. Both methods gave similar conclusions but some inconsistencies were highlighted, especially for γ-H2AX. Therefore,

using several mathematical models is highly useful when it comes to mixtures analysis, as suggested by Zhao et al., 2010 or Foucquier and Guedj, 2015.

Surprisingly, irrespective of the toxin, mixtures with OA always resulted at low concentrations in a diminished toxic response. Since PTX-2, YTX and SPX-1 have a different mechanism of action, it is likely that this protective effect resulted from a cellular defense mechanism rather than the disturbance of one OA-specific pathway by the second compound. For instance, OA was previously found to interact with regulatory nuclear receptors such as PXR (Fidler et al., 2012; Ferron et al., 2016) which regulate some specific cytochromes P450 expression (Wang et al., 2012). PTX-2 is believed to interact with AhR since it induced CYP1A in hepatic cells (Alarcan et al., 2017). Moreover, OA, PTX-2 and SPX have been shown to be metabolized through cytochromes P450 (Guo et al., 2010, Kittler et al., 2014, Alarcan et al., 2017, Hui et al., 2012). Therefore, at low concentrations, mixtures might have enhanced CYP and efflux transporters expression, resulting in higher detoxification/excretion of toxins and thus diminishing the toxic effects, as named hormesis effect.

Noteworthy, we pointed out a strong synergistic effect with high concentrations of the OA/PTX-2 mixture towards cytotoxicity. As toxins of the OA group and toxins of the PTX group share a common European regulatory limit, if synergism can be confirmed *in vivo* this may lead to reconsider the established limit.

In this study, we assessed the effects of binary mixtures of lipophilic phycotoxins *in vitro* on human intestinal cells towards multiple toxicity endpoints. Mainly antagonistic effects were depicted at low concentrations and, in few cases, a strong synergism was detected at higher concentrations. The mechanisms involved in the combined effects require further investigation. Our study pointed out that more data on hazard assessment of lipophilic toxins mixtures as well as on co-exposure conditions are required to state if the current EU toxin limits in shellfish are sufficient to protect consumers in case of co-exposure.

Authorship Contributions

Participated in research design: Alarcan, Le Hégarat, Fessard

Conducted experiments: Alarcan, Barbé

Contributed new reagents or analytical tools:

Performed data analysis: Alarcan

Wrote or contributed to the writing of the manuscript: Alarcan, Le Hégarat, Kopp, Hessel-Pras, Lampen and Fessard

References

Aasen JAB, Espenes A, Miles CO, Samdal IA, Hess P, Aune T. Combined oral toxicity of azaspiracid-1 and yessotoxin in female NMRI mice. Toxicon. 2011 May;57(6):909–17.

Alarcan J, Dubreil E, Huguet A, Hurtaud-Pessel D, Hessel-Pras S, Lampen A, Fessard V, Le Hegarat L. Metabolism of the Marine Phycotoxin PTX-2 and Its Effects on Hepatic Xenobiotic Metabolism:

Activation of Nuclear Receptors and Modulation of the Phase I Cytochrome P450. Toxins (Basel). 2017 Jul 5;9(7).

Alassane-Kpembi I., Puel O., Pinton P., Cossalter A.M., Chou T.C., Oswald I.P. Co-exposure to low doses of the food contaminants deoxynivalenol and nivalenol has a synergistic inflammatory effect on intestinal explants. Arch. Toxicol. 2017;91:2677–2687.

Alexander, J., Benford, D., Boobis, A., Ceccatelli, S., Cravedi, J.-P., Di, A., Domenico, D.D., Dogliotti, E., Edler, L., Farmer, P., et al. (2009). Marine biotoxins in shellfish–Summary on regulated marine biotoxins Scientific Opinion of the Panel on Contaminants in the Food Chain. EFSA J 1306, 1–23.

Allingham JS, Miles CO, Rayment I. A Structural Basis for Regulation of Actin Polymerization by Pectenotoxins. J Mol Biol. 2007 Aug;371(4):959–70.

Aráoz R, Ouanounou G, Iorga BI, Goudet A, Alili D, Amar M, et al. The Neurotoxic Effect of 13,19-Didesmethyl and 13-Desmethyl Spirolide C Phycotoxins Is Mainly Mediated by Nicotinic Rather Than Muscarinic Acetylcholine Receptors. Toxicol Sci. 2015 Sep;147(1):156–67.

Belyaeva E.A., Dymkowska D., Wieckowski M.R., Wojtczak L. Reactive oxygen species produced by the mitochondrial respiratory chain are involved in Cd2+-induced injury of rat ascites hepatoma AS-30D cells. Biochim. Biophys. Acta. 2006;1757:1568–1574.

Chou TC. (2006). Theoretical basis, experimental design, and computerized simulation of synergism and antagonism in drug combination studies. Pharmacol Rev 58:621–681.

Chou TC, Talalay P. (1984). Quantitative analysis of dose-effect relationships: the combined effects of multiple drugs or enzyme inhibitors. Adv Enzyme Regul 22:27–55

Fernández-Araujo A, Alfonso A, Vieytes MR, Botana LM. Key role of phosphodiesterase 4A (PDE4A) in autophagy triggered by yessotoxin. Toxicology. 2015 Mar;329:60–72.

Ferron, P.-J., Hogeveen, K., Fessard, V., and Hégarat, L. (2014). Comparative Analysis of the Cytotoxic Effects of Okadaic Acid-Group Toxins on Human Intestinal Cell Lines. Mar. Drugs 12, 4616–4634.

Ferron, P.J., Hogeveen, K., De Sousa, G., Rahmani, R., Dubreil, E., Fessard, V., and Le Hegarat, L. (2016). Modulation of CYP3A4 activity alters the cytotoxicity of lipophilic phycotoxins in human hepatic HepaRG cells. Toxicol. In Vitro 33, 136–146.

Ferron P-J, Dumazeau K, Beaulieu J-F, Le Hégarat L, Fessard V. Combined Effects of Lipophilic Phycotoxins (Okadaic Acid, Azapsiracid-1 and Yessotoxin) on Human Intestinal Cells Models. Toxins. 2016 Feb 19;8(2):50.

Fidler A.E., Holland P.T., Reschly E.J., Ekins S., Krasowski M.D. Activation of a tunicate (Ciona intestinalis) xenobiotic receptor orthologue by both natural toxins and synthetic toxicants. Toxicon. 2012;59:365–372.

Foucquier, J., Guedj, M., 2015. Analysis of drug combinations: current methodological landscape. Pharmacol. Res. Perspect. 3.

Hui JPM, Stuart Grossert J, Cutler MJ, Melanson JE. (2012). Strategic identification of in vitro metabolites of 13-desmethyl spirolide C using liquid chromatography/high-resolution mass spectrometry: Identification of in vitro metabolites of 13-desmethyl spirolide C. Rapid Commun Mass Spectrom. 26(3), 345–54.

Ito, E., Suzuki, T., Oshima, Y., and Yasumoto, T. (2008). Studies of diarrhetic activity on pectenotoxin-6 in the mouse and rat. Toxicon 51, 707–716.

Munday R, Quilliam MA, LeBlanc P, Lewis N, Gallant P, Sperker SA, et al. Investigations into the Toxicology of Spirolides, a Group of Marine Phycotoxins. Toxins. 2011 Dec 30;4(12):1–14.

Rodríguez L, González V, Martínez A, Paz B, Lago J, Cordeiro V, et al. Occurrence of Lipophilic Marine Toxins in Shellfish from Galicia (NW of Spain) and Synergies among Them. Mar Drugs. 2015 Mar 25;13(4):1666–87.

Jafar Shahraki, Abbasali Motallebi, Iman Barekati, Enayatollah Seydi & Jalal Pourahmad (2014) Comparison of cellular and molecular cytotoxic mechanisms of Cochlodinium polykrikoides in isolated trout and rat hepatocytes, Toxicological & Environmental Chemistry, 96:6, 917-930.

Sosa S, Ardizzone M, Beltramo D, Vita F, Dell'Ovo V, Barreras A, et al. Repeated oral co-exposure to yessotoxin and okadaic acid: A short term toxicity study in mice. Toxicon. 2013 Dec;76:94–102.

Takai, A., Murata, M., Torigoe, K., Isobe, M., Mieskes, G., and Yasumoto, T. (1992). Inhibitory effect of okadaic acid derivatives on protein phosphatases. A study on structure-affinity relationship. Biochem. J. 284 (Pt 2), 539–544.

Tubaro A, Dell'Ovo V, Sosa S, Florio C. Yessotoxins: A toxicological overview. Toxicon. 2010 Aug;56(2):163–72.

Valdiglesias, V., Prego-Faraldo, M.V., Pásaro, E., Méndez, J., and Laffon, B. (2013). Okadaic acid: more than a diarrheic toxin. Mar. Drugs 11, 4328–4349.

Visciano P., Schirone M., Berti M., Milandri A., Tofalo R., Suzzi G. (2016). Marine biotoxins: occurrence, toxicity, regulatory limits and reference methods. Front. Microbiol. 7:1051.

Wang Y.M., Ong S.S., Chai S.C., Chen T. Role of CAR and PXR in xenobiotic sensing and metabolism. Expert Opin. Drug Metab. Toxicol. 2012;8:803–817.

Weber, F.; Freudinger, R.; Schwerdt, G.; Gekle, M. A rapid screening method to test apoptotic synergisms of ochratoxin A with other nephrotoxic substances. Toxicol. In Vitro 2005, 19, 135–143.

Zhao L, Au JL, Wientjes MG. Comparison of methods for evaluating drug-drug interaction. Front Biosci (Elite Ed) 2010;2:241–249.

Final summary

Table 17: Summary of results

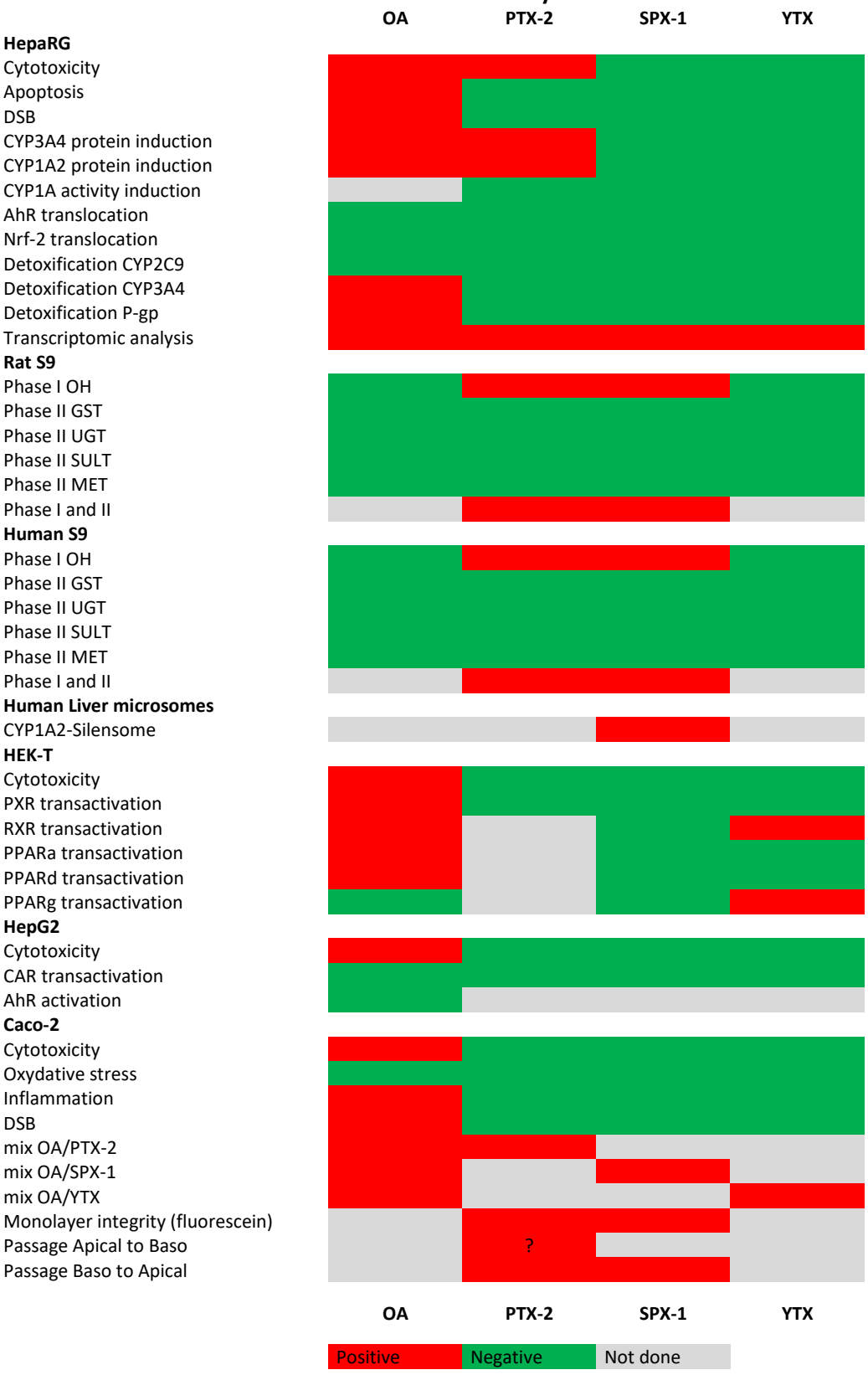

Discussion

The purposes of this PhD project were to bring further knowledge on the ADME of some key lipophilic toxins as well as to investigate their mixture effects focalizing on *in vitro* studies with human small intestine and liver cell models. The main goals were to:

- Assess the intestinal passage of lipophilic phycotoxins through Caco-2 monolayers,
- Assess the metabolism of lipophilic phycotoxins using liver fractions and HRMS method,
- Decipher the metabolic pathways involved in lipophilic phycotoxins biotransformation,
- Investigate the molecular modes of action by q-PCR approach and transactivation assay,
- Assess possible mixture effects using a panel of *in vitro* toxicity endpoints on intestinal cells.

Assessment of the intestinal passage of lipophilic phycotoxins through Caco-2 monolayers

Since data on OA intestinal absorption were already available (Ehlers et al., 2010, Ehlers et al., 2014), we focused our investigation on PTX-2, SPX-1 and YTX. We examined PTX-2 passage and SPX-1 efflux using monolayers of Caco-2 cells. PTX-2 showed a low passage across the intestinal barrier *in vitro* model and we suggested that PTX2 may be prone to an extensive metabolism inside the intestinal cells. This hypothesis needs to be confirmed. For instance, screening the metabolites in the two compartments using high-resolution mass spectrometry would help to clarify if any metabolism had occurred. Espiña et al. (2011) solely investigated the apical to basolateral passage of SPX-1 and demonstrated a high permeability predicting a human absorption superior to 80%. We showed when SPX-1 was loaded on the basolateral side that it also crossed the intestinal barrier to a large extent, meaning that part of the toxin would not enter the circulatory system and could be excreted back to the intestinal lumen. Interestingly, SPX-1 efflux was not time dependent as a state of equilibrium was reached after 3 h, indicating probably a passive mechanism. Unfortunately, YTX passage could not be investigated due to binding issues to the membrane of the Transwell.

Further investigations are needed to characterize deeper the *in vitro* passage of lipophilic phycotoxins, especially the involvement of active transporters. Several strategies are commonly used to investigate the functional involvement of transporters. The assessment of a specific transporter can be done whether by the use of chemical inhibitors (for instance verapamil to inhibit P-gp) or by the use of transfected cell lines that overexpress or are knock-down for one transporter. Using MDCK-II cell monolayers overexpressing P-gp, Ehlers et al., 2014 showed a P-gp-mediated efflux of OA. To circumvent possible analytical issues when dosing toxins with MS, the use of specific fluorescent substrates (for instance rhodamine 123 that is substrate for P-gp) can be a good alternative.

It is noteworthy that, so far, no intestinal cell line expressing a relevant full set of Phase 0, I, II and III exists and that the bioavailability of a drug can not easily be established *in vitro*. The Caco-2 cells, considered as a model of interest, are poorly expressing CYP compared to human enterocytes. In fact, a xenobiotic is likely to undergo biotransformation even before reaching the liver. Therefore, as intestinal metabolism is fully part of the xenobiotic metabolism, it is necessary to develop metabolically competent intestinal models.

Establishing new models that are more closely mimicking the physiological state of cells is also a further step towards more predictive models. Co-cultures of cell lines are an easy way to mimic the diversity of a cell population *in vivo*. In the case of the intestinal barrier, a co-culture of Caco-2/HT29 has been established (Béduneau et al., 2014). Other models such as 3D intestinal tissues and organoids are also promising tools.

Assessment of the metabolism of lipophilic phycotoxins using liver fractions and HRMS method

In order to investigate lipophilic phycotoxins metabolism, we first established a HRMS method allowing the quantification of the parent toxin as well as the screening of metabolites using the Metworks software. We validated our experimental incubation conditions with positive controls for the different reactions, ie hydroxylation, sulfation, glucuronidation, GSH conjugation. Using human and rat S9, we showed that PTX-2 was approximately half biotransformated and several hydroxylated metabolites previously described (Kittler et al., 2010) were detected. Regarding SPX-1, our results indicate that the toxin was metabolized almost completely with both rat and human S9. A mixture of different metabolites was detected, most of them similar to those described by Hui et al., 2012. YTX metabolism assessment was hampered due to analytical issues. Indeed, even when incubating YTX with inactivated S9, we barely detected it. Protein binding may be involved since 100 ng/ml YTX in BSA gave a signal level approximately equal to the one for 10 ng/ml YTX calibration standard.

Compared to Phase I, the role of Phase II conjugation reactions in the metabolism of lipophilic phycotoxins has not been much investigated. Therefore, we screened some main transferases reactions, ie glucuronidation, sulfation, GSH conjugation and methylation. No phase II metabolites were detected through our investigations but these transferases reactions were undertaken only with the parent compounds. Since we reported Phase I metabolites, mainly hydroxylated metabolites, possible conjugation following Phase I metabolism was assessed. For this purpose, screening of Phase I and II reactions were performed simultaneously after adding all the co-factors (for Phase I and Phase II enzymes) within the same incubation. Nevertheless, we did not detect any conjugated metabolite. Besides, it may not be the most appropriate way since our positive control, coumarin, was indeed hydroxylated but then failed to be glucuronidated as reported in humans (Egan et al., 1990). It could be more suitable to perform the reactions successively: Phase I metabolic conditions prior to transferring the supernatant (containing the Phase I metabolites) in Phase II metabolic conditions. The use of external metabolic activation systems such as S9 or HLM fractions proved to be appropriate to produce phase I metabolites.

Once having detected metabolites, the following step is their structural elucidation. This part was not investigated during this PhD project since no new metabolite was discovered. Two strategies are often employed: nuclear magnetic resonance (NMR) or fragmentation assays using MS. The quantification of the metabolites is also a key point but unfortunately, we cannot address this issue since no standards for metabolites are available. Indirect ways of measurement may be an alternative. For instance, the development of biotin-antibody specific of one metabolite would allow estimating the quantity of the metabolite expressed as equivalent of OPD substrate.

Investigating the biological activity of the metabolites is a requisite to determine if metabolism leads to detoxification or bioactivation. In the case of phycotoxins, it was demonstrated that hydroxylated metabolites of OA kept some inhibitory activity against PP2A (Guo et al., 2010), meaning that they

are likely to remain toxic. For SPX-1 metabolites, our results showed a decrease in the overall affinity towards nicotinic receptors compared to SPX-1. For PTX-2, although we detected several metabolites, we did not investigate if they were less toxic. It will be fruitful to verify if metabolism detoxifies or not PTX-2.

Deciphering which metabolic pathways are involved in the biotransformation of lipophilic phycotoxins

We first used XME inhibitors to see if a higher toxicity could be observed in hepatic cells. Using different CYP3A4 inhibitors (ketoconazole, azamulin), we showed an increase of toxicity only for OA. However, this approach was not appropriate in the case of the other tested lipophilic phycotoxins (PTX-2, SPX-1 and YTX) since they failed to induce any toxicity in hepatic cells. Therefore, it is not possible to detect any shift in toxicity due to biotransformation when the parent compounds are not toxic. Besides, another drawback of the use of XME inhibitors is that they are rarely very specific to one single target of the metabolism. For instance, ketoconazole, a well-known inhibitor of CYP3A4, has been also shown to partially inhibit P-gp, making it difficult to fully establish which pathways are involved and to which extent. If the role of CYP3A4 in the detoxification of OA was previously demonstrated (Kittler et al., 2014, Ferron et al., 2016) and confirmed in our studies, we also raised the question concerning the role of P-gp in OA toxicity. Transfected cell lines overexpressing or knock-down for one specific metabolism-associated protein are certainly a good complementary approach to XME inhibitors. The development of the new tool CRISPR/Cas9 is very promising and may become the gold standard for genome editing in the next years. Small interfering RNA (siRNA) has also proven efficiency to target one particular enzyme (Ehlers et al., 2014). Apart from the use of XME inhibitors, we tried a new *in vitro* Silensomes™ tool to investigate the CYP1A2 pathway. We demonstrated the role of the CYP1A2 in SPX-1 biotransformation and we estimated its implication up to approximately 50%. Undertaking proper CYP phenotyping assessment was unfortunately not possible due to the large amount of toxin required but Silensomes™ are available for the nine main CYP (1A2, 2A6, 2B6, 2C8, 2C9, 2C19, 2D6, 2E1, 3A4) which makes it possible to perform an advanced CYP phenotyping.

Investigation of the molecular modes of action of phycotoxins by q-PCR approach and transactivation assay

We investigated the modes of action of some phycotoxins on the liver using the HepaRG cells through a targeted transcriptomic analysis on a panel of metabolism-associated genes. Additionally to xenobiotic metabolism genes such as nuclear receptors, Phase I CYP, Phase II transferases, and transporters, we also analysed genes involved in oxidative stress, inflammation and autophagy. The positive controls OME and RIF greatly up-regulated *CYP1A* and *CYP3A4*, respectively.

Whereas PTX-2 mostly up-regulated the gene expression of *CYP1A1* and *CYP1A2*, no induction of these two CYP activities was further observed although an increase in protein level was shown by western blot and immunolabeling. The mRNA induction may be too weak to provoke an increase of enzymatic activity. Besides, the EROD assay may be not sensitive enough to reveal slight increases in fluorescence. Detection of enzymatic acitivy using key substrates and mass spectrometry could be a

good alternative to increase the sentitivity. For instance, CYP cocktail methods using the CYP1A2 specific substrate phenacetin have been established. Considering the regulation mechanism of XMEs, we also investigated the possible activation of nuclear receptors. PTX-2 did not act as an agonist of CAR or PXR. Regarding AhR, unfortunately, our model was biased by PTX-2 and therefore no conclusion could be drawn. Nonetheless, knowing the regulation of CYP1A, it is very likely that PTX-2 interferes with AhR.

Our results show that OA has an impact on the expression of many of the selected genes. The expression of metabolism genes was globally down-regulated whereas an up-regulation for inflammation genes expression was observed. Particularly *SLCO1A2*, *CYP3A4*, *SULT1A1*, *SULT1E1* and *UGT2B4* were strongly down-regulated while a strong up-regulation of *COX2*, *IL6* and *IL8* was observed. It is noticeable that *ABCB1* and *ABCG2* were slightly up-regulated. Data on oxidative stress shows a strong up-regulation for *HMOX1* whereas *CAT* was down-regulated. Considering the impact on metabolism genes, we further investigated the effects of OA on the activation of nuclear receptors. OA was found to inhibit PXR and RXRα transactivation, consistently with the down-regulation of the *CYP3A4* expression that is under the control of PXR. Nonetheless, since inflammation is known to induce a decrease in drug metabolism and as we reported strong up-regulations for some key cytokines genes, we investigated whether inflammation can play a role in the OA-mediated inhibition of PXR and RXRα transactivation. Using inflammation inhibitors, we did not show undisputed evidence for a role of OA-mediated inflammation in the inhibition of PXR or RXRα transactivation but the hypothesis driven from this preliminary assessment would require deeper investigation. Before assessing such mechanism-based hypothesis, it could be judicious to verify that OA treatment decrease CYP activities.

Data for SPX-1 shows little impact on the tested genes. Only an up-regulation of *CYP1A2* was noticeable but mRNA induction was not correlated at the protein level (immunolabeling and EROD assay). Besides, SPX-1 had no effect on the transactivation of nuclear receptors. Based on our results, we can conclude that SPX-1 is unlikely to interfere with the xenobiotic metabolism process. Assessing genes in relation to SPX-1 mechanism of action may bring more knowledge on its molecular modes of action.

Finally, our results indicated that YTX modulates the expression of many genes. The expression of metabolism genes was globally down-regulated whereas an up-regulation for inflammation genes expression was observed. Particularly, *NR1I2*, *CYP2C9*, *SULT1E1* and *UGT2B4* were strongly down-regulated while a strong up regulation of *COX2*, *IL6* and *IL8* was observed. Data on oxidative stress and autophagy shows both up and down regulation of some target genes. These findings need to be confirmed using for instance western blotting assay.

Assessment of possible mixture effects on a panel of toxicity endpoints in intestinal cells

We assessed the effects of mixtures of lipophilic phycotoxins on intestinal Caco-2 cells towards multiple toxicity endpoints. Three binary mixtures based on co-exposure data published in the literature were investigated: OA/PTX-2, OA/SPX-1 and OA/YTX. Our assays revealed that OA was cytotoxic, induced DNA breaks and triggered IL-8 release. PTX-2 only induced slightly DNA breaks at the highest concentrations, whereas SPX-1 and YTX showed a negative response for all endpoints.

We showed antagonistic effects at low concentrations, irrespective of the toxin, and strong synergistic effects in some cases at higher concentrations. Assessment of *in vivo* toxicity is required to confirm if this strong synergism can be detected in rodents. So far, *in vivo* studies on mixtures did not report any combined effects on mortality or pathological changes of internal organs (Aasen et al., 2011, Aune et al., 2012, Sosa et al., 2013). However, the distribution of toxins when mixtures were administrated was modified, leading to a higher elimination rate (Aasen et al., 2011, Aune et al., 2012). Therefore, it would be interesting to assess if mixtures could have an impact on the detoxification process.

There are lacking data on phycotoxins mixtures. On one side, the establishment of the mixtures (composition and ratio) appears the first concern. The work done with our literature review needs to be completed and pursued. In regard to the European situation, each country carries out a national program for phycotoxins monitoring in shellfish. It would be of interest that the EFSA establishes which mixtures are found based on the data provided by each European country. On the other side, the toxicity pathways should be investigated more deeply. If the toxic effects of some phycotoxins such as OA have been largely studied, others have been less characterized (yessotoxin for instance). *In vivo* studies dealing with mixtures highlighted that detoxification process could be an endpoint of interest. It was previously found that OA interacts with regulatory nuclear receptors such as PXR (Fidler et al., 2012; Ferron et al., 2016) and we showed in this work that PTX-2 probably interacts with AhR since it induced CYP1A in hepatic cells (Alarcan et al., 2017). Therefore, the assessment of how and to which extent the ADME of phycotoxins in mixtures are modulated seems a relevant axis for future research. Apart from effects on the metabolism, toxicity endpoints other than those we investigated will also complement the toxicological data on mixtures of lipophilic phycotoxins.

A high number of different approaches has been described to predict combined effects of a mixture (Foucquier and Guedj 2015). If antagonism and synergism are well-established concepts, however there is no consensus on the definition of additivity (Foucquier and Guedj, 2015). This lack of agreement results in a wide variety of proposed models. Besides, most models are designed for mixtures where each component is exerting an effect. Thus, in the case of binary mixtures where one compound fails to exert an effect, the prediction of mixture effect is difficult to establish. As proposed by Foucquier and Guedj (2015), the use of multiple approaches for the analysis of mixtures is a valuable option.

Conclusion

Although the acute risk related to the presence of phycotoxins in shellfish seems well controlled, several gaps still remain concerning emerging phycotoxins, phycotoxin analogues, phycotoxins with no regulatory limits while being very potent *in vivo*, mixtures, etc.

New *in vitro* models for toxicity investigation have emerged. Closer to the physiological state of cells inside the organ than the classical two-dimension cell cultures, they are expected to be even more predictive for toxicity assessment. Three-dimension cell culturing is a promising area with for instance spheroids and organoids depicting structural characteristics close to human organs. Co-cultures of cell lines are also an easy way to mimic the diversity of a cell population *in vivo*. The use of these innovative models would be helpful in the context of lipophilic phycotoxins. Indeed, these toxins induce potent effects on the GI tract but the the molecular pathways involved are not clearly elucidated. Such *in vitro* systems would certainly help in understanding the underlying mechanisms and establishing adverse outcome pathways (AOP) for lipophilic phycotoxins.

Our knowledge on the toxicokinetics of phycotoxins is still to be improved. *In vivo* assays are money-consuming and require a high amount of toxins, making it a limited approach. Moreover, the EFSA encourages the reduction of animal testing (the 3Rs principle – replacement, reduction and refinement). A combination of physiologically-based pharmacokinetic (PBPK) modeling and engineered advanced systems such as microfluidic organs-on-chips seems to be a good compromise.

Considering the role of the xenobiotic metabolism in the regulation of lipophilic phycotoxins behavior inside the human body, new methodological tools should be developed to investigate the amount of metabolites and their activity. HPLC biogram methodology is a powerful strategy used in pharmaceutical drug discovery programs. It allows the determination of the biological activity of each component inside a sample by combining HPLC and a functional bioassay in an automated process. Adapting such methodology to the lipophilic phycotoxins context would allow screening metabolites activity.

Risk assessment of phycotoxins mixtures needs to be pursued through deeper toxicity investigation. Using high-content screening is a convenient way to assess simultaneously multiple endpoints. It would help selecting only the combinations that display the most harmful effects and that require to be further assessed in *in vivo* studies.

Shellfish are not only exposed to lipophilic phycotoxins but to a wide variety of other contaminants such as heavy metals, dioxins, polychlorinated biphenyls (PCB) or polycyclic aromatic hydrocarbons (PAH). Assessing the effects of such complex mixtures may be ahead of time for the moment, but it should be reminded that shellfish matrices are not only accumulating marine biotoxins.

Bibliography

Aasen JAB, Espenes A, Miles CO, Samdal IA, Hess P, Aune T. Combined oral toxicity of azaspiracid-1 and yessotoxin in female NMRI mice. Toxicon. 2011 May;57(6):909–17.

Abdel-Misih SR, Bloomston M. Liver anatomy. Surg. Clin. North. Am. 2010;90:643–653.

Aimova, D.; Svobodova, L.; Kotrbova, V.; Mrazova, B.; Hodek, P.; Hudecek, J.; Václavíková, R.; Frei, E.; Stiborová, M. The Anticancer Drug Ellipticine Is a Potent Inducer of Rat Cytochromes P450 1A1 and 1A2, Thereby Modulating Its Own Metabolism. Drug Metab. Dispos. 2007, 35, 1926–1934.

Ajani P, Harwood D, Murray S. Recent Trends in Marine Phycotoxins from Australian Coastal Waters. Mar Drugs. 2017 Feb 9;15(2):33.

Alarcan J, Dubreil E, Huguet A, Hurtaud-Pessel D, Hessel-Pras S, Lampen A, Fessard V, Le Hegarat L. Metabolism of the Marine Phycotoxin PTX-2 and Its Effects on Hepatic Xenobiotic Metabolism: Activation of Nuclear Receptors and Modulation of the Phase I Cytochrome P450. Toxins (Basel). 2017 Jul 5;9(7).

Albano E, Rundgren M, Harvison PJ, Nelson SD, Moldéus P. (1985) Mechanisms of N-acetyl-p-benzoquinone imine cytotoxicity. Mol Pharmacol 28:306–311.

Alexander, J., Benford, D., Boobis, A., Ceccatelli, S., Cravedi, J.-P., Di, A., Domenico, D.D., Dogliotti, E., Edler, L., Farmer, P., et al. (2009). Marine biotoxins in shellfish–Summary on regulated marine biotoxins Scientific Opinion of the Panel on Contaminants in the Food Chain. EFSA J 1306, 1–23.

Alfonso, A.; de la Rosa, L.A.; Vieytes, M.R.; Yasumoto, T.; Botana, L.M. Yessotoxin a novel phycotoxin, activates phosphodiesterase activity. Effect of yessotoxin on cAMP levels in human lymphocytes. Biochem. Pharmacol. 2003, 65, 193–208.

Alfonso, C.; Alfonso, A.; Vieytes, M.R.; Yasumoto, T.; Botana, L.M. Quantification of yessotoxin using the fluorescence polarization technique, and study of the adequate extraccion procedure. Anal. Biochem. 2005, 344, 266–274.

Alfonso A, Vieytes MR, Botana LM. Yessotoxin, a Promising Therapeutic Tool. Mar Drugs. 2016;14(2).

Allingham JS, Miles CO, Rayment I. A Structural Basis for Regulation of Actin Polymerization by Pectenotoxins. J Mol Biol. 2007 Aug;371(4):959–70.

Álvarez G, Uribe E, Ávalos P, Mariño C, Blanco J. First identification of azaspiracid and spirolides in Mesodesma donacium and Mulinia edulis from Northern Chile. Toxicon. 2010 Feb;55(2–3):638–41.

Alves-de-Souza, C., Varela, D., Contreras, C., de La Iglesia, P., Fernández, P., Hipp, B., Hernández, C., Riobó, P., Reguera, B., Franco, J.M., Diogène, J., García, C., Lagos, N., 2014. Seasonal variability of Dinophysis spp. and Protoceratium reticulatum associated to lipophilic shellfish toxins in a strongly stratified Chilean fjord. Deep-Sea Research Part II: Topical Studies in Oceanography 101, 152-162.

Amphoux A, Vialou V, Drescher E, et al. (2006). Differential pharmacological in vitro properties of organic cation transporters and regional distribution in rat brain. Neuropharmacology. 50, 941–952.

Amzil Z, Sibat M, Royer F, Masson N, Abadie E. (2007). Report on the first detection of pectenotoxin-2, spirolide-A and their derivatives in French shellfish. Mar Drugs. 5(4), 168–179.

Amzil Z, Sibat M, Royer F, Savar V. First report on azaspiracid and yessotoxin groups detection in French shellfish. Toxicon. 2008 Jul;52(1):39–48.

An, T., Winshell, J., Scorzetti, G., Fell, J.W., and Rein, K.S. (2010). Identification of okadaic acid production in the marine dinoflagellate Prorocentrum rhathymum from Florida Bay. Toxicon 55, 653–657.

Anderson JM, Van Itallie CM (2009) Physiology and function of the tight junction. Cold Spring Harb Perspect Biol 1: a002584.

Anderson D.M., Cembella A.D., Hallegraeff G.M. Progress in understanding harmful algal blooms: Paradigm shifts and new technologies for research, monitoring, and management. Annu. Rev. Mar. Sci. 2012;4:143–176.

Andersson T.B., Kanebratt K.P., Kenna J.G. The HepaRG cell line: a unique in vitro tool for understanding drug metabolism and toxicology in human. Expert Opin. Drug Metab. Toxicol. 2012;8:909–920.

Antherieu, S., Chesne, C., Li, R., Camus, S., Lahoz, A., Picazo, L., Turpeinen, M., Tolonen, A., Uusitalo, J., Guguen-Guillouzo, C., et al. (2010). Stable Expression, Activity, and Inducibility of Cytochromes P450 in Differentiated HepaRG Cells. Drug Metab. Dispos. 38, 516–525.

Aráoz, R., Ramos, S., Pelissier, F., Guérineau, V., Benoit, E., Vilariño, N., Botana, L.M., Zakarian, A. and Molgó, J. (2012). Coupling the Torpedo microplate-receptor binding assay with mass spectrometry to detect cyclic imine neurotoxins. Anal Chem. 84(23), 10445-10453.

Aráoz R, Ouanounou G, Iorga BI, Goudet A, Alili D, Amar M, et al. (2015). The Neurotoxic Effect of 13,19-Didesmethyl and 13-Desmethyl Spirolide C Phycotoxins Is Mainly Mediated by Nicotinic Rather Than Muscarinic Acetylcholine Receptors. Toxicol Sci. 147(1), 156–67.

Artursson, P., Palm, K., Luthman, K., 2001. Caco-2 monolayers in experimental and theoretical predictions of drug transport. Adv. Drug Del. Rev. 46, 27–43.

Aune, T.; Sorby, R.; Yasumoto, T.; Ramstad, H.; Landsverk, T. Comparison of oral and intraperitoneal toxicity of yessotoxin towards mice. Toxicon 2002, 40, 77–82.

Aune, T., Larsen, S., Aasen, J.A.B., Rehmann, N., Satake, M., and Hess, P. (2007). Relative toxicity of dinophysistoxin-2 (DTX-2) compared with okadaic acid, based on acute intraperitoneal toxicity in mice. Toxicon 49, 1–7.

Aune T., Aasen J.A.B., Miles C.O., Larsen S. Effect of mouse strain and gender on LD50 of yessotoxin. Toxicon. 2008;52:535–540.

Aune T, Espenes A, Aasen JAB, Quilliam MA, Hess P, Larsen S. Study of possible combined toxic effects of azaspiracid-1 and okadaic acid in mice via the oral route. Toxicon. 2012 Oct;60(5):895–906.

Azaspiracids—Toxicological Evaluation, Test Methods and Identification of the Source Organism (ASTOX II). Available online: http://oar.marine.ie/handle/10793/970 (accessed on 19 February 2017).

Bacchiocchi S, Siracusa M, Ruzzi A, Gorbi S, Ercolessi M, Cosentino MA, et al. Two-year study of lipophilic marine toxin profile in mussels of the North-central Adriatic Sea: First report of azaspiracids in Mediterranean seafood. Toxicon. 2015 Dec;108:115–25.

Backlund M, Johansson I, Mkrtchian S, Ingelman-Sundberg M. Signal transduction-mediated activation of the aryl hydrocarbon receptor in rat hepatoma H4IIE cells, J. Biol. Chem. 272 (1997) 31755–31763.

Backlund M, Ingelman-Sundberg M. Regulation of aryl hydrocarbon receptor signal transduction by protein tyrosine kinases, Cell. Signal. 17 (2005) 39–48.

Barnes P. J. Anti-inflammatory actions of glucocorticoids: molecular mechanisms. Clinical Science (London, England) 1998;94(6):557–5722.

Bazin, E.; Mourot, A.; Humpage, A.R.; Fessard, V. Genotoxicity of a freshwater cyanotoxin, cylindrospermopsin, in two human cell lines: Caco-2 and HepaRG. Environ. Mol. Mutagen. 2010, 51, 251–259.

Béduneau, A., Tempesta, C., Fimbel, S., Pellequer, Y., Jannin, V., Demarne, F., and Lamprecht, A. (2014). A tunable Caco-2/HT29-MTX co-culture model mimicking variable permeabilities of the human intestine obtained by an original seeding procedure. Eur. J. Pharm. Biopharm. Off. J. Arbeitsgemeinschaft Pharm. Verfahrenstechnik EV.

Behrens I, Stenberg P, Artursson P, Kissel T. Transport of lipophilic drug molecules in a new mucus-secreting cell culture model based on HT29-MTX cells. Pharm Res. 2001;18:1138–1145.

Beischlag, T.V.; Morales, J.L.; Hollingshead, B.D.; Perdew, G.H. The aryl hydrocarbon receptor complex and the control of gene expression. Crit. Rev. Eukaryot. Gene Expr. 2008, 18, 207–250.

Belyaeva E.A., Dymkowska D., Wieckowski M.R., Wojtczak L. Reactive oxygen species produced by the mitochondrial respiratory chain are involved in Cd2+-induced injury of rat ascites hepatoma AS-30D cells. Biochim. Biophys. Acta. 2006;1757:1568–1574.

Ben Haddouch A, Amanhi R, Amzil Z, Taleb H, Rovillon G-A, Adly F, et al. Lipophilic Toxin Profile in Mytilus galloprovincialis from the North Atlantic Coast of Morocco: LC-MS/MS and Mouse Bioassay Analyses. Int J Sci Res IJSR [Internet]. 2017 [cited 2017 Aug 2];6(2). Available from: http://archimer.ifremer.fr/doc/00372/48342/

Berdalet E., Fleming L.E., Gowen R., Davidson K., Hess P., Backer L.C., Moore S.K., Hoagland P., Enevoldsen H. Marine harmful algal blooms, human health and wellbeing: Challenges and opportunities in the 21st century. J. Mar. Biol. Assoc. UK. 2015;2015.

Berthou, F.; Goasduff, T.; Dreano, Y.; Ménez, J.-F. Caffeine increases its own metabolism through cytochrome P4501A induction in rats. Life Sci. 1998, 57, 541–549.

Berven, G.; Seatre, F.; Halvorson, K.; Seglen, P.O. Effect of diarrhetic shellfish toxin, okadaic acid, on cytoskeletal element, viability and functionality of rat liver and intestinal cells. Toxicon 2001, 39, 349–362.

Bhatia, S.N., and Ingber, D.E. (2014). Microfluidic organs-on-chips. Nat. Biotechnol. 32, 760–772.

Bianchi, C.; Fato, R.; Angelin, A.; Trombetti, F.; Ventrella, V.; Borgatti, A.R.; Fattorusso, E.; Ciminiello, P.; Bernardi, P.; Lenaz, G.; et al. Yessotoxin, a shellfish biotoxin, is a potent inducer of the permeability transition in isolated mitochondria and intact cells. Biochim. Biophys. Acta 2004, 1656, 139–147.

Bialojan, C. and Takai, A., 1988. Inhibitory effect of a marine sponge toxin, okadaic acid, on protein phosphatases. Biochem. J. 256, 283-290.

Biré R, Trotereau S, Lemée R, Oregioni D, Delpont C, Krys S, Guérin T. Hunt for Palytoxins in a Wide Variety of Marine Organisms Harvested in 2010 on the French Mediterranean Coast. Mar Drugs. 2015 Aug 21;13(8):5425-46.

Botana, L. (2008). Seafood and Freshwater Toxins: Pharmacology, Physiology, and Detection, Second Edition.

Bourne, Y., Radic, Z., Aráoz, R., Talley, T. T., Benoit, E., Servent, D., Taylor, P., Molgó, J., and Marchot, P. (2010). Structural determinants in phycotoxins and AChBP conferring high affinity binding and nicotinic AChR antagonism. Proc. Natl. Acad. Sci. USA 107, 6076–6081.

Boyer JL. Bile formation and secretion. Compr Physiol. 2013;3(3):1035–1078.

Brockmoller J, Roots I. Assessment of liver metabolic function. Clinical implications. Clin Pharmacokinet. 1994;27:216–248.

Buratti S, Franzellitti S, Poletti R, Ceredi A, Montanari G, Capuzzo A, et al. Bioaccumulation of algal toxins and changes in physiological parameters in Mediterranean mussels from the North Adriatic Sea (Italy): Effects of Algal Toxins on Marine Mussels. Environ Toxicol. 2013 Aug;28(8):451–70.

Burgess VA, 2003. Toxicology investigation with the Pectenotoxin-2 seco acids. National Research Centre for Environmental Toxicology and the School of Public Health. Brisbane, Queensland, Australia, Griffith University, PhD thesis, February 2003.

Butler, S.C., Miles, C.O., Karim, A., and Twiner, M.J. (2012). Inhibitory effects of pectenotoxins from marine algae on the polymerization of various actin isoforms. Toxicol. In Vitro 26, 493–499.

Cabado, A.G.M.; Leira, F.; Vieytes, M.R.; Vieites, J.M.; Botana, L.M. Cytoskeletal disruption is the key factor that triggers apoptosis in okadaic acid-treated neuroblastoma cells. Arch. Toxicol. 2004, 78, 74–85.

Campbell, K., McNamee, S.E., Huet, A.C., Delahaut, P., Vilarino, N., Botana, L.M., Poli, M., Elliott, C.T., 2014. Evolving to the optoelectronic mouse for phycotoxin analysis in shellfish. Analytical and Bioanalytical Chemistry 406(27), 6867-6881.

Caraco Y, Sheller J, Wood AJ (1996) Pharmacogenetic determination of the effects of codeine and prediction of drug interactions. J Pharmacol Exp Ther 278:1165-1174.

Carvalho, P.-S., Catia, R., Moukha, S., Matias, W.G. and Creppy, E.E., 2006. Comparative Study of Domoic Acid and Okadaic Acid Induced - Chromosomal Abnormalities in the CACO-2 Cell Line. Int. J. Environ. Res. Publich Health. 3(1), 4-10.

Cashman J.R., Zhang J. Human flavin-containing monooxygenases. Annu. Rev. Pharmacol. Toxicol. 2006;46:65–100.

CBI. Market Intelligence. Trade Statistics Fish and Seafood in Europe. 2015.

Cembella, A.D., Lewis, N.I., Quilliam, M.A., (2000). The marine dinoflagellate Alexandriumostenfeldii (Dinophyceae) as the causative organism of spirolide shellfish toxins. Phycologia 39, 67–74.

Chai SC, Cherian MT, Wang YM, Chen T. Small-molecule modulators of PXR and CAR. Biochim. Biophys. Acta. 2016;1859:1141–1154.

Chambers TC, Raynor RL, Kuo JF. Multidrug-resistant human KB carcinoma cells are highly resistant to the protein phosphatase inhibitors okadaic acid and calyculin A. Analysis of potential mechanisms involved in toxin resistance. Int J Cancer. 1993 Jan 21;53(2):323–327.

Chang CK, Llanes S, Schumer W. Effect of dexamethasone on NF-κB activation, tumor necrosis factor formation, and glucose dyshomeostasis in septic rats. J Surg Res. 1997;72:141–145.

Chelikani P, Fita I, Loewen PD. Diversity of structures and properties among catalases. Cell Mol Life Sci. 2004; 61: 192–208.

Chen, Y., Tang, Y., Guo, C., Wang, J., Boral, D., and Nie, D. (2012). Nuclear receptors in the multidrug resistance through the regulation of drug-metabolizing enzymes and drug transporters. Biochem. Pharmacol. 83, 1112–1126.

Chhabra N, Aseri ML, Padmanabhan D. (2013). A review of drug isomerism and its significance. Int J Appl Basic Med Res. 3,16–18.

Choi H.-S., Chung M., Tzameli I., Simha D., Lee Y.-K., Seol W., Moore D.D., Differential transactivation by two isoforms of the orphan nuclear hormone receptor CAR, J. Biol. Chem. 272 (1997) 23565–23571.

Chou TC. (2006). Theoretical basis, experimental design, and computerized simulation of synergism and antagonism in drug combination studies. Pharmacol Rev 58:621–681.

Chou TC, Talalay P. (1984). Quantitative analysis of dose-effect relationships: the combined effects of multiple drugs or enzyme inhibitors. Adv Enzyme Regul 22:27–55

Ciminiello P, Fattorusso E, Forino M, Magno S, Poletti R, Satake M, et al. Yessotoxin in mussels of the northern Adriatic Sea. Toxicon. 1997;35(2):177–183.

Ciminiello, P., Dell'Aversano, C., Fattorusso, E., Forino, M., Magno, S., Guerrini, F., Pistocchi, R., and Boni, L. (2003). Complex yessotoxins profile in Protoceratium reticulatum from north-western Adriatic sea revealed by LC-MS analysis. Toxicon Off. J. Int. Soc. Toxinology 42, 7–14.

Ciminiello P, Dell'Aversano C, Fattorusso E, Forino M, Tartaglione L, Boschetti L, et al. Complex toxin profile of Mytilus galloprovincialis from the Adriatic sea revealed by LC–MS. Toxicon. 2010 Feb;55(2–3):280–8.

Cocucci E, Kim JY, Bai Y, Pabla N. Role of Passive Diffusion, Transporters, and Membrane Trafficking-Mediated Processes in Cellular Drug Transport. Clin Pharmacol Ther. 2017 Jan;101(1):121-129.

Cooper GM, The Cell, 2nd edition A Molecular Approach. Boston University, Sunderland (MA): Sinauer Associates; 2000. ISBN-10: 0-87893-106-6

Crinelli R., Antonelli A., Bianchi M., Gentilini L., Scaramucci S., Magnani M. (2000). Selective inhibition of NF-κB activation and TNF-α production in macrophages by red blood cell-mediated delivery of dexamethasone. Blood Cells Mol. Dis. 26, 211–222.

Cruz, P.G.; Norte, M.; Creus, A.H.; Fernández, J.J.; Daranas, A.H. Self-association of okadaic Acid: Structural and pharmacological significance. Mar. Drugs 2013, 11, 1866–1877.

Čustović S, Orhanović S, Skejić S, Pavela-Vrančič M. The predominant occurrence of YTX in the Eastern-mid Adriatic sea (Vranjic basin, Croatia). Fresenius Environ Bull. 2014;23(12c):3453–3458.

Daly AK. Significance of the minor cytochrome P450 3A isoforms. Clin Pharmacokinet 2006;45:13–31.

Daujat M., Peryt B., Lesca P., Fourtanier G., Domergue J., Maurel P., Omeprazole, an inducer of human CYP1A1 and 1A2, is not a ligand for the Ah receptor, Biochem. Biophys. Res. Commun. 188 (1992) 820–825.

de la Iglesia P, Gago-Martínez A. Determination of yessotoxins and pectenotoxins in shellfish by capillary electrophoresis-electrospray ionization-mass spectrometry. Food Addit Contam Part A. 2009 Feb;26(2):221–8.

De la Rosa, L.A.; Alfonso, A.; Vilariño, N.; Vieytes, M.R.; Botana, L.M. Modulation of cytosolic calcium levels of human lymphocytes by yessotoxin, a novel marine phycotoxin. Biochem. Pharmacol. 2001, 61, 827–833.

De Leeuw A.M., Brouwer A., Knook D.L. Sinusoidal endothelial cells of the liver: Fine structure and function in relation to age. J. Electron. Microsc. Tech. 1990;14:218–236.

Dell'Ovo, V.; Bandi, E.; Coslovich, T.; Florio, C.; Sciancalepore, M.; Decorti, G.; Sosa, S.; Lorenzon, P.; Yasumoto, T.; Tubaro, A. In vitro effects of yessotoxin on a primary culture of rat cardiomyocytes. Toxicol. Sci. 2008, 106, 392–399.

Dickey, R.W., Bobzin, S.C., Faulkner, D.J., Bencsath, F.A., and Andrzejewski, D. (1990). Identification of okadaic acid from a Caribbean dinoflagellate, Prorocentrum concavum. Toxicon 28, 371–377.

di Masi A., De Marinis E., Ascenzi P., Marino M. (2009). Nuclear receptors CAR and PXR: molecular, functional, and biomedical aspects. Mol. Aspects Med. 30 297–343.

Ding X., Staudinger J.L., Induction of drug metabolism by forskolin: the role of the pregnane X receptor and the protein kinase A signal transduction pathway, J. Pharmacol. Exp. Ther. 312 (2005) 849–856.

Ding X., Staudinger J.L., Repression of PXR-mediated induction of hepatic CYP3A gene expression by protein kinase C, Biochem. Pharmacol. 69 (2005) 867–873.

Diogène G, Fessard V, Dubreuil A, Puiseux-Dao S. Comparative studies of the actin cytoskeleton response to maitotoxin and okadaic acid. Toxicol. In Vitro, 9 (1995), pp. 1-10.

Diogène J; Soliño L; Turquet J; Widgy S; Pautonnier A; Loeffler C; Quintana HF; Hossen V; Leroy P; David E; Velge P; Dragacci S; Krys S; Reverté L; Rambla M (2017). Cell based assay and LC-MS/MS for the identification and quantification of ciguatoxins in fish. Application to the risk characterization of ciguatera. Poster. ECsafeSeafood congress held in Belgium.

Dixon L.J., Barnes M., Tang H., Pritchard M.T., Nagy L.E. Kupffer cells in the liver. Compr. Physiol. 2013;3(2):785–797.

Dominguez, H.J., Paz, B., Daranas, A.H., Norte, M., Franco, J.M., and Fernández, J.J. (2010). Dinoflagellate polyether within the yessotoxin, pectenotoxin and okadaic acid toxin groups: Characterization, analysis and human health implications. Toxicon 56, 191–217.

Draisci, R.; Lucentini, L.; Giannetti, L.; Boria, P.; Poletti, R. First report of pectenotoxin-2 (PTX-2) in algae (Dinophysis fortii) related to seafood poisoning in Europe. Toxicon 1996, 34, 923–935.

Draisci, R., Palleschi, L., Giannetti, L., Lucentini, L., James, K.J., Bishop, A.G., Satake, M., Yasumoto, T., 1999. New approach to the direct detection of known and new diarrhoeic shellfish toxins in mussels and phytoplankton by liquid chromatography-mass spectrometry. Journal of Chromatography A 847(1-2), 213-221.

Draisci R, Ferretti E, Palleschi L, Marchiafava C, Poletti R, Milandri A, Ceredi A, Pompei M. High levels of yessotoxin in mussels and presence of yessotoxin and homoyessotoxin in dinoflagellates of the Adriatic Sea. Toxicon. 1999 Aug;37(8):1187-93.

Dvorak Z. Opportunities and challenges in using human hepatocytes in cytochromes P450 induction assays. Expert Opin Drug Metab Toxicol. 2016; 12: 169–74.

Eberhart B-T, Moore L, Harrington N, Adams N, Borchert J, Trainer V. Screening Tests for the Rapid Detection of Diarrhetic Shellfish Toxins in Washington State. Mar Drugs. 2013 Sep 30;11(10):3718–34.

EFSA Journal (2008a). Marine biotoxins in shellfish – okadaic acid and analogues Scientific Opinion of the Panel on Contaminants in the Food chain. 589–,1–62.

EFSA Scientific Opinion on marine biotoxins in shellfish- Yessotoxin group. EFSA Panel on Contaminants in the Food Chain (CONTAM) EFSA J. 2008;907:1–62.

EFSA Scientific Opinion on marine biotoxins in shellfish- Pectenotoxin group. EFSA Panel on Contaminants in the Food Chain (CONTAM) EFSA J. 2009;1109:1–47.

EFSA Panel on Contaminants in the Food Chain (CONTAM); Scientific Opinion on marine biotoxins in shellfish – Cyclic imines (spirolides, gymnodimines, pinnatoxins and pteriatoxins). EFSA Journal 2010; 8(6):1628. [39 pp.]. doi:10.2903/j.efsa.2010.1628. Available online: www.efsa.europa.eu

European Food Safety Authority. International Frameworks Dealing with Human Risk Assessment of Combined Exposure to Multiple Chemicals: Combined exposure to multiple chemicals. EFSA J. 2013 Jul;11(7):3313.

Egan, D., O'Kennedy, R., Moran, E., Cox, D., Prosser, E. and Thornes, R.D. "The pharmacology, metabolism, analysis and applications of coumarin and coumarin-related compounds," Drug Metab. Rev., 22, 503-529(1990).

Ehlers A., Scholz J., These A., Hessel S., Preiss-Weigert A., Lampen A. Analysis of the passage of the marine biotoxin okadaic acid through an in vitro human gut barrier. Toxicology. 2011;279:196–202.

Ehlers A, These A, Hessel S, Preiss-Weigert A, Lampen A. Active elimination of the marine biotoxin okadaic acid by P-glycoprotein through an in vitro gastrointestinal barrier. Toxicol Lett. 2014 Mar;225(2):311–7.

Eichelbaum M, Ingelman-Sundberg M, Evans WE (2006) Pharmacogenomics and individualized drug therapy. Annu Rev Med 57:119–137.

Elgarch A, Vale P, Rifai S, Fassouane A. Detection of Diarrheic Shellfish Poisoning and Azaspiracids Toxins in Moroccan Mussels: Comparison of LC-MS Method with the Commercial Immunoassay Kit. Mar Drugs. 2008;6(4):587–594.

El-Kattan Ayman and Varma Manthena (2012). Oral Absorption, Intestinal Metabolism and Human Oral Bioavailability, Topics on Drug Metabolism, Dr. James Paxton (Ed.), InTech, DOI: 10.5772/31087. Available from: https://www.intechopen.com/books/topics-on-drug-metabolism/oral-absorption-intestinal-metabolism-and-human-oral-bioavailability-.

Elsby R, Surry DD, Smith VN, Gray AJ (2008). Validation and application of Caco-2 assays for the in vitro evaluation of development candidate drugs as substrates or inhibitors of P-glycoprotein to support regulatory submissions. Xenobiotica 38: 1140–1164.

Espenes A, Aasen JAB, Miles CO, Rehman N, Hess P, Smith A and Aune T, 2009. Combined oral toxicity of azaspiracid-1 and pectenotoxin-2 in female NMRI mice, manuscript in preparation.

Espina, B.; Louzao, M.C.; Ares, I.R.; Cagide, E.; Vieytes, M.R.; Vega, F.V.; Rubiolo, J.A.; Miles, C.O.; Suzuki, T.; Yasumoto, T.; et al. Cytoskeletal toxicity of pectenotoxins in hepatic cells. Br. J. Pharmacol. 2008, 155, 934–944.

Espiña B, Otero P, Louzao MC, Alfonso A, Botana LM. (2011). 13-Desmethyl spirolide-c and 13,19-didesmethyl spirolide-c trans-epithelial permeabilities: Human intestinal permeability modelling. Toxicology 287(1–3), 69–75.

Fang L, Yao X, Wang L, Li J. Solid-Phase Extraction-Based Ultra-Sensitive Detection of Four Lipophilic Marine Biotoxins in Bivalves by High-Performance Liquid Chromatography-Tandem Mass Spectrometry. J Chromatogr Sci. 2015 Feb 1;53(2):373–9.

FAO /WHO Joint. Technical paper on Toxicity Equivalency Factors for Marine Biotoxins associated with bivalve molluscs. 2016

Fernández L., M., Reguera, B., González-Gil, S., and Míguez, A. (2006). Pectenotoxin-2 in single-cell isolates of Dinophysis caudata and Dinophysis acuta from the Galician Rías (NW Spain). Toxicon 48, 477–490.

Fernandez D.A., Louzao M.C., Fraga M., Vilarino N., Vieytes M.R., Botana L.M. Experimental basis for the high oral toxicity of dinophysistoxin 1: A comparative study of DSP. Toxins. 2014;6:211–228.

Fernández-Araujo A, Tobio A, Alfonso A, Botana LM. Role of AKAP 149-PKA-PDE4A complex in cell survival and cell differentiation processes. Int J Biochem Cell Biol. 2014;53C:89–101.

Fernández-Araujo, A.; Alfonso, A.; Vieytes, M.R.; Botana, L.M. Yessotoxin activates cell death pathways independent of Protein Kinase C in K-562 human leukemic cell line. Toxicol. Vitro 2015, 29, 1545–1554.

Fernández-Araujo A, Alfonso A, Vieytes MR, Botana LM. Key role of phosphodiesterase 4A (PDE4A) in autophagy triggered by yessotoxin. Toxicology. 2015 Mar;329:60–72.

Ferreiro SF, Vilariño N, Carrera C, Louzao MC, Santamarina G, Cantalapiedra AG, Cifuentes JM, Crespo A, Botana LM. In vivo cardiomyocyte response to YTX- and AZA-1-induced damage: autophagy versus apoptosis. Arch Toxicol. 2017 Apr;91(4):1859-1870.

Ferron, P.-J., Hogeveen, K., Fessard, V., and Hégarat, L. (2014). Comparative Analysis of the Cytotoxic Effects of Okadaic Acid-Group Toxins on Human Intestinal Cell Lines. Mar. Drugs 12, 4616–4634.

Ferron, P.J., Hogeveen, K., De Sousa, G., Rahmani, R., Dubreil, E., Fessard, V., and Le Hegarat, L. (2016). Modulation of CYP3A4 activity alters the cytotoxicity of lipophilic phycotoxins in human hepatic HepaRG cells. Toxicol. In vitro 33, 136–146.

Ferron P-J, Dumazeau K, Beaulieu J-F, Le Hégarat L, Fessard V. Combined Effects of Lipophilic Phycotoxins (Okadaic Acid, Azapsiracid-1 and Yessotoxin) on Human Intestinal Cells Models. Toxins. 2016 Feb 19;8(2):50.

Fessard, V.; Grosse, Y.; Pfohl-Leszkowicz, A.; Puiseux-Dao, S. Okadaic acid treatment induces DNA adduct formation in BHK21 C13 fibroblasts and HESV keratinocytes. Mutat. Res. 1996, 361, 133–141.

Fidler A.E., Holland P.T., Reschly E.J., Ekins S., Krasowski M.D. Activation of a tunicate (Ciona intestinalis) xenobiotic receptor orthologue by both natural toxins and synthetic toxicants. Toxicon. 2012;59:365–372.

Fiorentini, C.; Matarrese, P.; Fattorossi, A.; Donelli, G. Okadaic acid induces changes in the organization of F-actin in intestinal cells. Toxicon 1996, 34, 937–945.

Fire, S.E., Wang, Z., Byrd, M., Whitehead, H.R., Paternoster, J., Morton, S.L., 2011. Co-occurrence of multiple classes of harmful algal toxins in bottlenose dolphins (Tursiops truncatus) stranding during an unusual mortality event in Texas, USA. Harmful Algae 10(3), 330-336.

Fletcher DA, Mullins RD. Cell mechanics and the cytoskeleton. Nature. 2010 Jan 28;463(7280):485-92.

Fogh, J., and Trempe, G. (1975). New Human Tumor Cell Lines. In Human Tumor Cells in Vitro, J. Fogh, ed. (Boston, MA: Springer US), pp. 115–159.

Foti R. S., Dalvie D. K. (2016). Cytochrome P450 and non-cytochrome P450 oxidative metabolism: contributions to the pharmacokinetics, safety, and efficacy of xenobiotics. Drug Metab. Dispos. 44, 1229–1245.

Franchini, A.; Marchesini, E.; Poletti, R.; Ottaviani, E. Lethal and sub-lethal yessotoxin dose-induced morpho-functional alterations in intraperitoneal injected Swiss CD1 mice. Toxicon 2004, 44, 83–90.

Franchini, A.; Marchesini, E.; Poletti, R.; Ottaviani, E. Acute toxic effect of the algal yessotoxin on Purkinje cells from the cerebellum of Swiss CD1 mice. Toxicon 2004, 43, 347–352.

Franchini A, Marchesini E, Poletti R, Ottaviania E. Swiss mice CD1 fed on mussels contaminated by okadaic acid and yessotoxins: effects on thymus and spleen. Eur J Histochem EJH. 2005;49(2):179.

Franchini A., Malagoli D., Ottaviani E. Targets and effects of yessotoxin, okadaic acid and palytoxin: A differential review. Mar. Drugs. 2010;8:658–677.

Friedman, M. (2008). Principles and models of biological transport. Springer. ISBN 978-0387-79239-2.

Friedman M.A., Fernandez M., Backer L.C., Dickey R.W., Bernstein J., Schrank K., Kibler S., Stephan W., Gribble M.O., Bienfang P. An updated review of ciguatera fish poisoning: Clinical, epidemiological, environmental and public health management. Mar. Drugs. 2017;15:72.

Fujiki, H.; Suganuma, M.; Suguri, H.; Yoshizawa, S.; Takagi, K.; Uda, N.; Wakamatsu, K.; Yamada, K.; Murata, M.; Yasumoto, T.; et al. Diarrhetic shellfish toxin, dinophysistoxin-1, is a potent tumor promoter on mouse skin. Jpn. J. Cancer Res. 1988, 79, 1089–1093.

Fujiwara R., Yokoi T., Nakajima M. Structure and protein-protein interactions of human UDP-glucuronosyltransferases. Front. Pharmacol. 2016;7:388.

Fux, E.; Rode, D.; Bire, R.; Hess, P. Approaches to the evaluation of matrix effects in the liquid chromatography-mass spectrometry (LC-MS) analysis of three regulated lipophilic toxin groups in mussel matrix (Mytilus edulis). Food Addit. Contam. Part A 2008, 25, 1024–1032.

Fux E, Bire R, Hess P. Comparative accumulation and composition of lipophilic marine biotoxins in passive samplers and in mussels (M. edulis) on the West Coast of Ireland. Harmful Algae. 2009 Feb;8(3):523–37.

Gago-Martinez A, Rodriguez-Vazquez JA, Thibault P, Quilliam MA. Simultaneous occurrence of diarrhetic and paralytic shellfish poisoning toxins in Spanish mussels in 1993. Nat Toxins. 1996;4(2):72–79.

Ganal, C.A., Asahina, A.Y., Hokama, Y., Miyahara, J.T., 1993. Characterization of marine toxin(s) in Myripristis sp. by immunological, mouse toxicity, and guinea pig assays. Journal of Clinical Laboratory Analysis 7(1), 41-45.

Garcia C, Rodriguez-Unda N, Contreras C, Barriga A, Lagos N. Lipophilic toxin profiles detected in farmed and benthic mussels populations from the most relevant production zones in Southern Chile. Food Addit Contam Part A. 2012 Jun;29(6):1011–20.

García C, Pérez F, Contreras C, Figueroa D, Barriga A, López-Rivera A, et al. Saxitoxins and okadaic acid group: accumulation and distribution in invertebrate marine vectors from Southern Chile. Food Addit Contam Part A. 2015 Jun 3;32(6):984–1002.

García C, Oyaneder-Terrazas J, Contreras C, del Campo M, Torres R, Contreras HR. Determination of the toxic variability of lipophilic biotoxins in marine bivalve and gastropod tissues treated with an industrial canning process. Food Addit Contam Part A. 2016 Nov;33(11):1711–27.

García-Altares M, Casanova A, Fernández-Tejedor M, Diogène J, de la Iglesia P. Bloom of Dinophysis spp. dominated by D. sacculus and its related diarrhetic shellfish poisoning (DSP) outbreak in Alfacs Bay (Catalonia, NW Mediterranean Sea): Identification of DSP toxins in phytoplankton, shellfish and passive samplers. Reg Stud Mar Sci. 2016 Jul;6:19–28.

García-Mendoza E, Sánchez-Bravo YA, Turner A, Blanco J, O'Neil A, Mancera-Flores J, et al. Lipophilic toxins in cultivated mussels (Mytilus galloprovincialis) from Baja California, Mexico. Toxicon. 2014 Nov;90:111–23.

Genies, C.; Maître, A.; Lefèbvre, E.; Jullien, A.; Chopard-Lallier, M.; Douki, T. The Extreme Variety of Genotoxic Response to Benzo[a]pyrene in Three Different Human Cell Lines from Three Different Organs. PLoS ONE 2013, 8, e78356.

Gerbe F., Jay P. Intestinal tuft cells: epithelial sentinels linking luminal cues to the immune system. Mucosal Immunology. 2016;9(6):1353–1359.

Gerssen A., Pol-Hofstad I.E., Poelman M., Mulder P.P., van den Top H.J., de Boer J. Marine toxins: Chemistry, toxicity, occurrence and detection, with special reference to the Dutch situation. Toxins. 2010;2:878–904.

Gerssen A, van Olst EHW, Mulder PPJ, de Boer J. In-house validation of a liquid chromatography tandem mass spectrometry method for the analysis of lipophilic marine toxins in shellfish using matrix-matched calibration. Anal Bioanal Chem. 2010 Aug;397(7):3079–88.

Gerssen A, Mulder PPJ, de Boer J. Screening of lipophilic marine toxins in shellfish and algae: Development of a library using liquid chromatography coupled to orbitrap mass spectrometry. Anal Chim Acta. 2011 Jan;685(2):176–85.

Gill S, Murphy M, Clausen J, Richard D, Quilliam M, MacKinnon S, et al. (2003). Neural Injury Biomarkers of Novel Shellfish Toxins, Spirolides: A Pilot Study Using Immunochemical and Transcriptional Analysis. NeuroToxicology 24(4–5), 593–604.

Gladan ŽN, Ujević I, Milandri A, Marasović I, Ceredi A, Pigozzi S, et al. Is Yessotoxin the Main Phycotoxin in Croatian Waters? Mar Drugs. 2010 Mar 5;8(3):460–70.

Gomez-Lechon MJ, Tolosa L, Donato MT. Upgrading HepG2 cells with adenoviral vectors that encode drug-metabolizing enzymes: application for drug hepatotoxicity testing. Expert Opin Drug Metab Toxicol. 2017;13:137–148.

González AV, Rodríguez-Velasco ML, Ben-Gigirey B, Botana LM. First evidence of spirolides in Spanish shellfish. Toxicon. 2006 Dec;48(8):1068–74.

Gonzalez F.J. The 2006 Bernard B. Brodie Award Lecture. Cyp2e1. Drug Metab. Dispos. 2007;35:1–8.

Gotoh, E.; Asakawa, Y.; Kosaka, H. Inhibition of protein serine/threonine phosphatases directly induces premature chromosome condensation in mammalian somatic cells. Biomed. Res. 1995, 16, 63–68.

Granade HR, Bencsath FA, Dickey RW. Isolation of analogues of okadaic acid from cultures of Prorocentrum lima. Bull Soc Pathol Exot. 1992;85(5 Pt 2):478-80.

Gripon, P., Rumin, S., Urban, S., Le Seyec, J., Glaise, D., Cannie, I., Guyomard, C., Lucas, J., Trepo, C., and Guguen-Guillouzo, C. (2002). Infection of a human hepatoma cell line by hepatitis B virus. Proc. Natl. Acad. Sci. 99, 15655–15660.

Groschwitz K. R., Hogan S. P. (2009). Intestinal barrier function: molecular regulation and disease pathogenesis. J. Allergy Clin. Immunol. 124, 21–22.

Gu X, Ke S, Liu D, Sheng T, Thomas PE, Rabson AB, et al. Role of NF-κB in Regulation of PXR-mediated Gene Expression: a mechanism for the suppression of cytochrome p-450 3a4 by proinflammatory agents. J Biol Chem. 2006;281:17882–9.

Guengerich FP. Cytochromes P450, drugs, and diseases. Molecular Interventions. 2003;3(4):194.

Guengerich, F. P., Wu, Z.-L., and Bartleson, C. J. (2005) Function of human cytochrome P450s: Characterization of the remaining orphans. Biochem. Biophys. Res. Commun. 338, 465–469.

Guillouzo A, et al. The human hepatoma HepaRG cells: A highly differentiated model for studies of liver metabolism and toxicity of xenobiotics. Chem.-Biol. Interact. 2007;168:66–73.

Guo, F.; An, T.; Rein, K.S. The algal hepatoxoxin okadaic acid is a substrate for human cytochromes CYP3A4 and CYP3A5. Toxicon 2010, 55, 325–332.

Guo, M., Tan, Z., Wu, H., Li, Z., Zhai, Y., 2012. Simultaneous determination of okadaic acid, dinophysistoxin, pectenotoxin and yessotoxin in shellfish by liquid chromatography-tandem mass spectrometry. Chinese Journal of Chromatography (Se Pu) 30(3), 256-261.

Halim R, Brimble MA. Synthetic studies towards the pectenotoxins: a review. Org Biomol Chem. 2006;4:4048–4058.

Hampf, M.; Gossen, M. A protocol for combined Photinus and Renilla luciferase quantification compatible with protein assays. Anal. Biochem. 2006, 356, 94–99.

Hashimoto, S., Suzuki, T., Shirota, Y., Honma, M., Itabashi, Y., Chyounan, T., Kamiyama, T., 2006. Lipophilic toxin profiles associated with diarrhetic shellfish poisoning in scallops, Patinopecten yessoensis, collected in Hokkaido and comparison of the quantitative results between LC/MS and mouse bioassay. Journal of the Food Hygienic Society of Japan 47(2), 33-40.

Hashizume, T.; Yoshitomi, S.; Asahi, S.; Matsumura, S.; Chatani, F.; Oda, H. In vitro micronucleus test in HepG2 transformants expressing a series of human cytochrome P450 isoforms with chemicals requiring metabolic activation. Mutat. Res. Toxicol. Environ. Mutagen. 2009, 677, 1–7.

Hattenrath-Lehmann TK, Marcoval MA, Berry DL, Fire S, Wang Z, Morton SL, et al. The emergence of Dinophysis acuminata blooms and DSP toxins in shellfish in New York waters. Harmful Algae. 2013 Jun;26:33–44.

Hauser T.A., Hepler C.D., Kombo D.C., Grinevich V.P., Kiser M.N., Hooker D.N., Zhang J.H., Mountfort D., Selwood A., Akireddy S.R., et al. Comparison of acetylcholine receptor interactions of the marine toxins, 13-desmethylspirolide C and gymnodimine. Neuropharmacolology. 2012;62:2239–2250.

Haystead, T.A., Sim, A.T.R., Carling, D., Honnor, R.C., Tsukitani, Y., Cohen, P. and Hardie, D.G., 1989. Effects of the tumor promoter okadaic acid on intracellular protein phosphorylation and metabolism. Nature 337, 78-81.

Hediger, M.A., Romero, M.F., Peng, J.-B., Rolfs, A., Takanaga, H., and Bruford, E.A. (2004). The ABCs of solute carriers: physiological, pathological and therapeutic implications of human membrane transport proteins. Pflugers Arch. Eur. J. Physiol. 447, 465–468.

Hidalgo I. J., Raub T. J., Borchardt R. T. (1989). Characterization of the human colon carcinoma cell line (Caco-2) as a model system for intestinal epithelial permeability. Gastroenterology 96, 736–749.

Hill J.A., Jr., Nghiem H.O., Changeux J.P. Serine-specific phosphorylation of nicotinic receptor associated 43 K protein. Biochemistry. 1991;30:5579–5585

Hoffmeyer S, Burk O, von Richter O, Arnold HP, Brockmoller J, Johne A, Cascorbi I, Gerloff T, Roots I, Eichelbaum M, Brinkmann U (2000) Functional polymorphisms of the human multidrug-resistance gene: multiple sequence variations and correlation of one allele with P-glycoprotein expression and activity in vivo. Proc Natl Acad Sci USA 97:3473-3478.

Hokama, Y.; Scheuer, P.J.; Yasumoto, T. Effect of a marine toxin on human peripheral blood monocytes. J. Clin. Lab. Anal. 1989, 3, 215–221.

Holmes, C.F., Luu, H.A., Carrier, F., and Schmitz, F.J. (1990). Inhibition of protein phosphatases-1 and -2A with acanthifolicin. Comparison with diarrhetic shellfish toxins and identification of a region on okadaic acid important for phosphatase inhibition. FEBS Lett. 270, 216–218.

Hori M, Matsuura Y, Yoshimoto R, Ozaki H, Yasumoto T and Karaki H, 1999. Actin depolymerizing action by marine toxin, Pectenotoxin-2. Folia Pharmacologica Japonica, 114, 225P-229P.

Hu, T., Doyle, J., Jackson, D., Marr, J., Nixon, E., Pleasance, S., Quilliam, M.A., Walter, J.A., and Wright, J.L.C. (1992). Isolation of a new diarrhetic shellfish poison from Irish mussels. J. Chem. Soc. Chem. Commun. 39.

Hu T, Curtis JM, Oshima Y, Quilliam MA, Walter JA, Watson-Wright WM and Wright JLC, 1995. Spirolides B and D, two novel macrocycles isolated from the digestive glands of shellfish. Journal of the Chemical Society, Chemical Communications, 2159-2161.

Hu T, Curtis JM, Walter JA and Wright JLC, 1996. Characterization of biologically inactive spirolides E and F: identification of the spirolide pharmacophore. Tetrahedron Letters, 37, 7671-7674.

Hu T, Burton IW, Cembella AD, Curtis JM, Quilliam MA, Walter JA and Wright JL, 2001. Characterization of spirolides a, c, and 13-desmethyl c, new marine toxins isolated from toxic plankton and contaminated shellfish. Journal of Natural Products, 64, 308-312.

Hui JPM, Stuart Grossert J, Cutler MJ, Melanson JE. (2012). Strategic identification of in vitro metabolites of 13-desmethyl spirolide C using liquid chromatography/high-resolution mass spectrometry: Identification of in vitro metabolites of 13-desmethyl spirolide C. Rapid Commun Mass Spectrom. 26(3), 345–54.

Ikema S, Takumi S, Maeda Y, et al. Okadaic acid is taken-up into the cells mediated by human hepatocytes transporter OATP1B3. Food Chem Toxicol 83, 229–236 (2015).

Ikuta T., Tachibana T., Watanabe J., Yoshida M., Yoneda Y., Kawajiri K., Nucleocytoplasmic shuttling of the aryl hydrocarbon Receptor1, J. Biochem. 127 (2000) 503–509.

Ingelman-Sundberg M (2005) Genetic polymorphisms of cytochrome P450 2D6 (CYP2D6): clinical consequences, evolutionary aspects and functional diversity. Pharmacogenomics J 5:6-13

Ishige, M.; Satoh, N.; Yasumoto, T. Pathological studies on mice administered with the causative agent of diarrhetic shellfish poisoning (okadaic acid and pectenotoxin-2). Hokkaidoritsu Eisei Kenkyushoho 1988, 38, 15–18.

Ito S, Tsukada K. Matrix effect and correction by standard addition in quantitative liquid chromatographic–mass spectrometric analysis of diarrhetic shellfish poisoning toxins. J Chromatogr A. 2002;943(1):39–46.

Ito, E., Yasumoto, T., Takai, A., Imanishi, S., and Harada, K. (2002). Investigation of the distribution and excretion of okadaic acid in mice using immunostaining method. Toxicon 40, 159–165.

Ito E, 2006. Abstract PO 08-01. 12th International Conference on Harmful Algae. 198.

Ito, E., Suzuki, T., Oshima, Y., and Yasumoto, T. (2008). Studies of diarrhetic activity on pectenotoxin-6 in the mouse and rat. Toxicon 51, 707–716.

Itoh M, Nagafuchi A, Moroi S, Tsukita S. Involvement of ZO-1 in cadherin-based cell adhesion through its direct binding to alpha catenin and actin filaments. J Cell Biol. 1997;138(1):181–92.

James KJ, Carey B, O'Halloran J, van Pelt FN, Skrabakova Z. Shellfish toxicity: human health implications of marine algal toxins. Epidemiol Infect. 2010;138:927–40.

Jančová P. and Šiller M. (2012). Phase II Drug Metabolism, Topics on Drug Metabolism, Dr. James Paxton (Ed.), ISBN: 978-953-51-0099-7, InTech, Available from: http://www.intechopen.com/books/topics-ondrug-metabolism/phase-ii-drug-metabolism

Jiang T, Liu L, Li Y, Zhang J, Tan Z, Wu H, et al. Occurrence of marine algal toxins in oyster and phytoplankton samples in Daya Bay, South China Sea. Chemosphere. 2017 Sep;183:80–8.

Jones C.R., Hatley O.J., Ungell A.L., Hilgendorf C., Peters S.A., Rostami-Hodjegan A. Gut Wall Metabolism. Application of Pre-Clinical Models for the Prediction of Human Drug Absorption and First-Pass Elimination. AAPS J. 2016;18:589–604.

Kanebratt KP, Andersson TB. (2008) HepaRG cells as an in vitro model for evaluation of cytochrome P450 induction in humans. Drug Metab Dispos 36:137–145.

Kanno Y., Suzuki M., Nakahama T., Inouye Y., Characterization of nuclear localization signals and cytoplasmic retention region in the nuclear receptor CAR, Biochim. Biophys. Acta (BBA) - Mol. Cell Res. 1745 (2005) 215–222.

Kasala ER, Bodduluru LN, Barua CC, Sriram CS, Gogoi R. Benzo(a)pyrene induced lung cancer: Role of dietary phytochemicals in chemoprevention. Pharmacol Rep. 2015;67:996–1009.

Kawamoto T, Sueyoshi T, Zelko I, Moore R, Washburn K, Negishi M, Phenobarbital-responsive nuclear translocation of the receptor CAR in induction of the CYP2B Gene, Mol. Cell. Biol. 19 (1999) 6318–6322.

Kazlauskas A, Sundström S, Poellinger L, Pongratz I, The hsp90 chaperone complex regulates intracellular localization of the dioxin receptor, Mol. Cell. Biol. 21 (2001) 2594–2607.

Kim, M.-O.; Moon, D.-O.; Heo, M.-S.; Lee, J.-D.; Jung, J.H.; Kim, S.-K.; Choi, Y.H.; Kim, G.-Y. Pectenotoxin-2 abolishes constitutively activated NF-B, leading to suppression of NF-B related gene products and potentiation of apoptosis. Cancer Lett. 2008, 271, 25–33.

Kim JH, Lee KJ, Suzuki T, Kang YS, Ho Kim P, Song KC, et al. Seasonal Variability of Lipophilic Shellfish Toxins in Bivalves and Waters, and Abundance of Dinophysis spp. in Jinhae Bay, Korea. J Shellfish Res. 2010 Dec;29(4):1061–7.

Kim, J.H., Lee, K.J., Suzuki, T., Mok, J.S., Park, K., Kwon, J.Y., Son, K.T., Song, K.C., 2012. First report of contamination of the abalone Haliotis discus hannai by okadaic acid and yessotoxin. Journal of Shellfish Research 31(4), 1199-1203.

Kim, Y., and Rajagopalan, P. (2010). 3D hepatic cultures simultaneously maintain primary hepatocyte and liver sinusoidal endothelial cell phenotypes. PloS One 5, e15456.

Kittler, K.; Preiss-Weigert, A.; These, A. Identification Strategy Using Combined Mass Spectrometric Techniques for Elucidation of Phase I and Phase II in Vitro Metabolites of Lipophilic Marine Biotoxins. Anal. Chem. 2010, 82, 9329–9335.

Kittler K, Fessard V, Maul R, Hurtaud-Pessel D. CYP3A4 activity reduces the cytotoxic effects of okadaic acid in HepaRG cells. Arch Toxicol. 2014;88(8):1519–1526.

Kmieć Z. (2001). Cooperation of liver cells in health and disease. Adv Anat Embryol Cell Biol 161, Iii–xiii, 1–151.

Knolle PA, Wohlleber D. Immunological functions of liver sinusoidal endothelial cells. Cell Mol Immunol (2016) 13(3):347–53.

Kodama S, Koike C, Negishi M, et al. Nuclear receptors CAR and PXR cross talk with FOXO1 to regulate genes that encode drug-metabolizing and gluconeogenic enzymes. Mol Cell Biol. 2004;24:7931–7940.

Kolrep F, Hessel S, Ehlers A, Lampen A. Impact of oxidated metabolites of okadaic acid in HepG2 cells—A comparative analysis. Toxicology Letters 211S (2012) S43–S216.

Kolrep F, Hessel S, These A, Ehlers A, Rein K, Lampen A, Differences in metabolism of the marine biotoxin okadaic acid by human and rat cytochrome P450 monooxygenases, Archives of toxicology. 90 (2016) 2025-2036.

Kong F, Singh RP. Disintegration of solid foods in human stomach. J Food Sci. 2008;73:R67–R80.

Korsnes, M.S.; Hetland, D.L.; Espenes, A.; Tranulis, M.A.; Aune, T. Apoptotic events induced by yessotoxin in myoblast cell lines from rat and mouse. Toxicol. Vitro 2006, 20, 1077–1087.

Korsnes, M.S.; Hetland, D.L.; Espenes, A.; Aune, T. Cleavage of tensin during cytoskeleton disruption in YTX-induced apoptosis. Toxicol. Vitro 2007, 21, 9–15.

Korsnes M.S., Espenes A. Yessotoxin as an apoptotic inducer. Toxicon. 2011;57:947–958.

Korsnes MS. Yessotoxin as a Tool to Study Induction of Multiple Cell Death Pathways. Toxins. 2012 Jul 23;4(12):568–79.

Korsnes, M.S.; Espenes, A.; Hermansen, L.C.; Loader, J.I.; Miles, C.O. Cytotoxic responses in BC3H1 myoblast cell lines exposed to 1-desulfoyessotoxin. Toxicol. Vitro 2013, 27, 1962–1969.

Kovacsics D., Patik I., Ozvegy-Laczka C. (2016). The role of organic anion transporting polypeptides in drug absorption, distribution, excretion and drug-drug interactions. Expert Opin. Drug Metab. Toxicol. 13, 409–424.

Pamela L. Krahl MD, MPH, LCDR, MC, USN (2009) Harmful Algal Bloom-Associated Marine Toxins: A Risk Assessment Framework, Archives of Environmental & Occupational Health, 64:2, 129-134.

Krause J. William (July 2005). Krause's Essential Human Histology for Medical Students. Universal-Publishers. ISBN 978-1-58112-468-2.

Küblbeck, J. Use of xenosensors for drug metabolism studies: focus on constitutive androstane receptor (2012). University of Eastern Finland Faculty of Health Sciences / School of Pharmacy. Dissertation. Publications of the University of Eastern Finland. Dissertations in Health Sciences., no 130. ISSN: 1798-5714. ISBN: 978-952-61-0889-6

Kurumbail GR, Stevens MA, Gierse KJ, Mc Donald JJ, Stegeman AR, Pak YJ, Gildehaus D, Miyashiro MJ, Pennung DT (1996) Structural basis for selective inhibition of cyclooxygenase-2 by anti-inflammatory agents. Nature 384:644–648.

Lago, J.; Santaclara, F.; Vieites, J.M.; Cabado, A.G. Collapse of mitochondrial membrane potential and caspases activation are early events in okadaic acid-treated Caco-2 cells. Toxicon 2005, 46, 579–586.

Larsen K., Petersen D., Wilkins A.L., Samdal I.A., Sandvik M., Rundberget T., Goldstone D., Arcus V., Hovgaard P., Rise F., et al. Clarification of the C-35 stereochemistries of dinophysistoxin-1 and dinophysistoxin-2 and its consequences for binding to protein phosphatase. Chem. Res. Toxicol. 2007;20:868–875.

Lee JS, Tangen K, Yasumoto T, Dahl E, Hovgaard P, Yasumoto T. Diarrhetic shellfish toxins in norwegian mussels. Nippon Suisan Gakkaishi. 1988;54(11):1953–1957.

Lee, J.-S., Igarashi, T., Fraga, S., Dahl, E., Hovgaard, P., and Yasumoto, T. (1989). Determination of diarrhetic shellfish toxins in various dinoflagellate species. J. Appl. Phycol. 1, 147–152.

Lee KJ, Mok JS, Song KC, Yu H, Jung JH, Kim JH. Geographical and Annual Variation in Lipophilic Shellfish Toxins from Oysters and Mussels along the South Coast of Korea. J Food Prot. 2011 Dec;74(12):2127–33.

Lee KJ, Mok JS, Song KC, Yu H, Lee DS, Jung JH, et al. First Detection and Seasonal Variation of Lipophilic Toxins Okadaic Acid, Dinophysistoxin-1, and Yessotoxin in Korean Gastropods. J Food Prot. 2012 Nov;75(11):2000–6.

Leira, F.; Alvarez, C.; Vieites, J.M.; Vieytes, M.R.; Botana, L.M. Study of cytoskeletal changes induced by okadaic acid in BE(2)-M17 cells by means of a quantitative fluorimetric microplate assay. Toxicol. Vitro 2001, 15, 277–282.

Leira, F.; Alvarez, C.; Vieites, J.M.; Vieytes, M.R.; Botana, L.M. Characterization of distinct apoptotic changes induced by okadaic acid and yessotoxin in the BE(2)-M17 neuroblastoma cell line. Toxicol. Vitro 2002, 16, 23–31.

Le Hégarat, L., Jacquin, A.-G., Bazin, E., and Fessard, V. (2006). Genotoxicity of the marine toxin okadaic acid, in human Caco-2 cells and in mice gut cells. Environ. Toxicol. 21, 55–64.

Le Hégarat, L., Dumont, J., Josse, R., Huet, S., Lanceleur, R., Mourot, A., Poul, J.-M., Guguen-Guillouzo, C., Guillouzo, A., and Fessard, V. (2010). Assessment of the genotoxic potential of indirect chemical mutagens in HepaRG cells by the comet and the cytokinesis-block micronucleus assays. Mutagenesis 25, 555–560.

Leonard, F., Collnot, E.-M., and Lehr, C.-M. (2010). A three-dimensional coculture of enterocytes, monocytes and dendritic cells to model inflamed intestinal mucosa in vitro. Mol. Pharm. 7, 2103–2119.

Lerga, A.; Richard, C.; Delgado, M.D.; Canelles, M.; Frade, P.; Cuadrado, M.A.; Leon, J. Apoptosis and mitotic arrest are two independent effects of the protein phosphatases inhibitor okadaic acid in K562 leukemia cells. Biochem. Biophys. Res. Commun. 1999, 260, 256–264.

Lesca P, Peryt B, Larrieu G, Alvinerie M, Galtier P, Daujat M, Maurel P, Hoogenboom L, Evidence for the ligand-independent activation of the AH receptor, Biochem. Biophys. Res. Commun. 209 (1995) 474–482.

Lesuffleur T, Porchet N, Aubert JP, Swallow D, Gum JR, Kim YS, Real FX, Zweibaum A. Differential expression of the human mucin genes MUC1 to MUC5 in relation to growth and differentiation of different mucus-secreting HT-29 cell subpopulations. J Cell Sci. 1993;106:771–783.

Levitt DG, Levitt MD.. Human serum albumin homeostasis: a new look at the roles of synthesis, catabolism, renal and gastrointestinal excretion, and the clinical value of serum albumin measurements. Int J Gen Med. 2016;9:229–55.

Lewis DF (2004) 57 Varieties: the human cytochromes P450. Pharmacogenomics 5:305–318.

Li, A.P.; Rasmussen, A.; Xu, L.; Kaminski, D.L. Rifampicin induction of lidocaine metabolism in cultured human hepatocytes. J. Pharmacol. Exp. Ther. 1995, 274, 673–677.

Li A, Ma J, Cao J, McCarron P. Toxins in mussels (Mytilus galloprovincialis) associated with diarrhetic shellfish poisoning episodes in China. Toxicon. 2012 Sep;60(3):420–5.

Li A, Sun G, Qiu J, Fan L. Lipophilic shellfish toxins in Dinophysis caudata picked cells and in shellfish from the East China Sea. Environ Sci Pollut Res. 2015 Feb;22(4):3116–26.

Li A, Chen H, Qiu J, Lin H, Gu H. Determination of multiple toxins in whelk and clam samples collected from the Chukchi and Bering seas. Toxicon. 2016 Jan;109:84–93.

Li H, Chen T, Cottrell J, Wang H, Nuclear translocation of adenoviral-enhanced yellow fluorescent protein-tagged-human constitutive androstane receptor (hCAR): A novel tool for screening hCAR activators in human primary hepatocytes, Drug Metab. Dispos. 37 (2009) 1098–1106.

Liang Y, Li S, Chen L. The physiological role of drug transporters. Protein Cell. 2015;6:334–350.

Lichti-Kaiser K, Brobst D, Xu C, Staudinger J.L, A systematic analysis of predicted phosphorylation sites within the human pregnane X receptor protein, J. Pharmacol. Exp. Ther. 331 (2009) 65–76.

Lieber CS (2004) The discovery of the microsomal ethanol oxidizing system and its physiologic and pathologic role. Drug Metab Rev 36:511–529.

Lin W, Wu J, Dong H, Bouck D, Zeng F.-Y, Chen T, Cyclin-dependent kinase 2 negatively regulates human pregnane X receptor-mediated CYP3A4 Gene Expression in HepG2 liver carcinoma cells, J. Biol. Chem. 283 (2008) 30650–30657.

Linton KJ. Structure and function of ABC transporters. Physiology (Bethesda). 2007;22:122–30.

Liu R, Liang Y, Wu X, Xu D, Liu Y, Liu L. First report on the detection of pectenotoxin groups in Chinese shellfish by LC–MS/MS. Toxicon. 2011 Jun;57(7–8):1000–7.

Louzao M.C., Fernández D.A., Abal P., Fraga M., Vilariño N., Vieytes M.R., Botana L.M. Diarrhetic effect of okadaic acid could be related with its neuronal action: Changes in neuropeptide y. Toxicol. Lett. 2015;237:151–160.

Luckert C., Ehlers A., Buhrke T., Seidel A., Lampen A., Hessel S. Polycyclic aromatic hydrocarbons stimulate human CYP3A4 promoter activity via PXR. Toxicol. Lett. 2013;222:180–188.

Luckert, C.; Hessel, S.; Lampen, A.; Braeuning, A. Utility of an appropriate reporter assay: Heliotrine interferes with GAL4/upstream activation sequence-driven reporter gene systems. Anal. Biochem. 2015, 487, 45–48.

Maayah Z, El Gendy M.M, El-Kadi A, Korashy H, Sunitinib, a tyrosine kinase inhibitor, induces cytochrome P450 1A1 gene in human breast cancer MCF7 cells through ligand-independent aryl hydrocarbon receptor activation, Arch. Toxicol. 87 (2013) 847–856.

MacKenzie L, Holland P, McNabb P, Beuzenberg V, Selwood A, Suzuki T. Complex toxin profiles in phytoplankton and Greenshell mussels (Perna canaliculus), revealed by LC–MS/MS analysis. Toxicon. 2002;40(9):1321–1330.

MacKenzie, L., Beuzenberg, V., Holland, P., McNabb, P., Suzuki, T., and Selwood, A. (2005). Pectenotoxin and okadaic acid-based toxin profiles in Dinophysis acuta and Dinophysis acuminata from New Zealand. Harmful Algae 4, 75–85.

MacKenzie, L.A., Selwood, A.I., McNabb, P., Rhodes, L., 2011. Benthic dinoflagellate toxins in two warm-temperate estuaries: Rangaunu and Parengarenga Harbours, Northland, New Zealand. Harmful Algae 10(6), 559-566.

Mackowiak B, Wang H. Mechanisms of xenobiotic receptor activation: Direct vs. indirect. Biochim Biophys Acta. 2016 Sep;1859(9):1130-40.

Madigan TL, Lee KG, Padula DJ, McNabb P, Pointon AM. Diarrhetic shellfish poisoning (DSP) toxins in South Australian shellfish. Harmful Algae. 2006 Mar;5(2):119–23.

Malagoli, D.; Marchesini, E.; Ottaviani, E. Lysosomes as the target of yessotoxin in invertebrate and vertebrate cell lines. Toxicol. Lett. 2006, 167, 75–83.

Malaguti, C.; Ciminiello, P.; Fattorusso, E.; Rossini, G.P. Caspase activation and death induced by yessotoxin in HeLa cells. Toxicol. Vitro 2002, 16, 357–363.

Mani S, Dou W, Redinbo MR. PXR antagonists and implication in drug metabolism. Drug metabolism reviews. 2013;45:60–72.

Martín-López, A.; Gallardo-Rodríguez, J.J.; Sánchez-Mirón, A.; García-Camacho, F.; Molina-Grima, E. Cytotoxicity of yessotoxin and okadaic acid in mouse T lymphocyte cell line EL-4. Toxicon 2012, 60, 1049–1056.

Martiny VY, Miteva MA. Advances in molecular modeling of human cytochrome P450 polymorphism. J Mol Biol. 2013; 425: 3978–3992.

Masahito Suiko, Katsuhisa Kurogi, Takuyu Hashiguchi, Yoichi Sakakibara & Ming-Cheh Liu (2017) Updated perspectives on the cytosolic sulfotransferases (SULTs) and SULT-mediated sulfation, Bioscience, Biotechnology, and Biochemistry, 81:1, 63-72.

Masubuchi, N.; Li, A.P.; Okazaki, O. An evaluation of the cytochrome P450 induction potential of pantoprazole in primary human hepatocytes. Chem. Biol. Interact. 1998, 114, 1–13.

Matias, W.G., Traore, A. and Creppy, E.E., 1999. Variations in the distribution of okadaic acid in organs and biological fluids of mice related to diarrhoeic syndrome. Human Exp. Toxicol. 18, 345-350.

Matsson, P., Bergstrom, C.A.S., Nagahara, N., Tavelin, S., Norinder, U., Artursson, P., 2005. Exploring the role of different drug transport routes in permeability screening. J. Med. Chem. 48, 604–613.

Matsushima R, Uchida H, Nagai S, Watanabe R, Kamio M, Nagai H, et al. Assimilation, Accumulation, and Metabolism of Dinophysistoxins (DTXs) and Pectenotoxins (PTXs) in the Several Tissues of Japanese Scallop Patinopecten yessoensis. Toxins. 2015 Dec 1;7(12):5141–54.

McCarron P, Wright E, Quilliam MA. Liquid Chromatography/Mass Spectrometry of Domoic Acid and Lipophilic Shellfish Toxins with Selected Reaction Monitoring and Optional Confirmation by Library Searching of Product Ion Spectra. J AOAC Int. 2014 Mar 1;97(2):316–24.

McMahon, T., and Silke, J. (1996). West coast of Ireland; winter toxicity of unknown aetiology in mussels. Harmfull Algae News.

McNabb P, Selwood AI, Holland PT. Multiresidue method for determination of algal toxins in shellfish: single-laboratory validation and interlaboratory study. J AOAC Int. 2005;88(3):761–772.

Messner, D.J.; Ao, P.; Jagdale, A.B.; Boynton, A.L. Abbreviated cell cycle progression induced by the serine/threonine protein phosphatase inhibitor okadaic acid at concentrations that promote neoplastic transformation. Carcinogenesis 2001, 22, 1163–1172.

Meyer UA, Zanger UM (1997) Molecular mechanisms of genetic polymorphisms of drug metabolism. Annu Rev Pharmacol Toxicol 37:269-296.

Miles, C.O.;Wilkins, A.L.; Munday, R.; Dines, M.H.; Hawkes, A.D.; Briggs, L.R.; Sandvik, M.; Jensen, D.J.; Cooney, J.M.; Holland, P.T.; et al. Isolation of pectenotoxin-2 from Dinophysis acuta and its conversion to pectenotoxin-2 seco acid, and preliminary assessment of their acute toxicities. Toxicon 2004, 43, 1–9.

Miles C.O., Wilkins A.L., Munday J.S., Munday R., Hawkes A.D., Jensen D.J., Conney J.M., Beuzenberg V. Production of 7-epi-pectenotoxin-2 seco acid and assessment of its acute toxicity to mice. J. Agric. Food Chem. 2006;54:1530–1534.

Miles CO, Rundberget T, Sandvik M, Aasen JAB and Selwood AI, 2010. The presence of pinnatoxins in Norwegian mussels. Report 07b - 2010, Veterinærinstituttet, National Veterinary Institute. Available from http://www.vetinst.no/eng/Research/Publications/Report-Series/Rapportserie-2010/7b-2010-The-presence-of-pinnatoxins-in-Norwegian-mussels.

Mohana Krishnamoorthy & Achary Anant (2017) Human cytosolic glutathione-S-transferases: quantitative analysis of expression, comparative analysis of structures and inhibition strategies of isozymes involved in drug resistance, Drug Metabolism Reviews, 49:3, 318-337.

Molgó J, Marchot P, Aráoz R, Benoit E, Iorga BI, Zakarian A, Taylor P, Bourne Y, Servent D. Cyclic imine toxins from dinoflagellates: a growing family of potent antagonists of the nicotinic acetylcholine receptors. J Neurochem. 2017 Aug;142 Suppl 2:41-51.

Monshouwer M, Witkamp RF, Nujmeijer SM, Van Amsterdam JG, Van Miert AS. Suppression of cytochrome P450- and UDP glucuronosyl transferase-dependent enzyme activities by proinflammatory cytokines and possible role of nitric oxide in primary cultures of pig hepatocytes. Toxicol Appl Pharmacol. 1996;137(2):237–244.

Moon, D.-O.; Kim, M.-O.; Kang, S.-H.; Lee, K.-J.; Heo, M.-S.; Choi, K.-S.; Choi, Y.-H.; Kim, G.-Y. Induction of G2/M arrest, endoreduplication, and apoptosis by actin depolymerization agent pextenotoxin-2 in human leukemia cells, involving activation of ERK and JNK. Biochem. Pharmacol. 2008, 76, 312–321.

Moore MN, Depledge MH, Fleming L, Hess P, Lees D, et al. (2013) Oceans and Human Health (OHH): European perspective from the Marine Board of the European Science Foundation (Marine Board-ESF). Microb Ecol 65(4): 889-900.

Moroz E, Matoori S, Leroux J-C. Oral delivery of macromolecular drugs: where we are after almost 100 years of attempts. Adv Drug Deliv Rev. 2016;101:108–121.

Morton SL, Vershinin A, Smith LL, Leighfield TA, Pankov S, Quilliam MA. Seasonality of Dinophysis spp. and Prorocentrum lima in Black Sea phytoplankton and associated shellfish toxicity. Harmful Algae. 2009 Jun;8(5):629–36.

Munday JS, 2008. Toxicology of the pectenotoxins. In: Seafood and Freshwater toxins: Pharmacology, Physiology and Detection, 2nd edition. CRC Press (Taylor and Francis Group), Botana LM (ed), Boca Raton, Florida, pp. 371-380.

Munday R, Quilliam MA, LeBlanc P, Lewis N, Gallant P, Sperker SA, Ewart HS, MacKinnon SL. (2012). Investigations into the toxicology of spirolides, a group of marine phycotoxins. Toxins. 4(1), 1-14.

Murata, M., Shimatani, M., Sugitani, H., Oshima, Y., and Yasumoto, T. (1982). Isolation and structural elucidation of the causative toxin of the diarrhetic shellfish poisoning. Bull. Jpn. Soc. Sci. Fish.

Murata, M., Kumagai, M., Lee, J.S., and Yasumoto, T. (1987). Isolation and structure of yessotoxin, a novel polyether compound implicated in diarrhetic shellfish poisoning. Tetrahedron Lett. 28, 5869–5872.

Mutoh S, Sobhany M, Moore R, Perera L, Pedersen L, Sueyoshi T, Negishi M, Phenobarbital indirectly activates the constitutive active androstane receptor (CAR) by inhibition of epidermal growth factor receptor signaling, Sci. Signal. 6 (2013) ra31.

Nassar A.F, Hollenberg P.F, Scatina J. (2009). Drug Metabolism Handbook: Concepts and Applications. JohnWiley, Chichester.

Ninčević-Gladan Ž, Skejić S, Bužančić M, Marasović I, Arapov J, Ujević I, et al. Seasonal variability in Dinophysis spp. abundances and diarrhetic shellfish poisoning outbreaks along the eastern Adriatic coast. Bot Mar [Internet]. 2008 Jan 1 [cited 2017 Sep 14];51(6). Available from: https://www.degruyter.com/view/j/bot.2008.51.issue-6/bot.2008.067/bot.2008.067.xml.

Nincevic Gladan Z, Ujevic I, Milandri A, Marasovic I, Ceredi A, Pigozzi S, et al. Lipophilic Toxin Profile in Mytilus galloprovincialis during Episodes of Diarrhetic Shellfish Poisoning (DSP) in the N.E. Adriatic Sea in 2006. Molecules. 2011 Jan 21;16(12):888–99.

Nishibe, Y.; Hirata, M. Effect of phenobarbital and other model inducers on cytochrome P450 isoenzymes in primary culture of dog hepatocytes. Xenobiotica 1993, 23, 681–692.

Ogino, H., Kumagai, M., and Yasumoto, T. (1997). Toxicologic evaluation of yessotoxin. Nat. Toxins 5, 255–259.

Omiecinski CJ, Vanden Heuvel JP, Perdew GH, Peters JM. (2011). Xenobiotic Metabolism, Disposition, and Regulation by Receptors: From Biochemical Phenomenon to Predictors of Major Toxicities. Toxicol Sci. 120(Supplement 1), S49–75.

Opsahl, JA.; Ljostveit, S.; Solstad, T.; Risa, K.; Roepstorff, P.; Fladmark, K.E. Identification of dynamic changes in proteins associated with the cellular cytoskeleton after exposure to okadaic Acid. Mar. Drugs 2013, 11, 1763–1782.

Orans J, Teotico D.G, Redinbo M.R, The nuclear xenobiotic receptor pregnane X receptor: recent insights and new challenges, Mol. Endocrinol. 19 (2005) 2891–2900.

Orellana G, Van Meulebroek L, De Rijcke M, Janssen CR, Vanhaecke L. High resolution mass spectrometry-based screening reveals lipophilic toxins in multiple trophic levels from the North Sea. Harmful Algae. 2017 Apr;64:30–41.

Orsi, C.F.; Colombari, B.; Callegari, F.; Todaro, A.M.; Ardizzoni, A.; Rossini, G.P.; Blasi, E.; Peppoloni, S. Yessotoxin inhibits phagocytic activity of macrophages. Toxicon 2010, 55, 265–273.

Otero P., Perez S., Alfonso A., Vale C., Rodriguez P., Gouveia N.N., Gouveia N., Delgado J., Vale P., Hirama M., Ishihara Y., Molgo J., Botana L.M. (2010) First toxin profile of ciguateric fish in Madeira Arquipelago (Europe). Anal. Chem. 82, 6032–6039.

Otero P, Alfonso A, Rodríguez P, Rubiolo JA, Cifuentes JM, Bermúdez R, et al. (2012). Pharmacokinetic and toxicological data of spirolides after oral and intraperitoneal administration. Food Chem Toxicol. 50(2), 232–7.

Paerl HW (2014) Mitigating harmful cyanobacterial blooms in a human- and climatically-impacted world. Life (Basel) 4(4): 988-1012.

Paine MF, Hart HL, Ludington SS, Haining RL, Rettie AE, Zeldin DC. The human intestinal cytochrome P450 'pie'. Drug Metab Dispos. 2006;34:880–886.

Pang, M.;Wang, Z.L.; Gao, C.L.; Qu, P.; Li, H.D. Characterization of apoptotic changes induced by yessotoxin in the Bel7402 human hepatoma cell line. Mol. Med. Rep. 2011, 4, 547–552.

Pang M., Qu P., Gao C.L., Wang Z.L. Yessotoxin induces apoptosis in HL7702 human liver cells. Mol. Med. Rep. 2012;5:211–216.

Pang M., Qu P., Gao C.L., Tang X., Wang Z.L. Effect of yessotoxin on cytosolic calcium levels in human hepatocellular carcinoma cells. Biomed. Rep. 2014;2:93–96.

Pappenheimer J, Michel C. Role of villus microcirculation in intestinal absorption of glucose: coupling of epithelial with endothelial transport. The Journal of physiology. 2003; 553: 561–574.

Parmentier Y, Pothier C, Delmas A, Caradec F, Trancart M-M, Guillet F, et al. (2016). Direct and quantitative evaluation of the human CYP3A4 contribution (fm) to drug clearance using the in vitro SILENSOMES model. Xenobiotica 3, 1–14.

Pascussi JM, Gerbal-Chaloin S, Pichard-Garcia L, et al. Interleukin-6 negatively regulates the expression of pregnane X receptor and constitutively activated receptor in primary human hepatocytes. Biochem Biophys Res Commun. 2000;274:707–713.

Pasquel D, Doricakova A, Li H, et al. Acetylation of lysine 109 modulates pregnane X receptor DNA binding and transcriptional activity. Biochim Biophys Acta. 2016.

Pavek P (2016) Pregnane X Receptor (PXR)-Mediated Gene Repression and Cross-Talk of PXR with Other Nuclear Receptors via Coactivator Interactions. Front. Pharmacol. 7:456.

Pavela-Vrančič M, Meštrović V, Marasović I, Gillman M, Furey A, James KK. The occurrence of 7-epi-pectenotoxin-2 seco acid in the coastal waters of the central Adriatic (Kaštela Bay). Toxicon. 2001;39(6):771–779.

Pavela-Vrančič M, Meštrović V, Marasović I, Gillman M, Furey A, James KJ. DSP toxin profile in the coastal waters of the central Adriatic Sea. Toxicon. 2002 Nov;40(11):1601-7.

Pavela-Vrančič M, Meštrović V, Marasović I, Gillman M, Furey A, James KJ. DSP toxin profile in the coastal waters of the central Adriatic Sea. Toxicon. 2002 Nov;40(11):1601-7.

Pavela-Vrančić M, Ujević I, Ninčević Gladan Ž, Furey A. Accumulation of Phycotoxins in the mussel Mytilus galloprovincialis from the Central Adriatic Sea. Croat Chem Acta. 2006;79(2):291–297.

Paz, B.; Riobo, P.; Fernandez, M.L.; Fraga, S.; Franco, J.M. Production and release of yessotoxins by the dinoflagellates Protoceratium reticulatum and Lingulodinium polyedrum in culture. Toxicon 2004, 44, 251–258.

Pazos, M.; Alfonso, A.; Vieytes, M.; Yasumoto, T.; Botana, L. Resonant mirror biosensor detection method based on yessotoxin-phosphodiesterase interactions. Anal. Biochem. 2004, 335, 112–118.

Pazos, M.J.; Alfonso, A.; Vieytes, M.R.; Yasumoto, T.; Botana, L.M. Kinetic analysis of the interaction between yessotoxin and analogs and immobilized phosphodiesterases using a resonant mirror optical biosensor. Chem. Res. Toxicol. 2005, 18, 1155–1160.

Pazos M., Alfonso A., Vieytes M., Yasumoto T., Botana L. Study of the interaction between different phosphodiesterases and yessotoxin using a resonant mirror biosensor. Chem. Res. Toxicol. 2006;19:794–800.

Pelkonen O, Turpeinen M, Hakkola J, Honkakoski P, Hukkanen J, Raunio H. Inhibition and induction of human cytochrome P450 enzymes: current status. Arch Toxicol. 2008;82:667–715.

Pelkonen O., Ahokas J.T., Hakkola J., Turpeinen M. (2014) Consideration of Metabolism in In Vitro Cellular Systems. In: Bal-Price A., Jennings P. (eds) In Vitro Toxicology Systems. Methods in Pharmacology and Toxicology. Humana Press, New York, NY

Peng, J.; Bowden, G.T.; Domann, F.E. Activation of AP-1 by okadaic acid in mouse keratinocytes associated with hyperphosphorylation of c-jun. Mol. Carcinog. 1997, 18, 37–43.

Perez-Gomez A., Ferrero-Gutierrez A., Novelli A., Franco J., Paz B., Fernandez-Sanchez M.T. Potent neurotoxic action of the shellfish biotoxin yessotoxin on cultured cerebellar neurons. Toxicol. Sci. 2006;90:168–177.

Picot C, Roudot A-C. A Practical Example of Risk Assessment–Risk Assessment to Phycotoxins in a Recreational Shellfish Harvester's Subpopulation. In: Novel Approaches and Their Applications in Risk Assessment [Internet]. InTech; 2012 [cited 2017 Aug 2]. Available from: https://www.intechopen.com/download/pdf/35499

Picot C, Limon G, Durand G, Parent-Massin D, Roudot AC. (2013). Probabilistic dietary exposure to phycotoxins in a recreational shellfish harvester subpopulation (France). J Expo Sci Environ Epidemiol. 23(4), 435-441.

Pistocchi, R., Guerrini, F., Pezzolesi, L., Riccardi, M., Vanucci, S., Ciminiello, P., Dell'Aversano, C., Forino, M., Fattorusso, E., Tartaglione, L., et al. (2012). Toxin levels and profiles in microalgae from the north-Western Adriatic Sea--15 years of studies on cultured species. Mar. Drugs 10, 140–162.

Pitcher GC, Krock B, Cembella AD. Accumulation of diarrhetic shellfish poisoning toxins in the oyster Crassostrea gigas and the mussel Choromytilus meridionalis in the southern Benguela ecosystem. Afr J Mar Sci. 2011 Aug;33(2):273–81.

Pontier C., Pachot J., Botham R., Lenfant B., Arnaud P. HT29-MTX and Caco-2/TC7 monolayers as predictive models for human intestinal absorption: Role of the mucus layer. J. Pharm. Sci. 2001;90:1608–1619.

Postic C, Dentin R, Girard J (2004) Role of the liver in the control of carbohydrate and lipid homeostasis. Diabetes Metab 30: 398–408.

Price E.R., Brun A., Caviedes-Vidal E., Karasov W.H. Digestive adaptations of aerial lifestyles. Physiology. 2015;30:69–78.

Puente PF, Sáez MJF, Hamilton B, Lehane M, Ramstad H, Furey A, et al. Rapid determination of polyether marine toxins using liquid chromatography–multiple tandem mass spectrometry. J Chromatogr A. 2004 Nov;1056(1–2):77–82.

Pulido OM (2016) Phycotoxins by Harmful Algal Blooms (HABS) and Human Poisoning: An Overview. Int Clin Pathol J 2(6): 00062.

Raddatz D, Ramadori G. Carbohydrate metabolism and the liver: Actual aspects from physiology and disease. Z Gastroenterol 2007; 45(1):51-62.

Ramadoss, P.; Marcus, C.; Perdew, G.H. Role of the aryl hydrocarbon receptor in drug metabolism. Expert Opin. Drug Metab. Toxicol. 2005, 1, 9–21.

Ramstad H, Hovgaard P, Yasumoto T, Larsen S, Aune T. Monthly variations in diarrhetic toxins and yessotoxin in shellfish from coast to the inner part of the Sognefjord, Norway. Toxicon. 2001;39(7):1035–1043.

Raucy JL, Kraner JC, Lasker JM (1993) Bioactivation of halogenated hydrocarbons by cytochrome P4502E1. Crit Rev Toxicol 23:1–20.

Reboldi A, Cyster JG. Peyer's patches: organizing B-cell responses at the intestinal frontier. Immunol Rev (2016) 271(1):230–45.

Reguera B, Riobó P, Rodríguez F, Díaz P, Pizarro G, Paz B, et al. Dinophysis Toxins: Causative Organisms, Distribution and Fate in Shellfish. Mar Drugs. 2014 Jan 20;12(1):394–461.

Reisz-Porszasz S, Probst M.R, Fukunaga B.N, Hankinson O, Identification of functional domains of the aryl hydrocarbon receptor nuclear translocator protein (ARNT), Mol. Cell. Biol. 14 (1994) 6075–6086.

Rhodes, L.; McNabb, P.; de Salas, M.; Briggs, L.; Beuzenberg, V.; Gladstone, M. Yessotoxin production by Gonyaulax spinifera. Harmful Algae 2006, 5, 148–155.

Richard D, Arsenault E, Cembella AD and Quilliam MA, 2001. Investigations into the toxicology and pharmacology of spirolides, a novel group of shellfish toxins. In: Harmful Algal Blooms 2000. Eds Hallegraef GM, Blackburn SI, Bolch CJ and Lewis RJ. Intergovernmental of Oceanographic Commision of UNESCO, 383-386.

Rieger JK, Klein K, Winter S, and Zanger UM, Expression variability of absorption, distribution, metabolism, excretion-related microRNAs in human liver: influence of non-genetic factors and association with gene expression, Drug Metab Dispos, 41, 1752-1762, (2013).

Riordan, F.A.; Foroni, L.; Hoffbrand, A.V.; Mehta, A.B.; Wickremasinghe, R.G. Okadaic acid-induced apoptosis of HL60 leukemia cells is preceded by destabilization of bcl-2 mRNA and downregulation of bcl-2 protein. FEBS Lett. 1998, 435, 195–198.

Roebuck KA. (1999). Regulation of interleukin-8 gene expression. J Interferon Cytokine Res. 19(5):429-38.

Rodríguez L.P., Vilariño N., Molgó J., Aráoz R., Botana L.M. High-throughput receptor-based assay for the detection of spirolides by chemiluminescence. Toxicon. 2013;75:35–43.

Rodríguez L, González V, Martínez A, Paz B, Lago J, Cordeiro V, et al. Occurrence of Lipophilic Marine Toxins in Shellfish from Galicia (NW of Spain) and Synergies among Them. Mar Drugs. 2015 Mar 25;13(4):1666–87.

Rossini, G.P.; Sgarbi, N.; Malaguti, C. The toxic responses induced by okadaic acid involve processing of multiple caspase isoforms. Toxicon 2001, 39, 763–770.

Rossini G.P., Hess P. Phycotoxins: Chemistry, mechanisms of action and shellfish poisoning. In: Luch A., editor. Molecular, Clinical and Environmental Toxicology. Birkhäuser; Basel, Switzerland: 2010. pp. 65–122.

Rostami-Hodjegan A, Tucker GT (2007) Simulation and prediction of in vivo drug metabolism in human populations from in vitro data. Nat Rev Drug Discov 6:140–148.

Roth A, Looser R, Kaufmann M, and Meyer UA, Sterol regulatory element binding protein 1 interacts with pregnane X receptor and constitutive androstane receptor and represses their target genes, Pharmacogenet Genomics, 18, 325–337, (2008).

Roth M, Obaidat A, Hagenbuch B. OATPs, OATs and OCTs: the organic anion and cation transporters of the SLCO and SLC22A gene superfamilies. British journal of pharmacology. 2012;165:1260–1287.

Rowlands JC, Gustafsson JA, Aryl hydrocarbon receptor-mediated signal transduction, Crit. Rev. Toxicol. 27 (1997) 109–134.

Rubio, F., Kamp, L., Carpino, J., Faltin, E., Loftin, K., Molgó, J. and Aráoz, R. (2014). Colorimetric microtiter plate receptor-binding assay for the detection of freshwater and marine neurotoxins targeting the nicotinic acetylcholine receptors. Toxicon 91, 45-56

Rubiolo, J.A.; Lopez-Alonso, H.; Martinez, P.; Millan, A.; Cagide, E.; Vieytes, M.R.; Vega, F.V.; Botana, L.M. Yessotoxin induces ER-stress followed by autophagic cell death in glioma cells mediated by mTOR and BNIP3. Cell Signal. 2014, 26, 419–432.

Sala GL, Ronzitti G, Sasaki M, Fuwa H, Yasumoto T, Bigiani A, et al. Proteomic Analysis Reveals Multiple Patterns of Response in Cells Exposed to a Toxin Mixture. Chem Res Toxicol. 2009 Jun 15;22(6):1077–85.

Sambuy Y., De Angelis I., Ranaldi G., Scarino M. L., Stammati A., Zucco F. (2005). The Caco-2 cell line as a model of the intestinal barrier: influence of cell and culture-related factors on Caco-2 cell functional characteristics. Cell Biol. Toxicol. 21, 1–26.

Sandvik M, Fæste C, Miles C. In vitro biotransformation of algal toxins. Poster presented during 11th International Conference on Molluscan Shellfish Safety, 2017, 14th - 18th May.

Saradhi M, Sengupta A, Mukhopadhyay G, Tyagi RK, Pregnane and xenobiotic receptor (PXR/SXR) resides predominantly in the nuclear compartment of the interphase cell and associates with the condensed chromosomes during mitosis, Biochim. Biophys. Acta (BBA) - Mol. Cell Res. 1746 (2005) 85–94.

Satake, M., Ichimura, T., Sekiguchi, K., Yoshimatsu, S., and Oshima, Y. (1999). Confirmation of yessotoxin and 45,46,47-trinoryessotoxin production by Protoceratium reticulatum collected in Japan. Nat. Toxins 7, 147–150.

Schneeman B. O. (2002). Gastrointestinal physiology and functions. Brit. J. Nutr. 88(Suppl. 2), S159–S163.

Schottelius, A.J.G., and Baldwin Jr., A.S. (1999). A role for transcription factor NF- k B in intestinal inflammation. Int. J. Colorectal Dis. 14, 18–28.

Shahraki J, Motallebi A, Barekati I, Seydi E & Pourahmad J (2014) Comparison of cellular and molecular cytotoxic mechanisms of Cochlodinium polykrikoides in isolated trout and rat hepatocytes, Toxicological & Environmental Chemistry, 96:6, 917-930.

Sheng Y., Abreu I. A., Cabelli D. E., Maroney M. J., Miller A. F., Teixeira M., et al. (2014). Superoxide dismutases and superoxide reductases. Chem. Rev. 114 3854–3918.

Shin, D.Y., Kim, G.Y., Kim, N.D., Jung, J.H., Kim, S.-K., Kang, H.S., and Choi, Y.H. (2008). Induction of apoptosis by pectenotoxin-2 is mediated with the induction of DR4/DR5, Egr-1 and NAG-1, activation of caspases and modulation of the Bcl-2 family in p53-deficient Hep3B hepatocellular carcinoma cells. Oncol. Rep. 19, 517–526.

Shin IJ, Ahn YT, Kim Y, Kim JM, An WG. Actin disruption agents induce phosphorylation of histone H2AX in human breast adenocarcinoma MCF-7 cells. Oncol Rep. 2011;25:1313–1319.

Shugarts S., Benet L.Z. The role of transporters in the pharmacokinetics of orally administered drugs. Pharm. Res. 2009;26:2039–2054.

Silva M., Rodriguez I., Barreiro A., Kaufmann M., Neto A.I., Hassouani M., Sabour B., Alfonso A., Botana L.M., Vasconcelos V. First report of ciguatoxins in two starfish species : Ophidiaster ophidianus and Marthasterias glacialis. Toxins. 2015;7:3740–3757.

Sim E, Abuhammad A, Ryan A (2014). Arylamine N-acetyltransferases: from drug metabolism and pharmacogenetics to drug dis covery. Br J Pharmacol 171: 270 5–2725.

Sirenko, O., Hesley, J., Rusyn, I., and Cromwell, E.F. (2014). High-content assays for hepatotoxicity using induced pluripotent stem cell-derived cells. Assay Drug Dev. Technol. 12, 43–54.

Sivakumar S and Gorbsky JG. Phosphatase-regulated recruitment of the spindle- and kinetochore-associated (Ska) complex to kinetochores. Biol Open. 2017 Nov 15; 6(11): 1672–1679.

Smienk H., Dominguez E., Rodriguez-Velasco M.L., Clarke D., Kapp K., Katikou P., Cabado A.G., Otero A., Vieites J.M., Razquin P., et al. Quantitative determination of the okadaic acid toxins group by a colorimetric phosphatase inhibition assay: Interlaboratory study. J. Aoac Int. 2013;96:77–85.

Smith M.C., Madec S., Coton E., Hymery N. Natural co-occurrence of mycotoxins in foods and feeds and their in vitro combined toxicological effects. Toxins. 2016;8:94.

Sonoda, Y.; Kasahara, T.; Yamaguchi, Y.; Kuno, K.; Matsushima, K.; Mukaida, N. Stimulation of interleukin-8 production by okadaic acid and vanadate in a human promyelocyte cell line, an HL-60 subline. Possible role of mitogen-activated protein kinase on the okadaic acid-induced NF-kappaB activation. J. Biol. Chem. 1997, 272, 15366–15372.

Sosa S, Ardizzone M, Beltramo D, Vita F, Dell'Ovo V, Barreras A, et al. Repeated oral co-exposure to yessotoxin and okadaic acid: A short term toxicity study in mice. Toxicon. 2013 Dec;76:94–102.

Stahn C, Löwenberg M, Hommes DW, Buttgereit F. Molecular mechanisms of glucocorticoid action and selective glucocorticoid receptor agonists. Mol Cell Endocrinol. 2007;275:71–78.

Stobo LA, Lacaze J-PC, Scott AC, Gallacher S, Smith EA, Quilliam MA. Liquid chromatography with mass spectrometry—detection of lipophilic shellfish toxins. J AOAC Int. 2005;88(5):1371–1382.

Stobo LA, Lacaze J-PCL, Scott AC, Petrie J, Turrell EA. Surveillance of algal toxins in shellfish from Scottish waters. Toxicon. 2008 Mar;51(4):635–48.

Sugano K, et al. Coexistence of passive and carrier-mediated processes in drug transport. Nature reviews. Drug discovery. 2010;9:597–614.

Suganuma, M.; Fujiki, H.; Suguiri, H.; Yoshizwa, S.; Hirota, M.; Nakayasu, M.; Ojika, M.; Wakamatsu, K.; Yamada, K.; Sugimura, T. Okadaic acid, an additional non-phorbol-12-tetrade-canoate-13-acetate type tumour promoter. Proc. Natl. Acad. Sci. USA 1988, 85, 1768–1771.

Suganuma M, Okabe S, Marino MW, Sakai A, Sueoka E, Fujiki H. Essential role of tumor necrosis factor α (TNF-α) in tumor promotion as revealed by TNF-α- deficient mice. Cancer Res. 1999;59:4516–4518.

Suganuma M, Okabe S, Kurusu M, Iida N, Ohshima S, Saeki Y, Kishimoto T, Fujiki H. Discrete roles of cytokines, TNF-alpha, IL-1, IL-6 in tumor promotion and cell transformation. International Journal of Oncology. 2002;20:131–136.

Sugatani J, Hattori Y, Noguchi Y, Yamaguchi M, Yamazaki Y, Ikari A, Threonine-290 regulates nuclear translocation of the human pregnane X receptor through its phosphorylation/dephosphorylation by

Ca2+/calmodulin-dependent protein kinase II and protein phosphatase 1, Drug Metab. Dispos. 42 (2014) 1708–1718.

Suzuki T, Yasumoto T. Liquid chromatography–electrospray ionization mass spectrometry of the diarrhetic shellfish-poisoning toxins okadaic acid, dinophysistoxin-1 and pectenotoxin-6 in bivalves. J Chromatogr A. 2000;874(2):199–206.

Suzuki, T., Beuzenberg, V., Mackenzie, L., and Quilliam, M.A. (2003). Liquid chromatographymass spectrometry of spiroketal stereoisomers of pectenotoxins and the analysis of novel pectenotoxin isomers in the toxic dinoflagellate Dinophysis acuta from New Zealand. J. Chromatogr. A 992, 141–150.

Suzuki T, Jin T, Shirota Y, Mitsuya T, Okumura Y, Kamiyama T. Quantification of lipophilic toxins associated with diarrhetic shellfish poisoning in Japanese bivalves by liquid chromatography–mass spectrometry and comparison with mouse bioassay. Fish Sci. 2005;71(6):1370–1378.

Suzuki T, Quilliam MA. LC-MS/MS analysis of diarrhetic shellfish poisoning (DSP) toxins, okadaic acid and dinophysistoxin analogues, and other lipophilic toxins. Anal Sci. 2011;27(6):571–571.

Swales K, Kakizaki S, Yamamoto Y, Inoue K, Kobayashi K, Negishi M, Novel CAR-mediated mechanism for synergistic activation of two distinct elements within the human cytochrome P450 2B6 Gene in HepG2 cells, J. Biol. Chem. 280 (2005) 3458–3466.

Tachibana, K., Scheuer, P.J., Tsukitani, Y., Kikuchi, H., Van Engen, D., Clardy, J., Gopichand, Y., and Schmitz, F.J. (1981). Okadaic acid, a cytotoxic polyether from two marine sponges of the genus Halichondria. J. Am. Chem. Soc. 103, 2469–2471.

Takahashi E, Yu Q, Eaglesham G, Connell DW, McBroom J, Costanzo S, et al. Occurrence and seasonal variations of algal toxins in water, phytoplankton and shellfish from North Stradbroke Island, Queensland, Australia. Mar Environ Res. 2007 Oct;64(4):429–42.

Takai A., Bialojan C., Troschka M., Ruegg J.C. Smooth muscle myosin phosphatase inhibition and force enhancement by black sponge toxin. FEBS Lett. 1987;217:81–84.

Takai, A., Murata, M., Torigoe, K., Isobe, M., Mieskes, G., and Yasumoto, T. (1992). Inhibitory effect of okadaic acid derivatives on protein phosphatases. A study on structure-affinity relationship. Biochem. J. 284 (Pt 2), 539–544.

Takakura N, Sanders P, Fessard V, Le Hégarat L. In vitro combined cytotoxic effects of pesticide cocktails simultaneously found in the French diet. Food Chem Toxicol. 2013 Feb;52:153–62.

Taleb H, Vale P, Amanhir R, Benhadouch A, Sagou R, Chafik A. First detection of azaspiracids in mussels in north west Africa. J. Shellfish Res., 25 (3) (2006), pp. 1067-1070.

Terao, K.; Ito, E.; Yanagi, T.; Yasumoto, T. Histopathological studies on experimental marine toxin poisoning. I. Ultrastructural changes in the small intestine and liver of suckling mice induced by dinophysistoxin-1 and pectenotoxin-1. Toxicon 1986, 24, 1141–1151.

Terao, K.; Ito, E.; Oarada, M.; Murata, M.; Yasumoto, T. Histopathological studies on experimental marine toxin poisoning-5. The effects in mice of yessotoxin isolated from Patinopecten yessoensis and of a desulfated derivative. Toxicon 1990, 28, 1095–1104.

Thomas P, Smart T. HEK293 cell line: A vehicle for the expression of recombinant proteins. J. Pharmacol. Toxicol. Methods. 2005;51:187–200.

Thompson, E.J.; MacGowan, J.; Young, M.R.; Colburn, N.; Bowden, G.T. Dominant negative c-jun specifically blocks okadaic acid-induced skin tumor promotion. Cancer Res. 2002, 62, 3044–3047.

Tillmann, U., Elbrächter, M., Krock, B., John, U., and Cembella, A. (2009). Azadinium spinosum gen. et sp. nov. (Dinophyceae) identified as a primary producer of azaspiracid toxins. Eur. J. Phycol. 44, 63–79.

Timsit YE, Negishi M. CAR and PXR: the xenobiotic-sensing receptors. Steroids. 2007;72(3):231–246.

Timsit YE, Negishi M, Coordinated regulation of nuclear receptor CAR by CCRP/DNAJC7, HSP70 and the ubiquitin-proteasome system, PLoS One 9 (2014), e96092.

Torgersen, T., Aasen, J., and Aune, T. (2005). Diarrhetic shellfish poisoning by okadaic acid esters from Brown crabs (Cancer pagurus) in Norway. Toxicon 46, 572–578.

Torgersen, T., Sandvik, M., Lundve, B., Lindegarth, S., 2008b. Profiles and levels of fatty acid esters of okadaic acid group toxins and pectenotoxins during toxin depuration. Part II: Blue mussels (Mytilus edulis) and flat oyster (Ostrea edulis). Toxicon 52(3), 418-427.

Touzet, N., Franco, J.M., Raine, R., (2008). Morphogenetic diversity and biotoxin composition of Alexandrium (dinophyceae) in Irish coastal waters. Harmful Algae 7, 782-797.

Townsend DM, Tew KD. The role of glutathione-S-transferase in anti-cancer drug resistance. Oncogene. 2003;22(47):7369–75.

Trainer V, Moore L, Bill B, Adams N, Harrington N, Borchert J, et al. Diarrhetic Shellfish Toxins and Other Lipophilic Toxins of Human Health Concern in Washington State. Mar Drugs. 2013 May 28;11(6):1815–35.

Trefts E, Gannon M, Wasserman DH. The liver. Curr Biol. 2017 Nov 6;27(21):R1147-R1151.

Tsuji N, Fukuda K, Nagata Y, Okada H, Haga A, Hatakeyama S, Yoshida S, Okamoto T, Hosaka M, Sekine K, Ohtaka K, Yamamoto S, Otaka M, Grave E, Itoh H, The activation mechanism of the aryl hydrocarbon receptor (AhR) by molecular chaperone HSP90, FEBS Open Bio 4 (2014) 796–803.

Tubaro A, Sosa S, Carbonatto M, Altinier G, Vita F, Melato M, et al. Oral and intraperitoneal acute toxicity studies of yessotoxin and homoyessotoxins in mice. Toxicon. 2003;41(7):783–92.

Tubaro, A., Sosa, S., Altinier, G., Soranzo, M.R., Satake, M., Della Loggia, R., and Yasumoto, T. (2004). Short-term oral toxicity of homoyessotoxins, yessotoxin and okadaic acid in mice. Toxicon 43, 439–445.

Tubaro A, Giangaspero A, Ardizzone M, Soranzo MR, Vita F, Yasumoto T, et al. Ultrastructural damage to heart tissue from repeated oral exposure to yessotoxin resolves in 3 months. Toxicon. 2008;51(7):1225–35.

Tubaro A, Dell'Ovo V, Sosa S, Florio C. Yessotoxins: A toxicological overview. Toxicon. 2010 Aug;56(2):163–72.

Turner AD, Goya AB. Occurrence and profiles of lipophilic toxins in shellfish harvested from Argentina. Toxicon. 2015 Aug;102:32–42.

Turpeinen M, Raunio H, Pelkonen O (2006) The functional role of CYP2B6 in human drug metabolism: substrates and inhibitors in vitro, in vivo and in silico. Curr Drug Metab 7:705–714.

Twiner, M.J., Doucette, G.J., Rasky, A., Huang, X.-P., Roth, B.L., and Sanguinetti, M.C. (2012a). Marine Algal Toxin Azaspiracid Is an Open-State Blocker of hERG Potassium Channels. Chem. Res. Toxicol. 25, 1975–1984.

Valdiglesias, V., Prego-Faraldo, M.V., Pásaro, E., Méndez, J., and Laffon, B. (2013). Okadaic acid: more than a diarrheic toxin. Mar. Drugs 11, 4328–4349.

Vale P. Differential dynamics of dinophysistoxins and pectenotoxins between blue mussel and common cockle: a phenomenon originating from the complex toxin profile of Dinophysis acuta. Toxicon. 2004 Aug;44(2):123–34.

Vale P. Differential dynamics of dinophysistoxins and pectenotoxins, part II: Offshore bivalve species. Toxicon. 2006 Feb;47(2):163–73.

Van Dolah F.M. Marine algal toxins: Origins, health effects, and their increased occurrence. Environ. Health Perspect. 2000;108:133–141.

Van Dolah, F.M.; Ramsdell, J.S. Review and assessment of in vitro detection methods for algal toxins. J. AOAC Int. 2001, 84, 1617–1625.

van den Top HJ, Gerssen A, McCarron P, van Egmond HP. Quantitative determination of marine lipophilic toxins in mussels, oysters and cockles using liquid chromatography-mass spectrometry: inter-laboratory validation study. Food Addit Contam Part A. 2011 Jul 28;1–13.

Van Vleet TR, Mace K, Coulombe Jr RA. (2002). Comparative Aflatoxin B1 Activation and Cytotoxicity in Human Bronchial Cells Expressing Human CYPs 1A2 and 3A4. ADVS Fac Publ.16.

Vershinin A, Moruchkov A, Morton SL, Leighfield TA, Quilliam MA, Ramsdell JS. Phytoplankton composition of the Kandalaksha Gulf, Russian White Sea: Dinophysis and lipophilic toxins in the blue mussel (Mytilus edulis). Harmful Algae. 2006 Oct;5(5):558–64.

Vieira A.C., Rubiolo J.A., Lopez-Alonso H., Cifuentes J.M., Alfonso A., Bermudez R., Otero P., Vieytes M.R., Vega F.V., Botana L.M. Oral toxicity of okadaic acid in mice: Study of lethality, organ damage, distribution and effects on detoxifying gene expression. Toxins (Basel) 2013;5:2093–2108.

Vilariño, N., Fonfría, E.S., Aráoz, R., Molgó, J. and Botana, L.M. (2009). Detection of gymnodimine-A and 13-desmethyl C spirolide phycotoxins by fluorescence polarization. Anal Chem. 81, 2708-2714.

Villar-González A, Rodríguez-Velasco ML, Ben-Gigirey B, Botana LM. Lipophilic toxin profile in Galicia (Spain): 2005 toxic episode. Toxicon. 2007 Jun;49(8):1129–34.

Visciano P., Schirone M., Berti M., Milandri A., Tofalo R., Suzzi G. (2016). Marine biotoxins: occurrence, toxicity, regulatory limits and reference methods. Front. Microbiol. 7:1051.

Walker, N. J., Crockett, P. W., Nyska, A., Brix, A. E., Jokinen, M. P., Sells, D. M., Hailey, J. R., Easterling, M., Haseman, J. K., Yin, M., Wyde, M. E., Bucher, J. R., and Portier, C. J. (2004) Dose-additive carcinogenicity of a defined mixture of "dioxin-like compounds. Environ. Health Perspect. 113, 43−48.

Wandscheer, C.B., Vilariño, N., Espiña, B., Louzao, M.C., and Botana, L.M. (2010). Human Muscarinic Acetylcholine Receptors Are a Target of the Marine Toxin 13-Desmethyl C Spirolide. Chem. Res. Toxicol. 23, 1753–1761.

Wang X., Chowdhury J. R., Chowdhury N. R. (2006). Bilirubin metabolism: applied physiology. Curr. Paediatr. 16, 70–74.

Wang X-Z, Cheng Y, Li N, Wen H-M, Liu R, Shan C-X, et al. Occurrence and Seasonal Variations of Lipophilic Marine Toxins in Commercial Clam Species along the Coast of Jiangsu, China. Toxins. 2015 Dec 25;8(1):8.

Wang, Y.-M.; Ong, S.S.; Chai, S.C.; Chen, T. Role of CAR and PXR in xenobiotic sensing and metabolism. Expert Opin. Drug Metab. Toxicol. 2012, 8, 803–817.

Wang Z, Broadwater MH, Ramsdell JS. Analysis of diarrhetic shellfish poisoning toxins and pectenotoxin-2 in the bottlenose dolphin (Tursiops truncatus) by liquid chromatography–tandem mass spectrometry. J Chromatogr A. 2015 Oct;1416:22–30.

Wardlaw Christopher P.; Protein phosphatase 2A contributes to separase regulation and the co-ordination of anaphase, Bioscience Horizons: The International Journal of Student Research, Volume 3, Issue 1, 1 March 2010, Pages 66–76.

Weber, F.; Freudinger, R.; Schwerdt, G.; Gekle, M. A rapid screening method to test apoptotic synergisms of ochratoxin A with other nephrotoxic substances. Toxicol. In Vitro 2005, 19, 135–143.

Weber L.W., Boll M., Stamp A. Hepatotoxicity and mechanism of action of haloalkanes: carbon tetrachloride as a toxicological model. CRC Crit. Rev. Toxicol. 2003;33:105–136.

Wild C.P., Turner P.C. The toxicology of aflatoxins as a basis for public health decisions. Mutagenesis. 2002;17:471–481.

Wilkens S. Structure and mechanism of ABC transporters. F1000Prime Rep. 2015;7:14.

Williams PA, Cosme J, Vinkovic DM, Ward A, Angove HC, Day PJ, et al. Crystal structures of human cytochrome P450 3A4 bound to metyrapone and progesterone. Science. 2004;305(5684):683–6.

Wu X, Kekuda R, Huang W, Fei YJ, Leibach FH, Chen J, Conway SJ, Ganapathy V. (1998). Identity of the organic cation transporter OCT3 as the extraneuronal monoamine transporter (uptake2) and evidence for the expression of the transporter in the brain. J. Biol. Chem. 273, 32776–32786.

Wu J-Y, Zheng L, Wang J-H. Contamination of shellfish from Shanghai seafood markets with paralytic shellfish poisoning and diarrhetic shellfish poisoning toxins determined by mouse bioassay and HPLC. Food Addit Contam. 2005 Jul;22(7):647–51.

Wu H, Guo M, Tan Z, Cheng H, Li Z, Zhai Y. Liquid chromatography quadrupole linear ion trap mass spectrometry for multiclass screening and identification of lipophilic marine biotoxins in bivalve mollusks. J Chromatogr A. 2014 Sep;1358:172–80.

Wu H, Yao J, Guo M, Tan Z, Zhou D, Zhai Y. Distribution of Marine Lipophilic Toxins in Shellfish Products Collected from the Chinese Market. Mar Drugs. 2015 Jul 14;13(7):4281–95.

Xie J, Zhu XY, Liu LM, Meng ZQ. Solute carrier transporters: potential targets for digestive system neoplasms. Cancer Manag Res. 2018 Jan 24;10:153-166.

Xu, R.X., Lambert, M.H., Wisely, B.B., Warren, E.N., Weinert, E.E., Waitt, G.M., Williams, J.D., Collins, J.L., Moore, L.B., Willson, T.M., et al. (2004). A Structural Basis for Constitutive Activity in the Human CAR/RXRα Heterodimer. Mol. Cell 16, 919–928.

Yamashita, K.; Yasuda, H.; Pines, J.; Yasumoto, K.; Nishitani, H.; Ohtsubo, M.; Hunter, T.; Sugimura, T.; Nishimoto, T. Okadaic acid, a potent inhibitor of type 1 and type 2A protein phosphatase, activates cdc2/H1 kinase and transiently induces a premature mitosis-like state in BHK21 cells. EMBO J. 1990, 9, 4331–4338.

Yamazaki H, Hatanaka N, Kizu R, Hayakawa K, Shimada N, Guengerich FP, et al. (2000). Bioactivation of diesel exhaust particle extracts and their major nitrated polycyclic aromatic hydrocarbon components, 1-nitropyrene and dinitropyrenes, by human cytochromes P450 1A1, 1A2, and 1B1. Mutat Res Toxicol Environ Mutagen. 472(1), 129–138.

Yanagi, T., Murata, M., Torigoe, K., and Yasumoto, T. (1989). Biological activities of semisynthetic analogs of dinophysistoxin-3, the major diarrhetic shellfish toxin. Agric. Biol. Chem. 53, 525–529.

Yang N, Sun R, Liao X, Aa J, Wang G. UDP-glucuronosyltransferases (UGTs) and their related metabolic cross-talk with internal homeostasis: A systematic review of UGT isoforms for precision medicine. Pharmacol Res. 2017 Jul;121:169-183.

Yano K, Tomono T, Ogihara T. Advances in Studies of P-Glycoprotein and Its Expression Regulators. Biol Pharm Bull. 2018;41(1):11-19.

Yasumoto, T.; Murata, M.; Oshima, Y.; Sano, M.; Matsumoto, G.K.; Clardy, J. Diarrhetic shellfish toxins. Tetrahedron 1985, 41, 1019–1025.

Yasumoto, T.; Murata, M.; Lee, J. Polyether toxins produced by dinoflagellates. In Mycotoxins andPhycotoxins ’88; Natori, S., Hashimoto, K., Ueno, Y., Eds.; Elsevier: Amsterdam, The Netherlands, 1989; pp. 375–382.

Yiannakopoulou E. (2013). Pharmacogenomics of phase II metabolizing enzymes and drug transporters: clinical implications. Pharmacogenomics J. 13 105–109.

Yoon, M.Y.; Kim, Y.C. Acute toxicity of pectenotoxin-2 and its effects on hepatic metabolising enzyme system in mice. Korean J. Toxicol. 1997, 13, 183–186.

Yoshinari K, Kobayashi K, Moore R, Kawamoto T, Negishi M, Identification of the nuclear receptor CAR:HSP90 complex in mouse liver and recruitment of protein phosphatase 2A in response to phenobarbital, FEBS Lett. 548 (2003) 17–20.

Yoshitomi S, Ikemoto K, Takahashi J, Miki H, Namba M, Asahi S. Establishment of the transformants expressing human cytochrome P450 subtypes in HepG2, and their applications on drug metabolism and toxicology. Toxicol In Vitro. 2001;15(3):245–256.

Young C., Truman P., Boucher M., Keyzers R., Northcote P., Jordan W.T. The algal metabolite yessotoxin affects heterogeneus nuclear ribonucleoproteins in HepG2 cells. Proteomics. 2009;9:2529–2542.

Yu A.-M. and Pan Y.-Z., Noncoding microRNAs: small RNAs play a big role in regulation of ADME? Acta Pharm Sin B, 2, 93-101, (2012).

Yu J, Zhou Z, Tay-Sontheimer J, Levy RH, Ragueneau-Majlessi I. Intestinal Drug Interactions Mediated by OATPs: A Systematic Review of Preclinical and Clinical Findings. Journal of pharmaceutical sciences. 2017;106:2312–2325.

Zamorano R, Marín M, Cabrera F, Figueroa D, Contreras C, Barriga A, et al. Determination of the variability of both hydrophilic and lipophilic toxins in endemic wild bivalves and carnivorous gastropods from the Southern part of Chile. Food Addit Contam Part A. 2013 Sep;30(9):1660–77.

Zendong, Z.; McCarron, P.; Herrenknecht, C.; Sibat, M.; Amzil, Z.; Cole, R.B.; Hess, P. High resolution mass spectrometry for quantitative analysis and untargeted screening of algal toxins in mussels and passive samplers. J. Chromatogr. A 2015, 1416, 10–21.

Zendong Z, Kadiri M, Herrenknecht C, Nézan E, Mazzeo A, Hess P. Algal toxin profiles in Nigerian coastal waters (Gulf of Guinea) using passive sampling and liquid chromatography coupled to mass spectrometry. Toxicon. 2016 May;114:16-27.

Zenser TV, Lakshmi VM, Davis BB. N-glucuronidation of benzidine and its metabolites role in bladder cancer. Drug Metab Dispos. 1998;26:856–859.

Zhang H, Tolonen A, Rousu T, Hirvonen J, Finel M (2011) Effects of cell differentiation and assay conditions on the UDP-glucuronosyltransferase activity in caco-2 cells. Drug Metabolism and Disposition 39: 456–464.

Zhang, X., Cai, X., 2012. [Isolation and identification of shellfish toxins from contaminated blue mussel (Mytilus edulis) from the East China Sea]. Wei sheng yan jiu = Journal of hygiene research 41(5), 819-823.

Zhao L, Au JL, Wientjes MG. Comparison of methods for evaluating drug-drug interaction. Front Biosci (Elite Ed) 2010;2:241–249.

Zhou S-F, Wang B, Yang L-P & Liu J-P (2010) Structure, function, regulation and polymorphism and the clinical significance of human cytochrome P450 1A2, Drug Metabolism Reviews, 42:2, 268-354.

Zhou Y.X., Xu J., Zhang X., Xu S., Du Q. Combined toxic effects of heavy metals and antibiotics on a pseudomonas fluorescens strain zy2 isolated from swine wastewater. Int. J. Mol. Sci. 2015;16:2839–2850.

(1999). A Unified Nomenclature System for the Nuclear Receptor Superfamily. Cell 97, 161–163.

Annexes

I. Training

« Préparation de l'après-thèse », formation provided by the UEB; 23th November 2015 (9h15 - 12h45; 13h40 - 18h35); Rennes: Amphi TA Faculté Sciences Eco - University of Rennes 1 (visioconference)

« Qualité et reproductibilité des publications », formation provided by Hervé Maisonneuve; 8th January 2016 (afternoon); Anses Fougères

« Rédaction d'articles scientifiques », formation provided by Hervé Maisonneuve; 26th-27th May 2016; Anses Maisons-Alfort

II. Collaborations

From September 2015 to March 2016 and from February to April 2017: development of LC/HRMS method for metabolism investigations; Estelle Dubreil, Dominique Pessel from Analysis of Residues and Contaminants Unit, ANSES Fougères

25th-29th January 2015: RT-qPCR assays; Patrick Fach, Cédric Woudstra from the IdentyPath platform, ANSES Maisons-Alfort

2nd-3rd March 2017: metabolism assays using Silensome®; Francoise Brée, Belkacem Bouati from Bioprédic International, Saint Grégoire

May 2017: Assessment of SPX-1 metabolites activity towards nAChR; Romulo Araoz from CNRS, Institut de Neurosciences, Gif sur Yvette

III. Communications

1. Conference

Jimmy Alarcan (JA), Stefanie Hessel-Pras (SH-P), Alfonso Lampen (AL), Ludovic Le Hégarat (LLH) and Valérie Fessard (VF); "Effect of co-exposure to marine lipophilic biotoxins on the intestinal barrier, bioactivation and molecular mode of actions"; **Journées scientifiques du GdR Phycotox et du GIS Cyano**; 31th Mars to 2nd April 2015, Institut Universitaire Européen de la Mer (IUEM) de Brest, France, oral communication

Jimmy Alarcan (JA), Ludovic Le Hégarat (LLH), and Valérie Fessard (VF); "Rôle des cytochromes P450 1A2 et 3A4 dans le métabolisme des phycotoxines lipophiles"; **Journées des doctorants et post-doctorants ANSES**; 19th November 2015, ANSES Maisons Alfort, Maisons Alfort, France, oral communication

Jimmy Alarcan (JA), Estelle Dubreil (ED), Ludovic Le Hégarat (LLH), Dominique Hurtaud-Pessl (DHP) and Valérie Fessard (VF); "In vitro investigation on the human metabolism of lipophilic phycotoxins PTX-2 and SPX-1 using liquid chromatography hyphenated with high resolution Orbitrap mass spectrometry"; **Journées scientifiques du GdR Phycotox**; 15th-16th March 2016, Villefranche sur mer, France, oral communication

Jimmy Alarcan (JA), Estelle Dubreil (ED), Ludovic Le Hégarat (LLH), Dominique Hurtaud-Pessl (DHP) and Valérie Fessard (VF); " In vitro investigation on the human metabolism of the lipophilic phycotoxin SPX-1 using liquid chromatography hyphenated with high resolution Orbitrap mass spectrometry "; **ECsafeSEAFOOD**; 25th-26th January 2017, Bruxells, Belgium, poster

Jimmy Alarcan (JA), Ronel Biré (RB), Ludovic Le Hégarat (LLH) and Valérie Fessard (VF); " Mixtures of lipophilic phycotoxins: exposure data and in vitro toxicity assessment"; **Journées scientifiques du GdR Phycotox et du GIS Cyano**; 14th-16th March 2017, Gif sur Yvette, campus CNRS, France, oral communication

Jimmy Alarcan (JA), Estelle Dubreil (ED), Antoine Huguet (AH), Dominique Hurtaud-Pessl (DH-P), Valérie Fessard (VF), Stefanie Hessel-Pras (SH-P), Alfonso Lampen (AL) and Ludovic Le Hégarat (LLH); " Metabolism of the marine biotoxin PTX-2 and its effects on hepatic xenobiotic metabolism: activation of nuclear receptors and modulation of CYP"; **ISSX 14th conference of the internationnal society for the study of xenobiotics**; 26th to 29th June 2017, Cologne, Germany, poster

Jimmy Alarcan (JA), Sabrina Barbé (SB), Stefanie Hessel-Pras (SH-P), Alfonso Lampen (AL), Valérie Fessard (VF)and Ludovic Le Hégarat (LLH); "In vitro assessment of binary mixture effects of phycotoxins in human intestinal Caco-2 cells"; **ECMNP 10th European Conference on Marine Natural Products**; September 3rd to 7th, 2017, Kolymbari – Crete, Greece, oral communication

Participation in the symposium « Current approaches to assess chemical contaminant mixture effects and regulatory implications » held in Paris the 19th June 2015.

2. Other

Radio interview for France Bleu Armorique: presenting the Ph.D job position. Recorded the 13th November 2015.

Abstract

Lipophilic phycotoxins are secondary metabolites produced by some phytoplankton species. They accumulate in filter-feeding molluscs and can cause intoxication in humans with a wide variety of symptoms. This work aimed at bringing better knowledge on their fate in humans and their effects after ingestion by providing data on their intestinal absorption and their hepatic metabolism since these phenomena affect the amount of toxin circulating in the body and therefore the generation of toxic effects. In addition, several phycotoxins are sometimes found simultaneously in shellfish while the effects of these mixtures are still unknown. Four lipophilic phycotoxins, okadaic acid (OA), pectenotoxin-2 (PTX-2), yessotoxin (YTX) and spirolide (SPX-1) were selected. The intestinal passage was evaluated using human intestinal Caco-2 cells mimicking the intestinal epithelium. If differences in absorption were observed for the 4 phycotoxins, our results showed that the intestinal epithelium was also able to send them back into the intestinal lumen, thus limiting the amount circulating in the body. Similarly, using liver extracts, we showed that the structure of the 4 phycotoxins was modified, mainly by hydroxylation reactions. For mixtures effects, the addition of another toxin (PTX-2, YTX or SPX-1) to OA results in lower effects at low concentrations, and additive or larger effects at higher concentrations. These results provide additional data that can be used to confirm or revise regulatory thresholds established for these toxins.

Résumé

Les phycotoxines lipophiles sont des métabolites secondaires produits par certaines espèces phytoplanctoniques. Elles s'accumulent dans les mollusques filtreurs et peuvent provoquer une intoxication chez l'homme avec une grande variété de symptômes. Ce travail s’est attaché à mieux connaitre leur devenir chez l’homme et leurs effets après ingestion en apportant des données sur leur absorption intestinale et leur métabolisme hépatique puisque ces phénomènes affectent la quantité de toxine circulant dans l’organisme et donc la génération d’effets toxiques. En outre, plusieurs phycotoxines se retrouvent parfois simultanément dans les coquillages alors que les effets de ces mélanges sont encore méconnus. Quatre phycotoxines lipophiles, l'acide okadaïque (AO), la pecténotoxine-2 (PTX-2), la yessotoxine (YTX) et le spirolide (SPX-1), ont été sélectionnées. Le passage intestinal a été évalué à l’aide de cellules intestinales humaines Caco-2 mimant l’épithélium intestinal. Si des différences d’absorption ont été observées pour les 4 phycotoxines, nos résultats ont montré que l’épithélium intestinal était également capable de les renvoyer dans la lumière intestinale, limitant ainsi la quantité circulant dans l’organisme. De même, à l’aide d’extraits de foie, nous avons montré que la structure des 4 phycotoxines était modifiée, principalement par des réactions d'hydroxylation. Concernant les effets mélanges, l'ajout d'une autre toxine (PTX-2, YTX ou SPX-1) à l'AO entraîne des effets moins importants avec de faibles concentrations, et des effets additifs ou plus importants avec des concentrations plus élevées. Ces résultats apportent des données complémentaires pouvant servir à confirmer ou réviser les seuils réglementaires établis pour ces toxines.

Les phycotoxines lipophiles sont des métabolites secondaires produits par certaines espèces phytoplanctoniques. Elles s'accumulent dans les mollusques filtreurs et peuvent provoquer une intoxication chez l'homme avec une grande variété de symptômes. Des limites réglementaires ont été fixées pour les toxines individuelles et les caractéristiques toxicologiques sont bien caractérisées pour certaines d'entre elles. Cependant, les connaissances concernant leur absorption et leur métabolisme sont restreintes. En outre, la contamination par les phycotoxines est souvent un phénomène de co-exposition et les données toxicologiques concernant les effets des mélanges sont rares. Ce travail vise à apporter de nouvelles informations sur un panel de quatre phycotoxines lipophiles: l'acide okadaïque (AO), la pecténotoxine-2 (PTX-2), la yessotoxine (YTX) et le spirolide (SPX-1) sur deux principaux axes de recherche: absorption intestinale/métabolisme hépatique des toxines et les effets de mélanges.

Nous avons d'abord examiné le passage intestinal des phycotoxines à l´aide de monocouches de cellules intestinales humaines Caco-2 ensemencées sur le système Transwell. Des travaux ayant été déjà publiés pour l´AO, nos efforts se sont concentrés sur les autres phycotoxines du projet. Bien qu´aucune cytotoxicité n´ait été rapportée après 24 h de traitement selon le test du rouge neutre, la PTX-2 désagrège l´intégrité de la monocouche comme en témoigne un passage paracellulaire accru du marqueur fluorescéine-dextran. Par conséquent, les travaux de passage ont été restreints à l´étude d´une faible concentration de PTX-2. Quel que soit le temps d´incubation (2, 6 ou 24 h), la PTX-2 est détectée en très faible quantité (moins de 20% de toxine initialement incubée) dans les compartiments apical et basolatéral, ce qui laisse supposer un fort métabolisme intestinal. Le SPX-1 n´a pas induit de toxicité et l´intégrité de la monocouche est restée inchangée. Les études de passage ont montré un fort efflux de la toxine vers le pôle apical. Cet efflux n´est pas temps-dépendent du fait qu´un maximum est atteint après 3 h et reste inchangé pour les autres temps étudiés (6 et 10 h). Concernant la YTX, les travaux ont été rapidement abandonnés dû à un problème de fixation de la toxine sur la membrane plastique du Transwell. Nos résultats indiquent donc que les phycotoxines traversent différentiellement les monocouches de cellules Caco-2, mais leur efflux se produit de manière plus prononcé.

Nous avons ensuite, dans un premier temps, étudié le métabolisme des toxines en utilisant des fractions de foie de rat et d´humain. Pour cela, une méthode d´analyse LC-HRMS a été mise au point. Puis, dans un second temps, les enzymes impliquées dans le processus de biotransformation ont été recherchées. Nous avons observé que la PTX-2 est métabolisée par les fractions S9 de rats et humaines, les quantités de PTX-2 diminuant simultanément avec l'apparition d'au moins un métabolite hydroxylé. Ce métabolite a déjà été décrit en utilisant des fractions S9 de rats. Nous avons observé deux métabolites supplémentaires avec les fractions S9 humaines, mais seulement dans l´essai où nous avons observé une perte presque totale de PTX-2. En ce qui concerne les métabolites formés, nous n'avons observé aucune différence inter-espèce entre le rat et l'humain, ce qui suggère que des enzymes de phase I similaires sont probablement impliquées dans le métabolisme de la PTX-2 chez les mammifères. Nos résultats sur l'expression des gènes ont révélé que la PTX-2 pouvait affecter la régulation de plusieurs gènes dans les cellules humaines HepaRG. Une régulation positive prononcée des ARNm du CYP1A1 et du CYP1A2 a en effet été observée, indiquant un rôle clé plausible pour ces deux enzymes dans l'hydroxylation de la PTX-2. La régulation à la hausse du SULT1E1 et de plusieurs UGT suggère que la PTX-2 elle-même ou les métabolites hydroxylés formés par le processus de phase I pourraient être conjugués. Les résultats sur l'expression des gènes de transporteur peuvent suggérer le rôle de la P-gp et de l'ABCG2 dans l'efflux de la PTX-2. L'induction des ARNm CYP1A a pu être corrélée avec l'induction des niveaux de

protéines, puisque nous avons montré l'induction du CYP1A2 en utilisant deux méthodologies différentes (immuno-marquage et western blot), et l'induction du CYP1A1 par Western blot. Cependant, nous n'avons détecté aucune augmentation de l'activité EROD dans les cellules HepaRG (jusqu'à 64 nM PTX-2 pendant 24 h ou 48 h). Il est possible que le niveau d'augmentation des ARNm CYP1A n'ait eu aucun impact sur les activités du CYP. D'autres investigations sont nécessaires pour révéler les mécanismes sous-jacents. En utilisant des essais de transactivation, nous avons montré que la PTX-2 n'active ni CAR ni PXR. Pour AhR, notre modèle a été biaisé par la PTX-2 et nous ne pouvons pas conclure. Cependant, il est peu probable que la PTX-2 n'interfère pas avec AhR, car la régulation des CYP1A1 et 1A2 a été démontrée comme quasi exclusivement par l´action du AhR. D'après nos résultats, nous pouvons émettre l´hypothèse que la PTX-2 est un inducteur de son propre métabolisme, impliquant que CYP1A1 et CYP1A2 seraient responsables de son hydroxylation.

En utilisant des fractions S9 humaines, nous avons observé une déplétion complète du SPX-1 simultanément à la formation de métabolites multiples. Nous avons confirmé cinq métabolites sur neuf déjà décrits. Les principaux métabolites ont été détectés avec succès dans les deux expériences menées, mais certains métabolites mineurs n'ont été détectés que dans une expérience. Malgré la formation de métabolites hydroxylés, aucun conjugué de phase II n'a été détecté. En utilisant des fractions S9 de rats, une déplétion similaire du SPX-1 a été observée. Les mêmes cinq métabolites ont été détectés chez le rat et l'homme. Cependant, quelques différences de temps de rétention ont été trouvées entre S9 humain et rat pour plusieurs métabolites. En particulier, le principal métabolite hydroxylé trouvé avec le S9 humain a un temps de rétention différent de celui trouvé avec le S9 rat. Cela peut indiquer que la biotransformation s'est produite sur un site différent de la SPX-1, ce qui signifie que les métabolites pourraient être des isomères. Nos résultats sur l'expression des gènes ont révélé que le SPX-1 régule à la hausse CYP1A2. Pour clarifier si cette enzyme est impliquée dans le métabolisme de la SPX-1, nous avons utilisé l'outil innovant Silensomes ™ et nous avons pu estimer que la contribution du CYP1A2 était de 48%, ce qui signifie que d'autres enzymes participent probablement au métabolisme du SPX-1.

La recherche des métabolites de l´AO à l´aide de fractions de foie étant déjà bien documentée, nos efforts se sont concentrés sur les enzymes impliquées. Nous avons cherché à évaluer le rôle de la P-gp dans la toxicité de l'AO et nous avons étudié en parallèle les effets de l'AO sur l´expression des gènes du métabolisme et de l'inflammation. Nos résultats montrent une toxicité accrue de l´AO lorsque la P-gp est inhibée par le vérapamil, indiquant ainsi un rôle clé de ce transporteur dans la modulation de la toxicité de l'AO. Nos résultats sur l'analyse de l'expression génique ont révélé que l'AO affecte la régulation de nombreux gènes du métabolisme dans les cellules HepaRG. Une régulation négative globale des ARNm CYP a en effet été observée, le *CYP3A4* étant le plus fortement régulé à la baisse. Les résultats sur la régulation des gènes des transporteurs ont confirmé le rôle de la P-gp et pourraient mettre en évidence le rôle possible de l'ABCG2 dans l'efflux de l'AO, ces deux gènes étant régulés à la hausse, favorisant l'excrétion de l'AO. Une explication possible de la diminution du métabolisme des xénobiotiques est l'implication des voies pro-inflammatoires. Ici, nous avons montré que l'AO régule fortement à la hausse certains gènes de l´inflammation tels que *COX2* ou *IL6/IL8*. En utilisant le test de transactivation, nous avons montré que l'AO inhibe à la fois le PXR et le RXRα. Comme l'AO régule à la hausse certains gènes clés de l´inflammation, nous avons voulu explorer la piste de l'inflammation comme explication possible de l'inhibition de PXR / RXRα. Dans ce but, nous avons utilisé des inhibiteurs de l'inflammation. Nos résultats sur la transactivation de PXR pourraient mettre en évidence le rôle de l'inflammation dans l'inhibition médiée par l'AO.

La recherche des métabolites de la YTX à l´aide de fractions de foie a dû être abandonnée suite à des problèmes analytiques. Devant les nombreux problèmes rencontrés, nous avons décidé de réorienter notre objectif vers une analyse des effets de la YTX sur un panel de 45 gènes liés aux récepteurs nucléaires, au métabolisme, à l'inflammation, au stress oxydatif et à l'autophagie dans la lignée cellulaire HepaRG en utilisant une approche qPCR. Les résultats indiquent que la YTX module l'expression de nombreux gènes. L'expression des gènes du métabolisme a été globalement régulée à la baisse tandis qu'une régulation à la hausse de l'expression des gènes de l'inflammation a été observée. En particulier, *NR1I2*, *CYP2C9*, *SULT1E1* et *UGT2B4* ont été fortement régulés à la baisse tandis qu'une forte régulation à la hausse de *COX2*, *IL6* et *IL8* a été observée. Les données sur le stress oxydatif et l'autophagie montrent à la fois une induction et une répression de certains gènes cibles. Ces résultats suggèrent donc que la YTX est susceptible de perturber plusieurs voies toxicologiques dans les cellules hépatiques. Ils peuvent également mettre en évidence le rôle clé de certaines protéines dans la toxicité YTX. Des études supplémentaires doivent être effectuées au niveau protéomique pour corréler les changements observés dans les niveaux d'ARNm.

La seconde partie du projet de thèse visait à étudier les effets de mélanges de toxines. Nous avons donc évalué un panel de différents paramètres de toxicité (viabilité cellulaire, stress oxydatif, inflammation et dommage des brins d'ADN) sur la lignée cellulaire humaine Caco-2 après traitement aux toxines (AO, PTX-2, YTX et SPX-1) seules ou en combinaisons binaires. Notre étude a révélé que l'AO est cytotoxique, induit des cassures double-brin d'ADN et déclenche la libération d'IL-8 dans les cellules différenciées Caco-2. La PTX-2 est sub-toxique et n'induit que faiblement des cassures double-brin d'ADN aux concentrations les plus élevées. Le SPX-1 et la YTX n'ont induit aucun effet sur les paramètres testés. Quel que soit la phycotoxine, aucune production de ROS n'a été détectée, ce qui peut être dû à un problème de cinétique car les ROS surviennent plutôt après une courte période de traitement. Dans notre étude, des effets antagonistes à faibles doses et de puissants effets synergiques dans certains cas à des doses plus élevées ont pu être démontrés. Il est intéressant de noter que les effets de mélange peuvent être différents d'un paramètre à un autre pour le même niveau de concentration. Par exemple, si les mélanges AO/YTX sont additifs en ce qui concerne la viabilité cellulaire, des effets synergiques ont été montrés pour la libération d'IL-8 et des effets antagonistes pour la phosphorylation de γ-H2AX. Ces données montrent l'importance d'étudier de multiples voies toxicologiques lorsque l´on étudie les effets de mélanges. Quelle que soit la toxine, les mélanges avec l'AO ont abouti à des réponses toxiques diminuées aux faibles concentrations. Dans la mesure où la PTX-2, la YTX et le SPX-1 ont tous un mécanisme d'action différent, il est probable que cet effet protecteur résulte d'un mécanisme de défense cellulaire plutôt que de la perturbation d'une voie spécifique de l'AO par le second composé. L'induction d'enzymes métabolisant les xénobiotiques telles que les cytochromes P450 pourrait être une explication. Un fort effet synergique a été observé pour le mélange AO/PTX-2 à forte concentration. Il convient d'évaluer la toxicité in vivo pour voir si cette forte synergie peut être corrélée chez les rongeurs. Si un effet combiné peut être établi, cela pourrait conduire à reconsidérer la limite réglementaire européenne des groupes des toxines AO et des toxines PTX. L'évaluation des effets des mélanges doit indiquer si les limites européennes actuelles de toxines dans les coquillages sont suffisantes pour protéger les consommateurs en cas de co-exposition. En raison des effets combinés notables sur certaines voies de toxicité clés, une plus grande attention devrait être accordée aux mélanges de phycotoxines.

Bien que le risque lié à la présence de phycotoxines dans les mollusques filtreurs semble bien maîtrisé, plusieurs lacunes subsistent concernant les phycotoxines émergentes, les analogues de phycotoxines, les phycotoxines sans limites réglementaires, les mélanges, etc.

De nouveaux modèles in vitro pour les études de toxicité ont été mis au point. La culture de cellules en trois dimensions est un domaine prometteur avec, par exemple, les sphéroïdes et les organoïdes qui présentent des caractéristiques structurelles proches des organes humains. Les co-cultures de lignées cellulaires sont également un moyen facile d'imiter la diversité d'une population cellulaire in vivo. L'utilisation de ces modèles innovants serait utile dans le contexte des phycotoxines lipophiles. En effet, ces toxines induisent des effets sur le tractus gastro-intestinal mais les voies moléculaires impliquées ne sont pas clairement élucidées. De tels systèmes in vitro aideraient certainement à comprendre les mécanismes sous-jacents des phycotoxines lipophiles. Nos connaissances sur la toxicocinétique des phycotoxines doivent encore être approfondies. Les études in vivo sont coûteuses et nécessitent une grande quantité de toxines, ce qui en fait une approche limitée. En outre, l'EFSA encourage la réduction des essais sur les animaux (principe des 3 R). Une combinaison d´outils de modélisation tel que le PBPK et de systèmes avancés tels que les organes microfluidiques sur puce semble être un bon compromis. Compte tenu du rôle du métabolisme des xénobiotiques dans la régulation du comportement des phycotoxines lipophiles à l'intérieur du corps humain, de nouveaux outils méthodologiques devraient être développés pour étudier les métabolites et leur activité. La méthodologie du biogramme HPLC est une stratégie utilisée dans les programmes de recherche de médicaments pharmaceutiques. Elle permet de déterminer l'activité biologique de chaque composant à l'intérieur d'un échantillon en combinant HPLC et un dosage biologique fonctionnel dans un processus automatisé. L'adaptation de cette méthodologie au contexte des phycotoxines lipophiles permettrait de déterminer l'activité des métabolites.

L'évaluation des risques liés aux mélanges de phycotoxines doit être poursuivie par une enquête plus approfondie de leur toxicité. L'utilisation du criblage à haut contenu ou « high-content screening » est un moyen pratique d'évaluer simultanément plusieurs paramètres biologiques. Cela aiderait à sélectionner en priorité les combinaisons présentant les effets les plus nocifs in vitro en vue de leur évaluation dans des études in vivo. Les mollusques filtreurs sont non seulement exposés aux phycotoxines lipophiles, mais aussi à une grande variété d'autres contaminants tels que les métaux lourds, les dioxines ou les hydrocarbures aromatiques polycycliques. L'évaluation des effets de ces mélanges très complexes est peut-être trop en avance pour le moment, mais il convient de garder à l´esprit que les mollusques n'accumulent pas que des biotoxines marines.